CHEMOTHERAPY INDUCES INTRA-TUMORAL EXPRESSION OF CHEMOKINES IN CUTANEOUS MELANOMA, FAVORING T CELL INFILTRATION AND TUMOR CONTROL

HONG LI WEN MICHELLE

NATIONAL UNIVERSITY OF SINGAPORE

2011

CHEMOTHERAPY INDUCES INTRA-TUMORAL EXPRESSION OF CHEMOKINES IN CUTANEOUS MELANOMA, FAVORING T CELL INFILTRATION AND TUMOR CONTROL

HONG LI WEN MICHELLE

(B.SCIENCE.(Hons.), NUS)

A THESIS SUBMITTED

FOR THE DEGREE OF DOCTOR OF PHILOSOPHY

NUS GRADUATE SCHOOL FOR INTEGRATIVE SCIENCES AND ENGINEERING

NATIONAL UNIVERSITY OF SINGAPORE

2011

ACKNOWLEDGEMENTS

First and foremost, I would like to express my deepest gratitude to my supervisor, Dr. Jean-Pierre Abastado, for his patience and invaluable guidance throughout the course of my PhD. I would like to express my heartfelt thanks and appreciation to my mentor, Dr. Anne-Laure Puaux, for believing in me and supporting me during the first two years of my PhD.

I would also like to acknowledge my lab members for their tremendous help and friendship, without which my stay in the lab would not have been so enjoyable and fulfilling. I would also like to thank my PhD Thesis Advisory Committee (TAC) members, Dr. Lu Jinhua and Dr. Lim Yaw Chyn for their advices, guidance and encouragements during my PhD studies. Furthermore, I would like to thank Dr. Joanne Keeble and Dr. Anne-Laure Puaux for proofreading my thesis.

I would like to thank all my collaborators, including Dr. Masashi Kato for kindly providing the RETAAD mouse model, Dr. Armelle Prévost-Blondel for providing the patients' RNA samples, Dr. Marie-Françoise Avril for the patients' samples, and Dr. Alessandra Nardin for the microarray analysis.

In addition, this project would not have been possible without the PhD opportunity from the NUS Graduate School for Integrative Sciences and Engineering (NGS) as well as the generous financial support from the Agency

for Science, Technology and Research (A*STAR) Biomedical Sciences Institute (BMSI) and the A*STAR Graduate Academy (A*GA).

Most importantly, I would like to express my deepest appreciation and love for my husband, my parents, and my siblings for their continuous love, support, encouragement and faith in my ability.

TABLE OF CONTENTS

SUMMARY

T cell-based immunotherapies for melanoma have limited success so far. Complete clinical responses are rarely observed. T cell recruitment to tumors is one of the potential rate-limiting steps in effective anti-tumor response in melanoma therapies. Therefore, the aim of the present study is to identify the molecular cues that control T cell infiltration into cutaneous melanoma and to find treatments promoting T cell infiltration. For this purpose, we used the RETAAD model of spontaneous melanoma and samples from melanoma patients treated with chemotherapy.

In the first part of the chemokine project, we show that the lack of T cell control of cutaneous melanoma in the RETAAD model of spontaneous melanoma is due to limited T cell infiltration into the tumors. This lack of T cell infiltration is not due to intrinsic defects in T cell migration to cutaneous sites. Rather, it is the result of lack of expression of T cell attracting chemokines within the local tumor microenvironment. We found that CXCR3 ligands (CXCL9 and CXCL10) and CCL5 synergize to attract T cells to cutaneous melanoma, and expression of these chemokines inhibits tumor growth. Most RETAAD skin tumors fail to express these chemokines and therefore escape T cell control.

In the second part of the chemokine project, we demonstrate that the chemotherapeutic drugs (dacarbazine, temozolomide, and cisplatin) induce specific expression of T cell-attracting chemokines (including CXCL9,

CXCL10 and CCL5) in several human melanoma cell lines *in vitro*. This increase in chemokine expression is dose- and time-dependent, indicating a direct effect of chemotherapy drugs on chemokine expression. Using global transcriptome analysis, we analyze cutaneous metastases resected from melanoma patients before and after chemotherapy, and detect increased T cell infiltration into chemotherapy-sensitive tumors. Response to chemotherapy correlates with up-regulation of the same chemokines. Furthermore, patients exhibiting enhanced chemokine expression after chemotherapy survive longer.

Collectively, our findings unravel a novel cell-extrinsic mechanism of action of common chemotherapy drugs by showing that chemotherapy works, in part, through the induction of chemokine expression in cancer cells and subsequent recruitment of effector T cells into the tumors. These findings may serve as a basis for new therapeutic strategies for the treatment of melanoma by identifying subgroups of patients with an increased chance of response to conventional chemotherapies. Furthermore, it suggests that screening for chemotherapy drugs that are able to induce the expression of T cell-attracting chemokines may improve conventional as well as immune-based therapies of cancer.

To further validate our findings in future investigations, we have generated a new reporter mouse melanoma model (Melucie) that enables visualization of spontaneous tumor development by *in vivo* bioluminescence imaging (BLI). *In vivo* BLI was able to detect bioluminescent primary tumor and metastases,

which were confirmed by *ex vivo* imaging and histology analysis. The Melucie model demonstrates a remarkable correlation between BLI signals and tumor weight, high sensitivity and positive predictive value, and enables longitudinal monitoring of disease progression *in vivo*. Taken together, this model will facilitate testing of future chemo-immunotherapeutic strategies against melanoma.

LIST OF TABLES

LIST OF FIGURES

LIST OF PUBLICATIONS

Publications:

Hong M, Puaux AL, Huang C, Loumagne L, Tow C, Mackay C, Kato M, Prevost-Blondel A, Avril MF, Nardin A, Abastado JP. Chemotherapy induces intratumoral expression of chemokines in cutaneous melanoma, favoring T cell infiltration and tumor control. Cancer Res. 2011 Oct 7. [Epub ahead of print]

Michelle Hong, Anne-Laure Puaux, Masashi Kato, and Jean-Pierre Abastado. A novel mouse model to monitor spontaneous primary melanoma development and metastases *in vivo* by bioluminescence imaging. (Manuscript in preparation)

Related publications:

Puaux AL, Ong LC, Jin Y, Teh I, **Hong M**, Chow PK, Golay X, Abastado JP. A comparison of imaging techniques to monitor tumor growth and cancer progression in living animals. *International Journal of Molecular Imaging*. 2011 [In press]

Bourgault-Villada I, **Hong M**, Khoo K, Tham M, Toh B, Wai LE and Abastado JP: Current insight into the metastatic process and melanoma cell dissemination. Melanoma 2011. ISBN 978-953-307-293-7. Editor: Mandi Murph Publisher Intech

Eyles J, Puaux AL, Wang X, Toh B, Prakash C, **Hong M**, Tan TG, Zheng L, Ong LC, Jin Y, Kato M, Prévost-Blondel A, Chow P, Yang H, Abastado JP. Tumor cells disseminate early, but immunosurveillance limits metastatic outgrowth, in a mouse model of melanoma. *J Clin Invest.* 2010, 120(6): 2030-9.

LIST OF ABBREVIATIONS

AAD	chimeric MHC class I molecule
ACT	adoptive cell transfer
APC	antigen-presenting cell
BiTE	bispecific T-cell engager
BLI	bioluminescence imaging
CAR	chimeric antigen receptor
CEA	carcinoembryonic antigen
CTL	cytotoxic T lymphocyte
CTLA-4	cytotoxic T-lymphocyte antigen 4
DC	dendritic cell
DCT	dopachrome tautomerase
DTIC	dacarbazine
FasL	Fas ligand
FDA	Food and Drug Administration
FLI	fluorescence imaging
GEMM	genetically modified mouse model
GM-CSF	granulocyte-macrophase colony-stimulating factor
GPCR	G-protein-coupled receptor
HLA	human leukocyte antigen
ICAM	intercellular adhesion molecule
IDO	indoleamine 2,3-dioxygenase
IFN-α	interferon-alpha
IFN-γ	interferon-gamma
IL-2	interleukin-2
LFA-1	leukocyte-function associated antigen-1
MDSC	myeloid-derived suppressor cell
MHC	major histocompatibility complex
MRI	magnetic resonance imaging
NSCLC	non-small cell lung carcinoma
NK	natural killer cells
NKG2DL	NKG2D ligands

NMC	nonmyeloablative chemotherapy
PD-1	programmed death-1
PET	positron emission tomography
PPV	positive predictive value
qRT-PCR	quantitative real-time polymerase chain reaction
RET	receptor tyrosine kinase
RETAAD	spontaneous mouse model of melanoma
RGP	radial growth phase
RLU	relative light unit
TAA	tumor associated antigen
TCR	T cell receptor
TEM	transendothelial migration
TGF-β	transforming growth factor beta
Th1	T helper type 1
Th2	T helper type 2
TIL	tumor-infiltrating lymphocyte
TNF	tumor necrosis factor
TRAIL	tumor necrosis factor–related apoptosis-inducing ligand
Treg	T regulatory cell
TLR	toll-like receptor
Trp2	tyrosinase-related protein 2
VGP	vertical growth phase
VLA4	very late antigen-4

CHAPTER 1

INTRODUCTION

1 INTRODUCTION

1.1 Melanoma

1.1.1 Melanoma incidence and etiological factors

Metastatic melanoma is one of the deadliest types of skin cancer. Globally, there is an estimated 132,000 cases a year (World Health Organization), and it accounts for most skin cancer deaths. It is the sixth most common cancer type in men and the seventh in woman, with a median survival of 6-10 months and a 5-year survival rate of about 10% (Cummins et al., 2006). Genetic susceptibility and exposure to ultraviolet radiation are thought to be the two most important risk factors for the development of malignant melanoma (Brozena et al., 1993). Comprehensive strategies such as comparative genomic hybridization and mutation analysis by gene sequencing have identified several genetic alterations in metastatic melanoma. This includes genetic alterations in oncogenes (*BRAF*, *C-KIT*, *NRAS*, *AKT3*), tumor suppressor genes (*CDKN2A*, *PTEN*, *APAF-1*, and *P53*), cell cycle genes (*CCND1*), and transcription factors (*MITF*)[i] (Gajewski, 2011; Gray-Schopfer et al., 2007).

1.1.2 Melanoma progression and the subtypes of cutaneous melanoma

Melanoma arise from aberrant melanocytes, and mutations in critical growth regulatory genes, the production of autocrine growth factors and the loss of

[i] BRAF – v-raf murine sarcoma viral oncogene homolog B1; C-KIT – v-kit Hardy-Zuckerman 4 feline sarcoma viral oncogene homolog; NRAS – neuroblastoma RAS viral (v-ras) oncogene homolog; AKT3 – v-akt murine thymoma viral oncogene homolog 3 (protein kinase B, gamma); CDKN2A – cyclin-dependent kinase inhibitor 2A; PTEN – phosphatase and tensin homolog; APAF1 – apoptotic peptidase activating factor 1; CCDN1 – cyclin D1; MITF – microphthalmia-associated transcription factor.

adhesion receptors have all been shown to contribute to disrupted intracellular signalling in melanocytes. This can result in the proliferation and spreading of melanocytes, thus, leading to the formation of a naevus or common mole. Melanocyte proliferation can be restricted to the epidermis (junctional naevus), the dermis (dermal naevus), or both (compound nevus). In general, naevi are benign but can progress to the radial-growth-phase (RGF) with some local invasion of the dermis, and subsequently, to the vertial-growth-phase (VGP) where invasion of the dermis and metastasis could occur. Not all melanomas will go through these sequential steps of progression – RGP or VGP can develop directly from benign melanocytes or naevi and can progress directly to metastatic melanoma (Gray-Schopfer et al., 2007) (Figure 1.1.1).

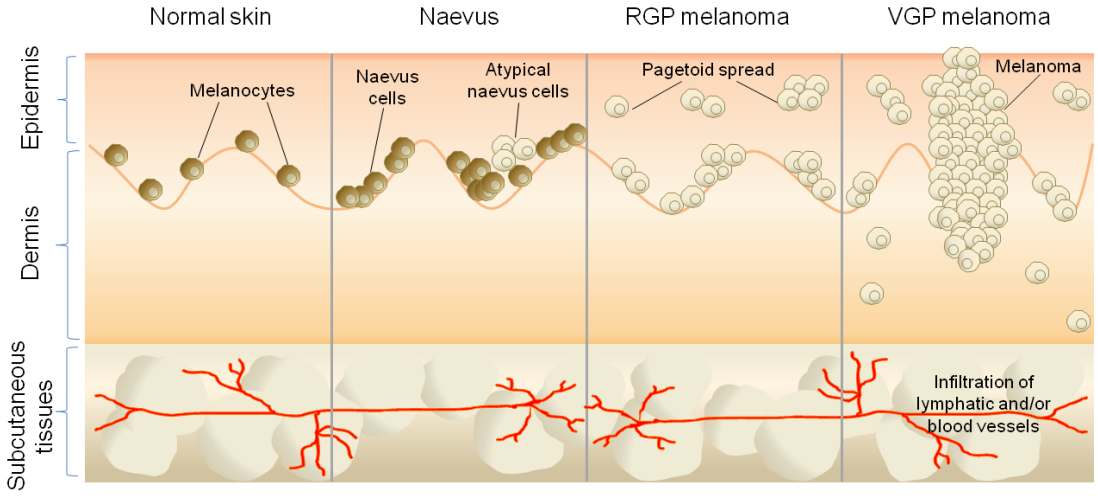

Figure 1.1.1 – Progression of melanocyte transformation into melanoma.
(A) In normal skin, normal melanocytes are evenly distributed within the basal layer of the epidermis. (B) Benign neavi can result from increased proliferation and spreading of aberrant melanocytes, and can be junctional, dermal or compound. Some neavi are dysplastic, characterized by morphologically atypical melanocytes. (C) Radial-growth-phase (RGP) is considered as the primary malignant stage. (D) Vertical-growth-phase (VGP) can lead directly to metastatic malignant melanoma. It is the most deadly stage, marked with infiltration of blood and lymphatic vessles. Pagetoid refers to upward spreading of melanocytes into the epidermis and is a histological characteristic of melanoma [adapted from (Gray-Schopfer et al., 2007)].

There are four main clinical subtypes of melanoma: nodular melanoma (raised nodules without flat portions), acral lentiginous melanoma or ALM (commonly found on the palms, soles and nail bed, not associated with sun exposure), lentigo maligna (generally flat in appearance, associated with chronic sun exposure especially in elderly), and superficial spreading melanoma or SSM (usually flat with an intra-epidermal component, the most common form of melanoma in young people in the UK and USA) (Gray-Schopfer et al., 2007; Johansson et al., 2009).

1.1.3 Melanoma diagnosis and treatment

Diagnosis of melanoma has been based on pathology, but interestingly, Bastian and colleagues have demonstrated that genome wide alterations in DNA copy number together with individual somatic mutations have 70% accuracy in distinguishing the different subtypes of melanoma (Curtin et al., 2005).

Surgical excision is the mainstay therapy for early-stage melanoma. Non-surgical modalities used in the treatment of advanced disease include cytotoxic chemotherapy, immunotherapy, a combination approach such as biochemotherapy, and novel investigational therapies (Gray-Schopfer et al., 2007; Kadison and Morton, 2003; Keilholz and Gore, 2002; Kirkwood et al., 2008; Rosenberg and Dudley, 2009; Sundaresan et al., 2009). To-date, there are three US FDA (Food and Drug Administration)-approved drugs available for the treatment of advanced metastatic melanoma. The first is the chemotherapy drug dacarbazine (DTIC, approved in 1976), the second is the

immune-modulatory cytokine interleukin-2 (IL-2, approved in 1998), and the third is the cytotoxic T lymphocyte antigen-4 (CTLA-4) blocker (Ipilimumab, approved in 2011).

Dacarbazine (DTIC) is considered to be the most active drug for the treatment of metastatic melanoma, with a response rate of 20%, and a median duration of response of 4 to 5 months (Khayat et al., 2002; Nathan and Mastrangelo, 1998). Other cytotoxic compounds, such as temozolomide (a DTIC analogue) (Middleton et al., 2000), cisplatin and carboplatin (Bajetta et al., 2002), vinca alkaloids (Khayat et al., 2002), taxanes (Bafaloukos et al., 2002) and nitrosoureas (Cure et al., 1999) are associated with response rates of less than 15% with significant adverse effects reported.

Post-operative adjuvant therapies for malignant melanoma such as high dose IL-2 (a cytokine that stimulates T cell proliferation and function) demonstrated modest anti-tumor activity in clinical trials of metastatic melanoma patients. Responses were observed in approximately 15% of patients, with around 5% of patients achieving a durable complete response, and toxicity is a problem (Atkins et al., 1999; Dutcher et al., 1989; Rosenberg et al., 1989). Interferon-alpha 2b (IFN-α2b) has also been approved by FDA, but only for the adjuvant treatment of stage IIb/III melanoma, and not for metastatic disease (Kirkwood et al., 2001). It is a type I IFN with pleiotropic functions in various malignancies, including immuno-modulatory, anti-proliferative, differentiation-inducing, apoptotic, and anti-angiogenic properties (Kirkwood et al., 2008). High dose IFN-α2b demonstrated response rates of approximately 20% (as

single agent in a Phase II trial), with a slightly more durable response than DTIC (Dorval et al., 1986; Sertoli et al., 1989).

Melanoma appears to be unique among human cancers due to its ability to induce anti-tumor lymphocytes during the natural course of tumor growth (Rosenberg and Dudley, 2009). Therefore, novel investigational immunotherapies for melanoma (both current and evolving), such as adoptive T cell transfer (ACT), cancer vaccines, bi-specific antibodies, and anti-cytotoxic T lymphocyte antigen-4 (CTLA-4) antibody, are paving the way for exciting new areas for melanoma treatment (discussed in Section 1.3).

1.2 The role of the immune system in cancer

The concept that the immune system may recognize and eliminate tumors is an established one. The long-standing theory of immunosurveillance, suggested by Thomas (Thomas, 1959) and Burnet, and developed by Burnet (Burnet, 1970), proposes that cells and tissues are constantly monitored by an ever-alert immune system, and that such immune surveillance is responsible for recognizing and eliminating the vast majority of incipient cancer cells and thus nascent tumors (Hanahan and Weinberg, 2011).

Despite tumor immune surveillance, tumors can still develop in the presence of a functional immune system. Consequently, the theory of immune surveillance has gone through multiple phases of acceptance and discredit until a decade ago when an updated concept of tumor immunoediting was recognized as a more complete explanation for the role of the immune system in tumor development. According to this theory, the immune system not only suppresses tumor growth by eliminating cancer cells and preventing their outgrowth, but also interacts in a complex way with the tumor to shape its immune profile, resulting in cancer variants that escape immune control (Bourgault-Villada et al., 2011; Dunn et al., 2004; Schreiber et al., 2011; Smyth et al., 2006; Swann and Smyth, 2007).

1.2.1 Natural killer cells and tumor immunosurveillance

1.2.1.1 Natural killer cell subsets and effector mechanisms

Natural killer (NK) cells, first identified in mice in 1975, are lymphocytes of the innate immune system that play important roles in the protection against viral

infections and the development of cancers (Biron, 1997; Trinchieri, 1989). In humans, NK cells constitute ~5-20% of peripheral blood lymphocytes and are mostly defined as $CD3^{-}CD56^{+}$ lymphocytes, which can be futher subdivided into two major subsets, namely $CD56^{dim}CD16^{+}$ and $CD56^{bright}CD16^{-}$ populations (Waldhauer and Steinle, 2008). The $CD56^{dim}$ population exhibit high cytotoxic potential and broadly express MHC class I-specific inhibitory receptors, and these population is predominant in the blood (~95% of NK cells) and at sites of inflammation. On the other hand, the $CD56^{bright}$ population mainly produces cytokines upon activation. This NK population, considered to be the precursors of terminally differentiated $CD56^{dim}$ NK cells, is less cytotoxic and predominates in the lymph nodes (~75% of NK cells) (Waldhauer and Steinle, 2008). The CD56 molecule is absent in mouse NK cells and recent work has categorized mouse NK subsets according to the expression of CD27. Similar to $CD56^{bright}$ human NK cells, $CD27^{high}$ mouse NK cells produce large amounts of cytokines upon activation and are mostly found in the lymph nodes. However, in contrast to $CD56^{bright}$ human NK cells, the $CD27^{high}$ mouse NK cells are also potent cytolytic effectors (Waldhauer and Steinle, 2008).

Various molecular mechanisms of NK cell cytotoxicity have been described. Firstly, activated NK cells can release cytotoxic granules containing perforin and granzymes, leading to target cells apoptosis. In addition to the perforin/granyzme pathway, interaction between tumor necrosis factor (TNF) receptor superfamily (TNFRSF) members, including Fas/CD95, TRAIL receptors, and TNFR1 on tumor cells with the corresponding ligands (FasL,

TRAIL and TNF) expressed or secreted by NK cells can lead to NK cytotoxicity under certain conditions. Furthermore, NK cells are also a potent source of a variety of cytokines and chemokines, including interferon-γ (IFN-γ), TNF, GM-CSF (granulocyte-macrophage colony stimulating factor), MIP-1α (macrophage inflammatory protein-1α) and RANTES (regulated upon activation, normal T cell expressed and secreted), which can promote the differentiation, activation and/or the recruitment of other immune cells. Moreover, NK cell-derived IFN-γ is crucial in priming T helper 1 (Th1) T cell responses (Waldhauer and Steinle, 2008).

1.2.1.2 NK cells and tumor immunosurveillance

Numerous studies have demonstrated the importance of NK cells in the eradication of tumors cells. Most of these studies were performed using syngeneic tumor cells implanted in mice deficient in NK cells (genetically or by antibody depletion) or with impaired NK cell functions. In these mice, tumors grew more aggressively and metastasize more frequently in the absence of NK cells (Hayakawa and Smyth, 2006; Kim et al., 2000; Smyth et al., 2002). Interestingly, Shreiber and colleagues have demonstrated that spontaneous tumors or tumors induced by methylcholanthrene (MCA) were higher in mice genetically deficient in key effector molecules of NK cells or their receptors, including perforin, IFN-γ, IFN-γR, or STAT1 (signal transducer of type I and type II IFN receptors) (Kaplan et al., 1998; Shankaran et al., 2001), suggesting that NK cells could play a role in controlling spontaneous tumor growth. Similarly, higher rates of spontaneous adenocarcinoma have been reported in mice deficient in both RAG2 (recombinase activating gene) and

STAT1 compared to mice deficient only for RAG2, implicating NK cells in tumor immunosurveillance. In humans, most evidences of NK cells in tumor immunosurveillance came from correlative studies. Low NK cell cytotoxic activity in the peripheral blood was correlated with increased risk of cancer (Imai et al., 2000). Furthermore, intra-tumoral infiltration of NK cells has been shown to represent a positive prognostic marker and improved survival in different human cancers (Chew et al., 2010; Ishigami et al., 2000). A more direct evidence for the role of NK cells in controlling malignancies is the transfer of alloreactive NK cells during allogeneic haematopoietic stem cell transplantion in leukaemic patients. Patients lacking HLA class I ligands for donor inhibitory killer cell Ig-like receptors (KIR) showed increased survival and protection from relapse (Hsu et al., 2005; Ruggeri et al., 2007).

Tumor cell recognition by NK cells is based on their unique ability to recognize and attack cells with diminished levels of the cell surface major histocompatibility class I (MHC-I) molecules, which are present at normal levels in all cells of the body. Abnormal tumor cells or virally-infected cells often down-regulate MHC-I, allowing them to escape detection by cytotoxic T cells. However, this down-regulation of MHC-I (loss of self molecules) makes these cells sensitive to NK cell cytotoxicity, a concept known as “missing self” recognition (Algarra et al., 2000; French and Yokoyama, 2003). However, the “missing self” hypothesis failed to explain why autologous cells which lack MHC-I expression are spared (eg. erythrocytes) and why tumor cells with normal MHC-I expression are killed (Waldhauer and Steinle, 2008). The discovery and characterization of several activating NK receptors, eg. NKG2D

receptor which recognizes stress-induced self ligands on ‘dangerous’ cells, led to the proposal of the “induced-self” recognition model (Bauer et al., 1999; Raulet, 2004). According to this model, NK cell triggering requires the expression of inducible ligands for activating NK receptors (Waldhauer and Steinle, 2008). It has since become clear that the activation of NK cells depends on an intricate balance between inhibitory and activating signals (Lanier, 2005).

1.2.1.3 NK cells inhibitory and activating receptors

NK cells make use of a large repertoire of germline-encoded inhibitory and activating receptors to sense ‘danger’ in the form of ‘altered-self’ cell surfaces (Waldhauer and Steinle, 2008). The main types of NK inhibitory receptors that recognize MHC class I molecules are the inhibitory killer cell Ig-like receptors (KIR) in humans, the Ly49 receptors in mice, and the heterodimeric NKG2A/CD94 receptor in both humans and mice. Inhibitory KIR and Ly49 receptors bind to classical MHC class I molecules, while NKG2A/CD94 detects the non-classical MHC class I molecule (HLA-E in humans and Qa-1^b in mice) (Purdy and Campbell, 2009). Interaction between the inhibitory NK receptors with MHC class I molecules establishes NK cell tolerance towards normal cells. Upon binding MHC class I ligands on target cells, the inhibitory receptors’ cytoplasmic immunoreceptor tyrosine-based inhibitory motifs (ITIM) undergo phosphorylation, leading to the recruitment of protein tyrosine phosphatases to the plasma membrane, which could counteract the activating receptor signals to inhibit cytotoxicity and cytokine production (Purdy and Campbell, 2009).

In contrast, the major NK cell activating receptors are the natural cytotoxicity receptors (NCR: NKp30, NKp44 and NKp46), the C-type lectin-like receptor (CTLR: NKG2D), the low affinity IgG receptor Fc_{γ}RIII CD16, and the activating KIRs. The ligands for NCR have only just begun to be identified; NKG2D recognizes the non-classical MHC class I molecules MICA/MICB (MHC class I chain-related molecules A and B) and ULBP (UL16-binding proteins) in humans and Rae1 proteins, the minor histocompatibility protein H60, and the murine UL-16-binding protein-like transcript 1 (MULT1) in mice; while activating KIR seem to recognize classical MHC class I molecules (Purdy and Campbell, 2009; Waldhauer and Steinle, 2008). On the other hand, CD16 binds to the Fc portion of IgG antibodies to mediate antibody-dependent cellular cytotoxicity (ADCC) (Ahmad and Menezes, 1996), thus allowing NK cells to recognize and kill target cells opsonized with antibodies. Activating receptors lack signaling motifs in their cytoplasmic sequences; instead, they associated with adaptor molecules via charged amino acids in the transmembrane domain (Waldhauer and Steinle, 2008). All these activating NK receptors promote cytotoxicity and cytokine production via the downstream activation of intracellular protein tyrosine kinase cascades.

NKG2D is one of the most well characterized activating NK receptors. It is a type II transmembrane-anchored glycoprotein expressed as a disulfiled-linked homodimer on the surface of almost all NK cells (Ljunggren, 2008). The distinctive feature of NKG2D is the multitude of NKG2D ligands (NKG2DL) with varying receptor affinity. NKG2D ligands are frequently expressed on primary tumor cells, tumor cell lines, and cells infected with pathogens

(Ljunggren, 2008). NKG2DL is inducible by various forms of cellular stress, such as heat shock, viral infection, DNA damage or UV irradiation (Waldhauer and Steinle, 2008) and has been detected in various human cancers including melanoma (Vetter et al., 2002). Interestingly, the expression of NKG2DL has been shown to be regulated by genotoxic stress and the activation of the DNA damage response pathway, which has been reported to occur in precancerous lesions and in many human tumors (Gasser et al., 2005). Several reports have demonstrated the critical role of NKG2D in immunosurveillance not only for early epithelial tumors but also for lymphoid malignancies, however, they do not seem to be important in controlling carcinogen-induced sarcomas (Ljunggren, 2008).

1.2.1.4 Tumor evasion strategies from NK surveillance

While NKG2D-mediated tumor rejection can be effective at early stages of tumor growth, sustained expression of NKG2DL by late stage human tumors can negatively impact anti-tumor responses, leading to tumor immune evasion. In mice, persistent, ectopic expression of NKG2DL resulted in local and systemic downregulation of NKG2D expression, impairing anti-tumor immune responses (Ljunggren, 2008). In addition, chronic exposure of mouse NK cells to cell-bound NKG2DL affects NKG2D signalling and interferes with signalling from other activating receptors (Ljunggren, 2008). In humans, shedding of NKG2D ligands have been observed in patients with epithelial and hematopoetic malignancies (Waldhauer and Steinle, 2008). Shedding of soluble ligands critically affects tumor immunogenicity by reducing activating signals for NK cells. Furthermore, soluble NKG2D ligands has been shown to

downregulate NKG2D expression on tumor infiltrating T and NK cells and counteract recognition of cell-bound NKG2D ligands by NK cells (Ljunggren, 2008; Nausch and Cerwenka, 2008). In addition, several immunosuppressive cytokines secreted by myeloid cells and/or tumor cells, such as TGF-β and L-kynurenine (a tryptophan catabolite generated by indoleamine 2,3-dioxygenase, IDO), have been shown to downregulate the expression of NKG2D receptor and its ligands, thus suppressing NKG2D-mediated immunosurveillance (Nausch and Cerwenka, 2008; Waldhauer and Steinle, 2008).

1.2.2 T cells and tumor immunosurveillance

It is now well established that the adaptive arm of the immune system, in particular T lymphocytes, plays a critical role in controlling malignant progression (Pages et al., 2010). Several lines of evidence support this notion. For example, spontaneous cancer remissions in patients, although rare, have long been recognized in ovarian cancer, melanoma, renal cancer and neuroblastoma patients (Cole, 1974; Prestwich et al., 2008). For primary melanoma, partial regression is commonly reported, but complete spontaneous regression is rare. Histologically, regressing melanoma lesions are associated with a perivascular lymphocyte infiltrate, along with a clonal T cell expansion and an increase in T helper cells, all of which are suggestive of an immune-mediated mechanism (Prestwich et al., 2008).

In mouse tumor models, carcinogen-induced tumors were more frequent and/or grew more rapidly in immunodeficient mice relative to

immunocompetent controls. In particular, there was an increase in tumor incidence in mice deficient in the development or function of $CD8^+$ cytotoxic T lymphocytes (CTL) and/or $CD4^+$ T helper 1 (Th1) cells (Kim et al., 2007; Teng et al., 2008). This data indicates the important contribution of the immune system, in particular T cells, in immune surveillance and tumor eradication.

Further support from clinical epidemiological data demonstrates that T cell infiltration is a predictor of patient survival in several human solid cancers, including colorectal carcinoman (CRC), ovarian cancers, bladder cancer, non small cell lung carcinomas (NSCLC), head and neck cancer, esophageal cancer, breast cancer, melanoma, renal cell carcinoma, prostrate adenocarcinoma, and hepatocellular carcinoma (HCC) (Clemente et al., 1996; Galon et al., 2006; Kawai et al., 2008; Pages et al., 2010; Sato et al., 2005; Schumann et al., 2010). For example, patients with colon and ovarian tumors that are heavily infiltrated with CTL and natural killer (NK) cells have a better prognosis than those that lack such infiltrates (Pages et al., 2010). In melanoma, melanoma-reactive T cells circulating in the blood, in contrast to tumor infiltrating lymphocytes (TIL), do not predict survival (Haanen et al., 2006). This shows that T cell infiltration into tumors is a prerequisite for an effective anti-tumor response. However, the existence of tumor-reactive T cells is not sufficient to confer a favorable prognosis. Intra-tumoral T cell nests, as opposed to peri-tumoral T cells, are prognostic indicators in colorectal cancer (Naito et al., 1998) and ovarian carcinoma (Al-Attar et al., 2009), suggesting that the localization of T cell infiltrates is also an important determinant of the clinical outcome.

Taken together, this increasing body of evidence strongly support the notion that T cells are indeed one of the critical mediators of an effective anti-tumor immune response, and their density, distribution and quality are pivotal determinants of clinical outcome.

1.2.3 Pathways of T cell-mediated killing of tumors

Antigen recognition by T cells involves binding of the T cell receptor (TCR) to cognate major histocompatability complex (MHC)-peptide combinations on tumor cells, leading to tumor cell elimination. Much of our understanding of the mechanisms underlying lymphocyte-mediated cytotoxicity has come from *in vitro* studies. The dominant mechanisms of contact-dependent, lymphocyte-mediated cytotoxicity that have been described are the perforin/granzyme-mediated and the Fas/FasL mediated pathways (Kagi et al., 1996) (Figure 1.2.1).

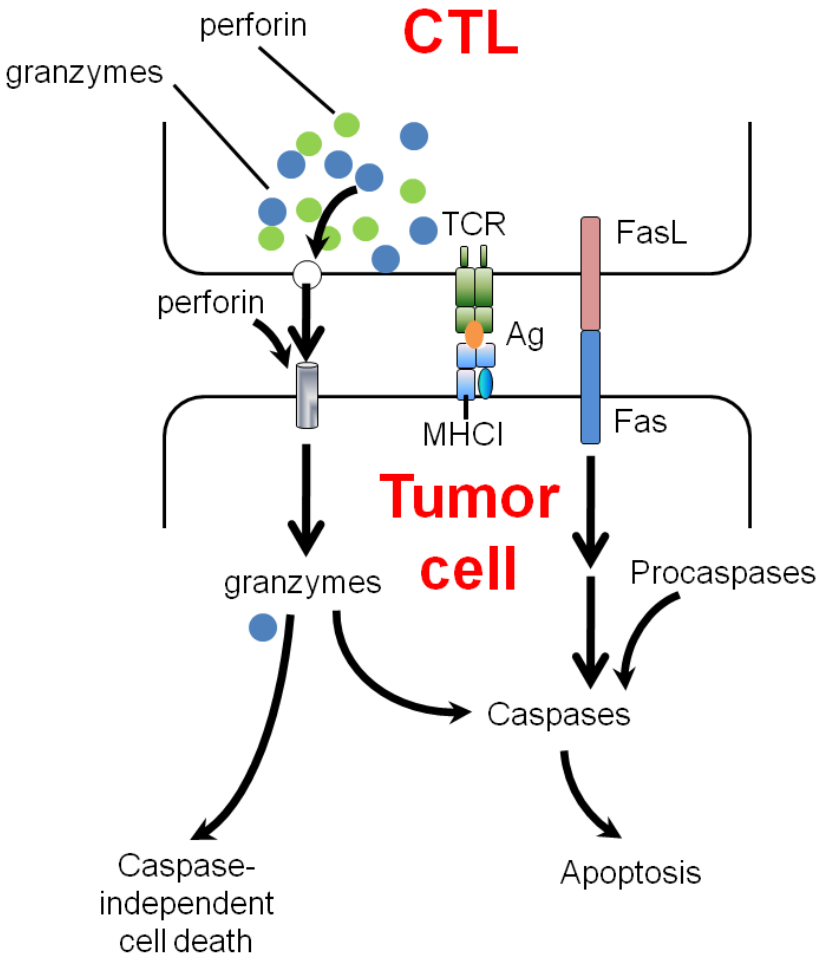

Figure 1.2.1 – Mechanisms of T cell-mediated killing of tumor cells.
Simplified view of the perforin/granzyme pathway (left) and the Fas/FasL pathway (right) in T cell-mediated killing of tumor cells. In the perforin/granzyme pathway, perforin forms a channel on the tumor cell membrane through which granzymes and other constituent granule proteins pass into the cell. The death receptor Fas on tumor cell can interact with its ligand, FasL, expressed on CTL. Both pathways lead to downstream activation of the caspase cascade, resulting in tumor cell apoptosis. Caspase-independent cell death has also been described.

Animal models with deficiencies in various T cell effector molecules have been instrumental in elucidating the roles of T cells during tumor regression (Breart et al., 2008). Several mechanisms of T cell action have been proposed, including: (1) direct killing of tumor cells, (2) recruitment of inflammatory cells by $CD8^+$ T cell-derived interferon-gamma (IFN-γ), (3) IFN-γ-dependent increase in MHC class I expression on tumor cells, leading to lower activation threshold for T cell cytotoxic activity, (4) IFN-γ mediated inhibition of angiogenesis, and (5) inhibition of tumor cell proliferation (Breart et al., 2008; Eyles et al., 2010; Nelson and Ganss, 2006). In human cancers, intra-tumoral T cell infitlration has been correlated with increased tumor cell apoptosis (Dolcetti et al., 1999; Schumann et al., 2010) and decreased tumor cell proliferation (Schumann et al., 2010).

A better understanding of how effector T cells survey cancer cells and eliminate tumors *in vivo* may provide clues as to how the local tumor microenvironment may subvert anti-tumor immune responses, and may offer new perspectives in designing rational immunotherapies for the treatment of cancers.

1.2.4 Mechanisms of T cell trafficking to tumors

Lymphocyte trafficking to lymphoid organs and to peripheral sites of injury, inflammation, infection and tumors is a multi-step process that involves distinct adhesive and activation steps (Johnston and Butcher, 2002). This includes: (1) primary tethering and rolling, (2) activation and secondary firm adhesion, (3) crawling, (4) transendothelial migration (TEM) (paracellular and transcellular), (5) extravasation, and (6) interstitial migration (Fisher et al., 2006; Hiraoka, 2010) (Figure 1.2.2). The basic processes are common, but multiple molecular choices exist at each step (i.e. adhesion molecules and chemokines) to provide a large degree of combinatorial diversity (Hiraoka, 2010), which serves as the basis for different lymphocyte subsets with different functions and activation status being recruited in a site- and time-specific manner (Hiraoka, 2010).

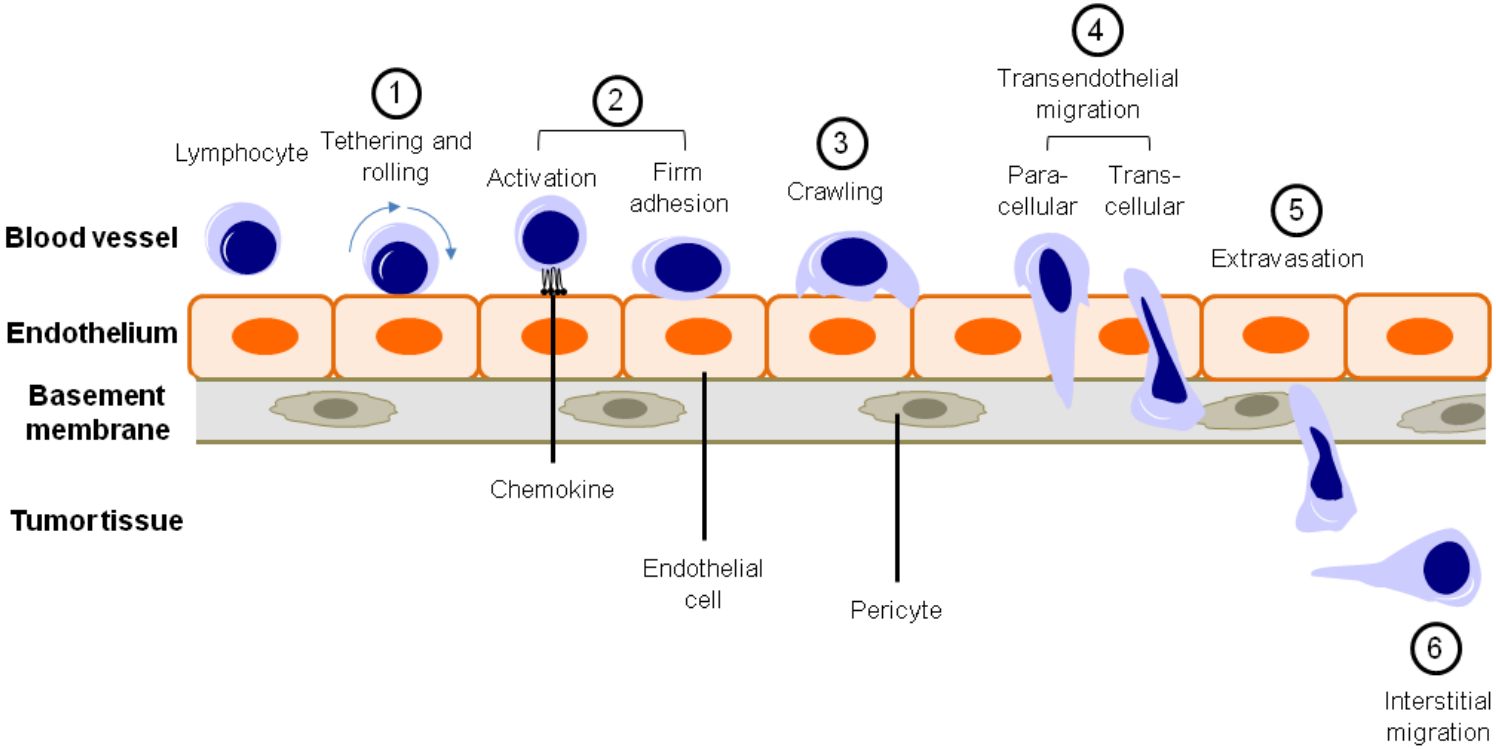

Figure 1.2.2 – The multistep model of lymphocyte trafficking to tumor tissues.
The recruitment of circulating lymphocytes from the blood to the tumor tissues through the tumor endothelial barriers involves six distinct adhesive and activation steps. These sequential events include tethering and rolling, activation and firm adhesion, crawling, transendothelial migration (consists of both paracellular and transcellular routes), extravasation and interstitial migration. Common and unique sets of trafficking molecules (including adhesive molecules and chemokine signals) dictate the nature of adhesion events that occur in each step in the cascade during lymphocyte trafficking to tumor tissues [adapted from (Hiraoka, 2010)].

1.2.4.1 Tethering and rolling

Lymphocyte tethering and rolling along the endothelium is mostly mediated by the selectin family of adhesion molecules. L-selectin is constitutively expressed on most circulating lymphocytes, while P-selectin and E-selectin are inducibly expressed on activated endothelial cells. These selectins bind to ligands modified with specific carbohydrate epitopes, which are expressed on the endothelium of high endothelial venules (HEV) in secondary lymphoid organs (except spleen), and at peripheral sites of injury and inflammation (Hiraoka, 2010). This rolling process (due to hemodynamic shear forces) slows down circulating lymphocytes, thus enabling interactions to occur between G-protein-coupled chemokine receptors (GPCR) expressed on lymphocytes with chemokines or other chemoattractants displayed on the endothelium.

1.2.4.2 Activation and firm adhesion

It has been traditionally thought that leukocytes are directed by soluble chemoattractant gradients to migrate across the endothelium, and through the extracellular matrix into the tissue. However, it has been suggested that soluble chemokine gradients are unlikely to exist at the luminal endothelial surface, as soluble chemokines are exposed to continuous shear flow and are rapidly washed away from the apical surface (Middleton et al., 2002).

There is an increasing body of evidence suggesting that many chemokines can bind to the surface of endothelial cells either by binding to heparin sulfate and other glycosylaminoglycans (GAG) or to the Duffy antigen receptor for

chemokines (DARC) (Johnston and Butcher, 2002). Activated endothelial cells can produce and bind to a number of such chemokines and mediate lymphocyte arrest (Johnston and Butcher, 2002). In addition, endothelial cells have been shown to transport chemokines from the basolateral to the luminal surface, indicating that chemokines secreted in the tissues can impact on the recruitment of intravascular lymphocytes (Middleton et al., 1997).

Chemokines bound to the endothelium can transduce robust signals to lymphocytes mediating firm adhesion to immoblized integrin ligands. This occurs via upregulation of integrin affinity through conformational changes or an increase in integrin avidity through integrin clustering (Johnston and Butcher, 2002). Chemokine-induced activation of chemokine receptors triggers intracellular signalling pathways, resulting in the activation of guanine nucleotide exchange factors (GEF) mediated by local phosphoinositide production and kinase activity. GEF activates Rho and Ras guanosine triphosphatase (GTPases), leading to cytoskeletal rearrangements and conformational changes in integrin molecules which regulate firm adhesion of lymphocytes to endothelial ligands. Avidity changes occur via clustering of low affinity receptors, which requires protease-dependent release of integrins from cytoskeletal restraints in order to facilitate lateral mobility of integrins on the plasma membrane (Johnston and Butcher, 2002). Chemokines can induce rapid clustering of integrins, thus leading to strengthened adhesion to immobilized integrin ligands. The binding of β_2-integrin, $\alpha_L\beta_2$ (or leukocyte-function associated antigen-1, LFA1) to their endothelial ligands, ICAM1 and ICAM2 (intercellular adhesion molecule), and between α_4 integrins, $\alpha_4\beta_1$ (or

VLA4, very late antigen-4) and $\alpha_4\beta_7$ with their ligands, VCAM1 (vascular cell adhesion molecule 1) and MADCAM1 (mucosal vascular addressin cell adhesion molecule 1), are important in this secondary adhesion event (Hiraoka, 2010).

1.2.4.3 Crawling

Lymphocyte crawling on endothelial cells requires the integration of three external signals: inside-out integrin activation signals from chemokine binding to GPCR, outside-in integrin activation signals, and chemokine-GPCR-triggered signals to actomyosin-remodeling Rho GTPases (Rosenberg et al., 2009). Migrating lymphocytes are flattened in shape, which is associated with polarization involving redistribution of intracellular signaling proteins, surface receptors, and adhesion molecules to specific sites of the cell (Hiraoka, 2010). Migrating lymphocytes form leading protrusions (or filopodia) and crawl along the endothelial surface supported by LFA1:ICAM1 interactions. Integrin ligands (such as ICAM1) clustered on the apical surface of endothelial cells trigger the activation of a variety of endothelial regulatory GTPases, including RhoA and RhoG, which may translate LFA1:ICAM1 focal contacts into endothelial invaginations surrounding lymphocyte filopodia, thus facilitating TEM (Rosenberg et al., 2009). Chemokines, cytokines and shear stress play major roles in lymphocyte crawling and triggering of additional promigratory actin remodeling machineries, leading to subsequent TEM under disruptive shear flow (Ascierto et al., 2011; Hiraoka, 2010).

1.2.4.4 Transendothelial migration (TEM)

Two routes of TEM have been reported, namely the paracellular (majority of events) and transcellular (minority of events) routes (Hiraoka, 2010) (Figure 1.2.2). In the paracellular route, leukocytes transmigrate between endothelial cells at cell junctions. This involves formation of a haptotactic gradient that guides lymphocytes to the junctional zones. The endothelial junctional molecules that actively mediate sequential steps in TEM includes CD31 (platelet-endothelial cell adhesion molecule 1, PECAM1), ICAM1, ICAM2, CD99, members of the JAM family (such as JAM-A, JAM-B, and JAM-C), and endothelial cell-selective adhesion molecule (ESAM) (Hiraoka, 2010). In the transcellular route, lymphocytes cross the endothelial barrier by transmigrating directly through individual endothelial cells. This process involves translocation of apical ICAM1 to caveolae and F-actin-rich regions and the transport of caveolin-1 to the basal membrane, resulting in a channel through which the lymphocytes can migrate (Hiraoka, 2010). This pathway has been identified in various *in vitro* models and is reported to operate in the central nervous system and at sites of inflammation (Gerard et al., 2009; Hiraoka, 2010).

1.2.4.5 Extravasation

To extravasate into tumors, lymphocytes breach the vascular basement membrane and pericyte coverage of venular walls to reach the tumor parenchyma. Basement membranes are composed of tightly packed networks of laminins and type IV collagen inter-connected with perlecan and nigogens that are suggested to be more resistant than endothelium (Hiraoka, 2010).

There is no unifying theory on the exact molecular mechanisms whereby lymphocytes penetrate the basement membrane. However, it has been reported that the penetration involves binding of the integrin $\alpha_6\beta_1$, the principal laminin receptor on lymphocytes, to the substrate. In addition, endothelial-associated or lymphocyte-derived proteases have been implicated in cleaving the structural proteins of the basement membrane (Hiraoka, 2010).

1.2.4.6 Interstitial migration

Lymphocytes migrate within the interstitial environment in an amoeboid manner, consisting of the leading edge where short-lived pseudopods form by actin-mediated forward flow, the protruding membrane and surface receptors interact with the tissue substrate, followed by actomyosin-mediated contraction of the mid region of the cell body, and finally the posterior tail, known as the uropod, moves forward (Hiraoka, 2010; Weigelin et al., 2011). In contrast to other migration modes, amoeboid cell locomotion is independent of integrin-mediated adhesion (Hiraoka, 2010; Weigelin et al., 2011). The use of weakly adhesive and nonadhesive interactions and traction mechanisms allows T cells to move rapidly (up to 30µm/min) within tissues (Weigelin et al., 2011).

Besides its function in T cell trafficking, amoeboid migration of T cells contributes to enhanced capability to sense and respond to signals from the extracellular environment, including chemoattractant signals and cognate antigens expressed on tumor cells. The trailing uropod contains adhesion receptors, including ICAM1, integrins and the highly glycosylated surface

receptors CD43 and CD44, which likely regulate attachment to cell surfaces and extracellular matrix (ECM) during migration (Weigelin et al., 2011). Upon recognition of the cognate antigen, $CD8^+$ T cells form long lasting contacts (30min to 6h) with target cells, resulting in tumor cell destruction. Some integrins, such as LFA-1, VLA-4 and $\alpha_E\beta_7$ promote adhesion and function as costimulatory molecules to enhance effector function by supporting interaction between T cells and tumor cells (Hiraoka, 2010). CD44, a receptor for ECM proteins and glycosaminoglycans, has been shown to maintain cell polarity during interstitial T cell migration and is critical for scanning of target cells needed for an efficient anti-tumor immune reaction (Mrass et al., 2008) .

In conclusion, T cell effector functions are critically dependent on efficient trafficking of T cells from the blood into the tumors, which in turn is tightly regulated by a complex array of adhesion molecules and chemokine signals. Therefore, proper functions of the vasculature and the lymphocytes as well as the inflammatory state of the tissues are essential for lymphocyte trafficking through tumor-associated blood vessels to reach the parenchyma.

1.3 T cell-based immunotherapies

By analyzing the T cells that recognize tumors, many tumor-associated antigens (TAA) have now been identified and successfully cloned. In melanoma, examples of known TAA include gp100 (glycoprotein 100), melan-A/MART-1 (melanoma-associated antigen recognized by T cells), tyrosinase, MAGEs, SSX-2 and -4 (synovial sarcoma X), NY-ESO-1 and others (Buonaguro et al., 2011; Jandus et al., 2009). In a single tumor, tumor-infiltrating lymphocytes (TIL) directed towards multiple TAA can be identified (Prestwich et al., 2008). The identification of TAA that can be potentially targeted by anti-tumor T cells generated great interest for the establishment of T cell-based immunotherapies to treat cancer. This includes approaches that target T cells directly (such as adoptive T cell transfer or ACT, cancer vaccines, and bispecific antibodies) or indirectly (via suppression of T cell inhibitory mechanisms, such as CTLA-4 blockade). These T cell-based immunotherapies serve as novel treatments for patients with cancer, and has allowed for the design of new strategies to break immune tolerance in these patients (Lizee et al., 2007).

1.3.1 Adoptive T cell transfer (ACT)

T cell adoptive therapies are an attractive approach in treating cancers and have yielded some promising results in melanoma, however, complete clinical responses are only observed in a minority of patients (Rosenberg and Dudley, 2009). ACT immunotherapy relies on *ex vivo* expansion and activation of tumor-specific lymphocytes followed by transfer of these cells into autologous tumor-bearing hosts (Figure 1.3.1). A significant breakthrough in the

development of effective ACT for the treatment of melanoma patients was the first demonstration in 1987 that tumor-infiltrating lymphocytes in metastatic melanoma could be grown in IL-2 and exhibit major histocompatability complex (MHC) restricted recognition of both fresh and cultured melanoma cells *in vitro* (Rosenberg and Dudley, 2009).

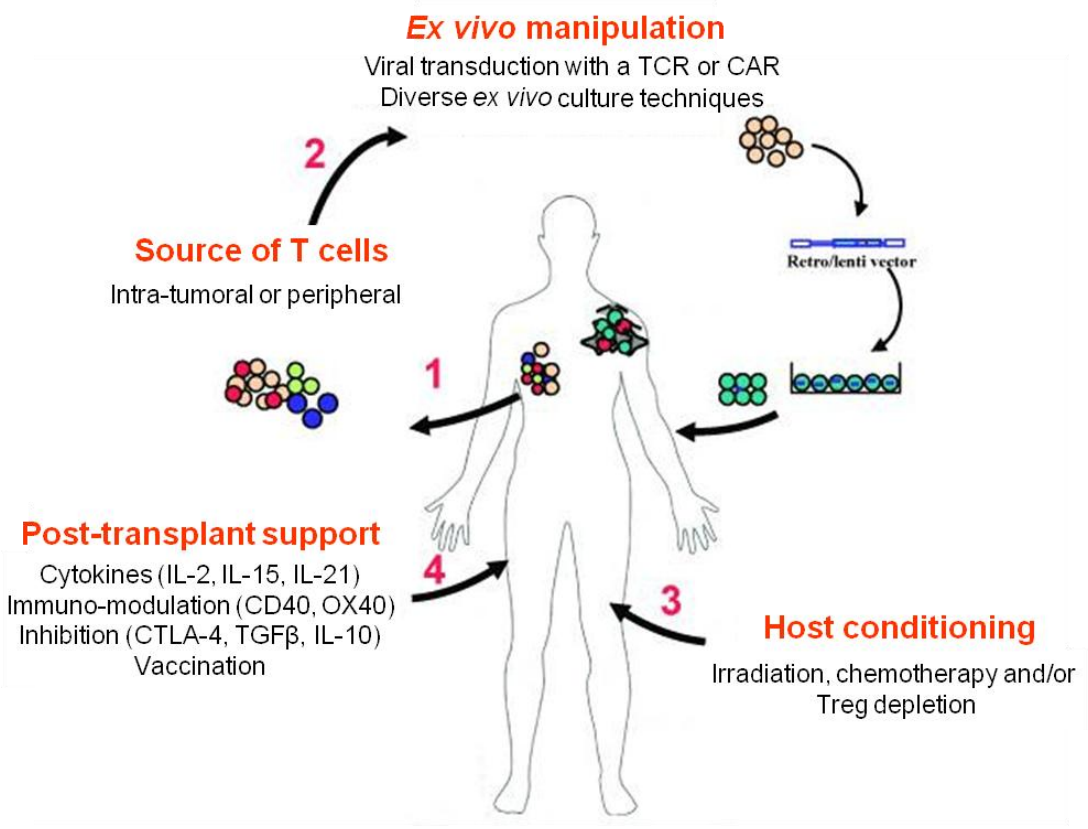

Figure 1.3.1 – Factors important for the success of ACT therapy against tumors. Several factors that can influence the efficacy of ACT include (1) the source of T cells (whether it is best to isolate from the tumor or from the peripheral blood), (2) *ex vivo* culture technique (bulk TIL, selected-TIL or young-TIL protocol) and manipulation [genetic modification to express either tumor-specific MHC-restricted T cell receptors (TCR) or non-MHC-restricted synthetic chimeric antigen receptors (CAR)], (3) host-conditioning (to favour the survival/persistence and the activity of the readministered cells), and (4) post-transplant support (to favour the *in vivo* expansion and activation of TIL). CTLA-4 – cytotoxic T lymphocyte antigen-4; IL-2 – interleukin-2; TGFβ – transforming growth factor beta; Treg – regulatory T cells [adapted from (Mondino et al., 2010).

1.3.1.1 Early ACT protocol

The first ACT-based immunotherapy was described in 1988 for the treatment of metastatic melanoma patients, with increased number of patients reported in 1994. In this study, eighty-six patients were treated with autologous TIL with high dose IL-2 (720,000 IU/kg). The TIL single cell suspension was generated by enzymatic digestion of the bulk tumor and expanded in high concentration of IL-2 until at least 10^{11} TIL were generated (Hershkovitz et al., 2010). TIL and IL-2 were administered in two cycles separated by approximately 2 weeks. Twenty-eight patients received TIL without a preparative regimen and fifty-eight patients receive an additional single low dose cyclophosphamide (25mg/kg) before the first TIL infusion (Hershkovitz et al., 2010). The overall objective response rate was 34% and was comparable to studies with high IL-2 alone (31%), or IL-2 with a combination of cyclophosphamide (35%). Although objective anti-tumor responses were seen in these early trials, many of the responses were short-lived. Of the twenty-nine patients with an objective clinical response, only five patients experienced a complete response and the median survival of all partial responders was only four months. Lack of persistence of transfused cells was the major reason for treatment failure. In fact, less than 0.1% of the transfused cells survived in the circulation after one week of administration (Rosenberg and Dudley, 2009).

Retrospective analyses revealed that objective clinical response was associated with cells with short period of culture, which exhibited high *in vitro* lysis of autologous tumor cells, and were able to traffic to the tumor targets *in vivo*. In addition, higher response rate was associated with patients receiving

TIL generated from subcutaneous tumors (49%) compared to those obtained from lymph nodes (17%), probably due to the presence of many non-tumor-specific T cells within the lymph nodes (Hershkovitz et al., 2010). This initial study paved the way for further modifications which led to dramatic improvement in the effectiveness of TIL therapy (Rosenberg and Dudley, 2009).

1.3.1.2 Selected-TIL protocol

Earlier trials involved the use of bulk TIL cultures that contained heterogeneous populations of lymphocytes, of which only some showed anti-tumor activity. Studies of the T cell receptor rearrangements in TIL revealed the variability of T cells present in these cultures and pointed towards the need for modified culture techniques that select only anti-tumor reactive lymphocytes without the presence of any other bystander cells. Thus, modifications were made to culture TIL from multiple small tumor fragments instead of a single bulk tumor, and *in vitro* IFN-γ release assays were used to identify tumor-specific TIL (Hershkovitz et al., 2010). Despite being more labor intensive (at least 21-35 days before large-scale expansion), the Selected-TIL protocol had the advantage of specifically selecting lymphocytes with anti-tumor activity. The potential disadvantage associated with this technique was the limited heterogeneity and polyclonality of the cells infused (Rosenberg and Dudley, 2009).

The decisive improvement in the efficacy of ACT came in 2002 with the introduction of an immunodepleting preparative regimen given before adoptive

transfer. This followed the success in preclinical models demonstrating improved ACT efficacy by administration of either total body irradiation or lymphodepleting nonmyeloablative chemotherapy (NMC) before cell transfer. Lymphodepletion appears to act predominantly by suppressing Tregs and by eliminating competition for homeostatic cytokines such as IL-7 and IL-15 that are vital for the survival of the infused TIL (Rosenberg and Dudley, 2009).

These results led researchers to explore the use of lymphodepleting strategies in patients before TIL transfer. Three consecutive studies involving 93 metastatic melanoma patients were performed using increasing levels of lymphodepletion before cell transfer. In the first study, 43 patients received a nonmyeloablative, lymphodepleting chemotherapy regimen consisting of cyclophosphamide and fludarabine before infusion of expanded, tumor-reactive, tumor-infiltrating lymphocytes and IL-2 therapy. In the following two consecutive studies, each cohort of 25 patients received an additional 200cGy or 1200cGy whole body irradiation before cell transfer. Preliminary results were promising with objective response rates of 49%, 52% and 72% respectively in these three consecutive protocols. Responses were often durable and clinical tumor regression was observed in all sites of the body with no long-term toxicities. Subsequently studies showed that clinical responses were highly correlated with *in vivo* persistence of the transferred cells, thus, highlighting the significant potential of lymphodepleting regimens to enhance the efficacy of ACT. Unfortunately, in the absence of a randomized clinical trial, it is not possible to determine how much

lymphoablative chemotherapy, high-dose IL-2 administration, and TIL therapy contributed to the promising results in these trials.

Continual efforts to improve the efficacy of ACT led to extensive studies to identify both patient and cell factors associated with objective clinical responses. In addition to the persistence of the transfused cells, studies in both mouse models and human patients predicted that the state of differentiation of the transferred cells was repeatedly reported to have a significant association with clinical response. The two main characteristics of cells able to mediate an effective anti-tumor response are long telomere length and high expression of CD27, both of which are markers of less differentiated cells (Rosenberg and Dudley, 2009). These findings led to the generation of very “young” TIL for subsequent ACT trials.

1.3.1.3 Young-TIL protocol

The Young-TIL protocol utilizes bulk unselected TIL, which spend shorter time in culture. Single cell suspensions are generated from bulk tumor instead of multiple small fragments, and enables rapid large-scale expansion in just 10-18d. This process simplified the laboratory procedures and significantly lowered the cost. Young TIL cultures were successfully established for approximately 90% of patients, making it more widely available for the treatment of more patients compared to the Selected-TIL procotol. Objective clinical response was 50%, including two ongoing complete responses (CR) and eight partial responses (PR). Dramatic improvement to the dropout rate (26% instead of 70% in the Selected-TIL protocol) was observed (Hershkovitz

et al., 2010). Toxicities related to the use of IL-2 and chemotherapy was similar to the Selected-TIL protocol. In short, the Young-TIL protocol provides a valuable tool to integrate ACT trials in more cancer centres worldwide for the treatment of more cancer patients (Hershkovitz et al., 2010).

1.3.1.4 Genetically engineered T cells

Technical issues with the production of tumor-specific lymphocytes present a formidable barrier to conducting ACT trials. Approximately 30-40% of biopsy samples yield satisfactory T cell populations and the procedure is labour-, cost- and time-intensive (Dudley et al., 2003). One of the methods vigorously pursued to improve the effectiveness of ACT therapy is the adoptive transfer of genetically modified peripheral blood lymphocytes instead of TIL. Autologous circulating blood lymphocytes can be genetically modified to express either MHC-restricted T cell receptors (TCR) or non-MHC-restricted synthetic chimeric antigen receptors (CAR) with defined antigen specificity.

The TCR approach is accomplished by the direct transfer of the α and β TCR chains from an antigen-specific T cell clone into peripheral blood T cells via transduction of a retroviral construct, thus generating large numbers of tumor antigen-specific T cells (Morse et al., 2002; Schmitt et al., 2009). An initial trial was conducted in metastatic melanoma patients whereby genetically engineered lymphocytes encoding TCR with low affinity for melanoma-associated antigen MART-1 was transfused to patients pre-conditioned with non-myeloablative chemotherapy (NMC) and IL-2. Although the response rate was low (13%), 2 out of 17 patients achieved full remission for more than a

year (Morgan et al., 2006). This initial trial demonstrated the potential of using genetically engineered T cells for patients with low TIL count. Retroviruses encoding T cell receptors with higher avidity to melanoma antigens and a broad array of cancer antigens such as p53, gp100, carcinoembryonic antigen (CEA), and the cancer-testis antigen NY-ESO-1 are now being evaluated in clinical trials for the treatment of other types of cancer in addition to melanoma (Rosenberg and Dudley, 2009).

Since the TCR for many antigens are not known and are difficult to generate, the chimeric antigen receptor (CAR) method was developed. This method utilizes the variable regions of the heavy and light chains of monoclonal antibodies recognising the tumor fused with T cell signalling chains derived from CD28, 41BB or CD3zeta (Hershkovitz et al., 2010). Clinical studies utilizing CAR to treat various cancers have induced modest responses, and many more clinical trials are underway to provide a more significant assessment of this approach. To date, no clinical trials involving the use of CAR have been reported. Nevertheless, several *in vitro* and preclinical studies have reported the feasibility of using lymphocytes encoding CAR for various melanoma tumor antigens such as ganglioside GD2, GD3 and MAGE-A1 (Hershkovitz et al., 2010). Although still in its infancy, the ability to genetically modify autologous lymphocytes from patients' blood to recognize tumor antigens and mediate cancer regression *in vivo* has opened doors for enhancing and extending the ACT approach to patients with a wide variety of cancer types.

1.3.2 Vaccines

Prophylactic vaccines have been proven to be clinically efficacious against infectious diseases, however, therapeutic cancer vaccines aimed at inducing effective anti-tumor activity are still unsatisfactory. The aim of cancer vaccines is to induce tumor regression by *in vivo* activation of tumor-specific T cells. Numerous strategies have been tested for therapeutic vaccination of cancer patients, including (1) whole cell-based vaccines: autologous and allogeneic whole tumor cells, (2) dendritic cell-based vaccines, and (3) antigen-based vaccines: peptides, proteins, plasmid DNA/mRNA, and viral vectors [reviewed in (Terando et al., 2007)]. Overall, the clinical results have been of limited impact (with some reported success as described below), even though tumor-specific immune responses could be measured in the majority of cases (Palucka et al., 2011; Rosenberg et al., 2004; Speiser and Romero, 2010).

1.3.2.1 Whole cell-based vaccines

Whole cell-based vaccines consist of either autologous or allogeneic whole tumor cell vaccines. Autologous whole tumor cells vaccines are derived from tumor cells obtained from operative specimens or tissue cultures generated from autologous tissues. These cells are rendered replication deficient through irradiation, and readministered back to the patients usually with an immune adjuvant, and/or after conjugation to a hapten (Terando et al., 2007). The main advantage of this vaccination strategy is that all of the antigens within a patient's tumor, whether know or unknown, will be readminstered back to the patient to initiate an optimal immune response. However, adequate amounts and the accessibility of tumor tissues is a major issue. In

addition, vaccine preparation has been extremely challenging, laborious and time-consuming. The most extensively studied autologous vaccine for melanoma, M-Vax (AVAX technologies, MO, USA), was developed by Berd and colleagues (Berd, 2002). This vaccine consists of autologous melanoma cells that have been irradiated and then modified with the hapten, dinitrophenyl (DNP). Patients with resected stage III melanoma treated with this vaccine, together with BCG (Bacille Calmette Guérin) and pre-treatment cyclophosphamide, demonstrated improved disease-free and overall survival compared to controls (Terando et al., 2007). To-date, a phase III, randomized, placebo-controlled, double-blind, multi-centered trial of M-Vax in patients with stage IV melanoma has been initiated.

Allogeneic whole tumor cell vaccines are generated from patients other than the intended recipient, and they consist of multiple tumor cell lines to maximize the antigen expression profiles (Terando et al., 2007). Two examples include Melacine (Corixa Corporation, Seattle, WA, USA) and Canvaxin (CancerVax Corporation, Carlsbad, CA, USA). Melacine is derived from two melanoma cell lines, and is rendered replication deficient through mechanical dissociation. A randomized trial to test the impact of Melacine in an adjuvant setting failed to demonstrate improved disease-free survival in vaccine-treated compared to non-treated melanoma patients (Sondak et al., 2002). Canvaxin is derived from three melanoma cell lines and is rendered replication defective through irradiation. Although this vaccine demonstrated survival benefit in two phase II studies in patients with resected stage III and stage IV melanoma, two recent phase III studies of Canvaxin + BCG versus

placebo + BCG in stage III and stage IV melanoma patients failed to show any clinical benefit (Atkins et al., 2006).

1.3.2.2 Dendritic cell-based vaccines

Dendritic cell (DC) is the most potent antigen-presenting cell, and the only cell type able to initiate de novo antigen-specific T cell responses. Therefore, attempts have been made to generate DCs loaded with peptides, proteins, whole tumor cell lysates or mRNA (messenger RNA) for clinical trial purposes [reviewed in (Jandus et al., 2009)]. Although DC vaccination has been shown to induce potent anti-tumor immune responses in patients, clinical benefit remains scarce. A randomized phase III trial investigating the use of autologous peptide-pulsed vaccine versus dacarbazine in stage III/IV melanoma did not demonstrate superiority of the DC-based immunotherapy compared to chemotherapy. Several parameters have been considered to better improve DC-based vaccinations, including the type and maturation stage of DC to be administered, the optimal density of epitopes on DC cell surface, optimal protocol to generate DC *in vitro*, and alternative protocol to target antigens directly to DCs *in vivo* (Jandus et al., 2009). DC-based vaccines for the treatment of other types of cancers have yielded encouraging clinical outcomes. Sipuleucel-T (Provenge), a cellular vaccine based on enriched blood APCs briefly cultured with a fusion protein of prostatic acid phosphatase with GM-CSF, demonstrated a 4-mo prolonged median survival in patients in a Phase III clinical trial and was the first therapeutic cancer vaccine approved by the Food and Drug Administration for the treatment of metastatic prostate cancer (Kantoff et al., 2010).

1.3.2.3 Antigen-based vaccines

Antigen-based vaccines that have been tested in clinical trials include peptides, proteins, plasmid DNA/mRNA, and viral vectors. Most cancer vaccine trials employ peptide vaccines derived from either cancer-testis antigens or differentiation TAAs (Buonaguro et al., 2011). For melanoma, peptide vaccines targeting melanocyte differentiation antigens (MART-1, gp100, tyrosinase) and cancer testis antigens (MAGE and NY-ESO) have been investigated alone, or in multi-peptide combinations, together with class II-restricted peptides, with or without cytokines (IL-2, IL-12, GM-CSF, IFN-α), and with a variety of adjuvants (incomplete Freund's adjuvant or IFA, Alum, ASO2B) (Terando et al., 2007). Peptide-based immunotherapies have been shown in some cases to elicit detectable anti-tumor T cells in the circulation, but clinical responses are rare (Jandus et al., 2009). The first prospective, randomized, multicenter, phase III clinical trial to demonstrate clinical benefit involved the treatment of 185 melanoma patients with $gp100_{209\text{-}217}$ analogue peptide with high dose IL-2. Improved response rate and progression-free survival were observed in patients treated with peptide plus IL-2, compared to IL-2 alone (Schwartzentruber et al., 2009).

One of the limitations in using peptides as immunogens is that each peptide-based vaccine is limited to a subset of melanoma patients with defined HLA (human leukocyte antigen) haplotypes. In addition, most immunization protocols include MHC class I-restricted epitopes, which precludes targeting of tumor-specific CD4 helper T cells (Jandus et al., 2009). In this context, vaccination using recombinant proteins has the potential to target both $CD4^+$

and $CD8^+$ T cells specific for a variety of epitopes of a TAA independently of the HLA haplotype (Jandus et al., 2009). Interestingly, vaccination of metastatic melanoma patients with a recombinant MAGE-A3 fusion protein, together with an adjuvant combination of monophosphoryl lipid A, QS-21, and CpG-ODNs (CpG oligodeoxynucleotides), improved clinical and immune responses compared to patients receiving the peptide plus vaccine formulation without CpG-ODNs (Kruit et al., 2008). A large phase III trial using MAGE-A3 vaccine with the same adjuvant is ongoing in resected NSCLC patients (Brichard and Lejeune, 2008). Several drawbacks of recombinant protein vaccines have been described, including the poor ability to cross-prime MHC class I-restricted $CD8^+$ T cells and high cost of production. A compromise between short peptides and full length recombinant proteins is the use of synthetic long peptides (20-30 amino acids long), and this has resulted in significant improvement in the immunogenicity of peptide vaccines (Jandus et al., 2009).

Recombinant viral vectors (either recombinant adenovirus or fowlpox virus) encoding TAAs have demonstrated variable success in several phase I trials in melanoma patients. Recombinant viral vectors are commonly used to enhance gene transduction efficiencies. However, the presence of pre-treatment anti-viral antibodies, or the induction of such antibodies following vaccination, can neutralize the effects of subsequent treatments (Terando et al., 2007). In addition, the immunodominance of viral antigens may dampen the generation of tumor antigen-specific responses (Jandus et al., 2009).

The shortcomings of recombinant viral vectors may be overcome with the use of naked DNA. Vaccination with DNA encoding melanoma antigens has shown some success in phase I trials (Terando et al., 2007). Administration of plasmid DNA has been performed by intramuscular or intradermal injections, or by intranodal infusion (Jandus et al., 2009; Terando et al., 2007). The main advantage of this technique is the continuous production of tumor antigens following gene transduction, in contrast to the short half-life of peptide vaccines. Heterologous prime-boost regimens, whereby the vector used for priming vaccinations (eg. plasmid DNA) is different from that used for booster vaccinations (eg. retroviral vector), may contribute to optimized cancer vaccine development. In addition to DNA, intradermal injection of total tumor mRNA has been shown to be feasible and immunogenic in a phase I trial (Jandus et al., 2009).

In summary, although significant technical and scientific progress has been achieved in the field of cancer vaccines, the clinical benefit from such treatments are still lacking. As such, much remains to be accomplished in terms of efficacy and applicability. The identification of target antigen and route of delivery as well as immune-modulatory strategies to counter immunosuppression mechanisms within the tumor microenvironment are key strategies to improve the success of cancer vaccines.

1.3.3 Bi-specific antibodies

An alternative approach to engage T cells for cancer therapy are antibodies, which are bispecific for a surface antigen on cancer cells and for T cell co-receptor molecule CD3 on T cells. The concept of using bispecific antibodies to engage cytotoxic T cells to kill cancer cells was first demonstrated by Staerz and colleagues (Staerz et al., 1985). Further progress in the development of bispecific antibodies lead to a new subclass of bispecific antibodies called BiTE (for “bispecific T cell engager”).

Generally, BiTEs are polypeptides of approximately 55 kDa composed of two single chain fragment variables (scFv) in tandem (Bird and Walker, 1991) (Figure 1.3.2). These antibodies are capable of binding any T cell to a cancer cell, independently of T cell receptor specificity, costimulation, or peptide antigen presentation (Baeuerle and Reinhardt, 2009). BiTEs have been shown to kill cancer cells by inducing immunological synapse between T cells and tumor cells (Offner et al., 2006), leading to BiTE-mediated T cell activation, and tumor cell killing via perforin-mediated membrane perforation and influx of granzyme proteases (Haas et al., 2009). Pioneering work by Kufer and colleagues demonstrated that these bispecific antibodies have high potency, and could engage both $CD4^+$ and $CD8^+$ T cells for redirected lysis of cancer cells at low effector to target (E:T) ratios (Mack et al., 1995).

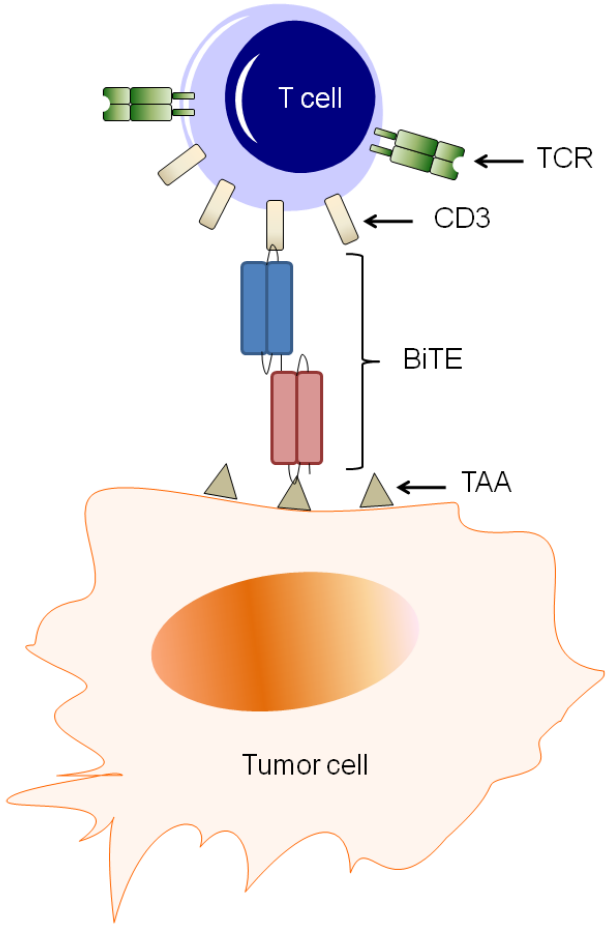

Figure 1.3.2 – Redirected lysis of a tumor cell by a T cell using a bispecific T cell-engager (BiTE) antibody.
A BiTE antibody is generated from the variable domains of two distinct monoclonal antibodies. BiTEs simultaneously bind the CD3 subunit common to all TCRs and a surface antigen on tumors cells, triggering a tumor-specific, cytotoxic event. TCR – T cell receptor. TAA – tumor associated antigen.

There are currently two BiTE antibodies being tested in clinical trials. Blinatumomab (MT103) is bispecific for CD3 and CD19. This bispecific antibody is now being tested in a phase I trial in patients with late-stage, relapsed non-Hodgkin's lymphoma (NHL) (Bargou et al., 2008) and in a phase II trial in patients with B-precursor acute lymphoblastic leukemia (B-ALL) having minimal residual (MRD) disease in their bone marrow (Topp et al., 2011). The phase I study in NHL patients confirmed the remarkable potency

of blinatumomab for engaging T cells within cancer patients for redirected tumor cell lysis. All seven patients in the study who received continuous infusion with BiTE at 0.06mg/m^2 per day reported objective tumor regression, including five partial responses and two complete responses with elimination of tumor cells from the blood, bone marrow and liver (Choi et al., 2011). Adverse events such as central nervous system (CNS) side effects were fully reversible and there was no dose-limiting cytokine release syndrome or autoimmune phenomena (Choi et al., 2011). However, this BiTE led to nearly complete depletion of CD19-expressing normal B cells. A recently completed phase II trial in B-ALL patients with MRD after therapy showed that 16 out of 21 patients treated with Blinatumomab became MRD negative with probability for relapse-free survival of 78% at a median follow-up of 405 days (Topp et al., 2011). An ongoing phase II trial with a second cohort of patients demonstrated complete remission or complete remission with only partial hematologic recovery in 9 of 12 patients with relapsed/refractory B-ALL in a small study (Topp, 2011).

The second BiTE antibody being tested in clinical trial is MT110, which is bispecific for CD3 and epithelial cell adhesion molecule (EpCAM) (Brischwein et al., 2006). It is currently being tested in phase I trial on patients with lung, gastrointestinal, and colorectal cancers. Early results from this phase I study showed disease stabilization in 7 of 19 evaluable patients following infusion with clinically-tolerable doses of MT110, and clinical evaluation of higher doses is ongoing (Fiedler et al., 2010). BiTE antibodies have now been constructed to more than 10 different target antigens, including CD19, EpCAM,

Her2/neu, EGFR (epidermal growth factor receptor), CEA, CD33, EphA2 (ephrin type-A receptor 2), and MCSP (melanoma chondroitin sulfate proteoglycan) (Baeuerle and Reinhardt, 2009; Choi et al., 2011).

The advantages of BiTE technology compared to other T cell based therapies for cancer are that they are fully antibody-derived and thus, obviate the need for *ex vivo* enrichment and modification as well as *in vivo* maintenance. Furthermore, BiTE antibodies are able to maintain tumor lysis despite certain classical tumor escape mechanisms as they engage T cells without requirements for MHC presentation or TCR specificity (Choi et al., 2011). The challenges associated with BiTE technology are perhaps similar to other forms of cancer therapy including the identification of appropriate tumor-specific targets, and the ability of BiTE-engaged T cells to overcome downstream barriers to T cell-mediated tumor rejection such as mechanical barriers, disorganized vasculature, and highly immunosuppressive microenvironments (Baeuerle and Reinhardt, 2009).

In conclusion, BiTE antibodies may hold promise as a future cancer immunotherapy strategy. However, further investigations are needed to study the impact of other immune cell types such as Tregs on BiTE-activated T cells, the possible mechanisms to evade BiTE-engaged T cells, and the broader utility of BiTE antibodies to treat human malignancies (Baeuerle and Reinhardt, 2009). Strategies to improve the serum half-life of BiTE antibodies and to reduce the cost of production may ultimately advance this therapeutic platform for treating human cancers (Choi et al., 2011).

1.3.4 Anti-CTLA antibody

CTLA-4 is a type I transmembrane glycoprotein that exhibits close homology to the costimulatory molecule CD28. T cell inhibition by CTLA-4 is mediated by two mechanisms: competitive antagonism of CD28 signals and direct negative signaling [reviewed in (Teft et al., 2006)]. During early T cell responses, engagement of CD28 molecules by B7 expressed on antigen presenting cells initiates a costimulatory signaling cascade required for optimal T cell activation via the TCR. CTLA-4 is upregulated on activated T cells, and competes with CD28 for binding to B7 molecules due to its higher affinity and avidity for the B7 molecules (Lizee et al., 2007). This competitive ligand binding will likely sequester B7 molecules, thus reducing the amount of CD28-dependent costimulation available and turning off the activated T cells. The second mechanism in which CTLA-4 leads to T cell inactivation is through direct delivery of an inhibitory signal through its cytoplasmic tail. The precise signals delivered by CTLA-4 and the level of action remain uncertain, but ultimately it leads to downregulation of cytokine production by inhibiting the accumulation of AP-1, NF-κB, and NFAT (nuclear factor of activated T cells) in the nucleus of activated T cells. CTLA-4 also inhibits early events of T cell proliferation by inhibiting cyclin D3, cyclin-dependent kinases 4 and 6, and the cell-cycle inhibitor $p27^{kip1}$ [reviewed in (Teft et al., 2006)].

CTLA-4 has been found to be progressively upregulated on chronically stimulated and exhausted T cells (Wherry et al., 2007). Using affymetrix gene expression profiling of metastatic melanoma, Gajewski and colleagues have observed minimal/absence of expression of the co-stimulatory molecules B7-1

and B7-2, suggesting that the melanoma tumor microenvironment may promote induction of classic T cell anergy (Gajewski, 2007; Gajewski et al., 2010; Gajewski et al., 2006). $CD4^+$ T cells have been shown to undergo anergy, leading to the failure to reject tumor in a mouse model *in vivo* (Sotomayor et al., 1999). Several preclinical studies confirmed that by blocking CTLA-4, anti-tumor T cell activity was enhanced and tumor recurrence was prevented [reviewed in (Kirkwood et al., 2008)]. This led to the development of CTLA-4-specific human monoclonal antibody (Ipilimumab or MDX-010, Medarex/Bristol-Myers Squibb) as a potential cancer immunotherapy.

Ipilimumab is a recombinant human immunoglobulin G1κ monoclonal antibody that binds to CTLA-4 and blocks the interaction of CTLA-4 with CD80 or CD86 (Figure 1.3.3). In patients, treatment with Ipilimumab showed moderate single-agent efficacy in mediating cancer regression in melanoma and renal cell carcinoma (Klebanoff et al., 2011). Interestingly, Ipilimumab (administered at 3mg/kg via intravenous infusion every 3 weeks for four doses) was shown to extend the overall survival in a recent phase III clinical trial that involved 676 melanoma patients with unresectable or metastatic melanoma who have failed one or more standard therapies (Hodi et al., 2010). The median overall survival was 10 months in the ipilimumab plus the peptide vaccine gp100 group, 10.1 months in the ipilimumab group, and 6.4 months in the gp100 group. Objective response rates in the ipilimumab plus gp100 arm, ipilimumab arm, and gp100 arm was 5.7%, 10.9%, and 1.5%, respectively. The median duration of response was 11.5 months in the ipilimumab plus

gp100 arm, and this was not reached in the ipilimumab alone or gp100 alone arms (Balwit et al., 2011; Hodi et al., 2010). Common side effects include fatigue, diarrhea, skin rash, endocrine deficiencies (gland or hormone), and inflammation of the intestines (colitis), while severe to fatal autoimmune reactions were observed in 12.9% of patients. Consequently, Ipilimumab was approved by the FDA for the treatment of unresectable or metastatic melanoma, with a risk evaluation and mitigation strategy to ensure that treatment benefits outweigh risks (Balwit et al., 2011; Culver et al., 2011). Following the promising results of the anti–CTLA-4 anticancer therapy, monoclonal antibodies targeting other negative regulatory molecules such as PD-1 have been developed and Phase II/III trials are currently under evaluation (El-Aneed, 2004; Vijayanathan et al., 2002).

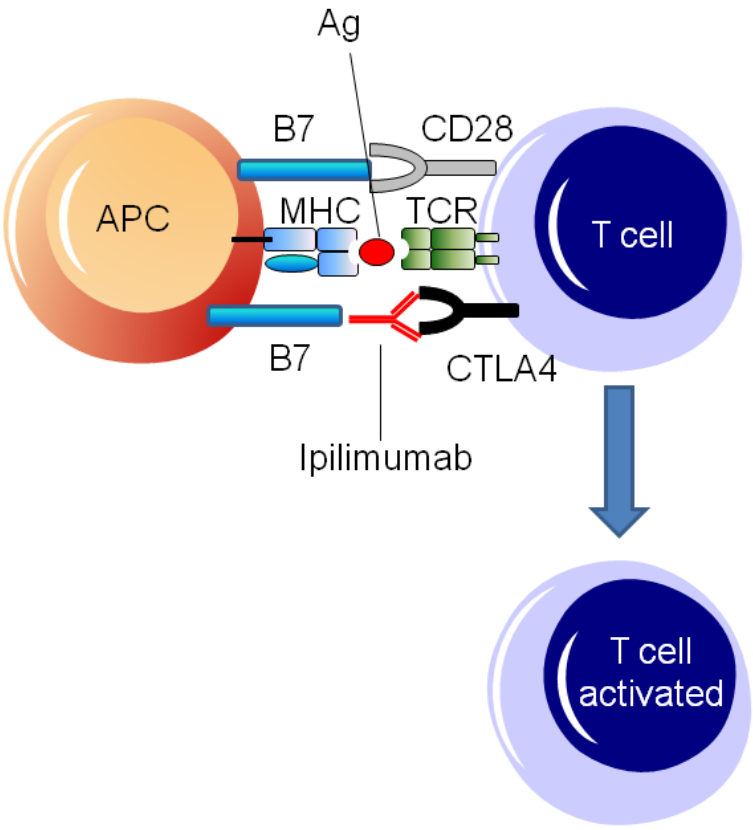

Figure 1.3.3 – Mechanism of action of anti-CTLA-4 antibody, Ipilimumab.
Ipilimumab binds to CTLA-4 and inhibits the interaction between B7 and CTLA-4. Thus, the inhibitory signal produced by B7 binding to CTLA-4 is blocked, and T cell activation is maintained. MHC – major histocompatibility complex; Ag – antigen; TCR – T cell receptor; CTLA-4 – cytotoxic T lymphocyte antigen 4; APC – antigen presenting cell.

1.4 Limitations of T cell-based immunotherapy

The continual growth of tumors in the presence of functional anti-tumor immune responses, whether spontaneous or induced by immunotherapy, is indeed the most disturbing paradox of tumor immunology (Zitvogel et al., 2006). The so far limited success of T cell based immunotherapies is largely due to our incomplete understanding of the mechanisms preventing the action of T cells locally. In order to generate an effective anti-tumor immune response, primed, activated T cells have to migrate into the tumor site and persist in the tumor tissues to execute their anti-tumor functions. This can explain largely why most T cell based immunotherapies fail: while large amounts of activated tumor-specific T cells can be detected in the circulation, many patients fail to benefit from these treatments. This argues for the importance of downstream barriers from the initial T cell priming step that needs to be addressed in order to translate immune responses into clinical tumor regressions. The obstacles faced by activated T cells include defective T cell migration to tumor site, tumor-induced T cell suppression mechanisms, and active immune evasion strategies employed by the tumor cells.

1.4.1 Defective T cell migration to tumor sites

The efficacy of immunotherapy strategies relies on the capacity of functional anti-tumor T cells to traffic effectively to sites of tumor development. Therefore, T cell recruitment to the tumor is one of the potential rate-limiting steps in immunotherapy. In melanoma patients, approximately one-third have tumor metastases with significant TIL infiltration. However, the majority of metastatic lesions lack TIL, demonstrating that proper T cell trafficking into tumors might

not occur in these patients (Gajewski et al., 2006). Furthermore, infusion of radiolabeled TIL in cancer patients did not lead to tumor localization (Chin et al., 1993), suggesting that there might be impaired trafficking of TIL to tumors, or there may be specific exclusion of T cells from the tumors.

The migration of T cells is dependent on the expression of a combination of selectins, chemokine receptors and integrins that regulate the trafficking and extravasation of T cells in different tumor microenvironments [reviewed in (Mondino et al., 2010)]. Thus, failure of T cell migration to tumor sites may be attributed to several factors, including low levels of T cell chemoattractants at the tumor site, active repulsion, lack of expression of chemokine receptors on T cells, and/or improper vascularisation. These factors are discussed in the following sections together with the therapeutic strategies aimed at interfering each of these factors to improve effector T cell trafficking into tumors.

1.4.1.1 Low levels of T cell chemoattractants

Little is known of the molecular cues critical for the recruitment of effector T cells into the tumor microenvironment. Intra-tumoral chemokines are likely to have a major impact on tumor-infiltrating T cells (Balkwill, 2003; Mantovani et al., 2004). Most information regarding the role of chemokines in effector T cell recruitment was derived from transduction of chemokine genes into transplantable tumor cell lines. To date, several chemokines have been suggested as potential recruiting factors for T cells into tumors, including XCL1 (lymphotactin) (Huang et al., 2005; Huang et al., 2002), CCL2 (Mcp-1) (Brown et al., 2007; Zhang et al., 2006), CCL3 (Mip-1α) (Crittenden et al.,

2003; Maric and Liu, 1999), CCL4 (Mip-1β) (Schall et al., 1993; Taub et al., 1993), CCL5 (Rantes) (Mule et al., 1996), CCL8 (Mcp-2) (Proost et al., 1996), CCL16 (LEC) (Giovarelli et al., 2000), CCL20 (LARC) (Crittenden et al., 2003), CCL21 (SLC) (Kirk et al., 2001; Sharma et al., 2000; Yang et al., 2004), CXCL12 (SDF-1α) (Bleul et al., 1996; Williams et al., 2010), CX3CL1 (fractalkine) (Tang et al., 2007; Xin et al., 2005), and the non-ELR-CXC chemokines, CXCL9 (Mig), CXCL10 (IP-10), and CXCL11 (I-TAC) (Ben-Baruch, 2006). In contrast to the known T cell attracting properties of these chemokines, several reports have also demonstrated T cell chemorepulsive activity mediated by high concentrations of CXCL12 (Poznansky et al., 2000; Vianello et al., 2006), even though at low concentrations CXCL12 has been shown to attract T cells.

In addition to preclinical data, clinical pathological data have shown correlation between chemokine expression and the levels of T cell infiltration in human tumors. For example, the expression of CXCL9 and CXCL10 was associated with heavy T cell infiltration in primary melanoma lesions (Kunz et al., 1999). Furthermore, gene expression profiling studies in metastatic melanoma demonstrated that intra-tumoral expression of chemokines indeed correlate with T cell infiltration (Harlin et al., 2009). However, since T cells are also an important source of chemokines, the significance of such a correlation is unclear. Therefore, the expression of chemokines within a tumor has to be analyzed in relation to T cell infiltration, tumor responses and patient survival.

Given the critical roles of chemokines in T cell recruitment, it is likely that the failure of activated T cells to cause tumor regression is due to the lack of inflammation within the tumor microenvironment, which fails to express the appropriate proinflammatory chemokines necessary for T cell attraction. Consequently, researchers have used intratumoral delivery of chemokines or other immunostimulatory cytokines to recruit selected leukocyte populations to tumors as initiators or effectors of antitumor immune responses in preclinical models [reviewed in (Ruffini et al., 2007)] and in human cancers (Sangro et al., 2004).

1.4.1.2 Lack of expression of chemokine receptors

The migration of effector T cells into a proinflammatory tumor microenvironment is dependent on the expression of corresponding chemokine receptors that recognize tumor-derived chemokines. IFN-γ-producing T-helper type 1 (Th1) cells express the chemokine receptors CCR2, CCR5 and CXCR3, while T-helper type 2 (Th2) cells express CCR3, CCR4, CCR8 and CXCR4, suggesting that a partially distinct set of chemokines are involved in recruiting T cells with different polarization/differentiation state. Activated $CD8^+$ cytotoxic T lymphocytes (CTL) are believed to respond to a similar set of chemokines as do Th1 cells (Gajewski et al., 2006). However, it has been shown that tumor-reactive T cells often lack the appropriate chemokine receptors to migrate in respond to the chemokines produced by the tumors (Berry et al., 2009). Hence, T cells engineered to express defined chemokine receptors have been shown to improve migration of T cells to tumor sites. For example, T cells genetically modified to express the

chemokine receptor CXCR2 migrated towards the ligand CXCL1 *in vitro* (Kershaw et al., 2002); while forced expression of CCR4 on T lymphocytes improved homing to Hodgkin's lymphoma expressing the corresponding chemokines CCL17 and CCL22 *in vivo* (Di Stasi et al., 2009). These reports demonstrate the potential application of using T cells engineered to express defined chemokine receptors to redirect tumor-reactive T cells to tumor sites.

1.4.1.3 Improper vascularization

Tumor tissues can be segregated into distinct microanatomical regions based on differences in vascular parameters. The blood vessels in peritumoral regions, in contrast to intratumoral regions often have a high endothelial venule (HEV)-like morphology and express high levels of primary and secondary adhesion molecules. Thus, the peritumoral areas are frequently associated with dense lymphocyte infiltrates (Fisher et al., 2006). Intratumoral vessels express low levels of adhesion molecules or chemokines, which prevents efficient interaction with circulating lymphocytes and thus, limits lymphocyte trafficking through tumor-associated blood vessels. Several *in vitro* and *in vivo* studies have suggested that angiogenic factors or anti-inflammatory cytokines produced within the tumor microenvironment can negatively impact lymphocyte trafficking by preventing the expression of endothelial adhesion molecules (Hiraoka, 2010).

In addition, tumor-associated blood vessels in various human cancers are often morphologically aberrant, characterized by dilated and fragile vessels, increased permeability, intensive vessel sprouting, delayed maturation and

loss of hierarchical architecture (Hamzah et al., 2008; Hiraoka, 2010). Constant vessel remodeling leads to spontaneous haemorrhages and increased interstitial fluid pressure in the tumour environment and represents a major barrier to successful T cell migration into the tumor parenchyma (Hamzah et al., 2008). Therefore, strategies aimed at “normalizing” tumor blood vessels to promote T cell infiltration and improve anti-tumor responses have been adopted. G-protein signalling 5 (Rgs5), for example, has been identified as a master gene responsible for the abnormal tumour vascular morphology in mice and loss of Rgs5 improved spontaneous T cell infiltration into tumors (Hamzah et al., 2008). In a recent study, Shrimali et al demonstrated that normalization of tumor vasculature through disruption of the VEGF (vascular endothelial growth factor)/VEGFR-2 axis can increase extravasation of adoptively transferred T cells into the tumor and improve ACT-based immunotherapy (Shrimali et al., 2010).

1.4.2 T cell suppressive mechanisms after successful T cell recruitment into tumors

Even when effector T cells have successfully migrated into the tumor tissues, they have to persist within the tumor microenvironment and maintain their cytotoxic functions for effective tumor cell killing. However, T cells that infiltrated the tumors are often faced with many immunosuppressive cues within the tumor microenvironment that prevent the action of T cells locally. The immunosuppressive mechanisms that have been described include T cell inhibitory ligands, negative regulation by other suppressor cells, activation-induced T cell death, and metabolic inhibition.

1.4.2.1 T cell inhibitory ligands

T cells that have migrated into the tumors may be progressively impaired or 'exhausted' with respect to their functional and proliferative capacities. A diverse array of negative regulatory molecules expressed on T cell surface correlated with this 'exhausted' phenotype, including CTLA-4, programmed cell death-1 (PD1/CD279), lymphocyte-activation gene 3 (LAG3/CD223), and T cell Ig- and mucin-domain-containing molecule-3 (TIM-3), among others (Klebanoff et al., 2011). Apart from being markers of T cell exhaustion, signaling through these molecules has been demonstrated to actively suppress cytokine secretion and T cell proliferation (Klebanoff et al., 2011). Strategies to overcome such inhibitory mechanisms have been discussed previously (Section 1.3.4).

1.4.2.2 Negative regulation by other suppressor cells

Regulatory immune cells including Tregs, Tr1 cells, Th3 cells and myeloid derived suppressor cells (MDSC) have all been described to contribute to immune suppression within the tumor microenvironment. The immunosuppressive cytokines IL-10 and TGF-β secreted by regulatory T cells inhibit the activation of professional antigen-presenting cells and directly suppress the function of effector T cells and B cells. Moreover, regulatory T cells constitutively express cell surface CTLA-4, which binds to B7 molecules on APC, indirectly suppressing T cell activation (Du and Wang, 2011). Several studies in cancer patients have demonstrated that the prevalence of Treg cells is significantly higher in cancerous lesions compared to those in healthy

controls, and the percentage of Treg cells among tumor-infiltrating immune cells correlates with lower survival rate (Du and Wang, 2011).

Myeloid-derived suppressor cells (MDSC) represent a heterogeneous population of immunosuppressive cells with the expression of variable surface markers, such as $CD11c^+$, $CD11b^+$, $CD33^+$, $CD34^+$ and $CD15^+$ (in human) and $CD11b^+$, $Gr1^+$ (in mouse). Increasing numbers of MDSC have been detected in the blood and/or in intratumor lesions in patients with different types of cancer. In addition, the frequency of MDSC is also positively correlated with the incidence of recurrence or metastatic disease in patients (Du and Wang, 2011). Experimental studies have shown that MDSC can function as potent suppressors of cytotoxic activity of effector $CD8^+$ T cells via various mechanisms including the expression of arginase and/or reactive oxygen species, the induction of $Foxp3^+$ Treg cells, sequestration of cysteine necessary for T cell activation, and down-regulation of L-selectin on T cells (Du and Wang, 2011; Ostrand-Rosenberg, 2010). Interestingly, MDSC can also promote early cancer cell dissemination from primary melanoma tumor by inducing epithelial-mesenchymal transition (EMT) (Toh et al., 2011).

Clinical trials using denileukin diftitox (Ontak), a CD25-directed diphtheria toxin to eliminate Tregs, have already been initiated in renal cell carcinoma or melanoma patients and preliminary results are promising (Dannull et al., 2005; Rasku et al., 2008). Sunitinib, a receptor tyrosine kinase inhibitor, has been shown to reduce the levels of MDSC in the blood of renal cell carcinoma patients. However, no changes in tumor burden, response to treatment or

survival have been reported (Ko et al., 2009). Chemotherapeutics such as gemcitabine is also known to inhibit Tregs in humans (Correale et al., 2005) and interestingly, MDSCs in mouse (Le et al., 2009; Suzuki et al., 2005).

1.4.2.3 Activation-induced T cell death

Several reports indicated that Fas (CD95/Apo-1) ligand (FasL) expression on various types of tumor cells may induce apoptosis of T cells *in vitro* (Hahne et al., 1996; O'Connell et al., 1996; Strand et al., 1996) and *in vivo* (Cefai et al., 2001), and may promote tumor escape from immune attack. FasL is expressed by many human tumors and is associated with poor prognosis in breast, liver, and ovarian cancers, supporting the immunosuppressive "counterattack" hypothesis (Jansen et al., 2010). Several studies using gene therapy strategies to knockdown FasL expression on tumor cells demonstrated reduced T cell apoptosis (Zhang and Xu, 2007) and improved anti-tumor immune responses (Jansen et al., 2010). Nevertheless, the exact role of FasL in tumor escape mechanism is still controversial. Tumor-specific T cells have been shown to utilize the Fas/FasL system to kill tumor cells *in vivo* (Arai et al., 1997). Therefore, much remains to be done to investigate whether FasL knock-down therapy has the potential to enhance current immunotherapies, including interleukin delivery and tumor vaccines, to achieve tumor regression in a clinical setting.

Although less well studied, chemokine-induced T cell death has also been reported in melanoma. In melanoma, the binding of melanoma-induced expression of CCR5 ligands to CCR5 on $CD8^+$ T cells activates an apoptotic

pathway involving cytochrome c release into the cytosol and activation of caspase-9 and -3 (Mellado et al., 2001a). Further studies are needed to confirm whether this phenomenon can be broadly applicable to other chemokines known to activate T cells and are normally expressed within the tumor microenvironment.

1.4.2.4 Metabolic inhibition

Three metabolic enzymes have been identified to mediate immunosuppression within the tumor micronenvironment, including indoleamine 2,3-dioxygenase (IDO), arginase, and inducible nitric oxide synthase (iNOS). IDO can be produced by tumor cells and/or dendritic cells in the tumor microenvironment and it suppresses T cell responses through tryptophan depletion via the production of proapoptotic metabolites (Fallarino et al., 2002). Uyttenhove et al demonstrated that inhibition of IDO expression using 1-methyltryptophan (1-MT) can improve T cell mediated tumor control *in vivo* (Uyttenhove et al., 2003). In addition to IDO, arginase has been shown to inhibit T cell activation by degrading another essential amino acid, arginine. In advanced cancer patients and in preclinical models, defective T cell activation has been associated with arginase-mediated downregulation of CD3zeta expression on T cells. Another arginine-metabolizing enzyme, iNOS, can lead to the production of nitric oxide, which has detrimental effects on T cell priming, proliferation, and cytotoxicity (Lizee et al., 2007). iNOS expression in human melanoma is associated with poor clinical prognosis (Ekmekcioglu et al., 2006) and targeted inhibition of iNOS inhibited human melanoma growth

in mouse models (Sikora et al., 2010), suggesting that targeting iNOS could be attractive for clinical application.

1.4.3 Defects at the level of the cancer cell

Cancer cells have been shown to actively evade immune attack and elimination by the immune system, leading to enhanced tumor development and progression. In fact, the concept of avoiding immune destruction has been proposed as one of the two emerging hallmarks of cancer in Weinberg's latest revision of the classical hallmarks of cancer (Hanahan and Weinberg, 2011). Several immune escape strategies utilized by cancer cells that are commonly described includes downregulation or loss of tumor antigens or MHC class I molecule and defects in apoptotic machinery.

1.4.3.1 Down-regulation or loss of tumor antigens/MHC class I molecule

Tumor cells are known to escape immune control by losing the expression of tumor antigens or down-regulating multiple components of the MHC class I antigen presentation machinery including proteasome components, transporter associated with antigen processing-1 (TAP1) or TAP2, MHC class I molecule or β2-microglobulin. Loss of MHC class I expression has been documented more frequently on aggressive and metastatic cancers compared to early-stage or more differentiated cancers (Du and Wang, 2011). Conversely, higher class I expression in bladder carcinoma has been associated with longer patient survival (Du and Wang, 2011). Tumors with altered expression of class I molecule contain few $CD8^+$ T cells in both renal cell carcinomas and cervical carcinomas (Du and Wang, 2011). This

deficiency is also associated with diminished sensitivity to CTL-mediated lysis, but increased susceptibility to NK cell destruction. The frequency of class I deficiencies is dependent on the tumor type and varies from 15 to 95% (Seliger, 2008). Therefore, the assessment of MHC class I antigen processing machinery components might identify patients able to respond to immunotherapy. Prospective studies have to be performed to validate the value of identifying MHC class I abnormalities for prognosis and therapeutic purposes.

1.4.3.2 Defects in apoptotic machinery

Evasion of endogenous cell death processes via defects in normal cell death pathways contribute to cancer progression by permitting progressively aberrant cell behaviours and desensitizing tumor cells to immune-mediated attack, radiation, and chemotherapy. The mechanisms responsible for this deficiency have been attributed to constitutive NF-κB activation, expression of anti-apoptotic Bcl-2 family members, defective signalling by Fas or TRAIL (tumor necrosis factor–related apoptosis-inducing ligand), active Notch signalling, expression of survivin, among others (Gajewski et al., 2006). Several apoptosis-based therapies have been developed to trigger tumor apoptosis and clinical trials are underway. These include gene therapies by down-regulation of anti-apoptotic genes/over-expression of pro-apoptotic genes, small molecule inhibitors of IAP, nutlins to increase levels of p53, chemical inhibitors of c-AKT that targets several apoptosis-regulating proteins, and compounds that reduce activation of NF-κB family transcription factors (Reed, 2006).

1.5 Chemotherapy and anti-tumor immune responses

Chemotherapy drugs were originally selected for their direct cytotoxic effect on tumor cells. The clinical success of chemotherapy to treat tumors is still very limited and varies considerably with tumor types. Tumors that are usually cured by chemotherapy include childhood leukemia, Hodgkin's disease, testicular cancer, choriocarcinoma, Burkitt's lymphoma, and nephroblastoma (Kaye), whereas most solid tumors respond poorly to chemotherapy. For example, the use DTIC as a single agent can induce objective tumor regression in 15%–20% of metastatic melanoma patients. However, the median response duration is 5 to 6 months with a negligible complete response rate and no significant effect on survival (Hershkovitz et al., 2010).

Accumulating evidence indicates that chemotherapy drugs could also indirectly promote tumor cell killing by effector components of the immune system (Nardin et al., 2011) (Figure 1.5.1). Certain chemotherapeutic drugs may contribute to anti-tumor immune responses by eliciting specific cellular responses that render tumor cell death immunogenic (Zitvogel et al., 2011). This includes the production of "eat-me signals" via calreticulin translocation to the plasma membrane, which stimulates antigen uptake by dendritic cells and antigen presentation to T cells. The release of danger signals such as high mobility group box 1 (HMGB1) protein, stimulates TLR4 (toll-like receptor 4) and regulates antigen processing and presentation, and thereby influences DC maturation, co-stimulation, polarization, and trafficking (Zitvogel et al., 2008).

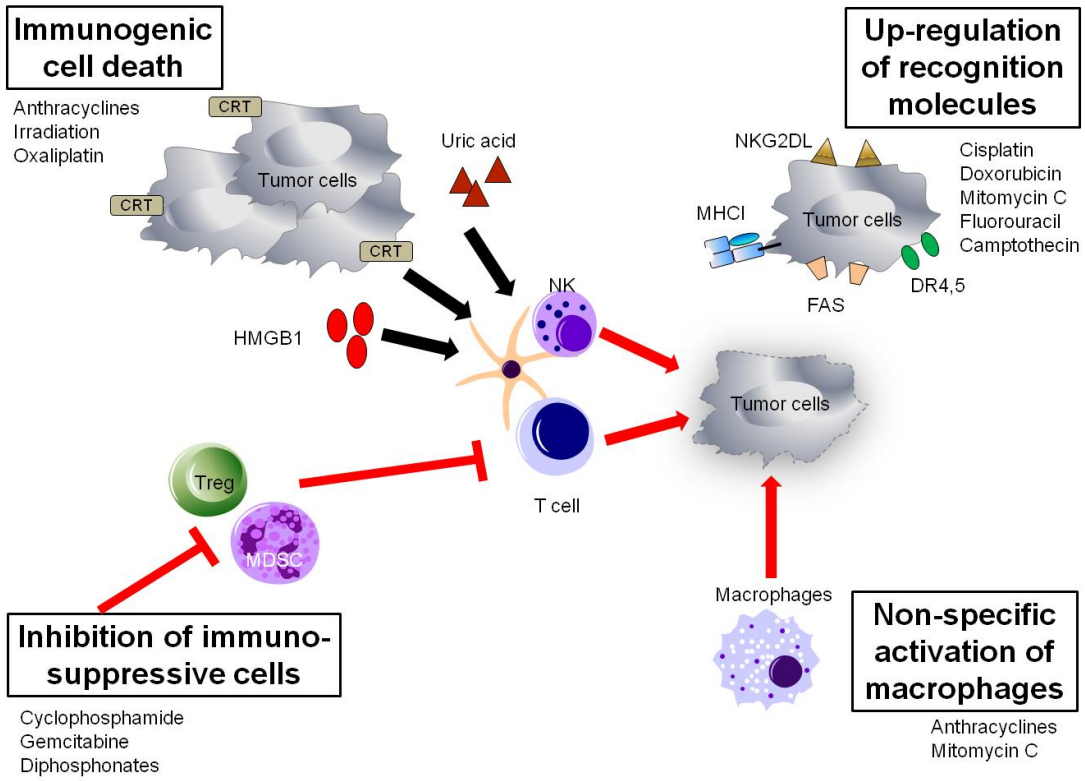

Figure 1.5.1 – Activation of the immune system by chemotherapy agents. Chemotherapy drugs have been shown to contribute to anti-tumor responses via the induction of immunogenic cell death mechanisms, upregulation of immune recognition molecules on tumor cells, inhibition of immunosuppressive cells, and non-specific activation of innate immune cells (see text for details). CRT – calreticulin; HMGB1 – high-mobility group protein B1; DR4,5 – death receptor 4 and 5 [adapted from (Menard et al., 2008)].

Other chemotherapy drugs may have side effects that stimulate the immune system, either directly or indirectly. Chemotherapy can induce stress signals leading to increased susceptibility of cancer cells to immune attack (Fine et al., 2010), including upregulation of NK stimulatory ligands (eg. NKG2D ligands after DNA damage) and/or death receptors (eg. Fas and TRAIL receptor) on tumor cells, leading to increased tumor cell killing. In addition, chemotherapeutic drugs could indirectly stimulate the immune system through transient lymphocyte depletion followed by more rapid homeostatic

proliferation, and subversion of immunosuppression mechanisms. For example, low dose cyclophosphamide (CPM) decreases the number and inhibitory function of $CD4^+$ $CD25^+$ Tregs by downregulating the expression of forkhead box P3 (FoxP3) and glucocorticoid-induced TNF-receptor-related protein (GITR) (Zitvogel et al., 2008), while gemcitabine reduces the frequency of $CD11b^+$ $Gr1^+$ MDSCs (Suzuki et al., 2005). Furthermore, chemotherapy may exert a direct effect on the activation of immune effector cells. For example, the vascular disrupting agent, 5,6-dimethyl-xanthenone-4-acetic acid (DMXAA) has been shown to activate tumor-associated macrophages (Jassar et al., 2005) or DC (Wallace et al., 2007), leading to increased tumor infiltration by CTL and myeloid cells. In addition, the taxane paclitaxel (Taxol; Bristol-Myers Squibb) can activate mouse macrophages and DCs by binding directly to TLR4, and has been shown to enhance T cell and NK cell activity in breast cancer patients (Zitvogel et al., 2008).

Recently, chemotherapeutic drugs have been shown to increase cytokine production in a variety of cell types *in vitro*. The significance of tumor-derived cytokine production in the therapeutic effectiveness or side effect profile of chemotherapeutic agents is unknown (Darst et al., 2004). However, significant levels of cytokines, including IL-8, TNF-α (tumor necrosis factor alpha), and others have been detected in the serum of patients undergoing chemotherapy for a variety of tumors (Darst et al., 2004). Another open question is whether T cell infiltration is a prognostic factor or predicts response to chemotherapy (Halama et al., 2009). While the presence of T cell infiltrates does not predict response to neoadjuvant chemotherapy in advanced laryngeal cancer

patients (Wolf et al., 2002), T cell infiltration after neoadjuvant chemotherapy in breast cancer patients is predictive of survival (Demaria et al., 2001; Ladoire et al., 2011).

In melanoma, mixed responses to chemotherapy are frequently observed (Bajetta et al., 2002). Systemic events such as improved induction of an immune response are unlikely to account for this variability, as this would most likely impact all lesions similarly. Tumor heterogeneity or differences in the tumor microenvironment is a more plausible explanation. It is not known whether differential T cell trafficking contributes to mixed responses after chemotherapy, and importantly, whether local factors controlling the recruitment of T cells into tumors could be affected by chemotherapy and therefore influence the clinical outcome.

Taken together, the ability of chemotherapy drugs to stimulate an anti-tumor immune response suggests that improved patient outcomes might be achieved using rational combinations of chemotherapy and immunotherapies (Nardin et al., 2011). Indeed, impressive clinical responses have been reported in patients treated with a combination of monoclonal antibodies (mAb) and chemotherapeutic drugs (Zhang and Herlyn, 2009). This raises great expectations for combination therapies using either vaccine or adoptive T cell transfer with chemotherapy, which have been shown to be promising in animal models and early clinical trials (Zhang and Herlyn, 2009).

1.6 Preclinical models in tumor immunotherapy studies

Mouse models of cancer have been instrumental in defining the mechanisms of tumor development and for the assessment of putative cancer therapeutics. The most widely used models are transplantation models, including murine tumors grown in syngeneic hosts or human tumor xenografts grown in immunodeficient mice. Autochthonous tumor models including carcinogen-induced tumor models and spontaneous tumor models (also known as genetically-modified mouse models, GEMM) are more recent developments that mirror defined steps of human carcinogenesis.

1.6.1 Transplanted tumor model

In transplanted tumor models, tumor cell lines implanted subcutaneously, intraperitoneally, or orthotopically into syngeneic mice generally grow rapidly (average doubling time < 2 days) and thus do not mimic the much slower doubling times of most human cancers. Extensive culturing of tumor cells will inadvertently select for cells with optimal growth and survival *in vitro*, and these tumor cells grow rapidly *in vivo* independent of the complex stroma/immune interactions (Tham and Abastado, 2011). The high proliferative capacity of these cells renders the tumors more sensitive to chemotherapeutic drugs that target actively dividing cells.

In the case of human tumor xenograft models, human tumor cells are grown in immune-deficient mice, therefore the role of the immune system cannot be evaluated. It is also unclear whether the tumor cells implanted at ectopic sites, which is a standard methodology, will respond to therapy the same way as

tumors grown at orthotopic site (i.e. in their organ of origin). In addition, studies of metastatic cancer therapy often involve artificial injection of tumor cells into the circulation. Therefore, transplanted tumor models are not suited for studying the early events of metastasis. Furthermore, large numbers of cells are required to induce tumor formation, which does not reflect the physiological condition of spontaneous tumor growth *in vivo* (Tham and Abastado, 2011). Despite these disadvantages, transplanted tumor models are still extensively used to study the immune response to tumor development and for the development of anticancer immune therapies, especially for advanced cancers.

1.6.2 Spontaneous tumor model

Carcinogen-induced models rely on administration of specific chemicals to generate cellular changes that rapidly lead to carcinogenesis. Several examples of widely used and studied models are the 7,12-dimethylbenzanthracene (DMBA) or N-methyl-N-nitrosourea (MNU) or hormonal 17b-estradiol (E2) induced mammary tumor models. In healthy female mice, these carcinogens induce a high incidence of mammary adenocarcinomas (MACs) that express similar histology and biomarker expressions to the human disease within 2–5 months (Ting et al., 2007).

Genetically-modified mouse models (GEMM) are generated through alterations in the level of expression (over-expression or deletion) of oncogenes or tumor suppressor genes. Examples of GEMM include the spontaneous models of breast cancers (including MMTV-PyMT and MMTV-

Erbb2) and pancreatic islet carcinoma (RIP-Tag). The main advantage of autochthonous models is that they can faithfully recapitulate key aspects of the human disease progression, including tumor initiation, local progression and distant metastases (Tham and Abastado, 2011). The tumors mostly develop at orthotopic sites, often reflect their respective human tumor histotypes, and contain a stroma and vasculature. As tumors develop over a long period of latency, there is sufficient time for tumor-host immune system interactions. While both of these autochthonous tumor models have been successful in predicting toxicity issues in humans, their value in predicting clinical results remains slow to progress (Walrath et al., 2010). This is, in part, due to low penetrance, long tumor latency, low incidence of distant metastasis, and asynchronous tumor development (Francia et al., 2011).

1.6.3 RETAAD model of spontaneous melanoma

To better mimic human disease, we are working on RETAAD mice, a recently characterized model of spontaneous melanoma that displays many critical features of the human disease (Lengagne et al., 2008). RETAAD mice are transgenic for the activated human *RET* oncogene and the chimeric mouse/human MHC antigen AAD (α1-α2 domains of HLA-A2 linked to α3 domain of H-2D^{d}). The *RET* oncogene, which encodes a receptor tyrosine kinase, is driven by the metallothionein-I (MT) promoter (Kato et al., 1998). In RETAAD mice, the *RET* oncogene is expressed by melanocytes (Iwamoto et al., 1991), driving enhanced melanogenesis, leading to skin melanosis and oncogenic transformation (Eyles et al., 2010).

In RETAAD mice, melanoma tumor development occurs step-wise starting with exophthalmos (i.e. bulging of the eye), followed by the development of spontaneous uveal melanoma (~28d), facial tumors (61d), neck/trunk tumors (135d), and eventually metastatic spread to various visceral organs (~250d), with each organ displaying a unique kinetic of tumor onset and tumor growth. SNP (single nucleotide polymorphism) analyses of 102 tumors derived from five mice revealed that most tumors arising in the same mouse share a common clonal origin. Consequently, most lesions (including cutaneous tumors) represent metastases and not independently transformed primary tumors (Eyles et al., 2010).

The expression of natural tumors antigens and the chimeric MHC molecule AAD in RETAAD mice facilitate the analysis of $CD8^+$ T cell responses against immunodominant HLA-A2-restricted human melanoma epitopes. Lengagne and co-workers have previously demonstrated that in the *RET* transgenic mice, a strong and broad anti-melanoma $CD8^+$ T cell response could be detected in the periphery as tumor grows (Lengagne et al., 2008; Lengagne et al., 2004). Using tyrosinase-related protein 2 (TRP2) as a model antigen, Umansky and colleagues showed that Trp2-specific $CD8^+$ T cells (mostly of the effector memory phenotype) could be detected in the bone marrow and tumors of transgenic mice (Umansky et al., 2008). Interestingly, these tumor-specific effector memory CD8+ T cells were also found in the bone marrow of transgenic mice without macroscopic tumors but showing microscopic lesions in the lymph nodes.

Recently, we have shown that tumor cells disseminate early to various organs in the RETAAD mice even before clinical detection of the primary eye tumor (Eyles et al., 2010). These early disseminated tumor cells (DTC) remain dormant for varying periods of time depending on the organ/tissue. $CD8^+$ T cells are required for the maintenance of tumor cell dormancy in visceral organs but not in the skin, as depletion of $CD8^+$ T cells significantly accelerated visceral tumor outgrowth and decreased survival in these mice, but had no effect on skin tumor development (Eyles et al., 2010; Lengagne et al., 2008).

The growth of immunogenic tumors in the presence of a functional anti-tumor immune response is clearly the most disturbing paradox of tumor immunology. The commonly proposed mechanisms to explain the paradoxical growth of tumors, including systemic ignorance, anergy, or tumor immunoediting alone cannot explain the growth of cutaneous tumors in the RETAAD mice, since most mice develop a strong tumor-specific $CD8^+$ T cell response and that these T cells have been shown to efficiently recognize tumor cell lines derived from cutaneous nodules (Lengagne et al., 2008). Local alteration of the immune system is a plausible explanation. In fact, several studies have focused on the role of immunosuppressive cells in cutaneous tumor development in the *RET* model. Increased frequencies of regulatory T cells (Treg) and myeloid-derived suppressor cells (MDSC) have been detected in cutaneous tumors and have been proposed to impair anti-tumor T cell responses in these tumors. However, depletion of Tregs had no effect on skin melanoma development (Kimpfler et al., 2009). While the depletion of MDSCs

led to partial restoration of T cell function in cutaneous tumors and increased survival in these mice (Meyer et al., 2011), we have found no effect of MDSC depletion on cutaneous tumor growth (Toh et al., 2011). Therefore, the escape of cutaneous tumors from the immune system involves other local suppression mechanism(s) that deserve futher exploration.

Taken together, the RETAAD model recapitulates many distinctive features of human disease, including natural progression of the disease, the paradoxical growth of immunogenic tumors in an immunocompetent host, and mixed efficacy of T cells, Therefore, the RETAAD model represents a unique model to investigate the basis of tumor escape from anti-tumor T cell responses, which could help to better understand and improve the efficacy of current T cell-based immunotherapies to treat cancers.

1.7 *In vivo* imaging to monitor tumor responses to immunotherapies

The two main objectives in modelling human diseases in animal models are (1) to recapitulate the pathophysiological characteristics of the human disease in the presence of a complete immune system to facilitate understanding of the complex molecular mechanisms underlying tumor development; and (2) to use these models to develop or test new targeted therapies. Since the growth and progression of spontaneous tumors varies widely from animal to animal, post-mortem tissue analysis of large cohorts of animals is often required to derive statistically meaningful data. Autopsy is often the most effective way to evaluate treatment efficacy and longitudinal studies examining the dynamics of tumor response and relapse to treatment is almost impossible.

The recent development of non-invasive imaging techniques has made it possible to follow tumor progression in mice with spontaneous tumor development. These include nuclear techniques such as magnetic resonance imaging (MRI) (Nelson et al., 2003), single-photon emission computed tomography (CT) and positron emission tomography (PET) (Mankoff et al., 2000; Mankoff et al., 2005; Ray et al., 2003; Yang et al., 2003), and optical techniques such as fluorescence imaging (FLI) (Hoffman and Yang, 2006) and bioluminescence imaging (BLI) (Rehemtulla et al., 2000). Detailed comparison of these molecular imaging techniques for tumor detection *in vivo* has been extensively reviewed (Koo et al., 2006; Lyons, 2005). For molecular imaging to be adapted more widely and to be complementary to other types molecular measurements, the read-out needs to meet certain criteria, i.e. it should be reliable, quantitative, high throughput, sensitive, high resolution,

longitudinal (allow imaging over time), and allow assessment of tumor burden in the whole animal.

We have previously compared the performances of various imaging modalities for whole body tumor imaging in transplanted and autochthonous melanoma models. Our data showed that BLI enables high-throughput, sensitive (detecting even non-palpable tumors), and quantitative whole-body tumor imaging for skin tumors and visceral metastases, and is suited for the determination of tumor burden in longitudinal studies. FLI is less sensitive than BLI and can only detect palpable tumors (≥2mm). Moreover, FLI signal is more subjected to tissue attenuation (3-fold vs 14-fold) and the presence of hair (70-fold vs 400-fold). Therefore, deep tissue imaging is unlikely due to the increased optical path through the tissues (Puaux et al., 2011). For nuclear imaging techniques, MRI and ^{18}FDG-PET allow early detection of small tumors and exhibit good sensitivity (81% and 70%) and positive predictive value (95% and 86%) compared to necropsy. In addition, MRI and ^{18}FDG-PET are not limited by the depth of the tumor, and both were able to provide precise locations of small nodules. For whole-body metabolic imaging, ^{18}FDG-PET is a better option for longitudinal follow-up of tumor burden. However, the high background observed in some organs (e.g. brain, heart and bladder) prevent tumor detection in these organs. MRI provides good contrast and anatomical information related to location, volume, vascularization and invasion. However this method is more challenging for whole-body tumor detection. Furthermore, both MRI and ^{18}FDG-PET scans are time-consuming

(low throughput), costly and require expertise for data analysis (Puaux et al., 2011).

Taken together, while each imaging modality has its own advantages, BLI is by far most suited for whole body detection of spontaneous tumor growth and for the purpose of evaluating preclinical therapies. BLI has been extensively validated in multiple transplanted and xenograft tumor models and its use in spontaneous tumor model is beginning to gain much attention.

1.8 Aims of the project

The success of T cell-based immunotherapies to treat cancers is still lacking. Therefore, the goal of the present study is to identify local factors that determine tumor control by T cells. We address this question using both the RETAAD mouse model of spontaneous melanoma and samples obtained from melanoma patients.

In RETAAD mice, $CD8^+$ T cells control visceral tumor outgrowth but have no effect on cutaneous tumors (Eyles et al., 2010; Lengagne et al., 2008), suggesting mixed T cell efficacy in the RETAAD mice. In melanoma patients treated with chemotherapy, mixed T cell responses were similarly observed. Using global transcriptome analysis on cutaneous melanoma metastases resected from melanoma patients before and after chemotherapy, increased T cell infiltration was identified specifically in chemotherapy-sensitive tumors (Nardin et al., 2011). Therefore, the aim of this study is to identify molecular cues that control T cell infiltration into cutaneous melanoma tumors in both human and mouse, and to evaluate the impact of therapeutic strategies on modulating the expression of such molecular cues in promoting T cell infiltration into tumors.

In addition, we addressed the need for a reliable imaging technique to follow disease progression and to evaluate responses to future chemo-immunotherapeutic treatments in spontaneous tumor models. This leads to the second aim of this study, i.e. to improve our current model of spontaneous mouse melanoma by developing a new transgenic mouse model that allows

longitudinal monitoring of disease progression and therapeutic responses by *in vivo* BLI.

CHAPTER 2

MATERIALS AND METHODS

2 MATERIALS AND METHODS

2.1 Development of a new spontaneous bioluminescent mouse melanoma model to monitor tumor growth and treatment responses

2.1.1 Tumor cell lines

The B16-F10 mouse melanoma cell line was from American Type Culture Collection (Cat Nr CRL-6475). B16-F10-luc cells (Xenogen, Alameda, CA) express firefly luciferase (sequence from pGL3, Promega) under the control of the SV40 promoter.

2.1.2 Animals

Animal care and experimental procedures were approved by the Institutional Animal Care and Use Committee of the Biological Resource Center, A*STAR, Singapore. RETAAD mice were generated as previously described (Kato et al., 1998).

2.1.3 Development of Melucie mouse

2.1.3.1 Gene expression analysis

RETAAD tumor samples were homogenized and RNA extraction was performed using NucleoSpin® RNA II kit (MACHEREY-NAGEL). Reverse transcription was performed and the expression of five melanocyte-specific genes relative to *Gapdh* was measured by quantitative real-time PCR (qRT-PCR) with SYBR green as previously described (Eyles et al., 2010).

2.1.3.2 Cloning of the Dct promoter

The mouse dopachrome tautomerase (Dct) promoter sequences with two different lengths were amplified from a BAC (bacterial artificial chromosome) probe (CHORI), denoted Dct1 (-3181 to +445) and Dct2 (-3181 to +63). Both Dct promoter sequences were individually cloned into the multiple cloning site (MCS) region of a pGL4.17 plasmid (Promega). Briefly, the pGL4.17 plasmid was digested with NheI and XhoI, dephosphorylated, and the Dct promoters were ligated separately with the luciferase vector to generate the final constructs, pGL4.17-Dct1 and pGL4.17-Dct2.

2.1.3.3 Luciferase reporter assay

The pGL4.17-Dct1 and -Dct2 constructs were transfected into B16-F10 mouse melanoma cells using Lipofectamine™ 2000 (Invitrogen) according to the manufacturer's protocol. The pGL4.13 vector (luc2 gene under the control of SV40 promoter) was used as a positive control. For luciferase assays, the cells were harvested 24h after transfection, and the luciferase activity was measured using a Dual Luciferase Reporter Assay kit (Promega) according to the manufacturer's protocol and firefly luciferase activity was normalized by renilla luciferase activity. Total protein content of the cell extracts was measured using BioRad Protein Assay Solution. Data was expressed as the relative light unit (RLU) per mg protein.

2.1.3.4 Transgenesis and founder screening

To generate the transgenic mouse, Dct-Luc, the pGL4.17-Dct2 construct was digested using SacII and StuI. Of the two resulting fragments, the larger

fragment (6341bp) containing the Dct promoter and luc2 gene was gel-purified. This linear DNA preparation was microinjected into fertilized C57BL/6 oocytes at the one-cell stage. Resulting mouse embryos were then implanted into pseudo-pregnant females. Pups were screened for transgene insertion by PCR. Luciferase expression was confirmed by *in vivo* BLI using a protocol described previously (Puaux et al., 2011) and the number of luciferase integration site(s) was determined by fluorescence in situ hybridization (FISH). Briefly, mouse chromosomes were prepared from mouse tail fibroblasts. To detect the transgene DNA, transgene-specific probes (300 bases to 2kb in size) were generated from the luciferase construct used for micro-injection. Cells were co-denatured with the probes during hybridization. Finally, two out of five luciferase founders were selected and independently crossed with MT-ret transgenic mice to generate double-transgenic Melucie mice.

2.1.4 Characterization of Melucie mouse

In vivo BLI of tumors was performed as previously described (Puaux et al., 2011). *Ex vivo* BLI of isolated organs was performed immediately after euthanasia of the animals. Dissected organs were plated into 48-well plates and imaged by IVIS after addition of 15mg/ml luciferin substrate. The presence of tumors in dissected organs was confirmed by hematoxylin and eosin (H&E) staining.

2.1.5 Data analysis and statistical analysis

BLI data were analyzed using Living Image Software (Xenogen, MA). Data was presented as relative light unit (RLU) (or photons per second, p/s). Correlation analyses was perfomed on log transformed values using Pearson correlation, one-tailed. The positive predictive value (PPV) was defined as: (number of tumors detected by imaging and confirmed at necropsy) / (total number of tumors detected by imaging); the sensitivity for tumor identification was defined as: (number of tumors detected by imaging and confirmed at necropsy) / (total number of tumors observed at necropsy).

2.2 Chemokines and intra-tumoral T cell trafficking in cutaneous mouse melanoma

2.2.1 Mouse melanoma cell lines

The B16-F10 (Cat Nr CRL-6475) cell line was from ATCC. The Melan-ret cell line, derived from a cutaneous tumor of a RET^+ mouse, was previously described (Lengagne et al., 2004).

2.2.2 Mice

Animal care and experimental procedures were approved by the Institutional Animal Care and Use Committee of the Biological Resource Center, A*STAR, Singapore.

2.2.3 Gene expression analysis

RETAAD tumor samples were homogenized and RNA extraction was performed using NucleoSpin® RNA II kit (MACHEREY-NAGEL). Reverse transcription was performed and the expression of various immune genes relative to *Gapdh* (for mouse) and *ACTB* (for human) was measured by qRT-PCR with SYBR green as previously described (Eyles et al., 2010).

To measure the expression of chemokine and chemokine receptor genes, reverse transcription was first carried out using RT^2 first strand kit (SABiosciences) with 1µg of RNA. The inflammatory cytokine-chemokine "RT^2 profiler PCR array" (SABiosciences) was used to measure the transcript levels of 40 inflammatory chemokines and their receptors. Data analysis was conducted according to the manufacturer's instructions.

2.2.4 Immunofluorescence

Formalin-fixed paraffin-embedded sections (5µm) were immunolabeled for CD3ε to identify T cells. Briefly, sections were heat-treated with Target Retrieval Solution (Dako S1699), blocked with 10% (v/v) normal goat serum (Dako) in PBS for 2h and Avidin/Biotin blocking solution (Dako X0590) for 10min, before overnight incubation at 4°C with rat monoclonal anti-CD3 antibody (Acris SM1754P; diluted 1:50 in PBS with 10% [v/v] normal goat serum). Anti-CD3 antibody binding was revealed with biotinylated donkey polyclonal anti-rat antibody (Jackson Lab; AffiniPure F(ab')2 Fragment; diluted 1:300) and AF594-conjugated strepavidin (Invitrogen S-11227; diluted 1:500 in PBS with 10% [v/v] normal goat serum). Nuclei were counterstained with DAPI. CD3 labeling was visualized using ImagePro Analyzer 6.2 software (Media Cybernetics Inc.).

2.2.5 Flow cytometry analyses

Single cell suspensions were obtained by digestion with Collagenase A (1mg/ml) and DNase I (0.1mg/ml) (Roche) in RPMI for 20min. After red blood cell lysis, Fc receptors were blocked with anti-mouse CD16/CD32 monoclonal antibodies (mAbs) for 30min before incubation with antigen-specific antibodies with a 1:50 dilution.

For the quantification of $CD3^+$ T cells, a total of 22 cutaneous and 4 visceral tumors were collected from tumor-bearing RETAAD mice. Tumors were dissociated and labeled with PerCP-Cy5.5-conjugated anti-CD45 mAb and PE-conjugated anti-CD3 mAb (Biolegend) for 20min.

For the characterization of chemokine receptors expressed on the surface of T cells subsets, whole blood was obtained from RETAAD mice and peripheral blood mononuclear cells (PBMC) were isolated. PBMC were incubated with PE-conjugated anti-CD3E mAb, PerCP-Cy5.5-conjugated anti-CD4 mAb, eFluor450-conjugated anti-CD8A mAb, PE-Cy7-conjugated anti-CD44 mAb, FITC-conjugated anti-CD62L mAb, and APC-conjugated anti-(human) CCR1 (R&D Systems) or anti-CCR2 (R&D Systems) or anti-CCR3 mAb. For CCR5, cells were labeled with FITC-conjugated CD3E mAb, PerCP-Cy5.5-conjugated anti-CD4 mAb, eFluor450-conjugated anti-CD8 mAb, PE-Cy7-conjugated anti-CD62L mAb, APC-Cy7-conjugated anti-CD44 mAb, and PE-conjugated anti-CCR5 mAb (R&D Systems). For CXCR3, cells were labeled with PE-conjugated anti-CD3E mAb, PerCP-Cy5.5-conjugated anti-CD4 mAb, eFluor450-conjugated anti-CD8 mAb, FITC-conjugated anti-CD62L mAb, APC-Cy7-conjugated anti-CD44 mAb, and PE-Cy7-conjugted anti-CXCR3 mAb. Corresponding isotype-matched control mAbs were used in control samples. All antibodies were from Biolegend unless otherwise stated. The same labeling protocol was used to characterize chemokine receptors on TIL. The markers for naïve, effector memory and central memory T cells were defined as $CD62L^+$ $CD44^-$ (naïve), $CD62L^-$ $CD44^+$ (effector memory) and $CD62L^+$ $CD44^+$ (central memory) for both $CD4^+$ and $CD8^+$ T cells.

All samples were acquired on a multicolor FACS LSRII and data analysis was performed using FlowJo software (Becton Dickinson).

2.2.6 Construction of chemokine expression plasmids

Total RNA from LPS-activated murine peritoneal macrophages was reverse transcribed then PCR amplified using specific primers for *Ccl5* (5' primer TACCGAGCTCGGATCCATGAAGATCTCTGCAGCTG; 3' primer AAACGGG CCCTCTAGAGCAGGGTCAGAATCAAGAAACC), and *Cxcl9* (5' primer TACCGAGCTCGGATCCGCCACCATGAAGTCCGCTGTTC; 3' primer GCCC TCTAGACTCGAGCTCTTATGTAGTCTTCCTTG). The 5' end of each primer contains 15 bases homologous to the 5' end of each cloning site in the vector and the 3' end of each primer is gene-specific. The *Ccl5* 5' primer contains a BamHI site, and the 3' primer contains a NheI site; the *Cxcl9* 5' primer contains a BamHI site, and the 3' primer contains a XhoI site. Specific chemokine bands were cloned into pcDNA3.1 Hygro(+) (Invitrogen) using the In-Fusion® Advantage PCR Cloning Kits from Clontech. Each construct was confirmed by restriction digestion and sequencing to generate pcDNA3.1(+)-CCL5 and pcDNA3.1(+)-CXCL9. Chemokine production was confirmed using commercially available ELISA kits for mouse CCL5 and CXCL9 following the manufacturer's instructions (R&D systems).

2.2.7 *In vivo* experiments

2.2.7.1 RETAAD T cell migration to skin tumor site

Five tumor-bearing RETAAD mice per group (aged between 30 to 40 weeks) were injected subcutaneously in the right flank with 200,000 B16-F10luc cells in 100μL of PBS. Mice were euthanized when the B16 tumor diameter reached 1cm. The B16 transplanted skin tumor and one to two RETAAD skin tumors were collected from the same mouse. Tumors were excised and

divided into two parts. One part was stored in RNALater for qRT-PCR of chemokine/cytokine expression, while the other was dissociated with Collagenase A and DNase I (Roche) for analysis of T cell infiltration by flow cytometry.

2.2.7.2 *In vivo* transfection of cutaneous tumors

Five to ten RETAAD tumor-bearing mice per group (aged 30 to 50 weeks) were used. For each mouse, 2 to 7 cutaneous tumors were transfected with 5ug of pcDNA3.1(+)-CCL5 or -CXCL9 or empty plasmid using in vivo JetPEI transfecting reagent (Polyplus Transfection). Three injections were performed on alternate days for 5 days. On day 6, the mice were euthanized and the tumors were excised, weighed and divided into two parts. One part was stored in RNALater in preparation for RNA extraction and qRT-PCR analysis of intra-tumoral mRNA expression of *Ccl5*, *Cxcl9*, *Cxcl10*, *Ifng*, *Gzma*, and *Gzmb*; the other was dissociated and analyzed for immune cell infiltration by flow cytometry. For *Ccl5* and *Cxcl9* co-injection studies, 2.5ug of pcDNA3.1(+)-CCL5, -CXCL9, empty plasmid or a combination of 5ug of pcDNA3.1(+)-CCL5 and -CXCL9 were injected into cutaneous RETAAD tumors using the protocol described above. On day 6, the mice were euthanized and tumors were excised, weighed and stored in RNALater. mRNA expression of *Cd3g*, *Ccl5* and *Cxcl9* was analyzed by qRT-PCR.

2.2.7.3 Transfection of Melan-ret cells

Melan-ret cells were seeded into 6-well plates and transfected with plasmid DNA encoding *Cxcl9* using Lipofectamine™ 2000 (Invitrogen) according to

the manufacturer's protocol. Six hours later, *Cxcl9*-transfected Melan-ret cells and control cells were harvested and injected subcutaneously into alternate flanks of C57 BL/6 mice with 200,000 cells per dose. Tumor growth was monitored by palpation every two to three days starting on day five after tumor cell injection. 16 days later, the mice were euthanized, and tumors were collected, weighed and *Cd3g* expression was analyzed by qRT-PCR. The same experiment was repeated using $Rag1^{-/-}$ mice.

2.2.8 Statistical analyses

Gene expression data were normalized, log-transformed and compared using Student's t-test or ANOVA. P values for multiple comparisons were adjusted using Bonferroni correction. Other parameters (tumor weight, tumor area, percentage of tumor-infiltrating cells) were compared using non-parametric tests (Mann-Whitney or Kruskal-Wallis).

2.3 Chemokines and intra-tumoral T cell trafficking in cutaneous human melanoma

2.3.1 Human melanoma cell lines

The HTB-71 cell line was from ATCC. The other four human melanoma cell lines (M88, M102, M131, and M134) were kindly provided by J-B Latouche and P. Musette.

2.3.2 Chemotherapeutic drugs

Temozolomide, cisplatin, and dacarbazine were purchased from Sigma-Aldrich. Stock solutions of temozolomide were prepared in DMSO (20mg/ml), cisplatin in DMF (10mg/ml) and dacarbazine in 0.6N HCl (10mg/ml).

2.3.3 Patient samples

Tumor samples were prospectively obtained from 13 stage III and IV melanoma patients recruited at the Cochin Hospital, Paris, France, between 2006 and 2009. The study was approved by the Ethics Committee of Ile de France. The Declaration of Helsinki protocols were followed and the patients gave their written, informed consent. Demographics and clinical characteristics of the patients, and microarray data analysis can be found in (Nardin et al., 2011).

2.3.4 Chemotherapy drug treatment and chemokine gene expression

Human melanoma cells were seeded into 12-well plates. After 48h, drugs were added at indicated concentrations. For dose-response studies, cells were incubated with escalating concentrations of drugs for three days before being harvested, while the supernatants were collected and frozen. RNA

extraction and cDNA conversion were performed as described previously, and the expression of *CCL5*, *CXCL9* and *CXCL10* relative to *ACTB* was analyzed by qRT-PCR. For kinetic studies, cells were incubated with a fixed dose of drug and were harvested at 6, 12, 24, 48 and 72h after addition of the drug. The expression of chemokines was determined using qRT-PCR at various timepoints.

2.3.5 Multiplex analysis of chemokine and cytokine production by tumor cells

Concentrations of various cytokines/chemokines in the supernatant of drug-treated cells were analyzed using multiplex bead-based assays based on xMAP technology, combining both the 21-plex (MF0-005KMII) and 27-plex (M50-0KCAF0Y) kits from Biorad. A total of 48 secreted factors were measured, including 28 cytokines (IL-1α, IL-2Rα, IL-3, IL-12 (p40), IL-16, IL-18, IL-1b, IL-1rα, IL-2, IL-4, IL-5, IL-6, IL-7, IL-8, IL-9, IL-10, IL-12 (p70), IL-13, IL-15, IL-17, IFN-α, IFN-α2, IFN-γ, LIF, MIF, TNFα, TNFβ, TRAIL), 10 chemokines [CTACK, CXCL1 (GROα), CXCL10 (IP-10), CCL2 (MCP-1), CCL7 (MCP-3), CXCL9 (MIG), CCL3 (MIP-1α), CCL4 (MIP-1β), CCL5 (RANTES) and CXCL12 (SDF-1α)], and 10 growth factors (basic-FGF, β-NGF, G-CSF, GM-CSF, HGF, M-CSF, PDGF-BB, SCF, SCGF-β and VEGF). Analyses of tumor supernatants were performed in a 96-well microplate format according to the manufacturer's protocol.

2.3.6 Statistical analyses

Gene expression data were normalized, log-transformed and compared using Student's t-test or ANOVA. P values for multiple comparisons were adjusted using Bonferroni correction. Other parameters (tumor weight, tumor area, percentage of tumor-infiltrating cells) were compared using non-parametric tests (Mann-Whitney or Kruskal-Wallis). Patient survival was analyzed by the Kaplan-Meier method using log-rank (Mantel-Cox) test.

CHAPTER 3

RESULTS

3 RESULTS

3.1 Development of a new spontaneous bioluminescent mouse melanoma model to monitor tumor growth and treatment responses

3.1.1 Generation of the ret$^{+/-}$ luc$^{+/-}$ transgenic mouse

In order to generate a unique model that allows non-invasive imaging of spontaneous melanoma tumor development and drug response, the advantages of both BLI and the spontaneous melanoma model, MT-ret, were exploited to develop a new transgenic mouse model called Melucie. The Melucie mouse is double-transgenic for the activated human RET oncogene and the luciferase reporter gene and is expected to develop spontaneous bioluminescent melanoma tumors and metastases.

To achieve melanocyte-specific transgenic expression, many laboratories use regulatory sequences of the tyrosinase family genes, such as tyrosinase (Tyr), tyrosinase-related protein 1 (Trp1) and tyrosinase-related protein 2 (Trp2) (or dopachrome tautomerase, Dct) (Murisier and Beermann, 2006) [reviewed in (Larue and Beermann, 2007)]. To determine the optimal promoter to drive luciferase expression in melanoma tumors, the relative expression of five different melanocyte-specific genes, including *Tyr*, *gp100*, *melan-A/Mart-1*, *Trp1*, and *Trp2* were analyzed in RETAAD tumors. Among the five genes analyzed, *Trp2* was found to be the most highly expressed melanocyte-specific gene in the tumors (Table 3.1.1). Therefore, the promoter of mouse dopachrome tautomerase (DCT), i.e. the homolog of human tyrosinase related protein 2 (Trp2), was chosen the melanocyte-specific promoter to

drive luciferase expression specifically in melanocytes. Consequently, melanoma tumors, which are enriched in melanocytes, are expected to express high levels of luciferase activity, thus allowing tumor detection via BLI.

Table 3.1.1 – Quantitative real-time PCR analysis of the expression of melanocyte-specific genes in RETAAD tumors.

Melanocyte-specific gene	**Mean Ct**
Tyrosinase related protein 2 (Trp2)	19
Tyrosinase (Tyr)	20.2
Melan-A/MART-1	22
Glycoprotein 100 (gp100)	>22
Tyrosinase related protein 1 (Trp1)	>22

Table shows the mean ct values of the expression of five melanocyte-specific genes in 20 RETAAD tumors. A higher ct value represents lower gene expression and vice versa.

The Dct promoter has been used previously to drive lacZ expression to study melanocyte differentiation during embryonic development (Mackenzie et al., 1997). Based on this earlier report, two constructs were generated: one containing the exact sequence of Dct promoter used by Mackenzie (-3181 to +445, denoted Dct1) and another one with a shortened 5' end (-3181 to +65, denoted Dct2) (Figure 3.1.1A). Both promoter sequences were cloned next to a codon-optimized luciferase reporter gene to generate the plasmids pGL4.17-Dct1 and pGL4.17-Dct2 respectively (Figure 3.1.1B). Transfection of these constructs into B16 mouse melanoma cell line confirmed the functionality of the enzymes after luciferin addition. In addition, higher

luciferase activity was observed for the construct with shorter non-coding sequence, i.e. pGL4.17-Dct2 (Figure 3.1.1C). Therefore, this construct was chosen for the generation of transgenic mouse.

A.

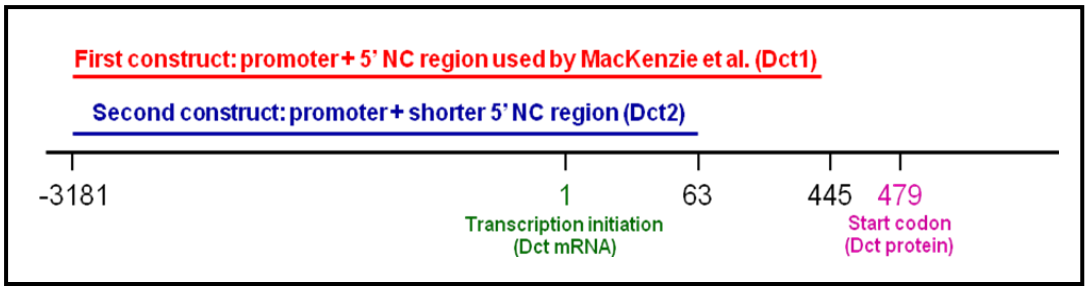
First construct: promoter + 5' NC region used by MacKenzie et al. (Dct1)
Second construct: promoter + shorter 5' NC region (Dct2)
-3181
1
63
445
479
Transcription initiation
(Dct mRNA)
Start codon
(Dct protein)

B.

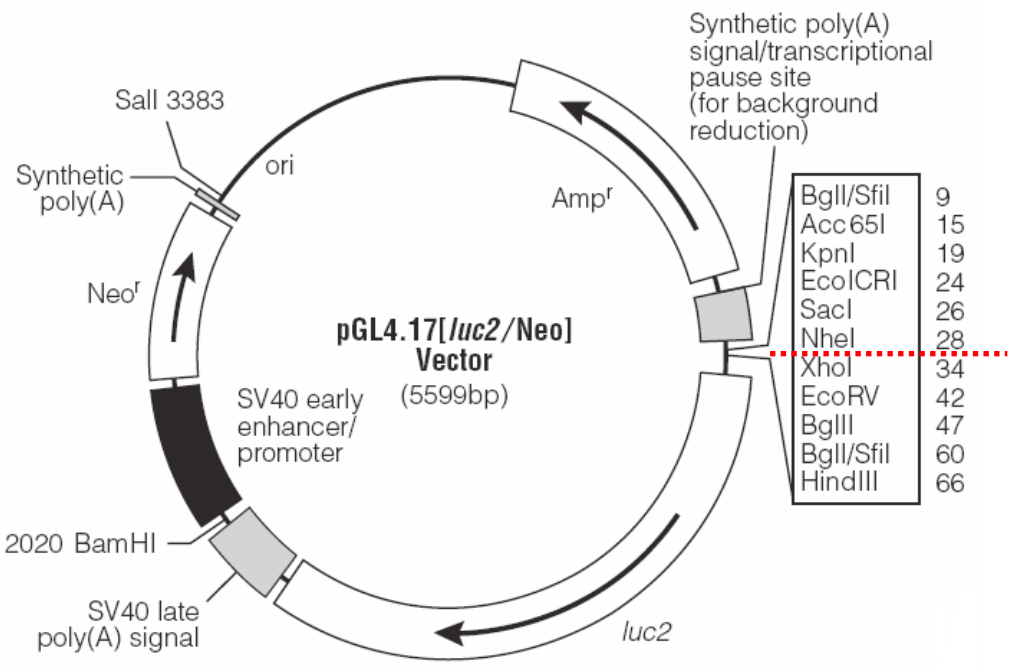
Synthetic poly(A) signal/transcriptional pause site (for background reduction)
SalI 3383
Synthetic poly(A)
ori
Amp^r
Neo^r
pGL4.17[luc2/Neo] Vector
(5599bp)
SV40 early enhancer/ promoter
2020 BamHI
SV40 late poly(A) signal
luc2
BglII/SfiI 9
Acc65I 15
KpnI 19
EcoICRI 24
SacI 26
NheI 28
XhoI 34
EcoRV 42
BglII 47
BglII/SfiI 60
HindIII 66

C.

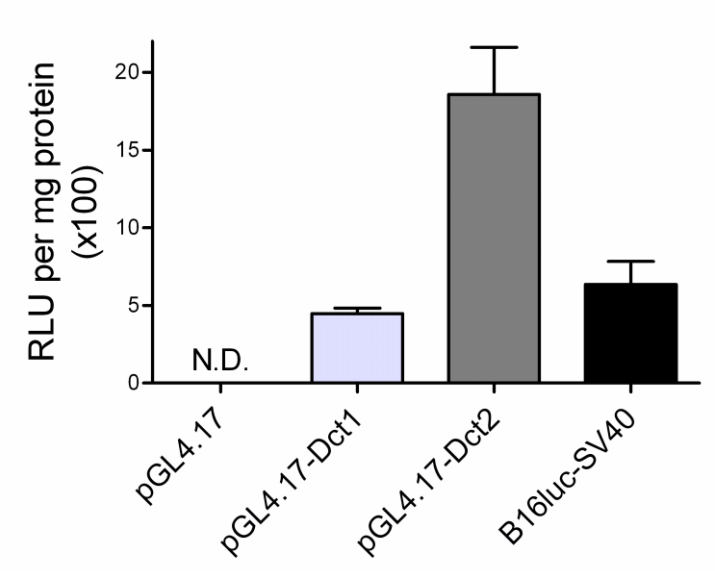
RLU per mg protein (x100)
20
15
10
5
0
N.D.
pGL4.17
pGL4.17-Dct1
pGL4.17-Dct2
B16luc-SV40

Figure 3.1.1 – Generation of luciferase construct for transgenesis.
(A) Mouse dopachrome tautomerase (Dct) promoter sequences used to drive luciferase transgene expression. Promoter sequences with two different lengths were amplified from a BAC (bacterial artificial chromosome) probe (CHORI), denoted Dct1 (-3181 to +445) and Dct2 (-3181 to +63). Both Dct promoter sequences were individually cloned into the multiple cloning site (MCS) of the pGL4.17 plasmid (Promega). NC = Non-Coding. (B) Vector map of the pGL4.17 plasmid (Promega) used for cloning. Red line indicates the position of insertion of the Dct promoter sequences within the multiple cloning site (MCS) of the pGL4.17 plasmid. (C) The two transgene constructs, pGL4.17-Dct1 and pGL4.17-Dct2 were individually transfected into B16-F10 mouse melanoma cells. Luciferase assay was performed 24h after transfection. The pGL4.17 vector and the pGL4.13 vector (luc2 gene under the control of SV40 promoter) were included as a negative and positive control, respectively. Total protein content of the cell extracts was measured using Bradford assay. Data is presented as relative light unit (RLU) per mg protein.

In general, for the development of a transgenic mouse, two methods of transgenesis are available. The first one is the knock-in approach, which involves homologous recombination of the gene of interest in the mouse genome of embryonic stem cells (ESC). This method allows specific targeting of the luciferase gene to the chosen locus, i.e. adjacent to a melanocyte-specific promoter. There is only a single transgene integration site and thus, only one transgenic line is necessary. This method is precise (targeted to the locus) but requires working with ESC (Smithies et al., 1985). The second approach is random insertion of a target construct containing both coding and regulatory elements. This requires having a construct containing the chosen promoter adjacent to the luciferase gene. The copy number of the transgene in the genome is unknown and may be high (usually 1-50 copies but can be up to 1000 copies). For random insertion, the presence of multiple copies of the transgene may lead to the formation of concatamers, i.e. they are joined to each other in a head-to-tail configuration. The precise location of the transgene in the genome is unknown. Therefore, “position effects” or “founder effect” may occur, making it necessary to analyze several transgenic lines derived from independent founders. This implies the need to screen large numbers of animals. This method is less precise, but it obviates the need to work with ESC. Most importantly, this method can lead to high levels of gene expression due to integration of multiple copies of the transgene (Gordon and Ruddle, 1981; Ittner and Gotz, 2007).

In our case, the level of the transgene expression is an important consideration because the level of luciferase expression in melanoma will

directly influence the sensitivity of tumor detection. This is especially important for early detection of both cutaneous and visceral tumors. Random insertion, therefore, was our method of choice for transgenesis because it may select for high expressors (with multiple copies of transgene). Furthermore, it allows selection of a transgenic line giving the best signal to noise ratio. In order to generate the luciferase transgenic mouse, the linearized luciferase construct pGL4.17-Dct2 (transgene sequence is shown in Appendix 1) was microinjected into pronuclear embryos from C57BL/6 mice and integration of the target construct into the mouse genome occurred by random insertion. Five independent transgenic founders denoted Dct-1-5 was generated.

The number of transgene insertion site(s) in each luciferase founder was determined by fluorescence in situ hybridization (FISH). As shown in Figure 3.1.2, only a single transgene insertion site was identified in each of the founders. In addition, BLI was performed to confirm the *in vivo* functionality of the luciferase enzyme after luciferin injection (Figure 3.1.3). Two out of five luciferase founders (Dct-1 and Dct-2, one low expressor and one high expressor) were subsequently selected and crossed independently with MT-ret transgenic mouse to obtain double-transgenic Melucie lines [which we refer to here as Centromeric Melucie (low expressor) and Telomeric Melucie (high expressor) based on the position of the luciferase transgene in the mouse chromosome].

Dct-1
Dct-2
Dct-3
Dct-4
Dct-5

Figure 3.1.2 – Identification of transgene integration site by fluorescence in situ hybridization (FISH).
Briefly, mouse chromosomes were prepared from mouse tail fibroblasts isolated from five different luciferase founders, denoted Dct-1 to Dct-5. To detect the luciferase transgene DNA, FISH probes (300bases to 2kb in size) labelled with spectrum green-dUTP were generated by nick translation of the luciferase construct used for micro-injection. The chromosomes were co-denatured with the FISH probes during hybridization. Hybridization signal is indicated by white arrow and two single dots (in green). Only a single transgene integration site is detected for all the luciferase founders analyzed. Blue – DAPI, Green spots – luciferase transgene.

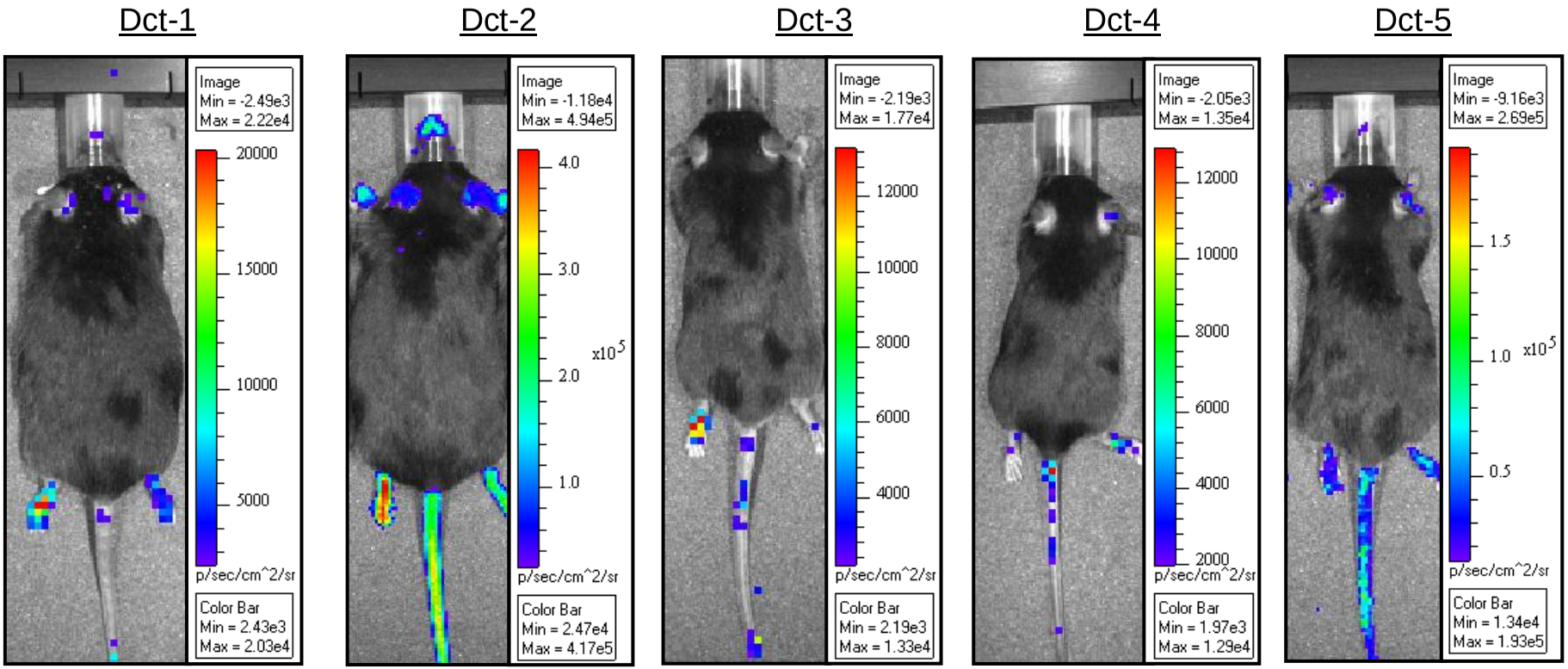

Figure 3.1.3 – Luciferase expression confirmed by *in vivo* bioluminescence imaging (BLI).
In vivo bioluminescence imaging (BLI) was performed to confirm the *in vivo* functionality of the luciferase enzyme in each of the luciferase founders, denoted Dct-1 to Dct-5. For *in vivo* imaging, mice were anesthetized with isoflurane and injected intraperitoneally with 150mg luciferin/kg body weight (D-luciferin, Caliper LifeSciences). 15min after substrate injection, mice were placed in the chamber and imaged for 1min with the camera set at the highest sensitivity by IVIS® Spectrum (Xenogen). Images were analyzed using Living Image Software (Xenogen, MA). Bioluminescence signal was detected in melanocytes in the skin of each mouse (i.e. ears, limbs, tail) with different signal intensities. No bioluminescence signal was observed from the body area due to signal attenuation by the mouse hair. Signal intensity was quantified as the sum of all detected photon counts from the whole body and presented as photons/sec.

3.1.2 Bioluminescence imaging of spontaneous melanoma tumor development in ret$^{+/-}$ luc$^{+/-}$ mice

The sensitivity and positive predictive value (PPV) of BLI in the detection of autochthonous melanoma tumors *in vivo* were evaluated in tumor-bearing Telomeric and Centromeric Melucie mice. For Telomeric Melucie, high background of luciferase expression was observed *in vivo* after intraperitoneal injection of the luciferin substrate (Figure 3.1.4A). Therefore, this Melucie line was excluded from further analysis, and we focused on the Centromeric Melucie for further characterization. *In vivo* BLI in Centromeric Melucie successfully detected luciferase expression from melanoma tumors with minimal/no background observed (Figure 3.1.4B). The overall sensitivity and PPV for tumor detection via BLI was 80% and 100%, respectively. For skin tumor detection, the sensitivity and PPV was 88% and 100%; while for visceral metastases detection, the values were 33% and 100% respectively. Taken together, this data indicates that the Melucie model is suited for whole-body detection of spontaneous skin and visceral metastases by *in vivo* BLI.

A.

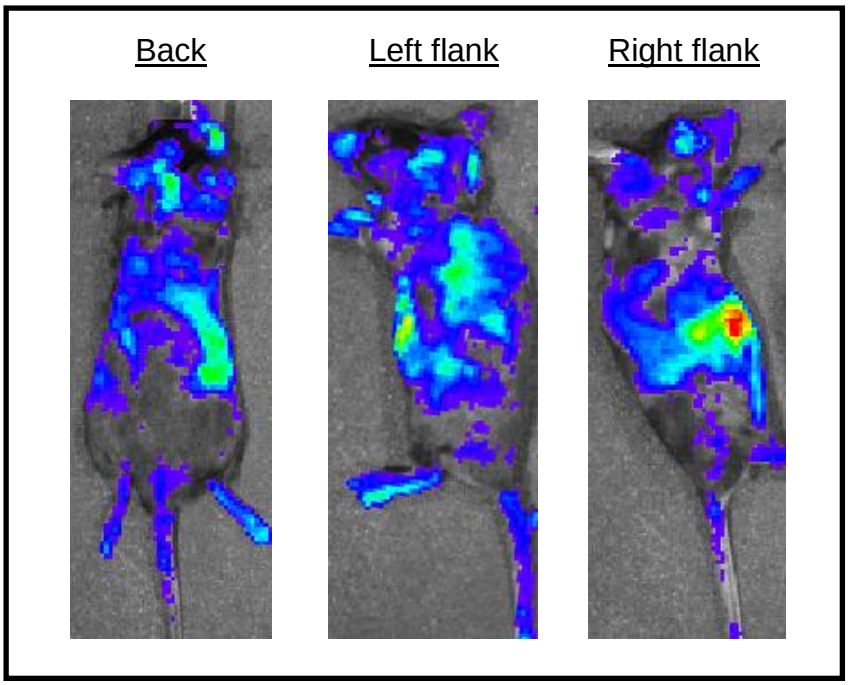

B.

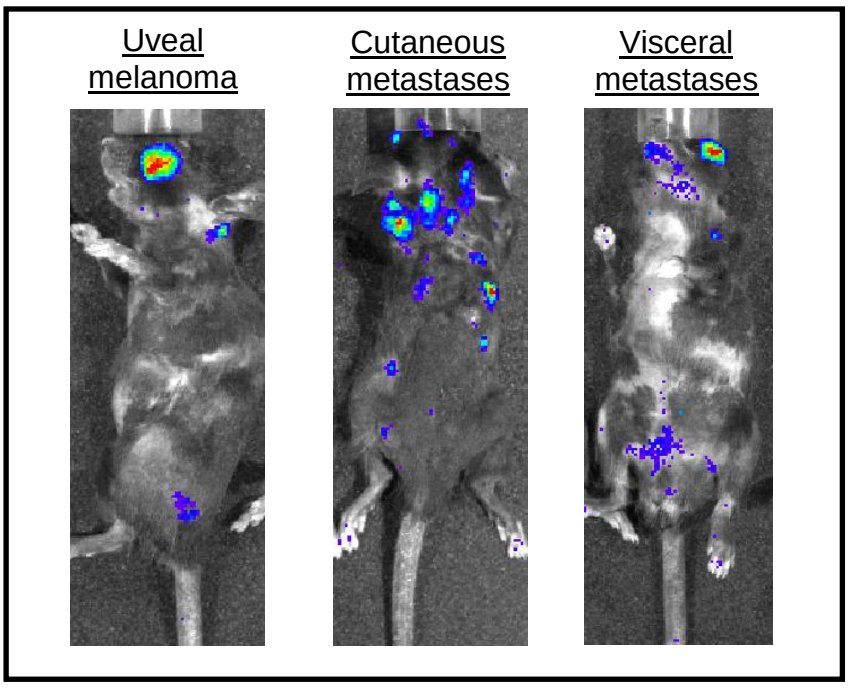

Figure 3.1.4 – Spontaneous melanoma tumor detection in Melucie mice by *in vivo* BLI.
(A) *In vivo* BLI of a tumor-bearing Telomeric Melucie mouse. High background of bioluminescent signal was observed throughout the whole animal. Images are representative of at least 10 mice. Exposure = 40s, Binning = 8. (B) *In vivo* detection of primary uveal melanoma (left panel), multiple cutaneous tumors (middle panel) and visceral metastases (reproductive tract tumor; right panel) in a Centromeric Melucie mouse by BLI. The BL signal was tumor-specific with no/low background observed. Images are representative of at least 3 mice. Exposure = 60s, Binning = 8.

The specificity of a reporter strain depends on the luminescence signal to noise ratio and consequently, on the background level of expression of the luciferase gene. Therefore, the *ex vivo* bioluminescence signal from selected organs were compared between $ret^{+/-}$ $luc^{+/-}$ Melucie mice [n=4] and $ret^{-/-}$ $luc^{+/-}$ littermate controls [n=3] after *in vivo* administration of luciferin. The background luminescence in all the organs tested from control mice was negligible. Higher emitted light was detected from the eyes, lungs and reproductive tract in the Centromeric Melucie compared to control mice, even in the absence of macroscopic tumors (Figure 3.1.5A). Interestingly, the presence of tumor cells in these organs was confirmed by histology (Figure 3.1.5B). No difference in signal was observed in the spleen, which serves as the control organ. The levels of emitted light from macroscopic tumors were comparatively higher (Figure 3.1.5A). This was expected as tumors are enriched with melanocytes and should express high levels of luciferase.

A.

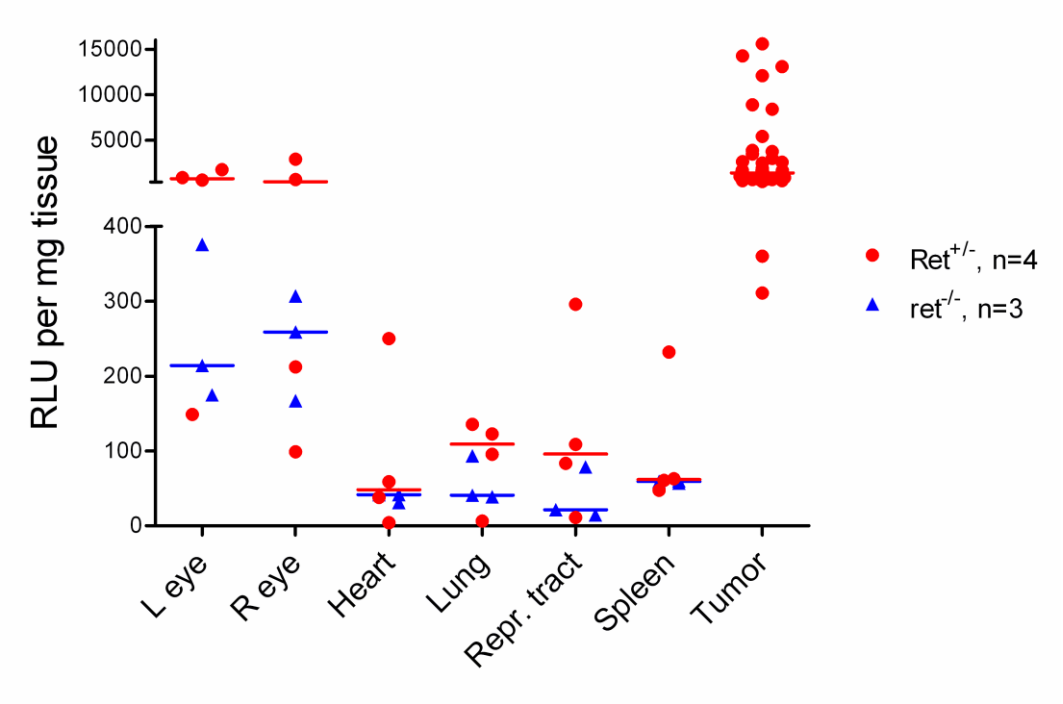
RLU per mg tissue
15000
10000
5000
400
300
200
100
0
L eye
R eye
Heart
Lung
Repr. tract
Spleen
Tumor
Ret+/-, n=4
ret-/-, n=3

B.

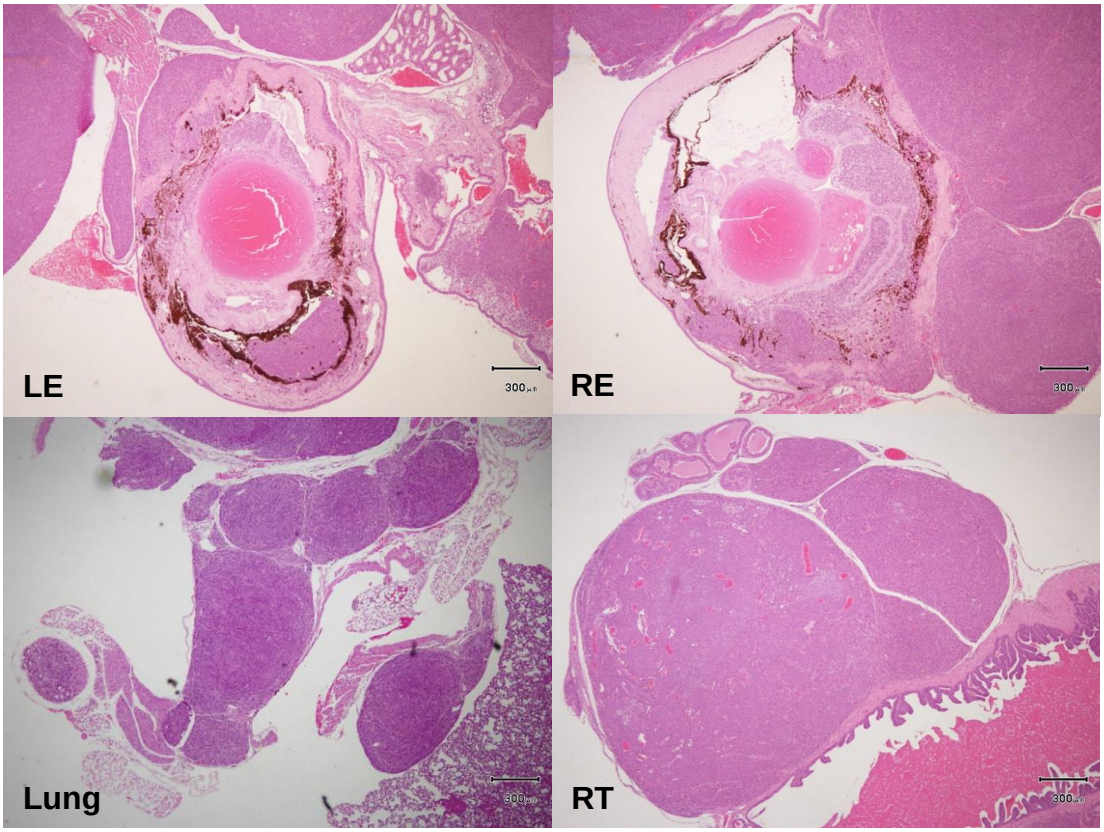
LE
RE
Lung
RT

Figure 3.1.5 – Detection of melanoma tumors in individual organs from Centromeric Melucie by *ex vivo* imaging and histology.
Tumor-bearing Centromeric Melucie [n=4] and age-matched littermate controls $ret^{-/-}$ $luc^{+/-}$ [n=3] were injected intraperitoneally with 150mg/kg body weight of luciferin. Mice were sacrificed 15mins post-luciferin injection and selected organs were harvested, weighed and placed into 24-well plates. *Ex vivo* imaging was performed and the bioluminescence signal was quantified using the Living Image Software (Xenogen). (A) Comparison of *ex vivo* BL signals from multiple organs of tumor-bearing Centromeric Melucie [n=4] and $ret^{-/-}$ $luc^{+/-}$ control mice [n=3]. Higher BL signal was observed in the eyes, lungs and reproductive tract, consistent with the presence of tumors in these organs. Macroscopic tumor nodules and spleens were included as positive and negative controls, respectively. High level of BL signal was detected in the tumors, as tumors are enriched in melanocytes and are expected to express high level of the luciferase enzymes. Data is shown as relative light unit (RLU) per mg tissue. (B) The presence of tumors in the eyes, lung and reproductive tract of Centromeric Melucie was confirmed on tissue sections by hematoxylin and eosin (H&E) staining. Images shown are representative of 4 Centromeric Melucie mice analyzed.

BLI of orthotopic xenografts in mice has demonstrated a linear correlation between tumor bioluminescence signal and tumor volume. To investigate whether such a correlation was also maintained during oncogene-driven tumor formation in our model, the luciferase activity of various tumors at different stages of growth was measured in several tumor-bearing Melucie mice. The tumors were imaged 15 minutes after i.p. injection of luciferin into the anaesthetized animals, and the signals were plotted against the wet tumor weights at necropsy. A remarkable correlation was observed between the detected photons and tumor weights (Pearson r = 0.7426, p-value = 4.72e-08) (Figure 3.1.6A). Furthermore, there was a good correlation between *ex vivo* and *in vivo* signals (Pearson r = 0.5340, p-value = 0.0063) (Figure 3.1.6B), and the *in vivo* signals correlated strongly to wet tumor weight (Pearson r = 0.602, p-value = 0.002) (Figure 3.1.6C). Our data indicates that the Melucie model is capable of volumetric detection of tumor growth *in vivo*.

We also followed melanoma tumor development in the Melucie by measuring bioluminescence from cutaneous tumors starting at 17 weeks of age when the tumor was first detected until the mice became moribund at 40 weeks. BLI was performed at three different time points, i.e. on day 121, 177, and 273 after birth. The mouse in Figure 3.1.6D showed an almost doubling of the signal every 30 days throughout the 150 day period, indicating exponential tumor growth.

A.

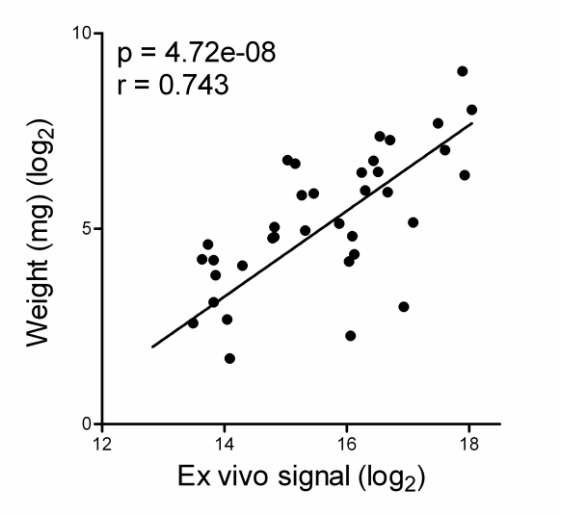
p = 4.72e-08
r = 0.743
Weight (mg) (log2)
Ex vivo signal (log2)
10
5
0
12
14
16
18

B.

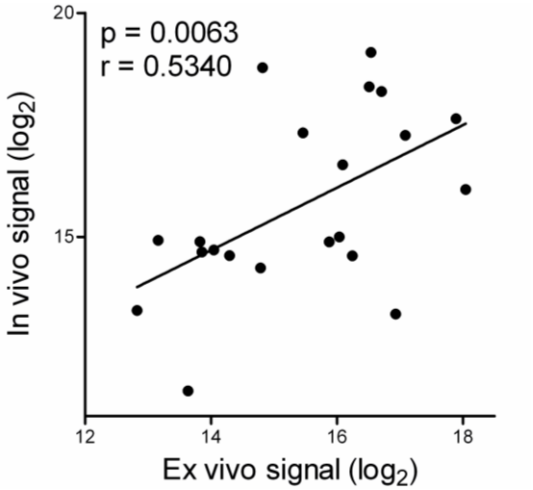
p = 0.0063
r = 0.5340
In vivo signal (log2)
Ex vivo signal (log2)
20
15
12
14
16
18

C.

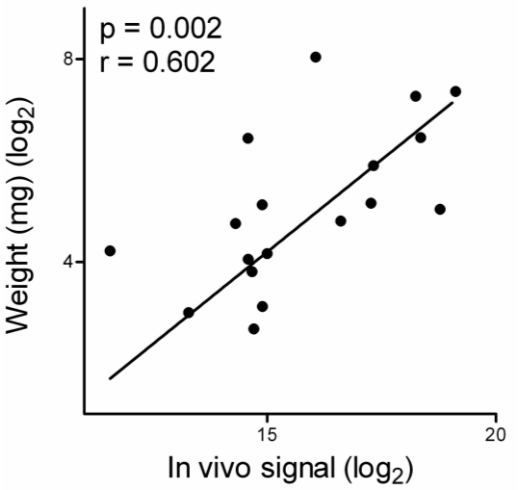
p = 0.002
r = 0.602
Weight (mg) (log2)
In vivo signal (log2)
8
4
15
20

D.

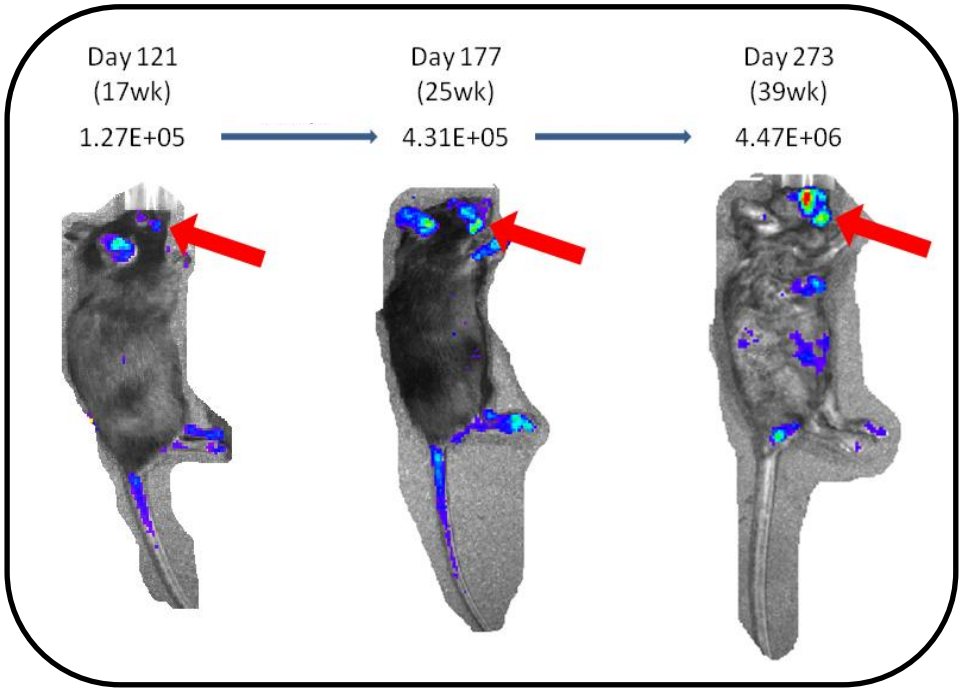
Day 121
(17wk)
1.27E+05
Day 177
(25wk)
4.31E+05
Day 273
(39wk)
4.47E+06

Figure 3.1.6 – Longitudinal monitoring of tumor growth by *in vivo* BLI.
Tumor bioluminescent signals were measured *in vivo* and *ex vivo* and correlation analyses were performed between *in vivo* BL signals, *ex vivo* BL signals, and wet tumor weight. Data demonstrates volumetric detection of tumor growth by BLI. (A) Correlation between *ex vivo* BL signals and wet tumor weight in 38 tumors collected from 3 Centromeric Melucie mice. (B-C) Correlation between *in vivo* and *ex vivo* BL signals (B), and between *in vivo* BL signals and wet tumor weight (C), in a total of 21 tumors collected from a tumor-bearing Centromeric Melucie. All correlation analyses were performed on log transformed values using *Pearson correlation, one-tailed*. (D) BL images of a Centromeric Melucie followed over a period of 39 weeks. Signal intensity was measured from a region of interest drawn around a cheek tumor. The numbers represent the BL signal intensity from a cheek tumor (indicated by an arrow) in photons per second (p/s).

In addition, we investigated whether BLI could detect early primary eye tumor growth in young Melucie mice. The development of primary eye tumors starts approximately at 3 weeks of age and is mostly confined within the choroid layer of the eye. Subsequently, tumors undergo distant metastases to the surrounding areas of the eye, together with local metastases leading to the development of multi-lobular nodules. These primary eye tumors are virtually non-palpable at early stages and their detection relies on clinical examination of exophthalmia (or bulging of the eye). Therefore, the ability of BLI to detect young primary eye tumors will provide a useful means to determine early events of tumor development and to assess response to therapy in our spontaneous mouse model.

In this study, young Melucie mice were analyzed at two different age groups, 2 weeks or 4 weeks, by *in vivo* imaging and *ex vivo* imaging. The presence of tumors was confirmed by histology. As shown in Figure 3.1.7A, no differences were detected between signals emitted *in vivo* and *ex vivo* from both eyes of the mice at 2 weeks of age. Histology confirmed the absence of uveal tumors at this age (Figure 3.1.7B). However, at 4 weeks of age, there was consistently higher signal from one eye compared to the contralateral eye within the same mouse both *in vivo* and *ex vivo* (Figure 3.1.7C). Most importantly, a higher BLI signal correlated with a higher number of tumor nodules as shown by histology (Figure 3.1.7D).

Altogether, we report the successful development of a new transgenic mouse model that permits non-invasive monitoring of spontaneous melanoma tumor

growth in live animals using *in vivo* BLI. Our data clearly demonstrates that the Melucie can be used to detect early events of tumor development and it represents a convenient model for longitudinal monitoring of primary tumor growth and metastases *in vivo*. Furthermore, we believe that the development of Melucie will invariably be an asset for the testing of future chemo-immunotherapeutic strategies against melanoma.

A.

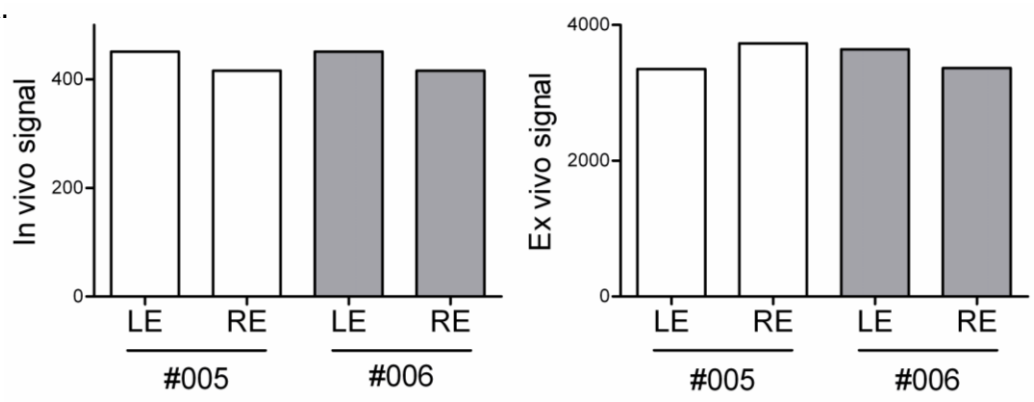
In vivo signal
400
200
0
LE
RE
LE
RE
#005
#006
Ex vivo signal
4000
2000
0
LE
RE
LE
RE
#005
#006

B.

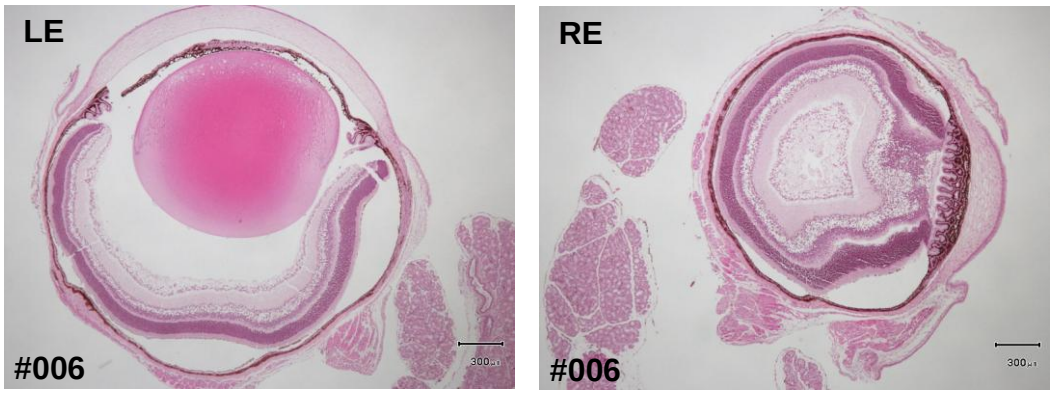
LE
#006
RE
#006

C.

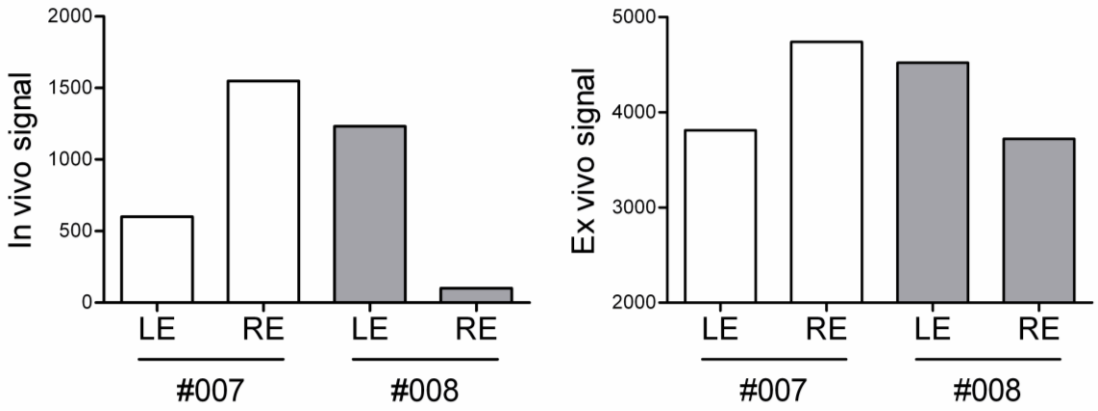
In vivo signal
2000
1500
1000
500
0
LE
RE
LE
RE
#007
#008
Ex vivo signal
5000
4000
3000
2000
LE
RE
LE
RE
#007
#008

D.

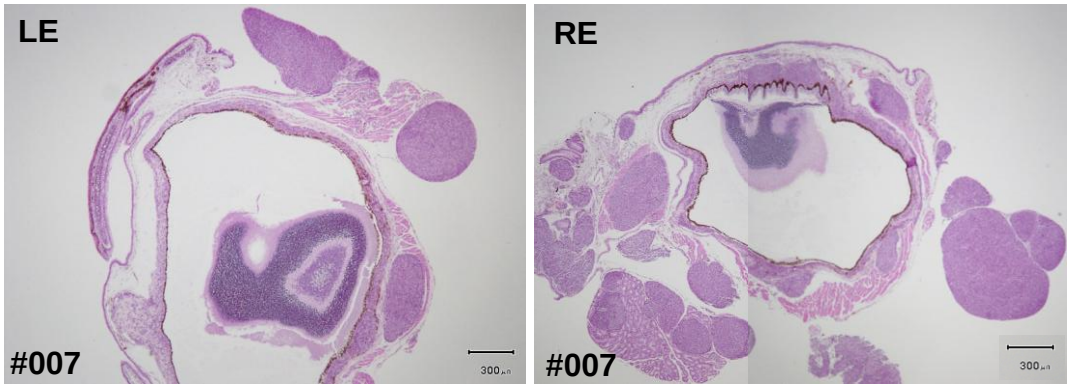
LE
#007
RE
#007

Figure 3.1.7 – Early detection of spontaneous uveal melanoma tumor development by *in vivo* BLI.
To determine the sensitivity of BLI to detect early primary eye tumor development, BLI was performed on contralateral eyes of young Centromeric Melucie mice (2 weeks old, n=2). BL signals were quantified from both the left eye (LE) and right eye (RE) after *in vivo* (A) and *ex vivo* (B) imaging. No difference was observed between the two contralateral eyes both by *in vivo* and *ex vivo* imaging. H&E staining confirm the absence of tumors in the eyes of 2-week old mice. (C) *In vivo* and *ex vivo* BL signals were similarly compared between contralateral eyes in 4 week-old Melucie [n=2]. The presence of tumors in these eye samples was confirmed by H&E staining. Interestingly, higher BL signal detected in right eye from a Centromeric Melucie (denoted #007) was associated with higher number of tumor nodules by H&E staining in the same eye (B and D).

3.2 Chemokines and intra-tumor T cell trafficking in cutaneous mouse melanoma

3.2.1 Distinct immune milieu in cutaneous metastases compared to visceral metastases in RETAAD mice

In the RETAAD mouse model of spontaneous melanoma, $CD8^+$ T cells have been shown to control the outgrowth of visceral metastases and disease progression but have no effect on cutaneous tumors (Eyles et al., 2010; Lengagne et al., 2008). The hypotheses on the lack of control of cutaneous tumors by T cells results from either the absence of T cell infiltration or from the loss of function of infiltrating T cells.

To understand why functional T cells fail to control cutaneous tumors, the tumor microenvironment of both cutaneous [n=19] and visceral metastases [n=10] from tumor-bearing RETAAD mice [n=5] were compared by qRT-PCR for the expression of 35 immune-related genes coding for various cytokines (*Ifng*, *Il*6, *Csf1*, *Csf2*, *Il1rn*, *Il10*, *Mif*, *Tnfa*, *Tgfb*1, *Vegfa*, *Mmp9*), chemokines (*Ccl2*, *Ccl3*, *Ccl5*, *Cxcl10*, *Cxcr4*), immune mediators (*Fizz1*, *Prf1*, *Gzma*, *Nos2*, *Arg1*, *Ltb4*, *Mpo, Anxa1, Cd274*) and lineage markers (*Cd3*, *Cd4*, *Cd8*, *Lck*, *Foxp3*, *Klrk1*, *Ly6g*, *Emr1*, *Mgl1*, *Ela2*).

Non-supervised hierarchical clustering revealed two distinct clusters, one for cutaneous tumors and a separate cluster for visceral metastases (Figure 3.2.1). In the cluster consisting of all the cutaneous tumors analyzed, no particular organization was observed between tumors collected from different parts of the body (eg. facial tumors or body tumors) or between different types of tumors (eg. attached to the skin or embedded within muscle). For visceral

metastases, the majority of the tumors (8 out of 10) cluster together. In particular, all the lung tumors formed a separate sub-cluster, which was distinct from visceral metastases collected from other organs.

Overall, this data demonstrates that cutaneous melanoma metastases display a distinct immune profile compared to visceral metastases and suggests that heterogeneity within the tumor microenvironment might play a role in the differential response to T cell mediated anti-tumor activity.

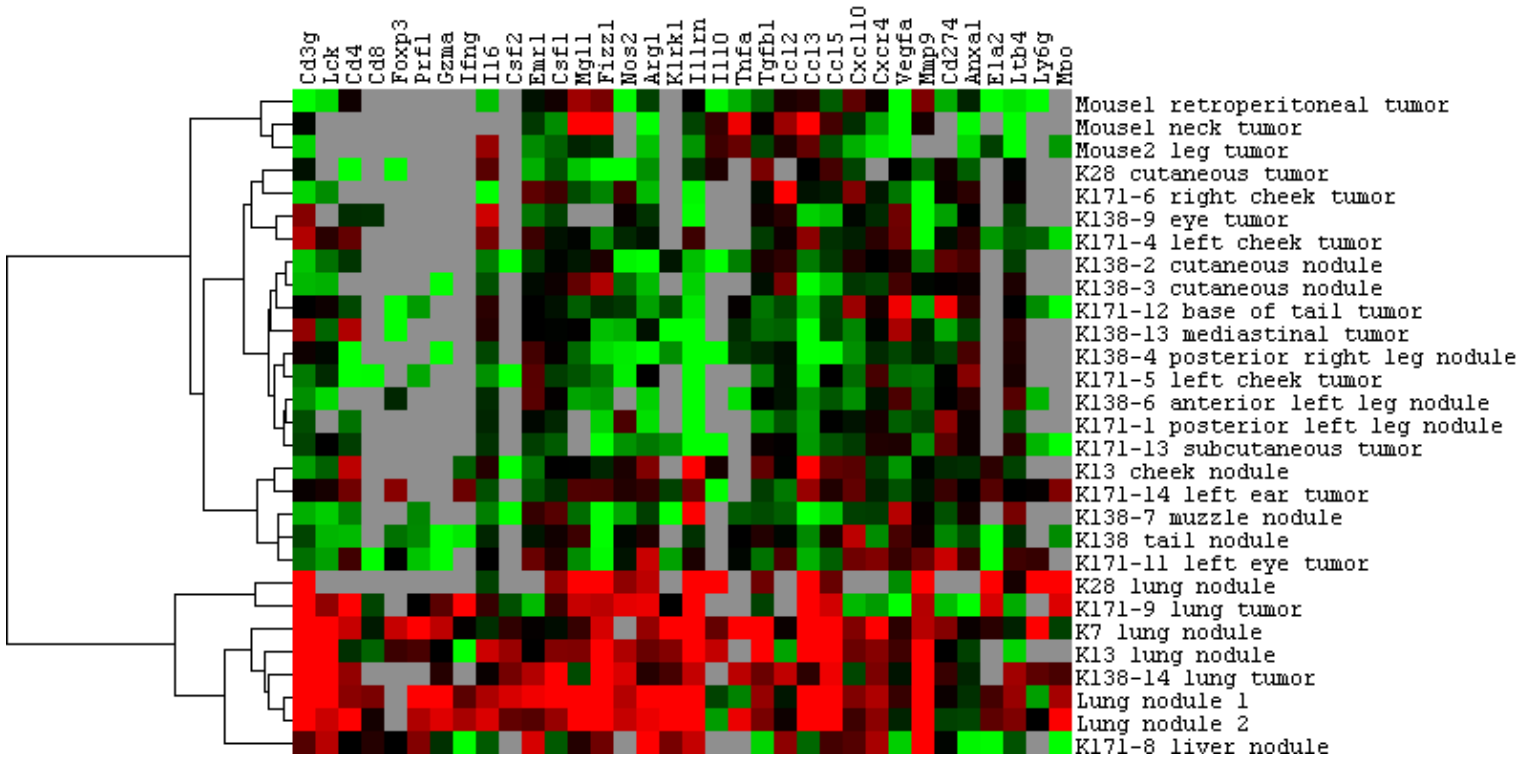

Figure 3.2.1 – Distinct immune milieu in cutaneous melanoma tumors compared to visceral metastases in RETAAD mice.
Non-supervised hierarchical clustering of 35 immune-related genes measured by qRT-PCR in 19 cutaneous tumors and 10 visceral tumors from 5 RETAAD mice. Data are color-coded gene expression compared to the median expression of each gene in all samples. Red – up-regulated; Green – down-regulated; Grey – no data.

3.2.2 Low T cell infiltration in cutaneous metastases

To further identify the immune genes whose expressions are significantly different between cutaneous and visceral metastases, differential gene expression (DGE) analysis was performed. In general, there was a trend for lower expression of immune-related genes in cutaneous tumors compared to visceral metastases (Figure 3.2.2). Among the list of genes analyzed, five immune genes (*Cd3g*, *Csf2*, *Nos2*, *Il1rn*, and *Anxa1*) were differentially expressed between cutaneous and visceral metastases (p-value < 0.05). All of these genes, with the exception of *Anxa1*, were higher in visceral tumors compared to cutaneous tumors. Interestingly, *Cd3g* was the most differentially expressed gene (p-value = 0.012), suggesting that cutaneous tumors contained less T cells compared to visceral tumors.

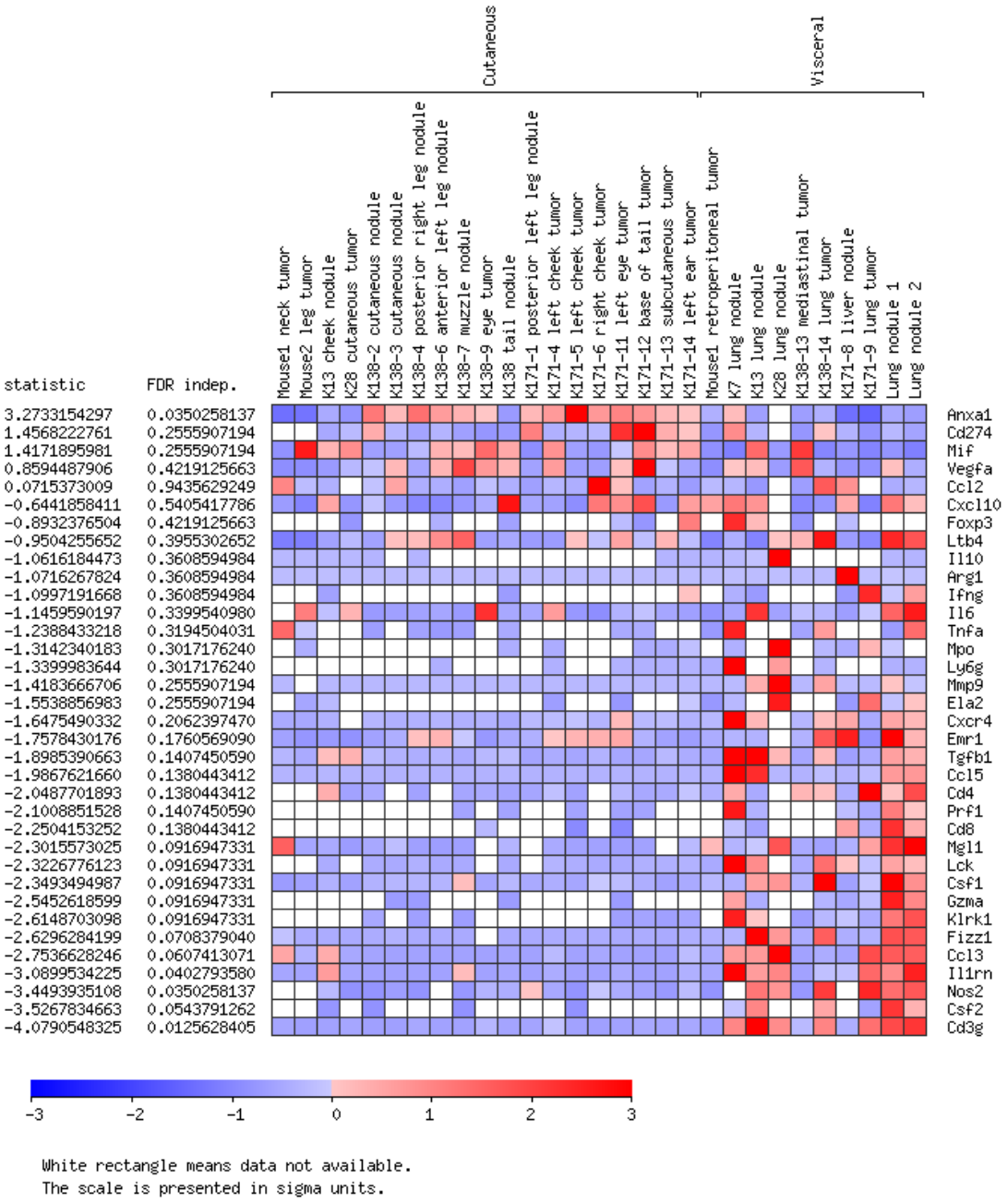

Figure 3.2.2 – Cutaneous tumors expresses low levels of immune-related genes compared to visceral metastases.
The expression of 35 immune-related genes relative to *gapdh* was measured by qRT-PCR in RETAAD cutaneous (n=19) and visceral (n=10) tumors. The relative expression of each gene was normalized against the median expression value of that particular gene, log transformed, and differential gene expression (DEG) analysis was performed using GEPAS 4.0 web-based software. The p-value between groups is indicated by FDR Indep. Most of the immune-related genes analyzed were more highly expressed in visceral metastases compared to cutaneous metastases. Data are color-coded gene expression compared to the median expression of each gene in all samples. Red – up-regulated; Blue – downregulated; White – no data.

To confirm this observation, the expression of other T cell markers (including *Cd4*, *Cd8a* and *Lck*) as well as T cell effector molecules (including *Ifng*, *Prf1b*, and *Gzmb*) were analyzed by qRT-PCR and their expression were found to be significantly lower in cutaneous metastases compared to visceral tumors (Figure 3.2.3A). The expression of both *Cd4* and *Cd8a* was lower in cutaneous tumors (p-values = 0.026 and 0.023), suggesting that both compartments were affected.

To measure T cell infiltration at the protein level, 22 cutaneous tumors and 4 visceral metastases were collected from tumor-bearing RETAAD mice and were compared for the presence of $CD3^+$ T cells by flow cytometry. The median percentage of $CD3^+$ T cells was 2.7 times lower (2-tailed Mann-Whitney test: p-value = 0.04) in cutaneous tumors compared to visceral tumors (Figure 3.2.3B). Immunofluorescent staining of cutaneous tumor sections confirmed that T cells were mostly confined to the peritumoral stroma with little or no infiltration into the tumor nest (Figure 3.2.3C, left). In contrast, T cells infiltrating visceral metastases were widely distributed (Figure 3.2.3C, right).

A.

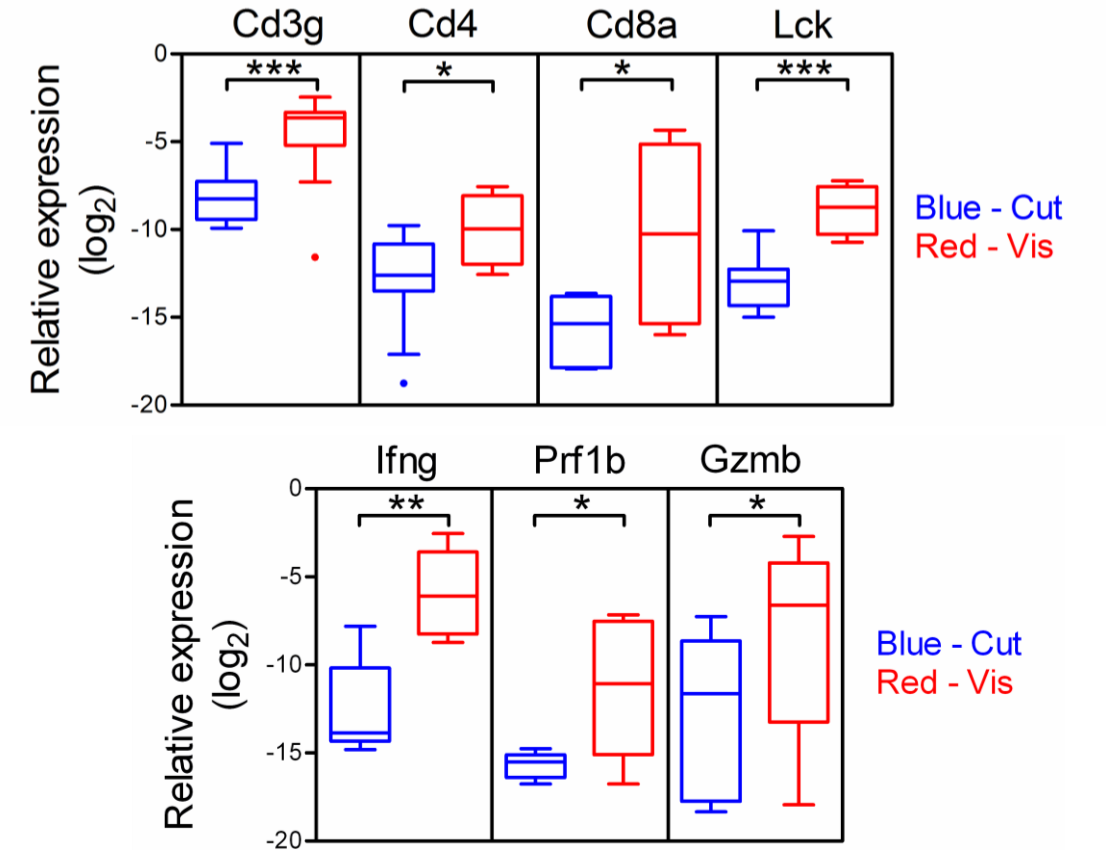
Cd3g
Cd4
Cd8a
Lck
***
*
*
***
Relative expression
(log2)
0
-5
-10
-15
-20
Blue - Cut
Red - Vis
Ifng
Prf1b
Gzmb
**
*
*
Relative expression
(log2)
0
-5
-10
-15
-20
Blue - Cut
Red - Vis

B.

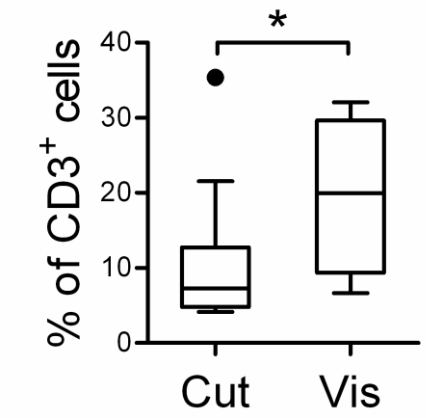
*
% of CD3+ cells
40
30
20
10
0
Cut
Vis

C.

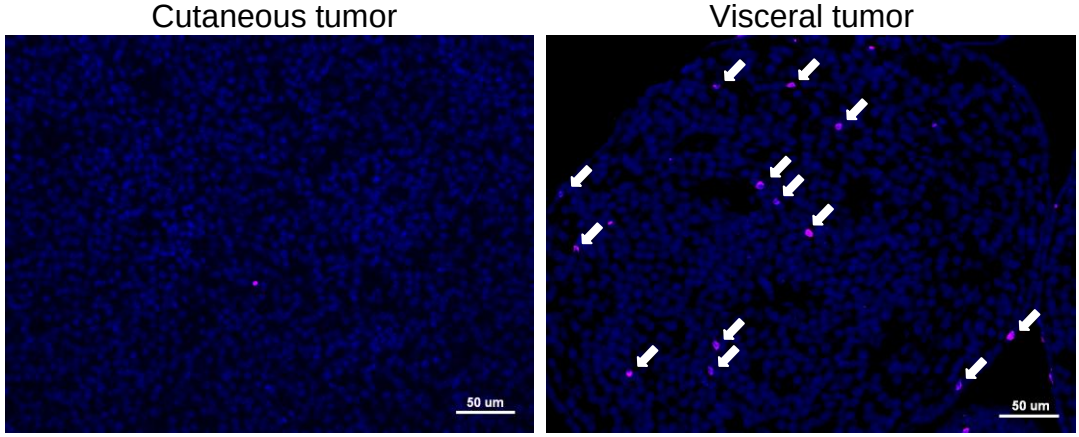
Cutaneous tumor
Visceral tumor
50 um
50 um

Figure 3.2.3 – Low T cell infiltration in cutaneous metastases.
(A) The relative expression of T cell markers (*Cd3g*, *Cd4*, *Cd8a*) and effector molecules (*Ifng*, *Prf1b*, *Gzmb*) to *gapdh* was measured in cutaneous (n=20) and visceral (n=10) tumors. Cutaneous tumors express significantly less T cell-related genes compared to visceral tumors. *Unpaired t-test, two-tailed*. (B) To measure T cell infiltration at the protein level, cutaneous (n=22) and visceral (n=4) tumors were collected from 9 RETAAD mice and analyzed for the presence of $CD3^+$ cells by flow cytometry. Data represents the percentage of $CD3^+$ cells among total live immune cells ($CD45^+DAPI^-$). *Mann-Whitney U test, two-tailed*. (C) Immunofluorescence labeling of CD3 (pink) in RETAAD cutaneous (left panel) and visceral (right panel) tumor. A representative reproductive tract tumor is shown. $CD3^+$ cells were low or absent in the cutaneous tumor bed and were more abundant in visceral tumor. Images are representative of 3 tumors analyzed in each group. Scale bar = 50μm. Statistical significance between groups is represented by * $p<0.05$; ** $p<0.01$; *** $p<0.001$; Cut – Cutaneous; Vis – Visceral.

In some cutaneous tumors, a few infiltrating T cells was observed. To determine whether the few T cells that infiltrated cutaneous tumors retained their functionality, the tumors weights were compared between tumors with different T cell densities. The results demonstrated an inverse correlation between tumor weights and the percentages of $CD3^+$, $CD4^+$ and $CD8^+$ infiltrating cells (Pearson's r coefficient=-0.67; -0.58; -0.64; p-values=0.009; 0.02; 0.01, respectively), suggesting that the few infiltrating T cells were able to control tumor growth (Figure 3.2.4A). In addition, the ratios of *Ifng* to *Cd4* and *Cd8a*, as well as the ratios of *Gzmb* and *Prf1* to *Cd8a* were not significantly different between cutaneous and visceral tumors (Figure 3.2.4B), implying that there was no gross alteration in the functionality of infiltrating T cells in cutaneous tumors.

Taken together, these data demonstrate that both $CD4^+$ and $CD8^+$ T cells poorly infiltrate cutaneous tumors in RETAAD mice. This observation is likely to explain the lack of T cell-mediated control over cutaneous tumors in the RETAAD model.

A.

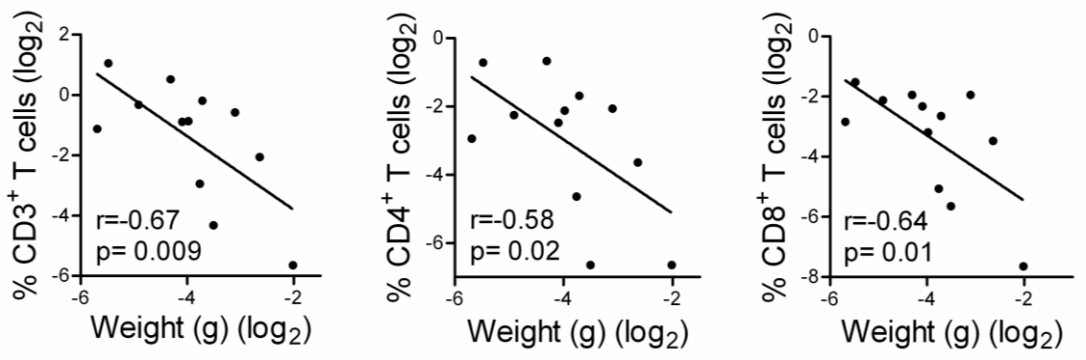

B.

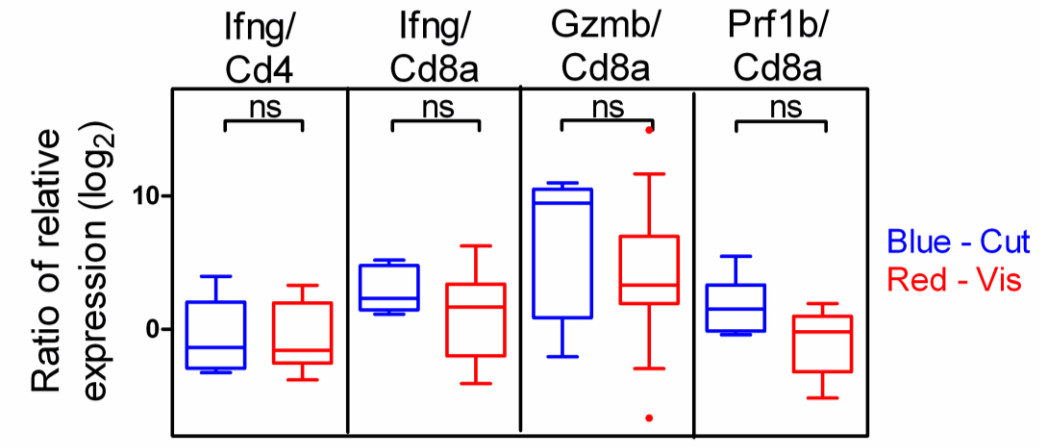

Figure 3.2.4 – The few infiltrating T cells in cutaneous tumors probably retain their functionality.
In a few cutaneous tumors, infiltrating T cells were observed. In order to determine the functionality of these infiltrated T cells, several cutaneous tumors were collected, weighed, and T cell infiltration and T cell effector molecules were measured by flow cytometry and qRT-PCR respectively. (A) Cutaneous tumor weights were compared between tumors with different T cell densities. The percentages of $CD3^+$, $CD4^+$ and $CD8^+$ T cells were inversely correlated with cutaneous tumor weight (n=12). *Pearson correlation, one-tailed.* (B) The ratios of expression of T effector molecules were compared between cutaneous (n=8) and visceral (n=16) tumors. No difference was observed between cutaneous and visceral tumors. *Unpaired t-test, two-tailed.* Statistical significance between groups is represented by * $p<0.05$; ** $p<0.01$; *** $p<0.001$; Cut – Cutaneous; Vis – Visceral.

3.2.3 RETAAD T cells infiltrate exogenous skin tumors

To determine whether the poor infiltration of T cells into cutaneous tumors was due to an intrinsic defect in endogenous T cell migration to the skin or to the tumors themselves, autochthonous RETAAD cutaneous tumors were compared to transplanted B16 cutaneous tumors within the RETAAD mice for the ability of the endogenous T cells to infiltrate into each tumor.

In this transplantation experiment, 200,000 B16 mouse melanoma cells were injected subcutaneously into both flanks of tumor-bearing RETAAD mice. Fourteen days after tumor cell injection, the transplanted B16 and autochthonous RETAAD cutaneous tumors were excised and compared for intra-tumor T cell infiltration by flow cytometry. As shown in Figure 3.2.5, the percentages of $CD3^+$, $CD4^+$ and $CD8^+$ T cells were respectively 11-fold, 9-fold and 11-fold more abundant in B16 than in RETAAD tumors within the same mouse (two-tailed Mann-Whitney p-values < 0.01).

These data show that T cells from RETAAD mice have the capacity to migrate to the skin and to infiltrate cutaneous tumors. Therefore, the paucity of T cells in RETAAD cutaneous tumors is most likely due to the tumor environment being poorly permissive to T cell infiltration.

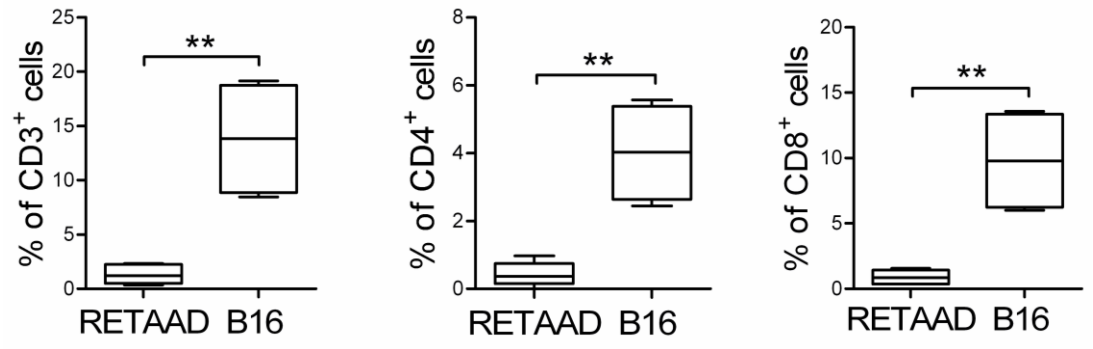

Figure 3.2.5 – RETAAD T cells infiltrate exogenous skin tumors.
B16 cells were injected subcutaneously into both flanks of tumor-bearing RETAAD mice. Fourteen days after injection, transplanted B16 and autochthonous RETAAD skin tumors from the same mice were analyzed for T cell infiltration. Results demonstrate the flow cytometric comparison of T cell infiltrates in transplanted B16 (n=4) and autochthonous RETAAD (n=6) skin tumors from the same mice. Data show the percentages of $CD3^+$, $CD4^+$ and $CD8^+$ T cells within total live cells. *Mann-Whitney U test, two-tailed*. Statistical significance between groups is represented by ** $p < 0.01$.

3.2.4 T cell infiltration of exogenous tumors correlates with high chemokine expression

Chemokines present in the tumors are likely to play a major role in T cell recruitment. Therefore, the repertoire of chemokine expression was compared between autochthonous RETAAD skin tumors and transplanted B16 skin tumors grown in RETAAD mice using low density PCR arrays. Thirty-nine genes including 26 chemokines and 13 chemokine receptors involved in inflammation were analyzed by qRT-PCR. As shown in Figure 3.2.6A, 14 out of 26 chemokine genes analyzed were differentially expressed in transplanted B16 compared to autochthonous RETAAD tumors (open squares; p-value < 0.05, fold-change > 2), with the vast majority of these chemokines (12 out of 14) being more highly expressed in B16 tumors. Among the list of differentially expressed chemokines, *Cxcl9* and *Cxcl10* were the two most differentially expressed chemokines, with 105- and 42-fold greater expression in B16 tumors, respectively. Five additional chemokines, *Ccl2*, *Ccl3*, *Ccl4*, *Ccl7* and *Cxcl5* were at least 10-fold more highly expressed in B16 tumors than in autochthonous RETAAD tumors.

To gain further insight into the possible roles of these differentially expressed chemokines in T cell recruitment, the expression of the corresponding chemokine receptors on peripheral blood T cells from RETAAD mice were analyzed by flow cytometry. The surface expression of the chemokine receptors CCR1, CCR2, CCR3, CCR5 and CXCR3 was analyzed on naïve, central memory and effector memory T cells subsets for both $CD4^+$ and $CD8^+$ T cells. The chemokine receptor CXCR3 was highly expressed by several subsets of circulating T cells while CCR1, CCR3 and CCR5 were only

expressed at marginal levels (Figure 3.2.6B). CCR2 was expressed by 25 ± 2% of effector memory $CD4^+$ T cells (Figure 3.2.6B). Within the $CD4^+$ T cells, 4 ± 1.9% of the central memory and 58 ± 10% of the effector memory cells expressed CXCR3, while among the $CD8^+$ T cell population, 93 ± 3.6% of the central memory and 75 ± 5.7% of the effector memory cells expressed CXCR3 (Figure 3.2.6C). CXCR3 has only 3 known ligands, CXCL9, CXCL10 and CXCL11. Therefore, these results strongly suggest a role for CXCL9 and CXCL10 in T cell recruitment into cutaneous melanoma tumors.

Having demonstrated a critical role of chemokines in T cell recruitment into cutaneous tumors, it was of interest to understand whether differential T cell recruitment between autochthonous cutaneous and visceral tumors could also be explained by inherent differences in local chemokine expression. Therefore, the profile of chemokine expression was compared by qRT-PCR between cutaneous tumors [n=9] and visceral tumors [n=7] collected from RETAAD mice [n=3]. As shown in Figure 3.2.6D, 4 chemokine genes and 5 chemokine receptor genes were more than 2-fold differentially expressed between cutaneous and visceral tumors, with all of the genes having greater expression in visceral tumors. This includes the chemokines *Ccl20*, *Ccl22*, *Ccl24* and *Ccl5*, as well as the chemokine receptors *Cxcr5*, *Ccr6*, *Ccr7*, *Ccr8*, and *Xcr1*. Interestingly, a distinct panel of chemokines and chemokine receptors were involved in T cell recruitment into visceral tumors in RETAAD mice.

Taken together, these results demonstrate that chemokines are critical local factors that determine effective T cell recruitment into cutaneous melanoma and suggest that different chemokines might dictate T cell recruitment into distinct tumor tissues.

A.

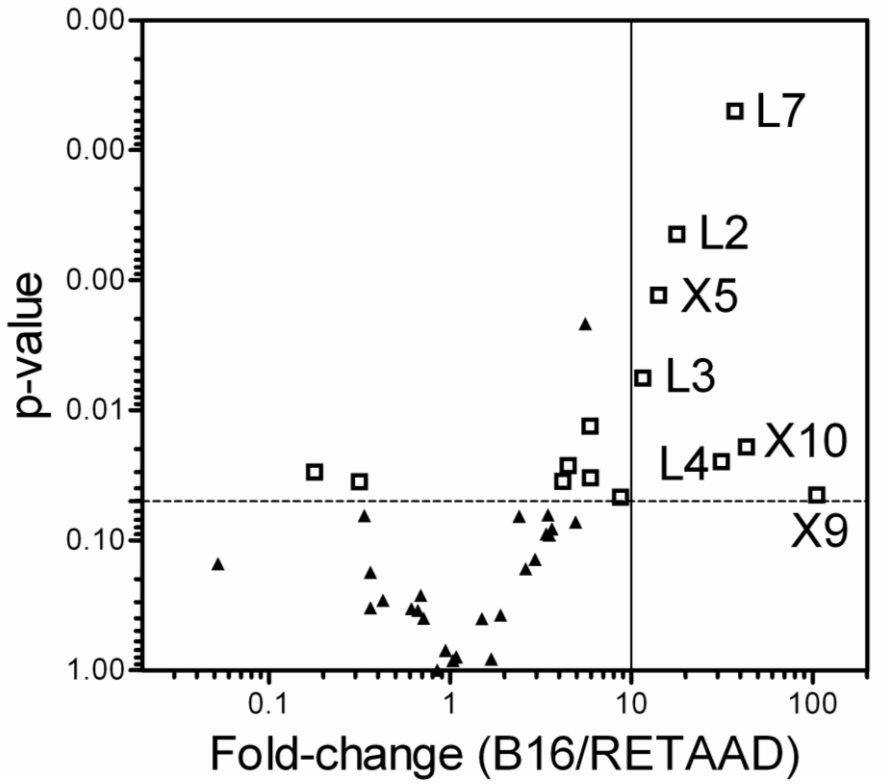
0.00
0.00
0.00
0.01
0.10
1.00
p-value
0.1
1
10
100
Fold-change (B16/RETAAD)
L7
L2
X5
L3
X10
L4
X9

B.

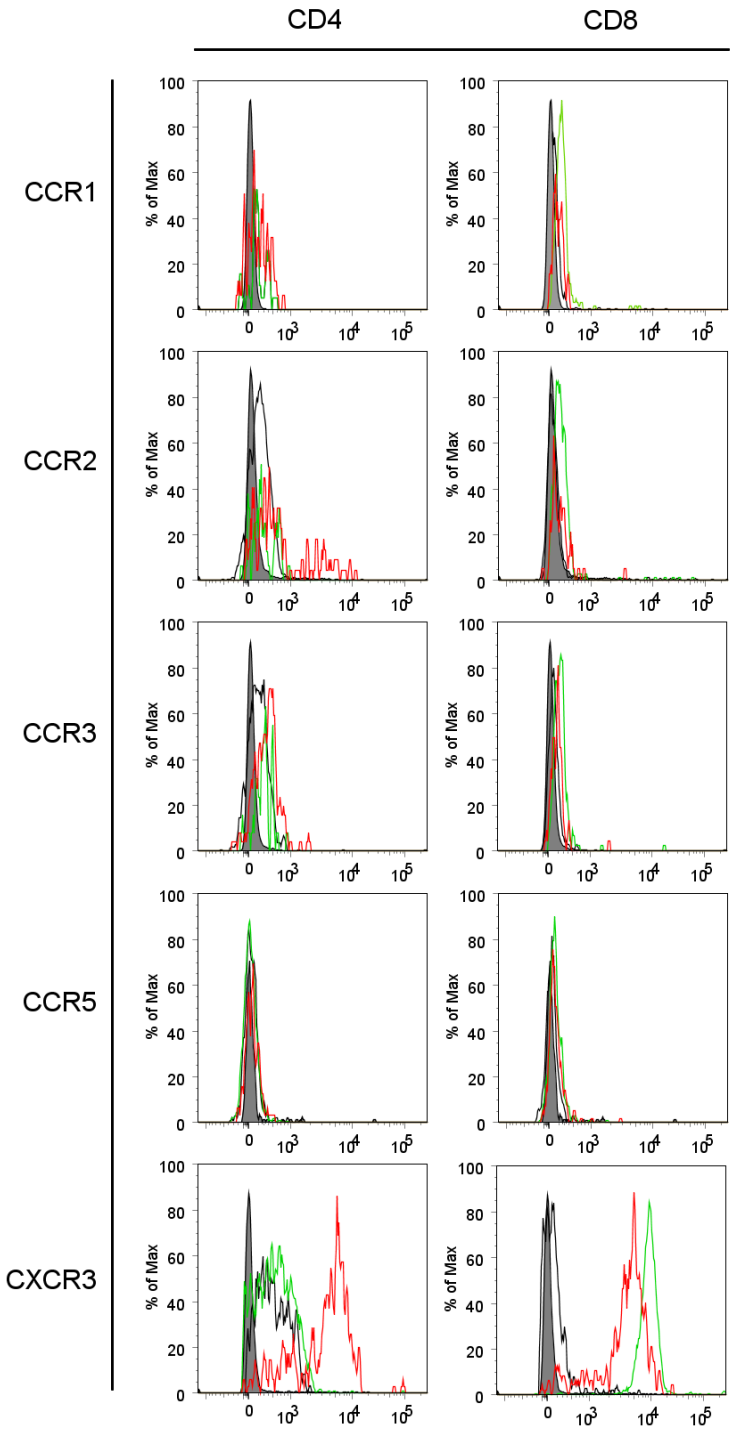
CD4
CD8
CCR1
CCR2
CCR3
CCR5
CXCR3
% of Max

C.

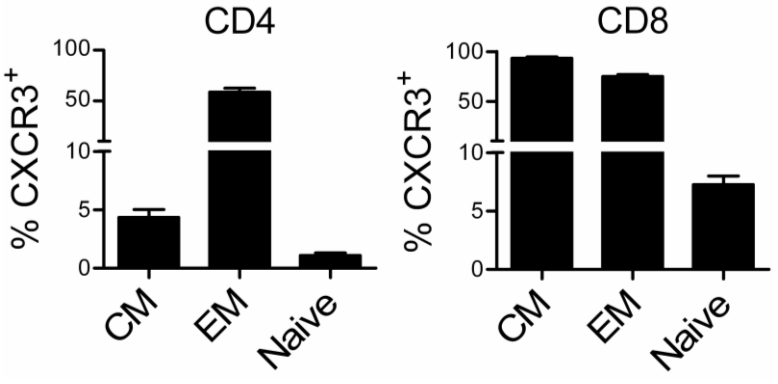
CD4
CD8
% CXCR3+
CM
EM
Naive

D.

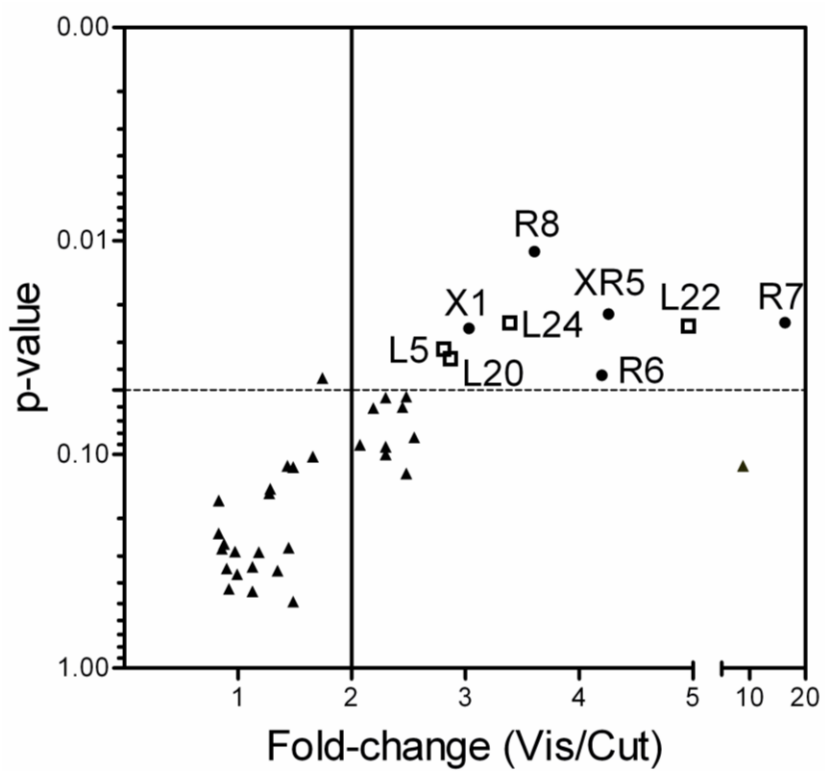

Figure 3.2.6 – T cell infiltration into tumors correlates with intra-tumoral chemokine expression.
(A) Intra-tumoral expression of chemokine and chemokine receptor genes in autochthonous and transplanted skin tumors. Volcano plot shows fold-change in gene expression in B16 skin tumors grown in RETAAD mice [n=3] compared to autochthonous RETAAD skin tumors [n=5]. Open square represent chemokine genes with > 2-fold differential expression and p-value < 0.05. Horizontal line shows p-value = 0.05. Vertical line represents 10-fold increase in B16 compared to RETAAD tumors. L2, L3, L4, L7, X5, X9 and X10 indicates the chemokine genes *Ccl2*, *Ccl3, Ccl4, Ccl7*, *Cxcl5*, *Cxcl9*, and *Cxcl10* respectively. (B) Surface expression of chemokine receptors on $CD4^+$ and $CD8^+$ T cells was analyzed in peripheral blood collected from RETAAD mice. Data are representative of 8 mice analyzed. Grey filled histogram – Isotype control; Black solid line – Naïve ($CD44^-$ $CD62L^+$); Red solid line – Effector memory ($CD44^+$ $CD62L^-$); Green solid line – Central memory ($CD44^+$ $CD62L^+$). (C) Percentages of $CXCR3^+$ cells within $CD4^+$ and $CD8^+$ T cell subsets of RETAAD mice (n=8). CM – Central Memory; EM – Effector Memory. (D) Intra-tumoral expression of chemokine and chemokine receptor genes in autochthonous cutaneous and visceral tumors. Volcano plot shows fold-change in gene expression in visceral tumors [n=7] compared to cutaneous tumors [n=9] in RETAAD mice. Open square and solid circles represent chemokine genes and chemokine receptor genes respectively, with > 2-fold differential expression and p-value < 0.05. Horizontal line shows p-value = 0.05. Vertical line represents 2-fold increase in visceral tumors compared to cutaneous tumors. The symbols L5, L20, L22 and L24 represents the chemokines genes *Ccl5*, *Ccl20*, *Ccl22* and *Ccl24* respectively while X1, XR5, R6, R7 and R8 represents the chemokine receptor genes *Xcr1*, *Cxcr5*, *Ccr6*, *Ccr7* and *Ccr8* respectively.

3.2.5 Transfection of RETAAD skin tumors with *Cxcl9* induces T cell infiltration

To directly demonstrate the role of CXCR3 ligands in T cell recruitment, established RETAAD autochthonous tumors were transfected with a plasmid encoding CXCL9. RETAAD mice bearing multiple cutaneous metastases (median weight = 60mg) were selected for this experiment. Three intra-tumoral injections were performed on alternate days. In each mouse, one or two tumors were injected with the CXCL9-encoding plasmid and one or two tumors were injected with a control plasmid. On day 6, tumors were excised, weighed and T cell infiltration was assessed by flow cytometry. The expression of *Cxcl9* in situ in tumor beds was confirmed by qRT-PCR (Figure 3.2.7A). The expression of *Cxcl10* was included as a negative control (Figure 3.2.7A). As shown in Figure 3.2.7B, CXCL9 transfection resulted in a 6-fold increase in both $CD4^+$ and $CD8^+$ T cell infiltration into RETAAD cutaneous tumors (one-tail Mann-Whitney p-value = 0.0026 and 0.0025 respectively). Injection of the control plasmid did not significantly alter the T cell infiltrate (Figure 3.2.7C).

To further characterize CXCL9-recruited T cells, the percentage of $CD44^+$ cells (a marker of memory T cells) among the $CD4^+$ and $CD8^+$ TIL were measured by flow cytometry. As shown in Figure 3.2.7D, the mean percentages of CD44-expressing $CD4^+$ and $CD8^+$ T cells were 99.2 ± 0.6% and 92.8 ± 9.9%, respectively. In addition, the expression of several effector molecules was measured by qRT-PCR. The expression of *Ifng*, *Gzma* and *Gzmb* was increased in CXCL9-treated tumors compared to control tumors by 7-, 5- and 5-fold, respectively (one-tailed t test p-values = 0.006, 0.01 and

0.02, respectively) (Figure 3.2.7E). Moreover, using flow cytometry, there was a 43% increase in tumor cell death (one-tailed Mann-Whitney p-value = 0.03) in treated tumors compared to control tumors (Figure 3.2.7F).

Taken together, these observations show that CXCL9 attracts effector T cells exhibiting type 1 polarization and cytotoxic potential.

A.

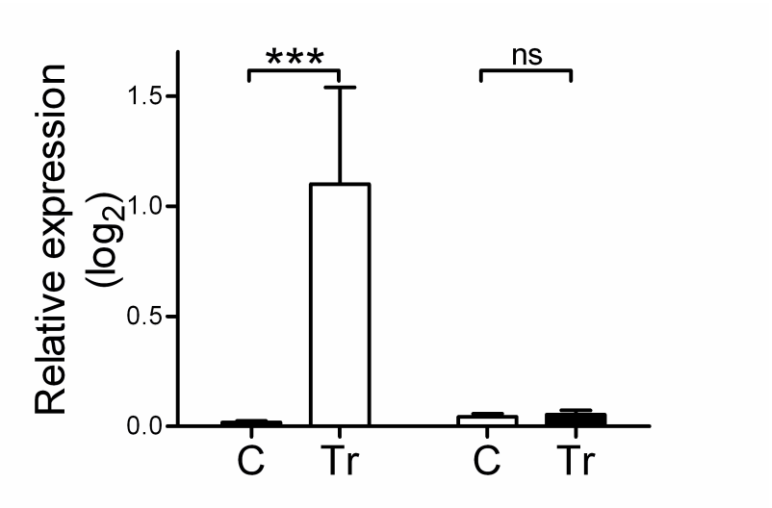
***
ns
Relative expression (log2)
1.5
1.0
0.5
0.0
C
Tr
C
Tr

B.

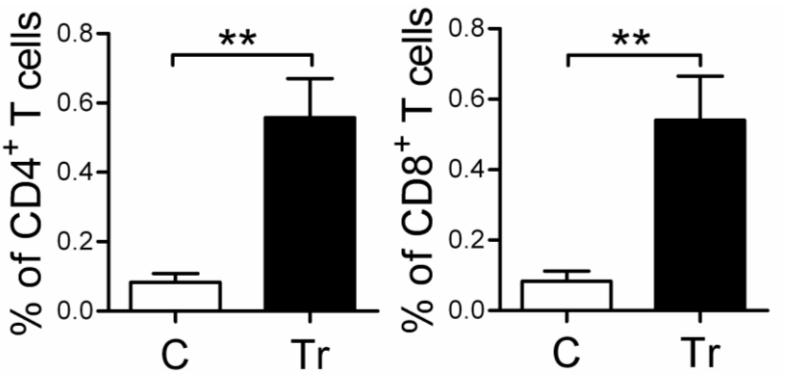
**
% of CD4+ T cells
0.8
0.6
0.4
0.2
0.0
C
Tr
**
% of CD8+ T cells
0.8
0.6
0.4
0.2
0.0
C
Tr

C.

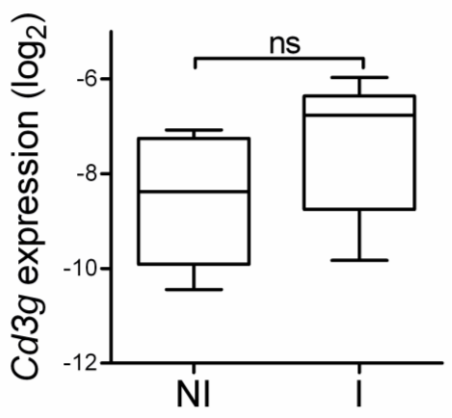
ns
Cd3g expression (log2)
-6
-8
-10
-12
NI
I

D.

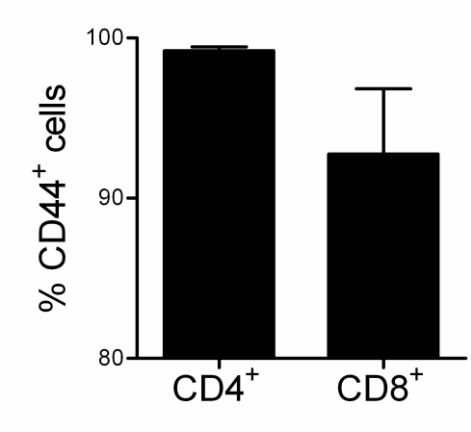
% CD44+ cells
100
90
80
CD4+
CD8+

E.

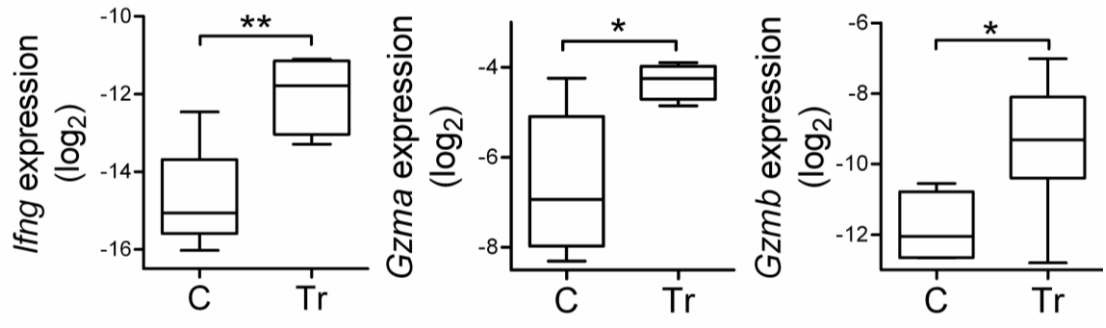

F.

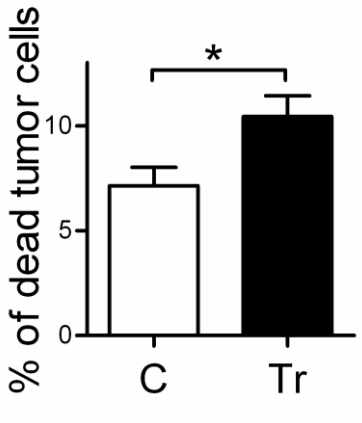

Figure 3.2.7 – Transfection of *Cxcl9* induces T cell infiltration in RETAAD cutaneous tumors.

Cxcl9-encoding or control plasmids (5µg) were injected into established RETAAD cutaneous tumors three times on alternate days. On day 6, tumors were analyzed for T cell infiltration. (A) Relative expression of *Cxcl9* to *Gadph* in tumors after *Cxcl9*-transfection [n=5] was confirmed by qRT-PCR. Relative expression of *Cxcl10* was shown as a negative control. *Unpaired t-test, one-tailed.* (B) The percentages of $CD4^+$ and $CD8^+$ T cells among total live cells in *Cxcl9*-treated tumors [n=5] and control tumors [n=7] were determined using flow cytometry. *Mann-Whitney U test, one-tailed.* (C) The relative expression of *Cd3g* to *Gapdh* measured by qRT-PCR between non-injected tumors [n=5] and tumors injected with control plasmid. [n=7]. NI = Non-Injected; I = Injected. *Unpaired t-test, one-tailed*. (D) Percentages of $CD44^+$ cells among $CD4^+$ and $CD8^+$ tumor-infiltrating T cells in *Cxcl9*-transfected tumors [n=5]. (E) Relative expression of several effector molecules, i.e. *Ifng*, *Gzma*, and *Gzmb* in *Cxcl9*-treated [n=8] and control tumors [n=5]. *Unpaired t-test, one-tailed*. (F) Percentage of dead tumor cells ($CD45^-DAPI^+/CD45^-$) in *Cxcl9*-treated [n=5] and control [n=5] tumors. *Mann-Whitney U test, one-tailed.* Data shown are representative of three different experiments. Statistical significance between treated and control groups is represented by *** $p<0.001$, ** $p<0.01$, * $p<0.05$. C – Control, Tr – Transfected.

3.2.6 *Cxcl9* expression inhibits exogenous tumor growth in a T cell-dependent manner

To investigate whether ectopic expression of *Cxcl9* could control tumor growth *in vivo*, *Cxcl9* transfection was performed on Melan-ret cells, a tumor cell line derived from a RETAAD cutaneous tumor. In this experiment, *Cxcl9*-transfected cells were injected subcutaneously into syngeneic C57BL/6 mice and tumor growth was monitored every two to three days for 16 days. The results showed that *Cxcl9*-expressing tumor cells demonstrated severely impaired tumor growth compared to control cells and tumor formation was even abolished in two out of five mice (Figure 3.2.8A). Mice were euthanized at day 16, and tumors were collected and weighed, and T cell infiltration was analyzed by qRT-PCR. As shown in Figure 3.2.8B, *Cxcl9*-expressing Melan-ret tumors were on average 10 times smaller (one-tailed Mann-Whitney p-value = 0.004; mean weight = 0.14g vs 0.014g) than control tumors, and this was associated with a 4-fold increase in *Cxcl9* expression and a 3-fold increase in *Cd3g* expression within the transfected tumors (Figure 3.2.8C). When the same experiment was repeated in $Rag1^{-/-}$ mice, there was no significant difference in the growth of *Cxcl9*-transfected and control Melan-ret tumors (Figure 3.2.8D). These data demonstrate that *Cxcl9* expression inhibits tumor growth and that this inhibition is dependent on a lymphoid cell population.

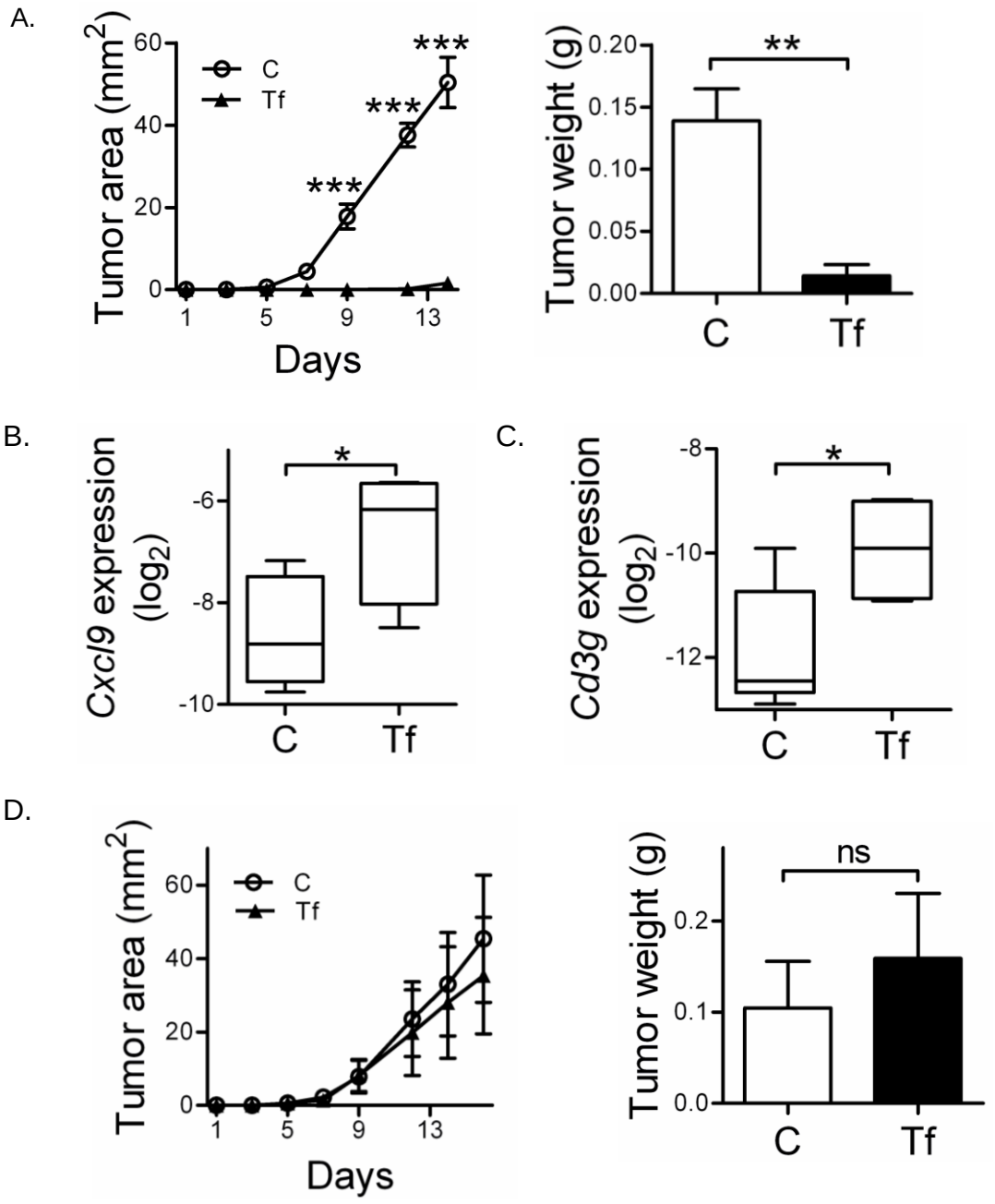

Figure 3.2.8 – Ectopic expression of *Cxcl9* inhibits tumor growth in a T-cell dependent manner.
Melan-ret cells were transfected with a CXCL9-encoding plasmid and injected subcutaneously into both flanks of C57BL/6 mice [n=5]. (A) Tumor size was measured every 2-3 days. Statistical analysis was carried out using two-way ANOVA, two-tailed. At necropsy on day 16, Cxcl9-transfected tumors [n=3] and control tumors [n=5] were collected and weighed. *Mann-Whitney U test, one-tailed*. (B-C) The expression of *Cxcl9* and *Cd3g* was measured by qRT-PCR in *Cxcl9*-transfected and control tumors. *Unpaired t-test, two-tailed.* (D) Tumor growth curves and tumor weights of *Cxcl9*-transfected [n=5] and control [n=5] tumors in Rag1$^{-/-}$ mice. *Two-way ANOVA, two-tailed* and *Mann-Whitney U test, one-tailed*. All data shown are from three independent experiments. Statistical differences between groups are represented by *** p<0.001; ** p<0.01; * p<0.05; ns=non-significant. C – Control; Tf – Transfected.

3.2.7 *Ccl5* synergizes with *Cxcl9* to recruit T cells

Knowing that CXCL9 promotes T cell recruitment and that chemokines often act in concert, the next question asked was whether other chemokines that were expressed in RETAAD tumors were also involved in T cell infiltration. By comparing a set of 33 cutaneous and visceral tumors, *Ccl5* expression was found to be highly correlated with *Cd3g* expression (Pearson's r coefficient = 0.65, p-value = 4.75E-6) (Figure 3.2.9A). CCL5 is the most potent T cell chemoattractant. However, surprisingly, RETAAD circulating T cells express very low levels of the known receptors of CCL5, namely CCR1, -3 and -5 (Figure 3.2.6B). Therefore, secretion of CCL5 by the T cells and/or tumor cells may account for the observed correlation. Alternatively, CCL5 might play an indirect role in T cell attraction, for example by synergizing with CXCR3 ligands.

To test the latter hypothesis, RETAAD cutaneous tumors were transfected with a plasmid encoding either CCL5 alone, CXCL9 alone, or a combination of both plasmids. Suboptimal doses of the CXCL9 plasmid were used. Three injections were performed on alternate days for four days. On day six, the mice were euthanized and the tumors were harvested, weighed and *Cd3g* expression was analyzed by qRT-PCR. As shown in Figure 3.2.9B, treatment with CCL5 plasmid alone did not lead to a significant enhancement in *Cd3g* expression in the treated tumors compared to control tumors. Similarly, treatment with suboptimal doses of CXCL9 plasmid had only a marginal effect. However, a combination of both CCL5 and CXCL9 resulted in a synergistic increase in *Cd3g* expression within the tumors (one-way ANOVA p-value <

0.0001). At the protein level, similar results were obtained using flow cytometry analyses. Specifically, co-transfection of CCL5 and CXCL9 led to a significant increase in $CD3^+$ T cells and $CD4^+$ T cells, when compared to CXCL9 alone (p=0.03 and 0.015, respectively). A similar trend was observed for $CD8^+$ T cells (p=0.051) (Figure 3.2.9C).

This increased infiltration of T cells in tumors co-injected with CCL5 and CXCL9 plasmids was not due to CCL5-mediated increase in CXCL9 production as no difference was observed between the levels of *Cxcl9* expression between the *Cxcl9*-injected and co-injected tumors (Figure 3.2.9C). Conversely, T cells may undergo changes in chemokine receptor expression upon infiltration into the tumor. Therefore, surface expression of CCR5 and CXCR3 was compared between TIL (n=16) and blood lymphocytes (n=6). As shown in Figure 3.2.9D, CXCR3 expression was significantly down-regulated on both $CD4^+$ and $CD8^+$ T cells in the tumor compared to the blood by 11% and 27.5% respectively. Interestingly, a small but reproducible increase in the percentage of CCR5-expressing $CD4^+$ and $CD8^+$ (40% and 80% increase, respectively) were detected in TIL compared to blood lymphocytes (Figure 3.2.9E).

Altogether, these data demonstrate a clear synergy between CXCL9 and CCL5 in T cell recruitment and suggest that CCR5 expression on TIL, due to either an upregulation of CCR5 or a preferential recruitment of the few CCR5-expressing T cells in the circulation, into the tumor microenvironment may favor T cell retention in CCL5-expressing tumors.

A.

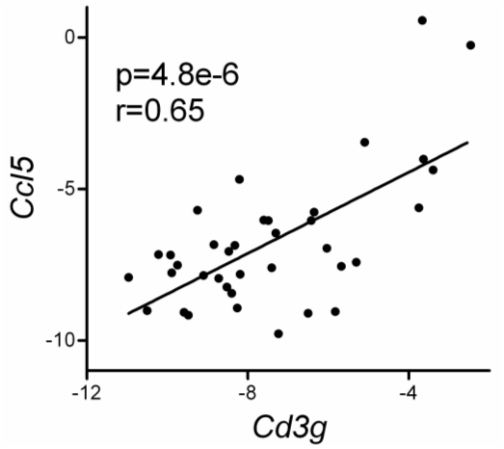
p=4.8e-6
r=0.65
Ccl5
Cd3g
0
-5
-10
-12
-8
-4

B.

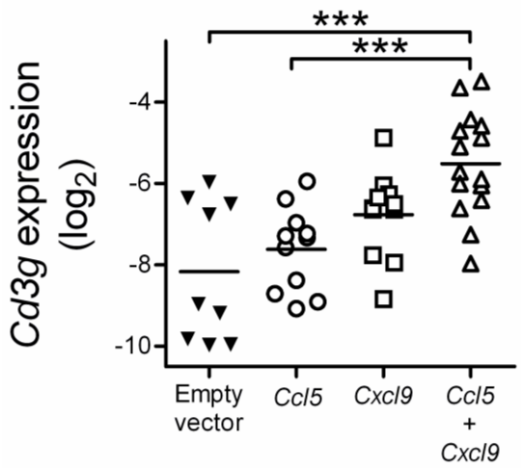
***
***
Cd3g expression (log2)
-4
-6
-8
-10
Empty vector
Ccl5
Cxcl9
Ccl5 + Cxcl9

C.

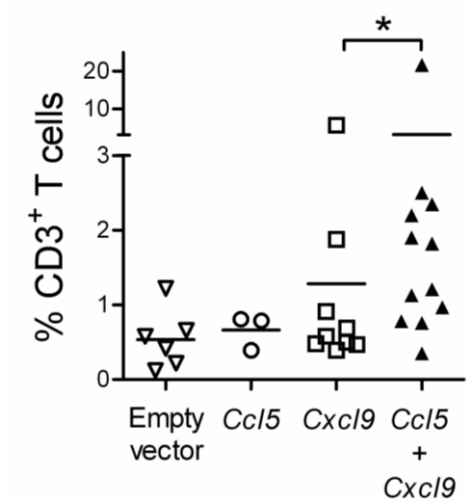
*
% CD3+ T cells
20
10
3
2
1
0
Empty vector
Ccl5
Cxcl9
Ccl5 + Cxcl9

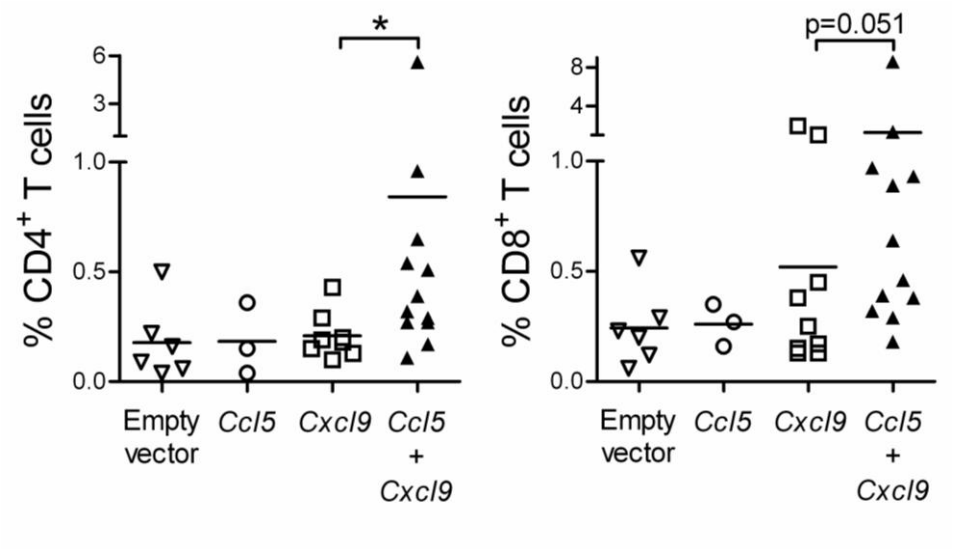
*
% CD4+ T cells
6
3
1.0
0.5
0.0
Empty vector
Ccl5
Cxcl9
Ccl5 + Cxcl9
p=0.051
% CD8+ T cells
8
4
1.0
0.5
0.0
Empty vector
Ccl5
Cxcl9
Ccl5 + Cxcl9

D.

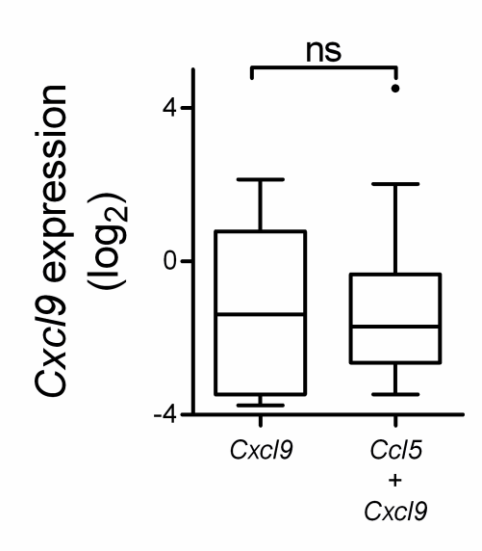
ns
Cxcl9 expression (log2)
4
0
-4
Cxcl9
Ccl5 + Cxcl9

E.

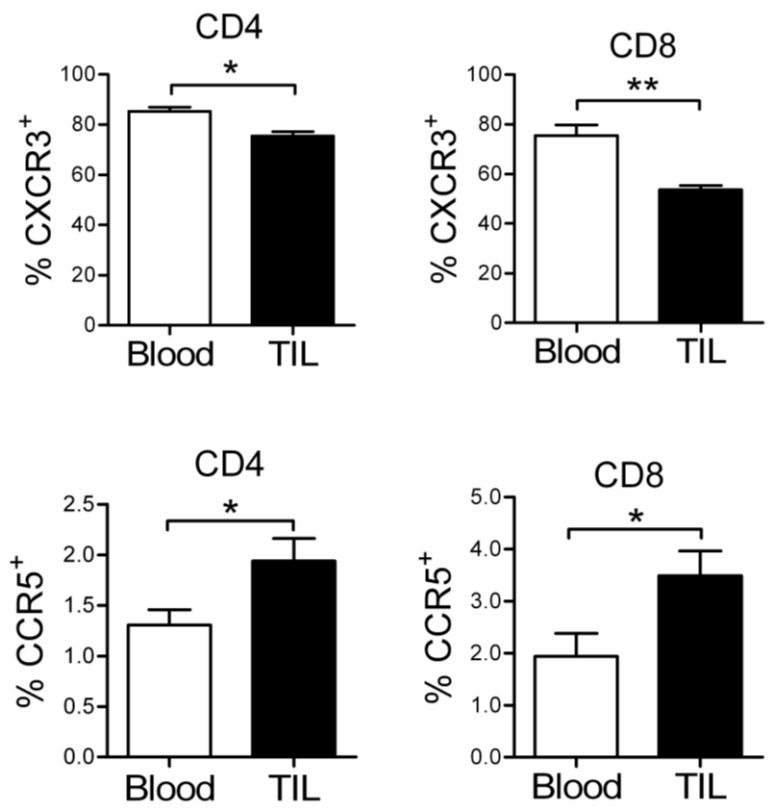
CD4
*
% CXCR3+
100
80
60
40
20
0
Blood
TIL
CD8
**
% CXCR3+
CD4
*
% CCR5+
2.5
2.0
1.5
1.0
0.5
0.0
CD8
*
% CCR5+
5.0
4.0
3.0
2.0
1.0
0.0

Figure 3.2.9 – *Ccl5* synergizes with *Cxcl9* to recruit T cells.
(A) A total of 37 cutaneous and visceral tumors were collected from 15 tumor-bearing RETAAD mice and analyzed for the expression of *Cd3g* and *Ccl5* by qRT-PCR. *Cd3g* expression was strongly correlated with *Ccl5* expression. *Pearson correlation, one-tailed*. (B-E) RETAAD cutaneous tumors were injected with 2.5µg of plasmid DNA encoding either CCL5 [n=10], CXCL9 [n=11], a combination of both plasmids [n=15], or control plasmid [n=9], on alternate days for 5 days. On day six, the tumors were analyzed for T cell infiltration. (B) The mean relative expression of *Cd3g* to *Gapdh* was compared by ANOVA and Bonferroni's multiple comparison post test. (C) The mean percentages of $CD3^+$, $CD4^+$ and $CD8^+$ T cells over live immune cells ($CD45^+$ $DAPI^-$) were compared between *Cxcl9*-injected and co-injected tumors. *Mann-Whitney U test, one-tailed*. (D) Relative expression of *Cxcl9* to *Gapdh* measured by qRT-PCR in *Cxcl9*-injected and co-injected tumors. *Unpaired t-test, one-tailed*. Surface expression of CXCR3 (E) and CCR5 (F) on $CD4^+$ and $CD8^+$ T cells in peripheral blood [n=6] and TIL [n=16] by flow cytometry. *Mann-Whitney U test, one-tailed*. All data are representative of three independent experiments. Statistical significance is shown by *** $p<0.001$; ** $p < 0.01$; * $p<0.05$.

3.3 Chemokines and intra-tumoral T cell trafficking in cutaneous human melanoma

3.3.1 Chemotherapeutic drugs induces chemokine production in human melanoma cell lines

Chemotherapy is known to alter the transcriptome of cancer cells and has been reported to modify their profile of chemokine secretion (Levina et al., 2008). Therefore, three chemotherapeutic drugs commonly used to treat stage IV melanoma (temozolomide, cisplatin and dacarbazine) were tested for their ability to induce T cell-attracting chemokines *in vitro*.

Five human melanoma cell lines (HTB-71, M88, M102, M131 and M134) were included in the study. Transcription of the *CXCL9*, *CXCL10* and *CCL5* genes was measured by qRT-PCR 72h after drug treatment. As shown in Figure 3.3.1A, each drug and each cell line displayed a unique pattern of chemokine expression; at least two T cell-attracting chemokines were actively transcribed in all cell lines after treatment with at least one drug. Temozolomide strongly induced all three chemokines in M102 and M134, and *CXCL10* in HTB-71 and M131 (more than 10-fold increase). Cisplatin induced all three chemokines in M102 but only the CXCR3 ligands in M134 and *CXCL10* in M88. Dacarbazine induced all three chemokines in HTB-71.

Dose-response relationships were observed for temozolomide and cisplatin (Figure 3.3.1B), but no reproducible dose-response relationships were observed for dacarbazine. This is likely due to the fact that dacarbazine requires conversion into the active metabolite 5-(3-methyltriazen-1-yl)imidazole-4-carboxamide (MTIC), which relies on spontaneous catalytic

reaction *in vitro* while liver enzymatic activity carries out this step *in vivo*. Therefore, the subsequent experiments focused on temozolomide (which shares the same active metabolite as dacarbazine) and cisplatin.

Time course experiments were performed to determine the kinetics of chemokine expression after drug treatment. Figure 3.1.1C shows the kinetics of *CCL5*, *CXCL9* and *CXCL10* induction in M102 cells following treatment with 100µg/ml temozolomide. Transcription of *CXCL10* was detectable as soon as 24h after treatment, while *CCL5* and *CXCL9* transcription was only detected at 48h and 72h respectively. Under these experimental conditions, cell death was not observed before 48h (Figure 3.3.1D), showing that *CXCL10* transcription preceded cell death. In fact, for lower concentrations of temozolomide that does not result in obvious cell death 72h after drug treatment (i.e. < 60ug/mL), the expression of *CCL5* and *CXCL9* were already detected (Figure 3.3.1B). This data demonstrates that drug-induced chemokine expression indeed precedes cell death.

The production of CCL5, CXCL9 and CXCL10 at the protein level was confirmed by analyzing supernatants of M102 cells 72h after treatment with temozolomide (100ug/mL) or cisplatin (10ug/mL). Using ELISA and Luminex-based Bio-Plex suspension arrays, the cell culture supernatants were tested for a variety of secreted proteins, including 24 cytokines (IL-1α, IL-1β, IL-1ra, IL-2, IL-2ra, IL-3, IL-4, IL-5, IL-6, IL-7, IL-9, IL-10, IL-12p40, IL-12p70, IL-13, IL-15, IL-16, IL-17, IL-18, IFN-α2, IFN-γ, TNF-α, TNF-β and TRAIL), 10 additional chemokines (CCL2, CCL3, CCL4, CCL7, CXCL1, CXCL8, CXCL12,

MIF, Eotaxin, CTACK), and 11 angiogenic and growth factors (VEGF, basic FGF, GM-CSF, HGF, M-CSF, PDGF, SCF, SCGFβ, LIF, b-NGF, G-CSF).

As shown in Figure 3.3.1E, temozolomide induced a more than 9-fold increase in the secretion of 5 chemokines (including CCL2, CCL5, CXCL8, CXCL9 and CXCL10), and one chemokine-like factor (MIF), while cisplatin induced a 5-fold or more increase in the secretion of CXCL8, CXCL10, and MIF. Importantly, none of the 40 other factors were significantly induced by chemotherapy (Table 3.3.1).

Altogether, these data demonstrate that the three chemotherapeutic drugs commonly used for the treatment of human metastatic melanoma induce specific expression of chemokines involved in T cell attraction.

A.

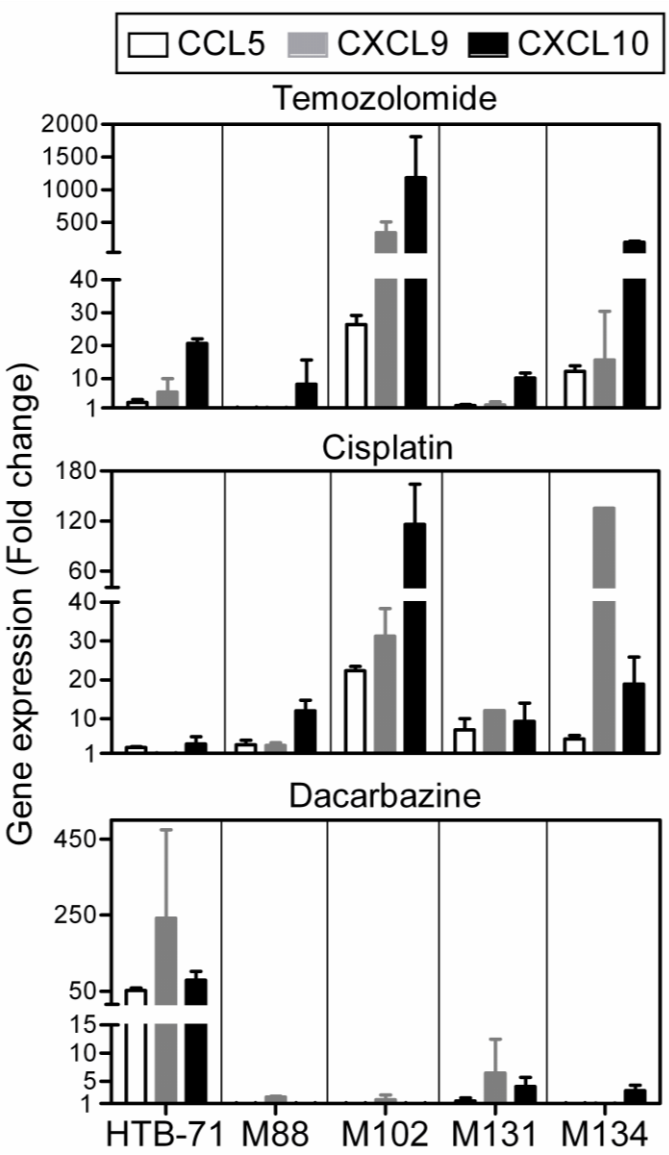
CCL5
CXCL9
CXCL10
Temozolomide
Cisplatin
Dacarbazine
Gene expression (Fold change)
2000
1500
1000
500
40
30
20
10
1
180
120
60
40
30
20
10
1
450
250
50
15
10
5
1
HTB-71
M88
M102
M131
M134

B.

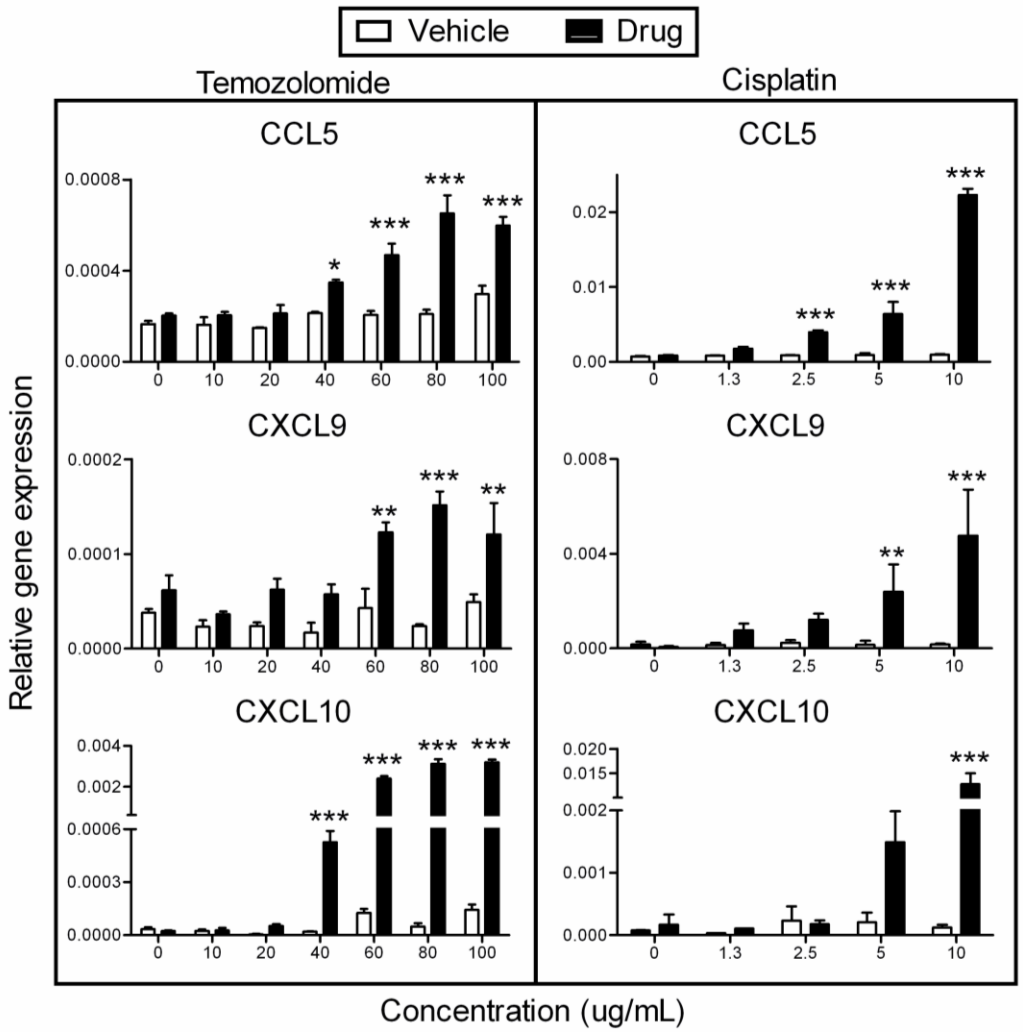
Vehicle
Drug
Temozolomide
Cisplatin
CCL5
CXCL9
CXCL10
Relative gene expression
Concentration (ug/mL)

C.

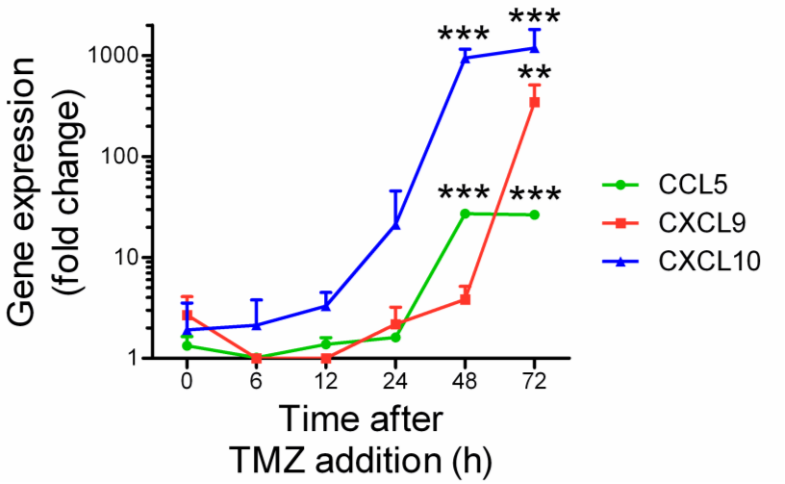
Gene expression
(fold change)
Time after
TMZ addition (h)
CCL5
CXCL9
CXCL10

D.

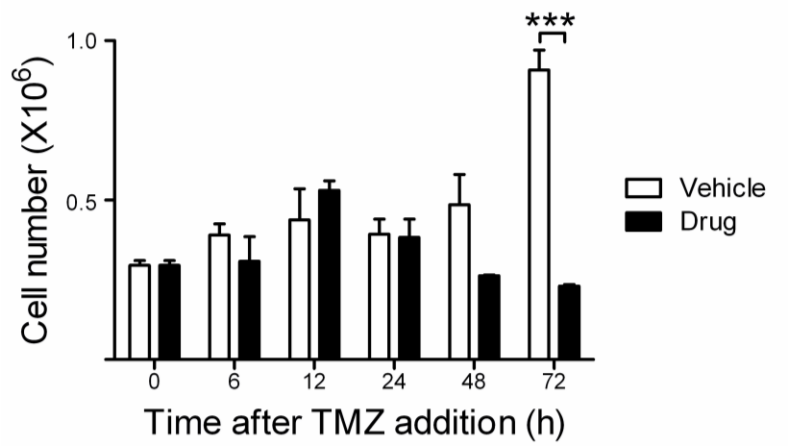

E.

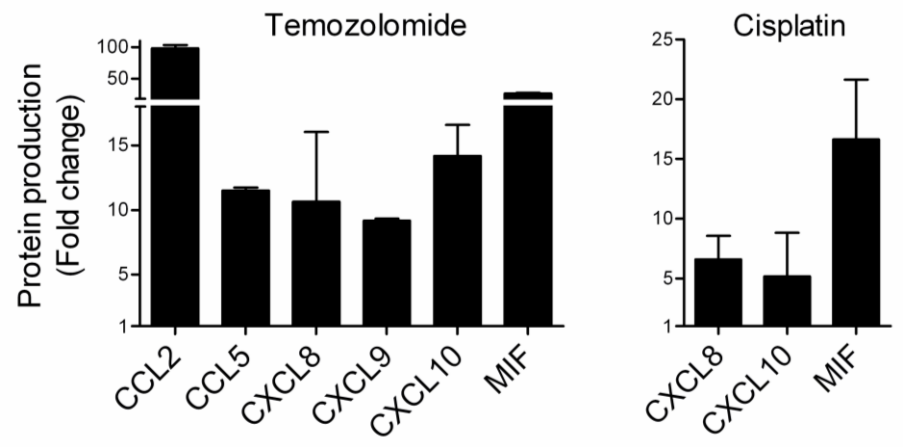

Figure 3.3.1 – Chemotherapeutic drugs induce chemokine expression in human melanoma cells *in vitro*.
Temozolomide, cisplatin, dacarbazine were tested on five different human melanoma cell lines (HTB-71, M88, M102, M131, M134) for their effect on CCL5, CXCL9 and CXCL10 production. (A) *CCL5*, *CXCL9* and *CXCL10* expression was measured by qRT-PCR in cells treated with either temozolomide (100µg/ml), cisplatin (10µg/ml), or dacarbazine (100µg/ml) for 72h. Data shows the fold-change in chemokine expression in drug-treated cells over control cells. (B) M102 cells were treated with increasing dose of temozolomide (0, 10, 20, 40, 60, 80, 100µg/ml) or cisplatin (0, 1.3, 2.5, 5, 10µg/ml) for 72h and the expression of *CCL5*, *CXCL9* and *CXCL10* was measured by qRT-PCR. Comparisons were performed using *two-way ANOVA*. (C) Kinetics of *CCL5*, *CXCL9* and *CXCL10* expression in M102 cells at 6, 12, 24, 48, and 72h after temozolomide (100µg/ml) and cisplatin (10µg/ml) treatment. Comparisons were performed using *two-way ANOVA*. (D) Total number of live cells were counted in drug-treated and control cells via trypan blue staining. *Two-way ANOVA.* (E) Concentrations of 40 different cytokines, chemokines, angiogenic factors, and growth factors in the supernatants of drug-treated and control cells were determined using multiplex immunobeads technology. (F) Data are presented as fold change in protein production from drug-treated cells compared to control cells. Only cytokines/chemokines with ≥ 9-fold increase in secretion after drug treatment and p-value < 0.05 are represented from temozolomide treatment group. Results are representative of 3 independent samples analyzed. *Mann-Whitney U test, one-tailed*.

Table 3.3.1 – Production of various cytokines, chemokines, angiogenic and growth factors after chemotherapy drug treatment.

Analyte	Mean ± SD (pg/mL) (Temozolomide)	Mean ± SD (pg/mL) (DMSO)	Fold increase	P value	Mean ± SD (pg/mL) (Cisplatin)	Mean ± SD (pg/mL) (DMF)	Fold increase	P value
b-NGF	ND	ND	NA	NA	ND	ND	NA	NA
CTACK	ND	ND	NA	NA	ND	ND	NA	NA
Eotaxin	42.1 ± 16.4	97.3 ± 89.8	0.43	0.25	84.5 ± 101	119.3 ± 133.6	0.71	0.35
FGF basic	41.5 ± 12.7	22.3 ± 18.7	1.86	0.10	44.8 ± 16.7	42.9 ± 45	1.04	0.35
G-CSF	ND	ND	NA	NA	ND	ND	NA	NA
GM-CSF	100.1 ± 73.8	75 ± 81.5	1.33	0.20	58.5 ± 58.7	124.6 ± 166.8	0.47	0.50
GROa	3776 ± 977.8	1009 ± 377.1	3.74	0.05	309.8 ± 87.4	293.9 ± 198.7	1.05	0.35
HGF	ND	ND	NA	NA	ND	ND	NA	NA
IFN-a2	ND	ND	NA	NA	ND	ND	NA	NA
IFNg	254 ± 199.3	319.6 ± 276.4	0.79	0.35	83.1 ± 42.4	700.5 ± 776.8	0.12	0.10
IL-1a	ND	ND	NA	NA	ND	ND	NA	NA
IL-1b	ND	ND	NA	NA	ND	ND	NA	NA
IL-1ra	200.2 ± 162.1	221.4 ± 184.1	0.9	0.41	131.3 ± 118.1	298 ± 256.4	0.46	0.35
IL-2	ND	ND	NA	NA	ND	ND	NA	NA
IL-2Ra	ND	ND	NA	NA	ND	ND	NA	NA
IL-3	ND	ND	NA	NA	ND	ND	NA	NA
IL-4	ND	ND	NA	NA	ND	ND	NA	NA
IL-5	ND	ND	NA	NA	ND	ND	NA	NA
IL-6	ND	ND	NA	NA	ND	ND	NA	NA
IL-7	ND	ND	NA	NA	ND	ND	NA	NA
IL-8/CXCL8	**83229 ± 67810**	**7869 ± 2354**	**10.58**	**0.05**	**11343 ± 1856**	**2144 ± 1243**	**5.29**	**0.05**
IL-9	75.3 ± 50.9	71.5 ± 55.5	0.92	0.50	10.2 ± 1.5	113 ± 117.1	0.09	0.05
IL-10	19.4 ± 16.2	48.1 ± 29.4	0.4	0.10	10.3 ± 7	65.8 ± 71	0.16	0.10
IL-12p40	ND	ND	NA	NA	ND	ND	NA	NA
IL-12p70	88 ± 87.8	91.6 ± 77.6	1.13	0.41	23.4 ± 19.4	143.6 ± 162.1	0.16	0.10
IL-13	ND	ND	NA	NA	ND	ND	NA	NA
IL-15	ND	ND	NA	NA	ND	ND	NA	NA
IL-16	40.8 ± 34.7	56.1 ± 62.3	0.73	0.50	41.8 ± 35.1	103 ± 123.3	0.41	0.35
IL-17	103.8 ± 97	130.1 ± 147.4	0.8	0.50	114.4 ± 125.8	125.6 ± 109.8	0.91	0.50
IL-18	ND	ND	NA	NA	ND	ND	NA	NA
IP-10/CXCL10	**3810 ± 1122**	**268.7 ± 268.8**	**14.18**	**0.05**	**667.3 ± 215.3**	**115.8 ± 100.2**	**5.76**	**0.05**
LIF	13478 ± 11843	6288 ± 5508	2.14	0.25	188.1 ± 16.4	2258 ± 383.4	0.08	0.05
MCP-1/CCL2	**522.8 ± 46.8**	**5.3 ± 1.6**	**98.29**	**0.04**	ND	ND	NA	NA
MCP-3/CCL7	ND	ND	NA	NA	ND	ND	NA	NA
M-CSF	86.7 ± 75.7	30.7 ± 35.7	2.92	0.17	121.4 ± 103.6	27.7 ± 30.5	4.38	0.17
MIF	**6475 ± 522.8**	**246.7 ± 54.9**	**26.25**	**0.05**	**13356 ± 3597**	**874.3 ± 236.8**	**15.28**	**0.05**
MIG/CXCL9	**47 ± 1.4**	**5.1 ± 5.1**	**9.17**	**0.05**	ND	ND	NA	NA
MIP-1a/CCL3	ND	ND	NA	NA	ND	ND	NA	NA
MIP-1b/CCL4	ND	ND	NA	NA	ND	ND	NA	NA
PDGF-bb	65.7 ± 44.1	57 ± 67	1.15	0.35	22.9 ± 14.4	93.3 ± 82.6	0.25	0.10
RANTES/CCL5	**330.4 ± 12.1**	**28.7 ± 11.6**	**11.5**	**0.05**	29 ± 10.4	27.3 ± 22.7	1.06	0.35
SCF	40.6 ± 35.6	44.4 ± 40.1	0.91	0.50	77.2 ± 66.9	20 ± 28.2	3.87	0.27
SCGF-b	1025 ± 405.7	1290 ± 431.5	0.79	0.20	832.9 ± 226.9	2916 ± 2790	0.29	0.05
SDF-1a	ND	ND	NA	NA	ND	ND	NA	NA
TNF-a	ND	ND	NA	NA	ND	ND	NA	NA
TNF-b	ND	ND	NA	NA	ND	ND	NA	NA
TRAIL	ND	ND	NA	NA	ND	ND	NA	NA
VEGF	36847 ± 6117	44477 ± 33965	0.83	0.35	16688 ± 5206	55394 ± 46310	0.3	0.35

Table shows the concentration of secreted factors in pg/mL ± SD from the supernatant of M102 human melanoma cells treated with chemotherapy drug or vehicle control. Secreted factors that were significantly upregulated after drug treatment are indicated in bold. ND = Not Detected; NA = Not Available. Data are representative of 3 independent samples analyzed. *Mann-Whitney U test, one-tailed*.

3.3.2 Enhanced expression of *CCL5*, *CXCL9* and *CXCL10* after chemotherapy is associated with tumor control and superior survival of melanoma patients

In a recent study, we showed increased T cell infiltration in chemotherapy-sensitive tumors of melanoma patients treated with dacarbazine (Nardin et al., 2011). In this previous study, global transcriptome analysis was performed on 35 cutaneous metastases resected before or after chemotherapy. A total of 13 melanoma patients with stage III/IV disease were included. For each patient, one tumor was collected at inclusion, and one to four tumors from the same patient were analyzed after chemotherapy.

Here, we now re-analyzed these data, asking whether there were any chemokine genes whose expression correlated with T cell infiltration. Among all the genes coding for chemokines, *CCL5, CXCL9* and *CXCL10* were the most significantly correlated with *CD3z* and *CD8A* expression, and were among the most significantly correlated with *CD4* (Figure 3.3.2A; Appendix 2a and 2b). For genes coding for chemokine receptors, *CXCR3* was the most significantly correlated with *CD4* and *CD8A* expression. Next, the levels of expression of *CD4* and *CD8A* were compared in three categories of tumor samples: those that expressed low levels of the three chemokines, those that expressed high levels of *CCL5* or high levels of CXCR3 ligands, and those that expressed high levels of *CCL5* and high levels of at least one CXCR3 ligand. This comparison revealed a clear synergy between *CCL5* and CXCR3 ligands for T cell infiltration (Figure 3.3.2B).

To determine whether chemotherapy had any impact on chemokine expression, the expression of *CCL5, CXCL9, CXCL10* and *CXCR3* was compared in tumors before and after chemotherapy. As shown in Figure 3.3.2C, while dacarbazine did not induce any significant changes in chemotherapy-resistant tumors, i.e. progressing lesions, an increase in *CCL5*, *CXCL9* and *CXCR3* expression was observed after treatment in chemotherapy-sensitive tumors (p-values = 0.018, 0.045 and 0.028, respectively). A similar trend was observed for *CXCL10* (p-value = 0.08). This increase in chemokine expression was associated with enhanced T cell infiltration, as demonstrated by a significant increase in *CD4* and *CD8A* expression in chemotherapy-sensitive tumors (p-values = 0.036 and 0.020, respectively; Figure 3.2.2D) Finally, Kaplan-Meier analysis showed that patients exhibiting enhanced chemokine expression after chemotherapy survived longer (p-value = 0.0002; HR = 35; Figure 3.2.2E).

Taken together, these data show that chemotherapy induces enhanced expression of CXCR3 ligands and *CCL5* in chemotherapy-sensitive tumors. Furthermore, increased expression of these chemokines translates into enhanced T cell infiltration, improved tumor control and prolonged overall survival.

A.

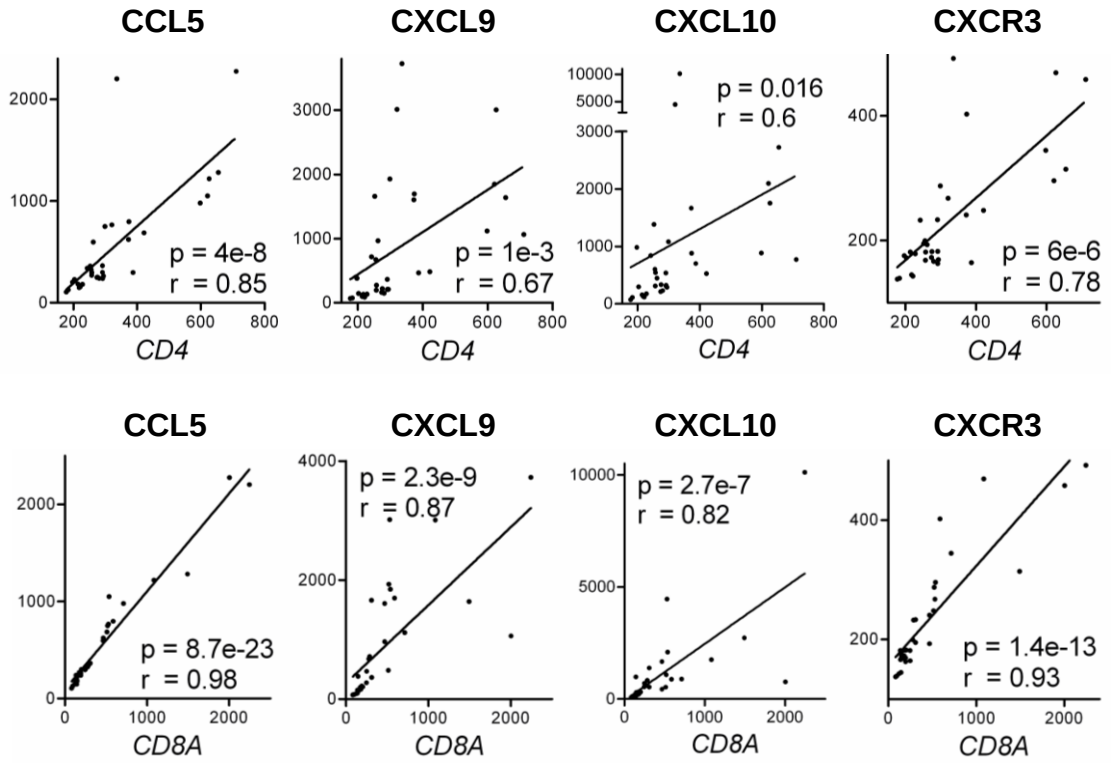
CCL5
CXCL9
CXCL10
CXCR3
p = 4e-8
r = 0.85
p = 1e-3
r = 0.67
p = 0.016
r = 0.6
p = 6e-6
r = 0.78
CD4
p = 8.7e-23
r = 0.98
p = 2.3e-9
r = 0.87
p = 2.7e-7
r = 0.82
p = 1.4e-13
r = 0.93
CD8A

B.

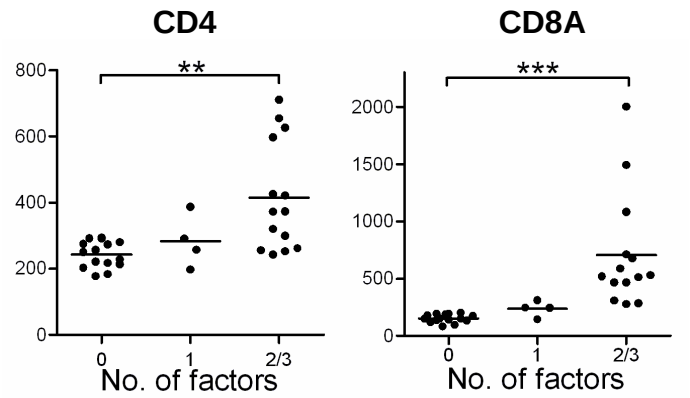
CD4
CD8A
**
***
No. of factors
0
1
2/3

C.

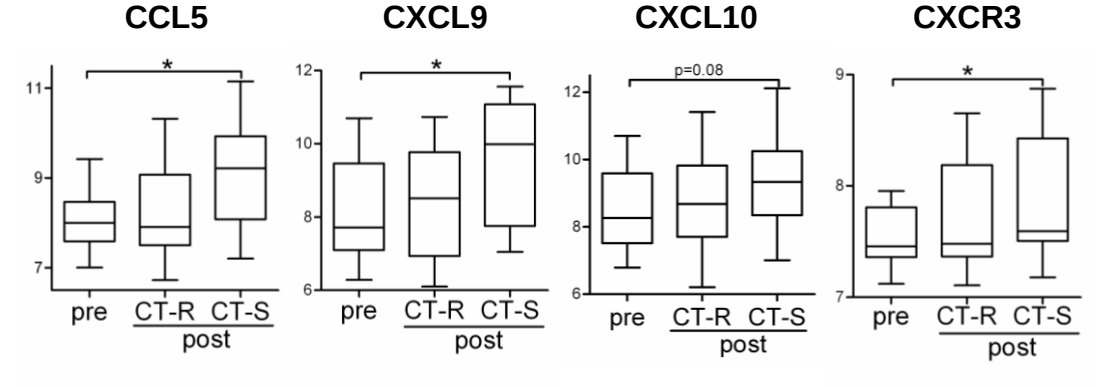
CCL5
CXCL9
CXCL10
CXCR3
*
p=0.08
pre
CT-R
CT-S
post

D.

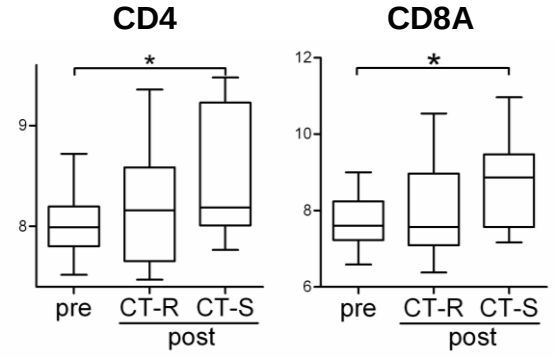

E.

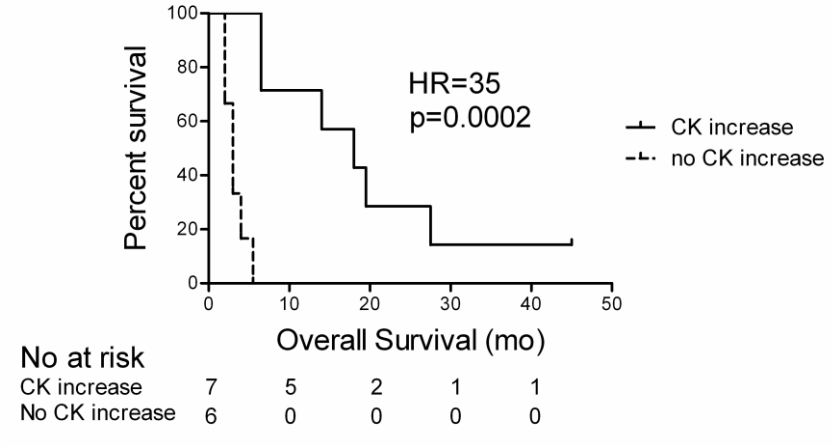

Figure 3.3.2 – Enhanced chemokine expression in human melanoma skin tumors after chemotherapy correlates with increased T cell infiltration, tumor control and patient survival.
A total of 35 cutaneous melanoma tumors from 13 stage III or IV patients were collected before and after chemotherapy and analyzed by gene expression microarray. (A) *CD4* or *CD8A* expression correlates with *CCL5*, *CXCL9, CXCL10* and *CXCR3* expression in the tumors. *Spearman correlation, one-tailed with Bonferroni's correction for multiple testing*. (B) The expression of *CD4* and *CD8A* was compared between tumors with high or low expression of *CCL5* and CXCR3 ligands. 0 – $CCL5^{lo}$ CXCR3 $ligands^{lo}$; 1 – $CCL5^{hi}$ or CXCR3 $ligands^{hi}$; 2 – $CCL5^{hi}$ and CXCR3 $ligands^{hi}$. *One-way ANOVA*. (C and D) Intra-tumoral expression of *CCL5*, *CXCL9* and *CXCR3* as well as *CD4* and *CD8A* was compared between cutaneous tumors before (pre; n=13) and after chemotherapy (post; n=22). Tumors collected after treatment were divided into chemotherapy-resistant (CT-R) [n=12] or chemotherapy-sensitive (CT-S) [n=10]. Differential gene expression between tumor samples collected before treatment and chemotherapy-sensitive tumors was assessed by one-tailed t test on Log-transformed expression values. (E) Kaplan-Meier analysis of patient survival with or without increase in intra-tumoral chemokine expression after chemotherapy.

CHAPTER 4

DISCUSSION

4 DISCUSSION

4.1 Development of a new spontaneous bioluminescent mouse melanoma model to monitor tumor growth and treatment responses

4.1.1 Generation of a ret$^{+/-}$ luc$^{+/-}$ transgenic mouse

Most preclinical studies of potential therapies for melanoma are done using transplanted tumor models. While these models are relatively appropriate for imaging tumor growth, they fail to recapitulate the natural clinical course of melanoma in humans. Over the past decade, many attempts have been made to use transgenic approaches to generate mouse models of spontaneous melanoma [reviewed in (Larue and Beermann, 2007)]. These models are often clinically relevant, however, they are limited in the ability to monitor tumor burden in animals accurately, especially for microscopic, non-palpable tumors. For longitudinal monitoring of cutaneous tumors, central necrosis, ulceration, or treatment-induced apoptosis may not be fully accounted for by gross tumor measurements (Craft et al., 2005). To circumvent these issues, we now report the development of a new genetically driven mouse model that allows non-invasive monitoring of spontaneous primary melanoma tumor growth and metastases *in vivo* by bioluminescence imaging (BLI). This novel mouse model, to our knowledge, is the only spontaneous model of metastatic melanoma that allows monitoring of metastasis development *in vivo*.

The use of optical imaging techniques for monitoring endogenous tumors can be achieved by the expression of a foreign gene in the tumors themselves. This is rather time-consuming and the feasibility of this technique has been

questioned primarily due to the immunogenicity of the foreign gene (Craft et al., 2005). Comparison of optical imaging techniques including BLI and FLI demonstrated that BLI is more sensitive than FLI in the detection of microscopic tumors due to lower tissue attenuation in BLI than in FLI. For FLI, tissues can absorb and scatter fluorescent light at both the excitation and emission level; while for BLI only the emission is subjected to attenuation since there is no excitation involved (Puaux et al., 2011). The effect of tissue attenuation is expected to be magnified for the imaging of visceral tumors compared to subcutaneous tumors due to the increased optical path through the tissues. Nevertheless, FLI has numerous other applications beyond the scope of this study, including fluorescent imaging of tumor cell mobility, invasion and angiogenesis (Puaux et al., 2011). In addition, FLI is the only imaging technology to give single cell resolution or even sub-cellular resolution *in vivo* (Puaux et al., 2011). In general, even though the resolution of optical imaging is not comparable to nuclear imaging techniques, recent advances have been made to enable signal collection in a three-dimensional plane.

In the case of melanoma, the use of BLI to monitor transplanted tumor growth has been extensively reported over the past few decades. This includes the widely used B16 syngeneic mouse melanoma model (Craft et al., 2005) and the A375 xenograft human melanoma model, among others (Craft et al., 2005). The method involves transfection *in vitro* and transplantation of cells *in vivo*, which are relatively simple procedures to perform. On the other hand, the use of BLI for monitoring spontaneous melanoma tumor growth and

metastases has not been reported. However, the development of spontaneous bioluminescent tumor model has been demonstrated for other types of cancers, including pituitary tumor (Vooijs et al., 2002), prostate adenocarcinoma (Liao et al., 2007), pancreatic cancer (Zhang et al., 2009), and mammary tumors (Goldman et al., 2011), indicating the feasibility of this approach in following autochthonous tumor growth. In these spontaneous bioluminescent tumor models, BLI effectively detected primary tumor development. Spontaneous metastases is absent in all the spontaneous models described, except for pancreatic cancer. In this model, primary pancreatic tumors metastasized to the intestines, liver and abdomen, but only a fraction of these metastatic tumors were detected by BLI (Zhang et al., 2009). Here, by showing that the BLI is able to detect both primary tumors and spontaneous metastases *in vivo*, the Melucie model represents a major step forward in the refinement of transgenic melanoma models and provides a valuable tool for evaluating novel anti-melanoma therapies, especially those targeting the metastatic cascade.

4.1.2 Bioluminescence imaging of spontaneous melanoma tumor development in ret$^{+/-}$ luc$^{+/-}$ mice

We have shown that in the Melucie, BLI successfully detected primary eye tumors and spontaneous metastases with sensitivity and positive predictive values that were comparable to nuclear imaging techniques such as MRI or ^{18}FDG-PET. *In vivo* BLI permitted sensitive and quantitative assessment of cutaneous metastases, but it was less than ideal for the detection of visceral metastases. It, nevertheless, still provides a means to highlight and localize visceral metastases at necropsy.

For cutaneous tumors, it should be noted that not all of the tumors were visible by *in vivo* luciferase imaging. This observation could not be explained by the loss of Dct promoter activity which drives luciferase expression as down-regulation of Dct enzyme was not observed for both cutaneous and visceral metastases from RETAAD mice (Lengagne et al., 2008). Other possible explanations include quenching of the luciferase signal due to hypoxia or necrosis which limits the availability of ATP required for the luciferase enzymatic activity. Alternatively, these tumors could harbor mutations within the luciferase gene which affects the functionality of the luciferase enzyme. Currently, it remains to be investigated what is the lower limit of detection for cutaneous tumors *in vivo*. Others have reported detection of as few as 500 cells in C57BL/6 mice (Craft et al., 2005) and a single tumor cell in nude mice *in vivo* (Kim et al., 2010). However, no such details have been demonstrated for spontaneous bioluminescent tumor models.

The strong correlation between detected photons and tumor weight both *in vivo* and *ex vivo* over a large dynamic range strongly support the notion that Melucie mice enables sensitive detection of tumor growth, stasis, regression or relapse. Although there was a remarkable correlation between BLI signal and tumor weight, the relationship was not linear. Low signal to mass ratios were observed for some tumors and this could be due to the presence of stromal cells or accumulated fluid in the tumors that contribute to the tumor mass, but not the signal. Alternatively, it could be due to quenching of the luciferase signal by hypoxia or necrosis. On the other hand, we have observed a few tumors with a higher signal to mass ratio, which possibly

reflects the rapid lost of fluid from these tumors after being harvested for *ex vivo* imaging. It is important to note that BLI detects only live tumors cells, and therefore, this technique is particularly suited to test the efficacy of various tumor therapies.

Ex vivo imaging of selected organs from Melucie mice demonstrated tumor-specific BLI signals with little or minimal background expression in control organs. Comparatively, the eyes displayed a higher luciferase signal compared to other organs in the Melucie and the same phenomenon was observed in control mice. This was most likely due to the presence of melanocytes in the choroid layer of the eyes. Since luciferase expression is driven by the Dct promoter and the Dct protein is present within melanocytes, we expected to detect background luciferase expression from the eyes of these mice. Interestingly, despite this, we were able to detect early, microscopic primary eye tumors in young mice by *in vivo* and *ex vivo* BLI before clinical detection of the primary tumor, highlighting the sensitivity of BLI in the detection of primary tumor onset in our model.

For future studies, it will be interesting to investigate whether the luciferase signal correlate with the number of tumor cells and whether we are able to measure the proliferation rate of tumors *in vivo* by longitudinal measurements of the tumor BLI signals. In addition, a proof-of-principle experiment needs to be performed to demonstrate the feasibility of this model to monitor tumor responses to therapies.

Taken together, our data demonstrates the feasibility of this new model for non-invasive monitoring of spontaneous melanoma tumor development and metastasis in living mice. The ability to detect early primary tumors, to track the stochastic onset of metastatic tumors, and to perform longitudinal monitoring of spontaneous tumor progression in live mice permit matching of animals on the basis of tumor burden, thus circumventing the inter-animal variation caused by the stochastic nature of spontaneous tumor formation (Vooijs et al., 2002), and ultimately reducing the number of animals required. Furthermore, it provides both temporal and spatial information throughout experiments, instead of just providing endpoint data obtained by more conventional approaches. Therefore, we strongly believe that our Melucie model will serve as an invaluable tool for the *in vivo* evaluation of the efficacy of future chemo-immunotherapeutic strategies against melanoma.

4.2 Chemokines and T cell trafficking in mouse and human cutaneous melanoma

In the second part of this work, we show that CCL5 and CXCR3 ligands are the main determinants of T cell infiltration into cutaneous melanoma tumors. Moreover, we show that chemotherapy induces expression of these chemokines in several human melanoma cell lines and that chemotherapy-induced chemokine expression in human melanoma tumors correlates with T cell infiltration, tumor control and prolonged patients' survival (refer proposed model, Fig 4.2.1).

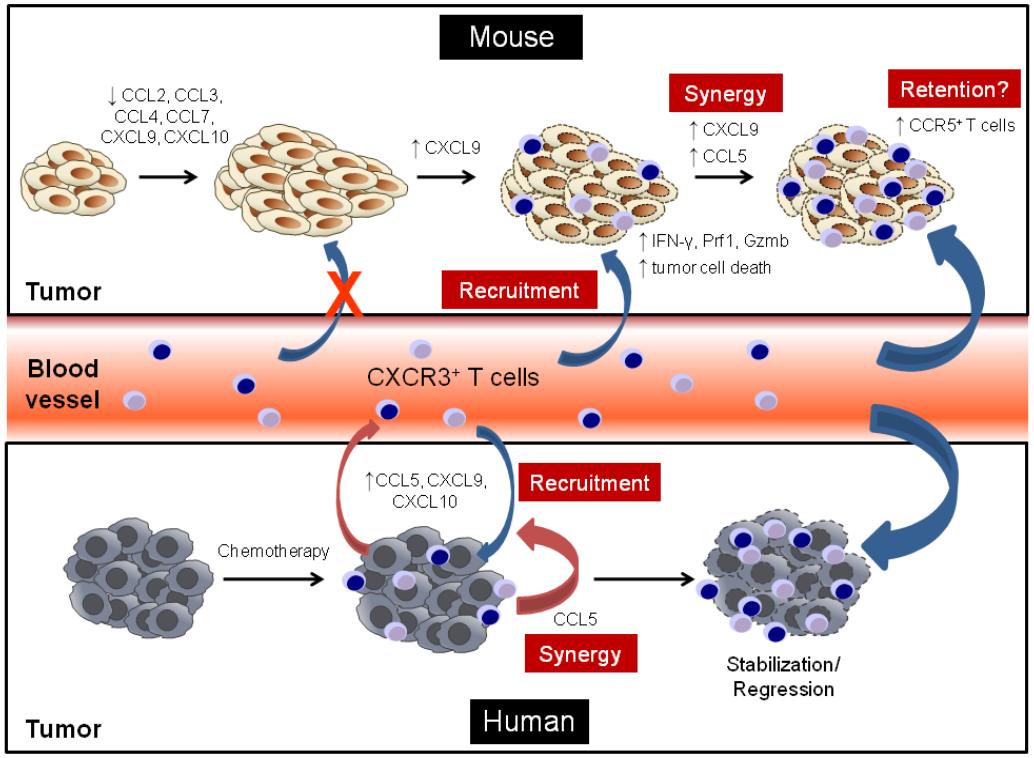

Figure 4.2.1 – Proposed model of chemokine-driven T cell recruitment into cutaneous melanoma tumors.
The chemokines CXCR3 ligands and CCL5 are main determinants of T cell infiltration into cutaneous melanoma tumors in both mouse and human. In RETAAD mice, cutaneous melanoma tumors express low levels of these chemokines, therefore escape T cell-mediated control. Transfection of CXCL9 into established cutaneous tumors augments the infiltration of circulating $CXCR3^+$ T cells into tumors. Interestingly, transfection of both CCL5 and CXCL9 induces a synergistic increase in T cell infiltration into tumors. This could be explained in part by the upregulation of CCR5 on tumor-infiltrating lymphocytes, which may play a role in the retention of T cells in the tumors. Chemokine-recruited T cells display a type 1 polarized/cytotoxic phenotype, leading to an increase in tumor cell death (Top panel). In human melanoma patients, chemotherapy (dacarbazine) increases the expression of CXCR3 ligands and CCL5 in chemotherapy-sensitive tumors. Chemotherapy-induced expression of these chemokines enhances $CXCR3^+$ T cell infiltration into chemotherapy-sensitive tumors, which in turn, favours tumor control and prolongs patient survival (Bottom panel).

4.2.1 Intra-tumoral T cell trafficking and tumor control *in vivo*

While anti-tumor T cells are often detected in the blood of melanoma patients, this only rarely translates into favorable patient clinical outcome (Salcedo et al., 2006). This applies to spontaneous T cell responses and those induced by cancer vaccines; the vast majority of cancer patients undergoing therapeutic vaccination display enhanced anti-tumor T cell responses, but only a small percentage control their tumors (Klebanoff et al., 2011). Several explanations have been proposed for this apparent paradox, including local immune-suppression, tumor immune-editing and escape from immune attack [reviewed in (Rabinovich et al., 2007)].

We addressed this question in the RETAAD model and found that the reason why T cells do not control cutaneous tumors *in vivo* is because they fail to traffic to these tumors. We had previously shown that cutaneous tumors are not immune edited (Lengagne et al., 2008): even if $CD8^+$ T cells fail to impact the growth of cutaneous tumors *in vivo*, resected cutaneous tumors are recognized *ex vivo* by anti-melanoma T cells (Lengagne et al., 2004). Moreover $CD8^+$ T cells retain their functionality *in vivo* since they control visceral metastases (Eyles et al., 2010).

In this present study, we show that very few T cells infiltrate skin tumors in comparison to visceral tumors or transplanted B16 skin tumors. The few T cells that infiltrate skin tumors probably retain their functionality since their number correlates inversely with tumor size. Further support for this conclusion comes from the observation that the ratios of expression of T cell

effector molecules (*Gzmb*, *Prf1b*, *Ifng*) and T cell markers (*Cd3g*, *Cd4* and *Cd8a*) are not different between cutaneous tumors and visceral tumors. Finally, transfection of CXCR3 ligand and *CCL5* in established cutaneous tumors results in increased T cell infiltration and reduced tumor growth. Therefore in this spontaneous model of melanoma, differential T cell trafficking is the main reason for the tissue-specific control of metastases. Importantly, we extended this finding to tumors from melanoma patients undergoing chemotherapy. In these patients, tumor control and prolonged survival are associated with increased T cell infiltration and expression of CXCR3 ligands and *CCL5*.

Taken together, our data clearly shows that homing of T cells with effector potential to the target tumor tissue is a prerequisite for its control or rejection by T cells, and suggests that local factors within the tumor microenvironment are major determinants of effective T cell trafficking to the tumors.

4.2.2 Chemokines and T cell recruitment to tumors

Chemokines play a critical role in determining the fate of the developing tumor by regulating the migration of different leukocyte subtypes into tumors. By transplanting B16 skin tumors in RETAAD mice, we identified a panel of 6 chemokines associated with superior T cell infiltration into B16 skin tumors, including CCL2, CCL3, CCL4, CCL7, CXCL9 and CXCL10. In fact, the two most differentially expressed chemokines, CXCL9 and CXCL10, are both ligands for the chemokine receptor CXCR3. As our data clearly demonstrate a differential, selective and strong expression of CXCL9 in the tumor, we

decided to focus on CXCL9 as a therapeutic target for over-expression in RETAAD cutaneous tumors.

Further support for the use of CXCL9 comes from the analysis of chemokine receptor expression on peripheral blood T cells, in which the cognate chemokine receptor for CXCL9, i.e. CXCR3, was found to be expressed by most circulating T cell subsets. Transfection of CXCL9 into cutaneous tumors augmented T cell infiltration and increased anti-tumor activity. Characterization of the CXCL9-recruited T cells demonstrated that > 90% of the infiltrated T cells were of the activated phenotype and T cell effector molecules were elevated in treated tumors, suggesting the recruitment of T cells with type 1 polarized/cytotoxic functions. Therefore, our results provide "proof-of-concept" that over-expression of CXCL9 within the cutaneous tumor microenvironment redirects circulating $CXCR3^+$ T cells into the tumors. Nevertheless, we cannot exclude that other chemokines with lymphocyte attractant properties might be additionally involved in TIL recruitment.

Exhaustion of tumor-specific $CD8^+$ T cells in metastases of late-stage melanoma patients has been reported recently (Baitsch et al., 2011). In our study, further experiments should be performed to determine the phenotype and antigen-specificity of the infiltrating T cells in cutaneous melanoma after treatment. Such studies are technically challenging, since tumor-specific T cells are rare and difficult to isolate for *ex vivo* analysis. However, the emergence of 'single-cell biology' (Bendall et al., 2011) may ultimately lead to comprehensive characterization of small cell numbers, even down to the single cell level.

We have shown that CXCL9 promotes T cell infiltration into cutaneous melanoma, most probably via interactions with CXCR3 expressed on circulating T cells. CXCR3 has two other known ligands, i.e. CXCL10 and CXCL11. We postulate that CXCL10 may function in the same way as CXCL9, since CXCL10 was also associated with high endogenous T cell infiltration in B16 skin tumors. However, the role of CXCL11 is less obvious. Although all three chemokines bind to CXCR3, and have been shown to attract activated T cells *in vitro* (Stanford and Issekutz, 2003) and *in vivo* (Hensbergen et al., 2005; Pertl et al., 2001; Tannenbaum et al., 1998; Walser et al., 2007), chemokine redundancy may not necessarily be operative *in vivo* (Groom and Luster, 2011). For example, several reports have demonstrated that the three CXCR3 ligands can collaborate (Yoneyama et al., 2002), and even compete or antagonize each other *in vivo* (Rosenblum et al., 2010). Thus, further experiments are required to clarify the exact roles of the other CXCR3 ligands in T cell recruitment into cutaneous melanoma *in vivo*. In addition to the ligands, the chemokine receptor CXCR3 is also known to be expressed by other immune cells, such as NK cells and dendritic cells. Although NK cells are not the focus of this study, it is possible that NK cells are recruited by CXCL9, leading to tumor cell killing.

In view of the critical roles of chemokines in mediating T cell recruitment to cutaneous melanoma, we were interested to know whether the differential T cell trafficking between visceral and cutaneous melanoma could be explained, in part, by differences in intra-tumor chemokine milieu. To do this, we

compared the chemokine expression profiles of visceral and cutaneous metastases using low-density PCR array. Four chemokine genes, *Ccl5*, *Ccl20*, *Ccl22*, and *Ccl24*, and five chemokine receptor genes, *Xcr1*, *Cxcr5*, *Ccr6*, *Ccr7* and *Ccr8*, were differentially expressed with greater expression in visceral tumors. Indeed, this data concurs with our finding that poor infiltration of T cells into cutaneous melanoma is due to lack of expression of T cell chemoattractants. Interestingly, the panel of chemokines differentially expressed between visceral and cutaneous tumors was distinct from those between transplanted and autochthonous cutaneous tumors, showing that different chemokines are involved in lymphocyte homing to different target tissues. As lymphocyte trafficking to tumor tissues is a tightly regulated process mediated by a complex array of adhesion molecules, chemokine signals and proper vasculature, it is possible that factors other than chemokines could account for the differential T cell trafficking between visceral and cutaneous tumors.

Several correlation studies have highlighted the importance of CXCR3 ligands and CCL5 in the progression of cutaneous melanoma. Harlin *et al* identified several chemokines (including CCL2, CCL3, CCL4, CCL5, CXCL9 and CXCL10) whose expression correlate with $CD8^+$ T cell infiltration, but this study did not distinguish between chemokines that attract T cells and those that are produced by T cells (Harlin et al., 2009). In primary malignant melanoma, marked infiltration of T cells was observed exclusively in areas with strong CXCL9 and to a lesser extent CXCL10 expression (Kunz et al., 1999). In the present study, by transfecting mouse tumors and analyzing the expression of the corresponding chemokine receptor in the blood, we could

establish a causal relationship between chemokine expression and T cell infiltration.

Expression of the chemokine receptor CXCR3 by circulating memory T cells in melanoma patients with stage III disease has been shown to correlate with prolonged survival (Mullins et al., 2004). IFN-α, a known inducer of CXCL9 and CXCL10, is approved for the treatment of high risk (stage IIb-III) cutaneous melanoma (Hauschild et al., 2008; Stadler et al., 2006). Based on the data presented in this study, it is tempting to speculate that CXCR3-ligand induction participates in IFN-α anti-melanoma activity. A recent study demonstrated increased plasma level of CXCL10 following IFN-α treatment in melanoma patients. However, it is not known whether this increase in CXCL10 is important for *in vivo* trafficking of $CD8^+$ effector T cells to tumor targets (Mohty et al., 2010). In another study, expression of CXCL10 by melanoma patients' PBMC was reported to correlate with tumor control (Antonicelli et al., 2011).

Interestingly, CXCR3 expression by cancer cells in cutaneous melanoma correlates negatively with lymphocyte infiltration (Monteagudo et al., 2007). The mechanism underlying this correlation is unclear but the present study suggests that cancer cells expressing CXCR3 might escape the immune response by competing for chemokines able to attract T cells. Expression of a non-functional variant of CCR5 results in decreased survival of melanoma patients receiving immunotherapy (Ugurel et al., 2008).

In addition to melanoma, CXCR3 ligands have also been involved in other types of cancer. For example, in colorectal cancer, expression of CXCL9, CXCL10 and CX3CL1 has been shown to correlate with prolonged disease-free survival (Mlecnik et al., 2010). In Ewing sarcoma, CXCL9, CXCL10 and CCL5 expression in the tumor microenvironment correlates with $CD8^+$, but not $CD4^+$ T cell infiltration (Berghuis et al., 2011). Expression of CXCL10 and CCL5 within the tumors of hepatocellular carcinoma patients correlates positively with NK and $CD8^+$ T cell densities and patient survival as well as negatively with tumor cell proliferation (Chew et al., 2011). None of these studies established a causal relationship between chemokine expression and T cell recruitment and most mouse studies addressing this question used transplanted tumor models, which as shown here for B16, may behave very differently than spontaneous tumors.

4.2.3 Chemokine synergy in immune cell recruitment to tumors

The present study also revealed a striking synergism between CXCR3 ligands and *CCL5* in attracting T cells into melanoma tumors. Synergistic interaction between chemokines has been observed in both human and mouse tumors. At this stage, the exact mechanism accounting for this synergy is unclear since circulating RETAAD T cells express very low levels of CCL5-receptors, i.e. CCR1, CCR3 and CCR5. In fact, less than 2% of the $CD8^+$ T cells in the RETAAD mice express CCL5 receptors. Transfection of *Ccl5* did not enhance *Cxcl9* expression in the tumor, and transfection of *Ccl5* alone has no effect on T cell attraction.

However, we did observe an increased percentage of $CD4^+$ and $CD8^+$ T cells expressing CCR5 among the TIL, suggesting either that CCR5-expressing T cells are preferentially attracted into the tumor or that upon infiltration, T cells upregulate CCR5. We propose that intra-tumoral expression of *Ccl5* might facilitate the retention of CCR5-expressing T cells, thereby augmenting the percentage of $CCR5^+$ TIL. In fact, CCR5 has been reported to play a role in T cell retention at the tumor site (Franciszkiewicz et al., 2009). Although we could not test this hypothesis in melanoma patients, we did find that intra-tumoral expression of CXCR3 ligands and *CCL5* in chemotherapy-treated tumors does lead to a synergistic increase in T cell infiltration. Since the chemokine CCL5 is also expressed in RETAAD visceral metastases, we postulate that CCL5 could synergize with other chemokines expressed within the tumors to mediate T cell recruitment into the tumors.

The cooperative action of chemokines in immune cell recruitment has been demonstrated mostly *in vitro*. Examples include neutrophils (Gijsbers et al., 2005; Gouwy et al., 2004; Gouwy et al., 2002; Struyf et al., 2001), interferon-producing cells/plasmacytoid dendritic cells (IPCs/pDCs) (Krug et al., 2002; Vanbervliet et al., 2003), dendritic cells, B cells and naïve T cells (Paoletti et al., 2005), T cells (Sebastiani et al., 2005), monocytes (Gouwy et al., 2008) and PBMCs (Mellado et al., 2001b). Synergistic interactions between chemokines have also been shown *in vivo* albeit in limited cases. Two studies demonstrated synergistic chemokine interactions in neutrophil recruitment (Struyf et al., 2005; Zwijnenburg et al., 2003), while only one such study on T cells has been reported (Stanford and Issekutz, 2003) although the combined chemotactic effect in this study was rather additive in nature. Chemokine synergism in T cell recruitment to tumors *in vivo* has not been reported thus far.

The molecular basis for the synergistic interactions between chemokines has been progressively studied in the past few years, although not yet been elucidated. Several proposed mechanisms include formation of chemokine heterodimers (Paoletti et al., 2005), co-expression of multiple chemokine receptors (Gouwy et al., 2004; Krug et al., 2002; Vanbervliet et al., 2003), and synergy between mediators at the post-receptor binding level (Mellado et al., 2001b). Further research is warranted to better understand the molecular mechanisms involved in the synergy between chemokines in order to fine tune the immune response for tumor therapy. In addition, further studies could explore the combination of chemokines and cytokines to recruit T cells and

promote local expansion and activation, a term referred to as the “attraction-expansion paradigm” (Ruffini et al., 2007).

Collectively, our study is the first to demonstrate synergy between chemokines in T cell recruitment into tumors *in vivo* in mice, and possibly in humans. Synergy between pro-inflammatory chemokines may be an important phenomenon to induce an adequate migratory response *in vivo* to sites of inflammation or tumors. Since multiple chemokines are often co-produced by various cell types within the tumor microenvironment, synergy between chemokines is biologically relevant and physiologically and pathologically important in a broad context.

4.3 Chemotherapy and the immune response

Chemotherapeutic drugs have been selected for their capacity to induce apoptosis in tumor cell lines, regression of transplanted tumors in animal models, and clinical responses in cancer patients (Herr and Debatin, 2001; Tiligada, 2006; Zhang and Herlyn, 2009; Zitvogel et al., 2008). Chemotherapies are probably acting, in part, through cell autonomous mechanisms. In addition, the immune system may contribute to chemotherapy efficiency. The concept of immunogenic chemotherapy has been recently proposed to describe compounds which rely on enhanced anti-tumor immune response to induce tumor regression (Zitvogel et al., 2011). For example, anthracyclines and platinum derivatives induce calreticulin exposure and release of danger signals such as HMGB1 or ATP, which activate dendritic cells, thereby stimulating the anti-tumor immune response (Obeid et al., 2007). DNA damaging agents used in cancer chemotherapy activate the DNA damage response pathway and trigger tumor cells to upregulate NKG2D ligands, which are recognized by innate immune cells (Gasser et al., 2005).

4.3.1 Chemotherapy induces chemokine expression in tumor cells

The present study provides evidence for a novel (third) mode of action in which some chemotherapeutic drugs could work by inducing chemokine expression and promoting T cell infiltration into the tumor. We provide direct evidence both *in vitro* using human melanoma cell lines, as well as *in vivo* in melanoma patients treated with chemotherapy. *In vitro*, we show that dacarbazine, cisplatin and temozolomide induce expression of T cell attracting chemokines in several melanoma cell lines. Transcription of CCL5, CXCL9

and/or CXCL10 was induced in all tested cell lines 72 hours after drug treatment, even though each cell line displayed a unique profile of response to the chemotherapeutic drugs. Dacarbazine, which is widely used to treat advanced melanoma, gave variable results, most likely due to the fact that it needs to be metabolized via a reaction that is unable to occur efficiently *in vitro* (unlike *in vivo*, where it takes place in the liver). We therefore focused on cisplatin and temozolomide, which has the same active metabolite as dacarbazine and is also used for the treatment of melanoma.

Both cisplatin and temozolomide are able to inhibit DNA replication and transcription leading to tumor cell death. In our study, tumor cell death was observed 48 hours after cisplatin (10µg/mL) treatment and 48-72 hours after temozolomide (100µg/mL) treatment *in vitro*. To preclude that the expression of chemokines was due to an indirect effect of tumor cell death, time course experiments were performed. Our results showed that under most experimental conditions tested, transcription of the chemokine genes preceded cell death, indicating clearly that the increased expression of chemokines is a direct effect of chemotherapy drugs.

Secretion of the chemokines in the culture medium was verified for one of the cell lines. The effect of chemotherapy drug on chemokine induction was highly specific since out of 48 soluble factors analyzed, only 5 chemokines and 1 chemokine-like factor were significantly induced by temozolomide; while only 2 chemokines and 1 chemokine-like factor were induced by cisplatin.

Production of other soluble factors including growth factors, angiogenic factors and cytokines was not affected after drug treatment.

4.3.2 Chemotherapy-induced chemokine expression triggers T cell infiltration, improves tumor control, and prolongs patient survival

Chemotherapy is a standard treatment of metastatic melanoma but it only induces clinical responses in about 20% of melanoma patients (Bajetta et al., 2002). Even in patients who responded to chemotherapy, mixed responses are frequently observed (Bajetta et al., 2002), but the reason for this variability is not clear.

In our limited cohort, tumor regression or stabilization was observed in 5 out of 13 patients and 10 out of 22 tumors resected after chemotherapy. Remarkably, enhanced expression of CCL5, CXCL9 and CXCL10 after chemotherapy correlated with increased T cell infiltration and tumor response. Most importantly, prolonged patient survival was associated with enhanced chemokine expression after chemotherapy. Therefore, our data clearly demonstrates that human melanoma tumors, in which chemotherapy induces chemokine expression and T cell infiltration, are more likely to be controlled. These findings could explain the mixed responses frequently observed in patients after chemotherapy.

Chemotherapies are known to alter cancer cell transcriptome [reviewed in (Hsu et al., 2002)]. By damaging the tumor and stimulating a wound healing response, chemotherapies may induce epithelial-mesenchymal transition and favor the outgrowth of cells with higher motility and invasiveness (Rosano et

al., 2011); it may also select drug-resistant cells with stem cell and metastasis-initiating properties (Ahmed et al., 2010). Levina *et al* previously reported that *in vitro* treatment of some human cancer cell lines with doxorubicin or cisplatin induces expression of several cytokines, chemokines and growth factors which protect the cancer cells from drug-induced apoptosis (Levina et al., 2008). These previous reports identified cancer cell alterations that limit chemotherapy-induced cell death. The present study, by showing that chemotherapy can alter cancer cell phenotype in a way which favourably impact immune cell trafficking to the tumor, reveals a novel mechanism of action of chemotherapy.

A limitation of the present study is that a direct functional link could not be tested with the available patients' material. Several important questions could not be addressed. One such example is the inability to perform kinetics experiments in humans. Therefore, it is not possible to know the timing at which the chemokines are being produced after chemotherapy treatment and whether the chemokine production is at an optimal level. In addition, we could not address the question of when T cells start to infiltrate into the tumors, i.e. before or after chemotherapy.

The use of preclinical models is tremendously beneficial to unequivocally test the hypothesis that induction of intra-tumor chemokines *in vivo* after chemotherapy can induce effective T cell infiltration, leading to tumor control. The development of a new transgenic Melucie model of spontaneous melanoma will serve as an important tool to allow us to provide the direct

functional links by investigating whether (1) cisplatin or temozolomide can induce CXCR3 ligands and *Ccl5* expression from tumor cells *in vivo*, (2) T cell infiltration into tumors and tumor regression are significantly increased in chemotherapy-treated mice compared to control mice, and (3) the efficacy of chemotherapy can be blocked by antagonists or blocking antibodies against the chemokines (i.e. CXCR3 ligands and CCL5) or the chemokine receptors (i.e. CXCR3 and CCR5) involved.

4.3.3 Proposed mechanisms of chemotherapy-induced intratumoral chemokine expression

Chemotherapy drugs have been reported to induce chemokine expression in tumor cells (Darst et al., 2004; Geller et al., 2010; Lev et al., 2004; Levina et al., 2008; Niiya et al., 2003). However, the exact mechanism(s) of chemotherapy-induced chemokine expression in cancer cells is not known. Levina et al reported activation of various transcription factors including NF-κB, AP-1, AP-2, ATF-2, CREB, HIF-1, STAT-1, STAT-3, and STAT-5 after doxorubicin treatment on tumor cells, and activation of these transcription factors paralleled the upregulation of *IL-6*, *IL-8*, *bFGF*, *G-CSF*, *CCL2* and *CCL5* gene expression (Levina et al., 2008). However, the authors merely demonstrated an association, and not a causal relationship between transcription factor activation and induction of chemokine expression. No mechanisms were proposed. Moreover, it is unclear whether a less than two-fold increase in activated transcription factors is sufficient for the induction of more than 15-fold expression of some of the cytokines/chemokine genes.

In another study, Lev and colleagues proposed that upregulation of Raf-Mek-Erk pathway was partially responsible for the over-expression of IL-8 and VEGF in dacarbazine-resistant tumor cells, and that inhibition of activated Mek rendered the cells more sensitive to dacarbazine (Lev et al., 2004). If the Raf-Mek-Erk pathway is involved in the upregulation of IL-8 and VEGF proposed by the authors, inhibition of pMek should result in downregulation of these cytokines. However, the authors did not demonstrate this in their study. Based on their results, it is likely that the Raf-Mek-Erk pathway is involved in cell proliferation and survival, rather than the induction of chemokines/cytokines.

As chemokine production is regulated via the activation of transcription factors (Karin, 2006; Richmond, 2002), it is important to first determine which transcription factors are involved in driving the expression of these chemokine genes. Multiple transcription factor binding sites are present upstream of the chemokine genes *CCL5*, *CXCL9* and *CXCL10*. For example, the promoters of *CXCL9* and *CXCL10* contain the interferon–stimulated response element (ISRE) sequences. In fact, CXCL9 and CXCL10 have been shown to be produced by a variety of interferons, including IFN-α, IFN-β and IFN-γ (Antonelli et al., 2010). IFN-γ, compared to IFN-α and IFN-β, is the most potent inducer of CXCL9 and CXCL10 (Antonelli et al., 2010). In addition, NF-κB binding sites are also present in the promoters of all three chemokine genes. Interestingly, a direct binding site for p53 is present in the promoter region of *CXCL9* (Table 4.3.1). It is, therefore, possible that more than one

pathway are simultaneously activated, leading to the induction of chemokine expression in response to chemotherapy agents.

Table 4.3.1 – Transcription factor binding sites in the promoters of *CCL5*, *CXCL9* and *CXCL10* chemokines genes.

Transcription factor	CCL5	CXCL9	CXCL10
AhR		Y	Y
AP-1	Y		
C/EBPβ	Y		
c-Jun	Y		
c-Rel	Y		Y
IRF-1	Y	Y	
IRF-2		Y	Y
IRF-7A	Y		
JunB			Y
NF-κB	Y	Y	Y
NF-κB1	Y	Y	Y
p53		Y	
PPARγ1	Y		
PPARγ2	Y		
STAT1			Y
STAT1α			Y
STAT1β			Y
STAT5A			Y

Table shows the list of transcription factor binding sites identied in the gene promoter regions of the chemokines genes CCL5, CXCL9 and CXCL10 as predicted by SABiosciences' Text Mining Application and the UCSC Genome Browser. AhR – aryl hydrocarbon receptor; AP-1 – activator protein 1; C/EBP – CCAAT-enhancer-binding proteins; IRF – interferon regulatory factor; NF-κB – nuclear factor kappa-light-chain-enhancer of activated B cells; NF-κB1 – encodes a subunit of the transcripton factor, NF-κB; PPAR – peroxisome proliferator-activated receptors; STAT – signal transducers and activators of transcription. The presence of a transcription factor binding site was indicated by the letter “Y”.

In our study, we propose that two major mechanisms could explain the induction of chemokines in chemotherapy-treated cancer cells (Figure 4.3.1). In the first proposed mechanism, we postulate that endogeneous components derived from dying cancer cells, termed damage-associated molecular patterns (DAMPs), such as RNA and DNA, can lead to type I IFN production. RNA released by necrotic or apoptotic cancer cells, could be sensed by TLR3 (toll-like receptor 3) (Beg, 2002; Cavassani et al., 2008; Lim and Wang, 2011). TLR3 signals via the adaptor protein, TRIF, which activates the kinase TBK1 (tank-binding kinase 1) and IRF3, leading to the production of type I IFNs (Takaoka and Taniguchi, 2008; Tow, 2010). In addition, TRIF associates with the mitochondria-localized adaptor molecule, RIP1, to activate NF-κB for the synthesis of proinflammatory cytokines (Tow, 2010). Chemotherapy drugs could also induce cytoplasmic DNA (Sumantran et al., 1995), which can be sensed by the cytosolic DNA sensors, DNA-dependent activator of interferon regulatory factors (DAI) or as yet an unknown cytosolic DNA receptor, DNA–RX, which trigger induction of type I IFN genes through TBK1-mediated and IRF3-mediated signalling (Trinchieri, 2010).

The second proposed mechanism is that chemotherapy drugs can induce DNA damage, leading to the activation of the DNA damage response pathway proteins, such as the protein kinases ATM (ataxiatelangiectasia mutated), CHK1/CHK2 (checkpoint kinase 1 or 2), and the transcription factor p53 (Zitvogel et al., 2008). Activated p53 can result in downstream activation of NF-κB through H-Ras, MEK1, and IKKa/b (Armstrong et al., 2006) or via the JNK (c-Jun NH_2-terminal kinase) pathway (Wu, 2004). Activated p53 can also

contribute to interferon response via transcriptional activation of IRF-9 and the enhancement of IFN signalling (Munoz-Fontela et al., 2008). In addition, IRF-1 (interferon regulatory factor-1) has also been reported to be induced via the ATM signalling pathway in response to genotoxic stress (Pamment et al., 2002).

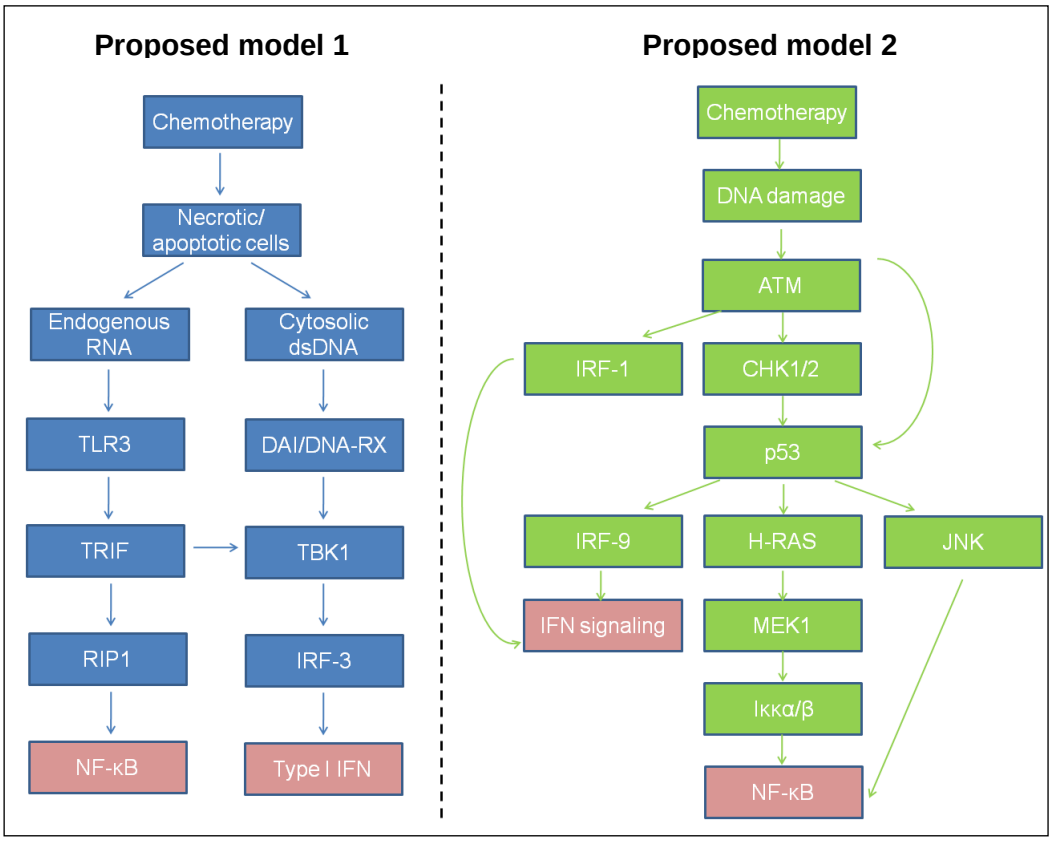

Figure 4.3.1 – Proposed models for the induction of chemokine expression from tumor cells after chemotherapy.
Chemotherapy could induce chemokine expression from tumor cells via at least two different mechansims that result in the same downstream responses. In the first proposed mechanism, endogenous components from dying cells (RNA and/or DNA) could be sensed by nucleic sensors (TLR3 or DAI/DNA-RX), leading to downstream activation of the transcription factor, NF-κB, and the production of type I IFN. In the second proposed model, DNA damage induced by chemotherapy activates the DNA-damage response pathway, resulting in downstream activation of NF-κB and IFN signalling. The corresponding transcription factor binding sites have been identified in the promoters of the *CCL5*, *CXCL9* and *CXCL10* chemokine genes.

To identify the pathway(s) involved, a multi-pronged approach including gene microarray and proteomic analyses will be performed. As we observed different kinetics in the induction of expression of these chemokine genes, it will be of interest to analyze tumor cells treated with chemotherapy at different time points. Activation of signal transduction pathways and transcription factors will be evaluated using western blot analyses and validated by microarray analyses (by looking at enrichment of transcription factor target genes). In addition, microarray analyses will serve to provide a comprehensive list of immediate early genes that may be involved in triggering the induction of chemokine expression after chemotherapy treatment. Furthermore, it provides insights as to whether chemotherapy-induced production of chemokines is a sequential event (Zitvogel et al., 2008).

Final proof-of-concept experiments should be performed to determine whether blocking the activation of pathways in these cells affects the response to chemotherapy treatment. It will also be interesting to determine whether these findings can be extended to more than one melanoma line. As shown previously, not all the melanoma cell lines included in our study respond to chemotherapy drug treatments by upregulating chemokine expression. Thus, it will be of interest to understand whether the basis of this 'non-responsiveness' could be in part due to defects in the activation of certain pathway(s). Finally, preliminary data obtained from this proposed study in cultured cells will need to be validated in patients by directly studying tumor tissues obtained before and after chemotherapy treatment.

4.3.4 Implications for the treatment of metastatic melanoma patients

Melanoma is a highly heterogeneous disease and it has recently become clear that indeed, there are many molecular subtypes of melanoma that may be associated with clinical responses to defined therapeutic strategies. This has led researchers to probe the tumor microenvironment for local factors that may determine the clinical outcome to such treatments. The molecular markers associated with responses to immunotherapeutic treatments in melanoma have been recently reviewed (Gajewski, 2011; Sznol, 2011).

For example, the identification of an 'inflamed' signature within the tumor microenvironment (that includes T cells and chemokines) by gene expression profiling is associated with favorable clinical benefit in recent cancer vaccine trials in advanced melanoma and non-small cell lung cancer (NSCLC) patients (Gajewski et al., 2009; Louahed et al., 2008; NCT00480025, [updated 02.06.2011]). In addition, the expression of defined tumor antigens is associated with improved disease-free interval (DFI) in patients treated with antigen-specific vaccines (i.e. MAGE-A3 Phase II vaccine trial in MAGE-A3-positive NSCLC patients) (Brichard and Lejeune, 2008). Furthermore, activating mutations in *B-raf* or *c-kit* are associated with clinical responses to the specific kinase inhibitors, PLX4032 and imatinib respectively and prospective Phase II and/or Phase III clinical trials are ongoing to demonstrate overall survival benefit (Gajewski, 2011).

In addition, several emerging molecular markers involved in signal transduction pathways have been identified in melanoma patients that may

predict clinical responses to specific immunotherapies and thus facilitate patient-specific therapy in subsets of melanoma patients harboring such biomarkers. This includes active Notch pathway, activating mutations in PI3 kinase/loss of PTEN suppressor, activating mutations in ErbB4, activating mutations in *c-met*, expression of stabilized β-catenin, and constitutive activation of Stat3, which are potential biomarkers for new targeted agents [reviewed in (Gajewski, 2011)]. All these observations clearly show that melanoma patients are highly heterogeneous in their tumor subtypes and this may render them susceptible to the therapeutic effect of one treatment modality and not the other.

The fact that clinical responses to immunotherapeutic agents may be predicted based on the molecular biomarkers present in the tumors of the patients raises the question of whether conventional chemotherapy drugs used for the treatment of metastatic melanoma patients might also be associated with a predictive biomarker. Chemotherapy drug resistance in melanoma is well known and several mechanisms have been postulated including dysregulation of apoptotic pathways, defects in drug transport, detoxification, and enhanced DNA repair (Lev et al., 2004).

Indeed, responses to the alkylating agents dacarbazine and temozolomide is predicted to be inversely correlated with the expression of DNA repair enzymes, such as 0^6-methylguanine methyltransferase (MGMT). While silencing of MGMT has been associated with a favourable clinical response of glioblastoma to temozolomide plus radiation (Hegi et al., 2005), the addition of

MGMT inhibitor 0^6-benzylguanine in melanoma failed to demonstrate any added clinical benefit (Gajewski et al., 2005).

A recent report demonstrated the use of p53 functional status as a biomarker to predict response to neoadjuvant chemotherapy in patients with locally advanced head and neck squamous cell carcinoma (HNSCC) in the oral cavity (Perrone et al., 2010). In this study, 40% of patients with wild-type or partially functional p53 showed complete pathologic response to chemotherapy, compared to approximately 10% of those having non-functional p53. While this study represents a step forward in risk stratification of patients and towards personalized therapy, many questions remain to be addressed (Mroz and Rocco, 2010). For example, it is unclear whether the functional/non-functional distinction is clearly superior to the simple mutated/nonmutated classification as not all the exons in p53 were screened. In addition, it is unknown whether the complete responses in the chemotherapy arm were confounded by the better surgical outcome in patients carrying wild-type p53. Most importantly, the exact functions of p53 in tumor biology and in mediating responses to chemotherapy in HNSCC remain unknown. At this moment, it is still too early to focus solely on p53 functional status as a biomarker of chemotherapy response and further experiments should be performed and followed up in clinical trials before it can be widely applied in clinical practice.

Based on these earlier reports, it is imperative in our case to identify the pathway(s) in which chemotherapy induces chemokine expression in

melanoma, leading to downstream activation of immune defense mechanisms. We believe that elucidation of the pathway(s) involved and the identification of the pathway proteins could have tremendous advantages for improving the therapeutic success for melanoma patients. Firstly, it could potentially serve as a novel predictive biomarker for response to chemotherapy agents commonly used to treat metastatic melanoma patients. Secondly, it allows stratifying patients based on pathway expression and selection of patients such that only those most likely to benefit are subjected to chemotherapy treatment. Thirdly, it enables identification of patients whom are likely to gain from additional treatment with immunotherapy, i.e. combination chemoimmunotherapy.

Patients with advanced metastatic melanoma are often treated with a combination of chemotherapy and immunotherapy, i.e chemoimmunotherapy. Combination treatments have been studied since the early 1990s (Khayat et al., 2002). Some reports have suggested that chemotherapeutic agents administered in combination with IL-2 or IFN-α, or both, can improve response rates (Legha et al., 1998; Richards et al., 1992) and increase the median survival of patients (Falkson et al., 1991). Based on these earlier reports, the use of chemoimmunotherapy is currently preferred in some institutions as a first-line treatment in advanced (stage IV) melanoma patients (Kadison and Morton, 2003; Keilholz and Gore, 2002). In contrast, a recent study suggests that adding IL-2 and IFN-α to a specific three-drug regimen of cisplatin, vinblastine, and dacarbazine did not prolong survival in a phase III trial (Atkins et al., 2008). Thus, the role of IL-2 and IFN-α in improving the response to

chemotherapy is still unresolved, and there is still lack of evidence to support the use of immunotherapy in conjunction with chemotherapy.

Our findings that chemotherapy can directly enhance intra-tumor chemokine expression and positively impacts T cell infiltration, tumor control and patient survival raises great hope for combination therapies consisting of vaccines or adoptive lymphocyte transfer combined with chemotherapy. Therefore, identifying the intrinsic characteristics of tumor cells and the immunological characteristic of tumors may yield valuable information for the optimal design of chemo-immunotherapies for the treatment of melanoma. Furthermore, future studies should consider screening for chemotherapeutic products that are able to induce specific expression of T cell attracting-chemokines in cancer cells so as to identify drugs that could potentially improve the efficacy of immunotherapy.

CHAPTER 5
CONCLUSION

5 CONCLUSION

T cell infiltration is known to impact tumor growth and is associated with cancer patient survival. However, the molecular cues that favor T cell infiltration remain largely undefined. Therefore, unraveling the signals that control T cell infiltration into the tumors is, without doubt, a pre-requisite to improve the efficacy of cancer vaccines and adoptive T cell therapies.

In the present study, using a genetically-engineered mouse model of melanoma, we identify CXCR3 ligands (CXCL9 and CXCL10) and CCL5 as the main determinants of T cell infiltration into cutaneous metastases. CXCR3 ligands and CCL5 synergize to attract effector T cells into cutaneous tumors leading to enhanced anti-tumor activity. In addition, expression of these chemokines in tumors inhibits tumor growth.

In melanoma patients, CXCR3 ligands and CCL5 are also up-regulated in chemotherapy-sensitive lesions following chemotherapy, and correlate with T cell infiltration, tumor control and patient survival. Mechanistically, we found that the chemotherapeutic agents commonly used to treat advanced melanomas (dacarbazine, temozolomide and cisplatin) induce specific expression of these T cell-attracting chemokines in several human melanoma cell lines *in vitro*.

These data unravel a novel mechanism of the action of chemotherapy, in which chemotherapy treatment induces intra-tumoral expression of T cell-

attracting chemokines, leading to anti-tumor immune responses. The combination of experiments performed *in vitro* and *in vivo* (using both spontaneous and transplanted model of melanoma, syngeneic and human melanoma cell lines, together with data from melanoma patients), provide a solid validation of the findings.

The findings from this study are important as they may provide the basis for new therapeutic approaches to treat melanoma by identifying patients with an increased chance of response to conventional chemotherapies as well as combination chemoimmunotherapies. For future studies, we propose that identifying chemotherapeutic drugs that are able to induce the expression of T cell-attracting chemokines in cancer cells may represent a novel strategy to improve the efficacy of cancer immunotherapy. To this end, the generation of a new reporter mouse model of melanoma, Melucie, will serve as a useful tool to facilitate testing of future chemo-immunotherapeutic strategies against melanoma.

CHAPTER 6

REFERENCES

6 REFERENCES

Ahmad, A., and Menezes, J. (1996). Antibody-dependent cellular cytotoxicity in HIV infections. FASEB J *10*, 258-266.

Ahmed, N., Abubaker, K., Findlay, J., and Quinn, M. (2010). Epithelial mesenchymal transition and cancer stem cell-like phenotypes facilitate chemoresistance in recurrent ovarian cancer. Curr Cancer Drug Targets *10*, 268-278.

Al-Attar, A., Shehata, M., Durrant, L., Moseley, P., Deen, S., and Chan, S. (2009). T cell density and location can influence the prognosis of ovarian cancer. Pathol Oncol Res *16*, 361-370.

Algarra, I., Cabrera, T., and Garrido, F. (2000). The HLA crossroad in tumor immunology. Hum Immunol *61*, 65-73.

Antonelli, A., Ferrari, S.M., Fallahi, P., Ghiri, E., Crescioli, C., Romagnani, P., Vitti, P., Serio, M., and Ferrannini, E. (2010). Interferon-alpha, -beta and -gamma induce CXCL9 and CXCL10 secretion by human thyrocytes: modulation by peroxisome proliferator-activated receptor-gamma agonists. Cytokine *50*, 260-267.

Antonicelli, F., Lorin, J., Kurdykowski, S., Gangloff, S.C., Le Naour, R., Sallenave, J.M., Hornebeck, W., Grange, F., and Bernard, P. (2011). CXCL10 reduces melanoma proliferation and invasiveness in vitro and in vivo. Br J Dermatol *164*, 720-728.

Arai, H., Gordon, D., Nabel, E.G., and Nabel, G.J. (1997). Gene transfer of Fas ligand induces tumor regression in vivo. Proc Natl Acad Sci U S A *94*, 13862-13867.

Armstrong, M.B., Bian, X., Liu, Y., Subramanian, C., Ratanaproeksa, A.B., Shao, F., Yu, V.C., Kwok, R.P., Opipari, A.W., and Castle, V.P. (2006). Signaling from p53 to NF-kappa B determines the chemotherapy responsiveness of neuroblastoma. Neoplasia *8*, 964-974.

Ascierto, P.A., De Maio, E., Bertuzzi, S., Palmieri, G., Halaban, R., Hendrix, M., Kashani-sabet, M., Ferrone, S., Wang, E., Cochran, A.*, et al.* (2011). Future perspectives in melanoma research. Meeting report from the "Melanoma Research: a bridge Naples-USA. Naples, December 6th-7th 2010". J Transl Med *9*, 32.

Atkins, M.B., Elder, D.E., Essner, R., Flaherty, K.T., Gajewski, T.F., Haluska, F.G., Hwu, P., Keilholz, U., Kirkwood, J.M., Mier, J.W.*, et al.* (2006). Innovations and challenges in melanoma: summary statement from the first Cambridge conference. Clin Cancer Res *12*, 2291s-2296s.

Atkins, M.B., Hsu, J., Lee, S., Cohen, G.I., Flaherty, L.E., Sosman, J.A., Sondak, V.K., and Kirkwood, J.M. (2008). Phase III trial comparing concurrent biochemotherapy with cisplatin, vinblastine, dacarbazine, interleukin-2, and interferon alfa-2b with cisplatin, vinblastine, and dacarbazine alone in patients with metastatic malignant melanoma (E3695): a trial coordinated by the Eastern Cooperative Oncology Group. J Clin Oncol *26*, 5748-5754.

Atkins, M.B., Lotze, M.T., Dutcher, J.P., Fisher, R.I., Weiss, G., Margolin, K., Abrams, J., Sznol, M., Parkinson, D., Hawkins, M.*, et al.* (1999). High-dose recombinant interleukin 2 therapy for patients with metastatic melanoma: analysis of 270 patients treated between 1985 and 1993. J Clin Oncol *17*, 2105-2116.

Baeuerle, P.A., and Reinhardt, C. (2009). Bispecific T-cell engaging antibodies for cancer therapy. Cancer Res *69*, 4941-4944.

Bafaloukos, D., Aravantinos, G., Fountzilas, G., Stathopoulos, G., Gogas, H., Samonis, G., Briasoulis, E., Mylonakis, N., Skarlos, D.V., and Kosmidis, P. (2002). Docetaxel in combination with dacarbazine in patients with advanced melanoma. Oncology *63*, 333-337.

Baitsch, L., Baumgaertner, P., Devevre, E., Raghav, S.K., Legat, A., Barba, L., Wieckowski, S., Bouzourene, H., Deplancke, B., Romero, P.*, et al.* (2011). Exhaustion of tumor-specific CD8+ T cells in metastases from melanoma patients. J Clin Invest *121*, 2350-2360.

Bajetta, E., Del Vecchio, M., Bernard-Marty, C., Vitali, M., Buzzoni, R., Rixe, O., Nova, P., Aglione, S., Taillibert, S., and Khayat, D. (2002). Metastatic melanoma: chemotherapy. Semin Oncol *29*, 427-445.

Balkwill, F. (2003). Chemokine biology in cancer. Semin Immunol *15*, 49-55.

Balwit, J.M., Kalinski, P., Sondak, V.K., Coulie, P.G., Jaffee, E.M., Gajewski, T.F., and Marincola, F.M. (2011). Review of the 25th annual scientific meeting

of the International Society for Biological Therapy of Cancer. J Transl Med *9*, 60.

Bargou, R., Leo, E., Zugmaier, G., Klinger, M., Goebeler, M., Knop, S., Noppeney, R., Viardot, A., Hess, G., Schuler, M.*, et al.* (2008). Tumor regression in cancer patients by very low doses of a T cell-engaging antibody. Science *321*, 974-977.

Bauer, S., Groh, V., Wu, J., Steinle, A., Phillips, J.H., Lanier, L.L., and Spies, T. (1999). Activation of NK cells and T cells by NKG2D, a receptor for stress-inducible MICA. Science *285*, 727-729.

Beg, A.A. (2002). Endogenous ligands of Toll-like receptors: implications for regulating inflammatory and immune responses. Trends Immunol *23*, 509-512.

Ben-Baruch, A. (2006). The multifaceted roles of chemokines in malignancy. Cancer Metastasis Rev *25*, 357-371.

Bendall, S.C., Simonds, E.F., Qiu, P., Amir el, A.D., Krutzik, P.O., Finck, R., Bruggner, R.V., Melamed, R., Trejo, A., Ornatsky, O.I.*, et al.* (2011). Single-cell mass cytometry of differential immune and drug responses across a human hematopoietic continuum. Science *332*, 687-696.

Berd, D. (2002). M-Vax: an autologous, hapten-modified vaccine for human cancer. Expert Opin Biol Ther *2*, 335-342.

Berghuis, D., Santos, S.J., Baelde, H.J., Taminiau, A.H., Egeler, R.M., Schilham, M.W., Hogendoorn, P.C., and Lankester, A.C. (2011). Pro-

inflammatory chemokine-chemokine receptor interactions within the Ewing sarcoma microenvironment determine CD8(+) T-lymphocyte infiltration and affect tumour progression. J Pathol *223*, 347-357.

Berry, L.J., Moeller, M., and Darcy, P.K. (2009). Adoptive immunotherapy for cancer: the next generation of gene-engineered immune cells. Tissue Antigens *74*, 277-289.

Bird, R.E., and Walker, B.W. (1991). Single chain antibody variable regions. Trends Biotechnol *9*, 132-137.

Biron, C.A. (1997). Activation and function of natural killer cell responses during viral infections. Curr Opin Immunol *9*, 24-34.

Bleul, C.C., Fuhlbrigge, R.C., Casasnovas, J.M., Aiuti, A., and Springer, T.A. (1996). A highly efficacious lymphocyte chemoattractant, stromal cell-derived factor 1 (SDF-1). J Exp Med *184*, 1101-1109.

Bourgault-Villada, I., Hong, M., Khoo, K., Tham, M., Toh, B., Wai, L., and Abastado, J. (2011). Current Insight Into the Metastatic Process and Melanoma Cell Dissemination. In Melanoma/Book 1, M. Murph, ed.

Breart, B., Lemaitre, F., Celli, S., and Bousso, P. (2008). Two-photon imaging of intratumoral CD8+ T cell cytotoxic activity during adoptive T cell therapy in mice. J Clin Invest *118*, 1390-1397.

Brichard, V.G., and Lejeune, D. (2008). Cancer immunotherapy targeting tumour-specific antigens: towards a new therapy for minimal residual disease. Expert Opin Biol Ther *8*, 951-968.

Brischwein, K., Schlereth, B., Guller, B., Steiger, C., Wolf, A., Lutterbuese, R., Offner, S., Locher, M., Urbig, T., Raum, T.*, et al.* (2006). MT110: a novel bispecific single-chain antibody construct with high efficacy in eradicating established tumors. Mol Immunol *43*, 1129-1143.

Brown, C.E., Vishwanath, R.P., Aguilar, B., Starr, R., Najbauer, J., Aboody, K.S., and Jensen, M.C. (2007). Tumor-derived chemokine MCP-1/CCL2 is sufficient for mediating tumor tropism of adoptively transferred T cells. J Immunol *179*, 3332-3341.

Brozena, S.J., Fenske, N.A., and Perez, I.R. (1993). Epidemiology of malignant melanoma, worldwide incidence, and etiologic factors. Semin Surg Oncol *9*, 165-167.

Buonaguro, L., Petrizzo, A., Tornesello, M.L., and Buonaguro, F.M. (2011). Translating tumor antigens into cancer vaccines. Clin Vaccine Immunol *18*, 23-34.

Burnet, F.M. (1970). The concept of immunological surveillance. Prog Exp Tumor Res *13*, 1-27.

Cavassani, K.A., Ishii, M., Wen, H., Schaller, M.A., Lincoln, P.M., Lukacs, N.W., Hogaboam, C.M., and Kunkel, S.L. (2008). TLR3 is an endogenous

sensor of tissue necrosis during acute inflammatory events. J Exp Med *205*, 2609-2621.

Cefai, D., Favre, L., Wattendorf, E., Marti, A., Jaggi, R., and Gimmi, C.D. (2001). Role of Fas ligand expression in promoting escape from immune rejection in a spontaneous tumor model. Int J Cancer *91*, 529-537.

Chew, V., Chen, J., Lee, D., Loh, E., Lee, J., Lim, K.H., Weber, A., Slankamenac, K., Poon, R.T., Yang, H.*, et al.* (2011). Chemokine-driven lymphocyte infiltration: an early intratumoural event determining long-term survival in resectable hepatocellular carcinoma. Gut.

Chew, V., Tow, C., Teo, M., Wong, H.L., Chan, J., Gehring, A., Loh, M., Bolze, A., Quek, R., Lee, V.K.*, et al.* (2010). Inflammatory tumour microenvironment is associated with superior survival in hepatocellular carcinoma patients. J Hepatol *52*, 370-379.

Chin, Y., Janssens, J., Bleus, J., Zhang, J., and Raus, J. (1993). In vivo distribution of radio-labeled tumor infiltrating lymphocytes in cancer patients. In Vivo *7*, 27-30.

Choi, B.D., Cai, M., Bigner, D.D., Mehta, A.I., Kuan, C.T., and Sampson, J.H. (2011). Bispecific antibodies engage T cells for antitumor immunotherapy. Expert Opin Biol Ther *11*, 843-853.

Clemente, C.G., Mihm, M.C., Jr., Bufalino, R., Zurrida, S., Collini, P., and Cascinelli, N. (1996). Prognostic value of tumor infiltrating lymphocytes in the vertical growth phase of primary cutaneous melanoma. Cancer *77*, 1303-1310.

Cole, W.H. (1974). Spontaneous regression of cancer: the metabolic triumph of the host? Ann N Y Acad Sci *230*, 111-141.

Correale, P., Cusi, M.G., Tsang, K.Y., Del Vecchio, M.T., Marsili, S., Placa, M.L., Intrivici, C., Aquino, A., Micheli, L., Nencini, C.*, et al.* (2005). Chemo-immunotherapy of metastatic colorectal carcinoma with gemcitabine plus FOLFOX 4 followed by subcutaneous granulocyte macrophage colony-stimulating factor and interleukin-2 induces strong immunologic and antitumor activity in metastatic colon cancer patients. J Clin Oncol *23*, 8950-8958.

Craft, N., Bruhn, K.W., Nguyen, B.D., Prins, R., Liau, L.M., Collisson, E.A., De, A., Kolodney, M.S., Gambhir, S.S., and Miller, J.F. (2005). Bioluminescent imaging of melanoma in live mice. J Invest Dermatol *125*, 159-165.

Crittenden, M., Gough, M., Harrington, K., Olivier, K., Thompson, J., and Vile, R.G. (2003). Expression of inflammatory chemokines combined with local tumor destruction enhances tumor regression and long-term immunity. Cancer Res *63*, 5505-5512.

Culver, M.E., Gatesman, M.L., Mancl, E.E., and Lowe, D.K. (2011). Ipilimumab: a novel treatment for metastatic melanoma. Ann Pharmacother *45*, 510-519.

Cummins, D.L., Cummins, J.M., Pantle, H., Silverman, M.A., Leonard, A.L., and Chanmugam, A. (2006). Cutaneous malignant melanoma. Mayo Clin Proc *81*, 500-507.

Cure, H., Souteyrand, P., Ouabdesselam, R., Roche, H., Ravaud, A., D'Incan, M., Viens, P., Fargeot, P., Lentz, M.A., Fumoleau, P.*, et al.* (1999). Results of a phase II trial with cystemustine at 90 mg/m(2) as a first- or second-line treatment in advanced malignant melanoma: a trial of the EORTC Clinical Studies Group. Melanoma Res *9*, 607-610.

Curtin, J.A., Fridlyand, J., Kageshita, T., Patel, H.N., Busam, K.J., Kutzner, H., Cho, K.H., Aiba, S., Brocker, E.B., LeBoit, P.E.*, et al.* (2005). Distinct sets of genetic alterations in melanoma. N Engl J Med *353*, 2135-2147.

Dannull, J., Su, Z., Rizzieri, D., Yang, B.K., Coleman, D., Yancey, D., Zhang, A., Dahm, P., Chao, N., Gilboa, E.*, et al.* (2005). Enhancement of vaccine-mediated antitumor immunity in cancer patients after depletion of regulatory T cells. J Clin Invest *115*, 3623-3633.

Darst, M., Al-Hassani, M., Li, T., Yi, Q., Travers, J.M., Lewis, D.A., and Travers, J.B. (2004). Augmentation of chemotherapy-induced cytokine production by expression of the platelet-activating factor receptor in a human epithelial carcinoma cell line. J Immunol *172*, 6330-6335.

Demaria, S., Volm, M.D., Shapiro, R.L., Yee, H.T., Oratz, R., Formenti, S.C., Muggia, F., and Symmans, W.F. (2001). Development of tumor-infiltrating

lymphocytes in breast cancer after neoadjuvant paclitaxel chemotherapy. Clin Cancer Res *7*, 3025-3030.

Di Stasi, A., De Angelis, B., Rooney, C.M., Zhang, L., Mahendravada, A., Foster, A.E., Heslop, H.E., Brenner, M.K., Dotti, G., and Savoldo, B. (2009). T lymphocytes coexpressing CCR4 and a chimeric antigen receptor targeting CD30 have improved homing and antitumor activity in a Hodgkin tumor model. Blood *113*, 6392-6402.

Dolcetti, R., Viel, A., Doglioni, C., Russo, A., Guidoboni, M., Capozzi, E., Vecchiato, N., Macri, E., Fornasarig, M., and Boiocchi, M. (1999). High prevalence of activated intraepithelial cytotoxic T lymphocytes and increased neoplastic cell apoptosis in colorectal carcinomas with microsatellite instability. Am J Pathol *154*, 1805-1813.

Dorval, T., Palangie, T., Jouve, M., Garcia-Giralt, E., Israel, L., Falcoff, E., Schwab, D., and Pouillart, P. (1986). Clinical phase II trial of recombinant DNA interferon (interferon alpha 2b) in patients with metastatic malignant melanoma. Cancer *58*, 215-218.

Du, C., and Wang, Y. (2011). The immunoregulatory mechanisms of carcinoma for its survival and development. J Exp Clin Cancer Res *30*, 12.

Dudley, M.E., Wunderlich, J.R., Shelton, T.E., Even, J., and Rosenberg, S.A. (2003). Generation of tumor-infiltrating lymphocyte cultures for use in adoptive transfer therapy for melanoma patients. J Immunother *26*, 332-342.

Dunn, G.P., Old, L.J., and Schreiber, R.D. (2004). The three Es of cancer immunoediting. Annu Rev Immunol *22*, 329-360.

Dutcher, J.P., Creekmore, S., Weiss, G.R., Margolin, K., Markowitz, A.B., Roper, M., Parkinson, D., Ciobanu, N., Fisher, R.I., Boldt, D.H.*, et al.* (1989). A phase II study of interleukin-2 and lymphokine-activated killer cells in patients with metastatic malignant melanoma. J Clin Oncol *7*, 477-485.

Ekmekcioglu, S., Ellerhorst, J.A., Prieto, V.G., Johnson, M.M., Broemeling, L.D., and Grimm, E.A. (2006). Tumor iNOS predicts poor survival for stage III melanoma patients. Int J Cancer *119*, 861-866.

El-Aneed, A. (2004). An overview of current delivery systems in cancer gene therapy. J Control Release *94*, 1-14.

Eyles, J., Puaux, A.L., Wang, X., Toh, B., Prakash, C., Hong, M., Tan, T.G., Zheng, L., Ong, L.C., Jin, Y.*, et al.* (2010). Tumor cells disseminate early, but immunosurveillance limits metastatic outgrowth, in a mouse model of melanoma. J Clin Invest *120*, 2030-2039.

Falkson, C.I., Falkson, G., and Falkson, H.C. (1991). Improved results with the addition of interferon alfa-2b to dacarbazine in the treatment of patients with metastatic malignant melanoma. J Clin Oncol *9*, 1403-1408.

Fallarino, F., Grohmann, U., Vacca, C., Bianchi, R., Orabona, C., Spreca, A., Fioretti, M.C., and Puccetti, P. (2002). T cell apoptosis by tryptophan catabolism. Cell Death Differ *9*, 1069-1077.

Fiedler, M., Ritter, B., Seggewiss, R., Bokemeyer, C., Fettes, P., Klinger, M., Vieser, E., Ruettinger, D., Kaubitzsch, S., and Wolf, M. (2010). Phase I safety and pharmacology study of the EpCAM/CD3-bispecific BiTE antibody MT110 in patients with metastatic colorectal, gastric, or lung cancer. In ASCO Annual Meeting Proceedings (Post-Meeting Edition), pp. 2573.

Fine, J.H., Chen, P., Mesci, A., Allan, D.S., Gasser, S., Raulet, D.H., and Carlyle, J.R. (2010). Chemotherapy-induced genotoxic stress promotes sensitivity to natural killer cell cytotoxicity by enabling missing-self recognition. Cancer Res *70*, 7102-7113.

Fisher, D.T., Chen, Q., Appenheimer, M.M., Skitzki, J., Wang, W.C., Odunsi, K., and Evans, S.S. (2006). Hurdles to lymphocyte trafficking in the tumor microenvironment: implications for effective immunotherapy. Immunol Invest *35*, 251-277.

Francia, G., Cruz-Munoz, W., Man, S., Xu, P., and Kerbel, R.S. (2011). Mouse models of advanced spontaneous metastasis for experimental therapeutics. Nat Rev Cancer *11*, 135-141.

Franciszkiewicz, K., Le Floc'h, A., Jalil, A., Vigant, F., Robert, T., Vergnon, I., Mackiewicz, A., Benihoud, K., Validire, P., Chouaib, S.*, et al.* (2009). Intratumoral induction of CD103 triggers tumor-specific CTL function and CCR5-dependent T-cell retention. Cancer Res *69*, 6249-6255.

French, A.R., and Yokoyama, W.M. (2003). Natural killer cells and viral infections. Curr Opin Immunol *15*, 45-51.

Gajewski, T., Zha, Y., Thurner, B., and Schuler, G. (2009). Association of gene expression profile in metastatic melanoma and survival to a dendritic cell-based vaccine. Paper presented at: ASCO Annual Meeting Proceedings.

Gajewski, T.F. (2007). Failure at the effector phase: immune barriers at the level of the melanoma tumor microenvironment. Clin Cancer Res *13*, 5256-5261.

Gajewski, T.F. (2011). Molecular profiling of melanoma and the evolution of patient-specific therapy. Semin Oncol *38*, 236-242.

Gajewski, T.F., Louahed, J., and Brichard, V.G. (2010). Gene signature in melanoma associated with clinical activity: a potential clue to unlock cancer immunotherapy. Cancer J *16*, 399-403.

Gajewski, T.F., Meng, Y., Blank, C., Brown, I., Kacha, A., Kline, J., and Harlin, H. (2006). Immune resistance orchestrated by the tumor microenvironment. Immunol Rev *213*, 131-145.

Gajewski, T.F., Sosman, J., Gerson, S.L., Liu, L., Dolan, E., Lin, S., and Vokes, E.E. (2005). Phase II trial of the O6-alkylguanine DNA alkyltransferase inhibitor O6-benzylguanine and 1,3-bis(2-chloroethyl)-1-nitrosourea in advanced melanoma. Clin Cancer Res *11*, 7861-7865.

Galon, J., Costes, A., Sanchez-Cabo, F., Kirilovsky, A., Mlecnik, B., Lagorce-Pages, C., Tosolini, M., Camus, M., Berger, A., Wind, P.*, et al.* (2006). Type,

density, and location of immune cells within human colorectal tumors predict clinical outcome. Science *313*, 1960-1964.

Gasser, S., Orsulic, S., Brown, E.J., and Raulet, D.H. (2005). The DNA damage pathway regulates innate immune system ligands of the NKG2D receptor. Nature *436*, 1186-1190.

Geller, M.A., Bui-Nguyen, T.M., Rogers, L.M., and Ramakrishnan, S. (2010). Chemotherapy induces macrophage chemoattractant protein-1 production in ovarian cancer. Int J Gynecol Cancer *20*, 918-925.

Gerard, A., van der Kammen, R.A., Janssen, H., Ellenbroek, S.I., and Collard, J.G. (2009). The Rac activator Tiam1 controls efficient T-cell trafficking and route of transendothelial migration. Blood *113*, 6138-6147.

Gijsbers, K., Gouwy, M., Struyf, S., Wuyts, A., Proost, P., Opdenakker, G., Penninckx, F., Ectors, N., Geboes, K., and Van Damme, J. (2005). GCP-2/CXCL6 synergizes with other endothelial cell-derived chemokines in neutrophil mobilization and is associated with angiogenesis in gastrointestinal tumors. Exp Cell Res *303*, 331-342.

Giovarelli, M., Cappello, P., Forni, G., Salcedo, T., Moore, P.A., LeFleur, D.W., Nardelli, B., Di Carlo, E., Lollini, P.L., Ruben, S.*, et al.* (2000). Tumor rejection and immune memory elicited by locally released LEC chemokine are associated with an impressive recruitment of APCs, lymphocytes, and granulocytes. J Immunol *164*, 3200-3206.

Goldman, S.J., Chen, E., Taylor, R., Zhang, S., Petrosky, W., Reiss, M., and Jin, S. (2011). Use of the ODD-luciferase transgene for the non-invasive imaging of spontaneous tumors in mice. PLoS One *6*, e18269.

Gordon, J.W., and Ruddle, F.H. (1981). Integration and stable germ line transmission of genes injected into mouse pronuclei. Science *214*, 1244-1246.

Gouwy, M., Struyf, S., Catusse, J., Proost, P., and Van Damme, J. (2004). Synergy between proinflammatory ligands of G protein-coupled receptors in neutrophil activation and migration. J Leukoc Biol *76*, 185-194.

Gouwy, M., Struyf, S., Mahieu, F., Put, W., Proost, P., and Van Damme, J. (2002). The unique property of the CC chemokine regakine-1 to synergize with other plasma-derived inflammatory mediators in neutrophil chemotaxis does not reside in its NH2-terminal structure. Mol Pharmacol *62*, 173-180.

Gouwy, M., Struyf, S., Noppen, S., Schutyser, E., Springael, J.Y., Parmentier, M., Proost, P., and Van Damme, J. (2008). Synergy between coproduced CC and CXC chemokines in monocyte chemotaxis through receptor-mediated events. Mol Pharmacol *74*, 485-495.

Gray-Schopfer, V., Wellbrock, C., and Marais, R. (2007). Melanoma biology and new targeted therapy. Nature *445*, 851-857.

Groom, J.R., and Luster, A.D. (2011). CXCR3 ligands: redundant, collaborative and antagonistic functions. Immunol Cell Biol *89*, 207-215.

Haanen, J.B., Baars, A., Gomez, R., Weder, P., Smits, M., de Gruijl, T.D., von Blomberg, B.M., Bloemena, E., Scheper, R.J., van Ham, S.M.*, et al.* (2006). Melanoma-specific tumor-infiltrating lymphocytes but not circulating melanoma-specific T cells may predict survival in resected advanced-stage melanoma patients. Cancer Immunol Immunother *55*, 451-458.

Haas, C., Krinner, E., Brischwein, K., Hoffmann, P., Lutterbuse, R., Schlereth, B., Kufer, P., and Baeuerle, P.A. (2009). Mode of cytotoxic action of T cell-engaging BiTE antibody MT110. Immunobiology *214*, 441-453.

Hahne, M., Rimoldi, D., Schroter, M., Romero, P., Schreier, M., French, L.E., Schneider, P., Bornand, T., Fontana, A., Lienard, D.*, et al.* (1996). Melanoma cell expression of Fas(Apo-1/CD95) ligand: implications for tumor immune escape. Science *274*, 1363-1366.

Halama, N., Michel, S., Kloor, M., Zoernig, I., Pommerencke, T., von Knebel Doeberitz, M., Schirmacher, P., Weitz, J., Grabe, N., and Jager, D. (2009). The localization and density of immune cells in primary tumors of human metastatic colorectal cancer shows an association with response to chemotherapy. Cancer Immun *9*, 1.

Hamzah, J., Jugold, M., Kiessling, F., Rigby, P., Manzur, M., Marti, H.H., Rabie, T., Kaden, S., Grone, H.J., Hammerling, G.J.*, et al.* (2008). Vascular normalization in Rgs5-deficient tumours promotes immune destruction. Nature *453*, 410-414.

Hanahan, D., and Weinberg, R.A. (2011). Hallmarks of cancer: the next generation. Cell *144*, 646-674.

Harlin, H., Meng, Y., Peterson, A.C., Zha, Y., Tretiakova, M., Slingluff, C., McKee, M., and Gajewski, T.F. (2009). Chemokine expression in melanoma metastases associated with CD8+ T-cell recruitment. Cancer Res *69*, 3077-3085.

Hauschild, A., Gogas, H., Tarhini, A., Middleton, M.R., Testori, A., Dreno, B., and Kirkwood, J.M. (2008). Practical guidelines for the management of interferon-alpha-2b side effects in patients receiving adjuvant treatment for melanoma: expert opinion. Cancer *112*, 982-994.

Hayakawa, Y., and Smyth, M.J. (2006). Innate immune recognition and suppression of tumors. Adv Cancer Res *95*, 293-322.

Hegi, M.E., Diserens, A.C., Gorlia, T., Hamou, M.F., de Tribolet, N., Weller, M., Kros, J.M., Hainfellner, J.A., Mason, W., Mariani, L.*, et al.* (2005). MGMT gene silencing and benefit from temozolomide in glioblastoma. N Engl J Med *352*, 997-1003.

Hensbergen, P.J., Wijnands, P.G., Schreurs, M.W., Scheper, R.J., Willemze, R., and Tensen, C.P. (2005). The CXCR3 targeting chemokine CXCL11 has potent antitumor activity in vivo involving attraction of CD8+ T lymphocytes but not inhibition of angiogenesis. J Immunother *28*, 343-351.

Herr, I., and Debatin, K.M. (2001). Cellular stress response and apoptosis in cancer therapy. Blood *98*, 2603-2614.

Hershkovitz, L., Schachter, J., Treves, A.J., and Besser, M.J. (2010). Focus on adoptive T cell transfer trials in melanoma. Clin Dev Immunol *2010*, 260267.

Hiraoka, N. (2010). Tumor-infiltrating lymphocytes and hepatocellular carcinoma: molecular biology. Int J Clin Oncol *15*, 544-551.

Hodi, F.S., O'Day, S.J., McDermott, D.F., Weber, R.W., Sosman, J.A., Haanen, J.B., Gonzalez, R., Robert, C., Schadendorf, D., Hassel, J.C.*, et al.* (2010). Improved survival with ipilimumab in patients with metastatic melanoma. N Engl J Med *363*, 711-723.

Hoffman, R.M., and Yang, M. (2006). Whole-body imaging with fluorescent proteins. Nat Protoc *1*, 1429-1438.

Hsu, B.L., Harless, S.M., Lindsley, R.C., Hilbert, D.M., and Cancro, M.P. (2002). Cutting edge: BLyS enables survival of transitional and mature B cells through distinct mediators. J Immunol *168*, 5993-5996.

Hsu, K.C., Keever-Taylor, C.A., Wilton, A., Pinto, C., Heller, G., Arkun, K., O'Reilly, R.J., Horowitz, M.M., and Dupont, B. (2005). Improved outcome in HLA-identical sibling hematopoietic stem-cell transplantation for acute myelogenous leukemia predicted by KIR and HLA genotypes. Blood *105*, 4878-4884.

Huang, H., Bi, X.G., Yuan, J.Y., Xu, S.L., Guo, X.L., and Xiang, J. (2005). Combined CD4+ Th1 effect and lymphotactin transgene expression enhance CD8+ Tc1 tumor localization and therapy. Gene Ther *12*, 999-1010.

Huang, H., Li, F., Gordon, J.R., and Xiang, J. (2002). Synergistic enhancement of antitumor immunity with adoptively transferred tumor-specific CD4+ and CD8+ T cells and intratumoral lymphotactin transgene expression. Cancer Res *62*, 2043-2051.

Imai, K., Matsuyama, S., Miyake, S., Suga, K., and Nakachi, K. (2000). Natural cytotoxic activity of peripheral-blood lymphocytes and cancer incidence: an 11-year follow-up study of a general population. Lancet *356*, 1795-1799.

Ishigami, S., Natsugoe, S., Tokuda, K., Nakajo, A., Che, X., Iwashige, H., Aridome, K., Hokita, S., and Aikou, T. (2000). Prognostic value of intratumoral natural killer cells in gastric carcinoma. Cancer *88*, 577-583.

Ittner, L.M., and Gotz, J. (2007). Pronuclear injection for the production of transgenic mice. Nat Protoc *2*, 1206-1215.

Iwamoto, T., Takahashi, M., Ito, M., Hamatani, K., Ohbayashi, M., Wajjwalku, W., Isobe, K., and Nakashima, I. (1991). Aberrant melanogenesis and melanocytic tumour development in transgenic mice that carry a metallothionein/ret fusion gene. EMBO J *10*, 3167-3175.

Jandus, C., Speiser, D., and Romero, P. (2009). Recent advances and hurdles in melanoma immunotherapy. Pigment Cell Melanoma Res *22*, 711-723.

Jansen, T., Tyler, B., Mankowski, J.L., Recinos, V.R., Pradilla, G., Legnani, F., Laterra, J., and Olivi, A. (2010). FasL gene knock-down therapy enhances the antiglioma immune response. Neuro Oncol *12*, 482-489.

Jassar, A.S., Suzuki, E., Kapoor, V., Sun, J., Silverberg, M.B., Cheung, L., Burdick, M.D., Strieter, R.M., Ching, L.M., Kaiser, L.R.*, et al.* (2005). Activation of tumor-associated macrophages by the vascular disrupting agent 5,6-dimethylxanthenone-4-acetic acid induces an effective CD8+ T-cell-mediated antitumor immune response in murine models of lung cancer and mesothelioma. Cancer Res *65*, 11752-11761.

Johansson, C.C., Egyhazi, S., Masucci, G., Harlin, H., Mougiakakos, D., Poschke, I., Nilsson, B., Garberg, L., Tuominen, R., Linden, D.*, et al.* (2009). Prognostic significance of tumor iNOS and COX-2 in stage III malignant cutaneous melanoma. Cancer Immunol Immunother *58*, 1085-1094.

Johnston, B., and Butcher, E.C. (2002). Chemokines in rapid leukocyte adhesion triggering and migration. Semin Immunol *14*, 83-92.

Kadison, A.S., and Morton, D.L. (2003). Immunotherapy of malignant melanoma. Surg Clin North Am *83*, 343-370.

Kagi, D., Ledermann, B., Burki, K., Zinkernagel, R.M., and Hengartner, H. (1996). Molecular mechanisms of lymphocyte-mediated cytotoxicity and their role in immunological protection and pathogenesis in vivo. Annu Rev Immunol *14*, 207-232.

Kantoff, P.W., Higano, C.S., Shore, N.D., Berger, E.R., Small, E.J., Penson, D.F., Redfern, C.H., Ferrari, A.C., Dreicer, R., Sims, R.B.*, et al.* (2010). Sipuleucel-T immunotherapy for castration-resistant prostate cancer. N Engl J Med *363*, 411-422.

Kaplan, D.H., Shankaran, V., Dighe, A.S., Stockert, E., Aguet, M., Old, L.J., and Schreiber, R.D. (1998). Demonstration of an interferon gamma-dependent tumor surveillance system in immunocompetent mice. Proc Natl Acad Sci U S A *95*, 7556-7561.

Karin, M. (2006). NF-kappaB and cancer: mechanisms and targets. Mol Carcinog *45*, 355-361.

Kato, M., Takahashi, M., Akhand, A.A., Liu, W., Dai, Y., Shimizu, S., Iwamoto, T., Suzuki, H., and Nakashima, I. (1998). Transgenic mouse model for skin malignant melanoma. Oncogene *17*, 1885-1888.

Kawai, O., Ishii, G., Kubota, K., Murata, Y., Naito, Y., Mizuno, T., Aokage, K., Saijo, N., Nishiwaki, Y., Gemma, A.*, et al.* (2008). Predominant infiltration of macrophages and CD8(+) T Cells in cancer nests is a significant predictor of survival in stage IV nonsmall cell lung cancer. Cancer *113*, 1387-1395.

Kaye, P. Notes on symptom control in hospice and palliative care (Hospice Education Institute).

Keilholz, U., and Gore, M.E. (2002). Biochemotherapy for advanced melanoma. Semin Oncol *29*, 456-461.

Kershaw, M.H., Wang, G., Westwood, J.A., Pachynski, R.K., Tiffany, H.L., Marincola, F.M., Wang, E., Young, H.A., Murphy, P.M., and Hwu, P. (2002). Redirecting migration of T cells to chemokine secreted from tumors by genetic modification with CXCR2. Hum Gene Ther *13*, 1971-1980.

Khayat, D., Bernard-Marty, C., Meric, J.B., and Rixe, O. (2002). Biochemotherapy for advanced melanoma: maybe it is real. J Clin Oncol *20*, 2411-2414.

Kim, J.B., Urban, K., Cochran, E., Lee, S., Ang, A., Rice, B., Bata, A., Campbell, K., Coffee, R., Gorodinsky, A.*, et al.* (2010). Non-invasive detection of a small number of bioluminescent cancer cells in vivo. PLoS One *5*, e9364.

Kim, R., Emi, M., and Tanabe, K. (2007). Cancer immunoediting from immune surveillance to immune escape. Immunology *121*, 1-14.

Kim, S., Iizuka, K., Aguila, H.L., Weissman, I.L., and Yokoyama, W.M. (2000). In vivo natural killer cell activities revealed by natural killer cell-deficient mice. Proc Natl Acad Sci U S A *97*, 2731-2736.

Kimpfler, S., Sevko, A., Ring, S., Falk, C., Osen, W., Frank, K., Kato, M., Mahnke, K., Schadendorf, D., and Umansky, V. (2009). Skin melanoma

development in ret transgenic mice despite the depletion of CD25+Foxp3+ regulatory T cells in lymphoid organs. J Immunol *183*, 6330-6337.

Kirk, C.J., Hartigan-O'Connor, D., and Mule, J.J. (2001). The dynamics of the T-cell antitumor response: chemokine-secreting dendritic cells can prime tumor-reactive T cells extranodally. Cancer Res *61*, 8794-8802.

Kirkwood, J.M., Ibrahim, J.G., Sosman, J.A., Sondak, V.K., Agarwala, S.S., Ernstoff, M.S., and Rao, U. (2001). High-dose interferon alfa-2b significantly prolongs relapse-free and overall survival compared with the GM2-KLH/QS-21 vaccine in patients with resected stage IIB-III melanoma: results of intergroup trial E1694/S9512/C509801. J Clin Oncol *19*, 2370-2380.

Kirkwood, J.M., Tarhini, A.A., Panelli, M.C., Moschos, S.J., Zarour, H.M., Butterfield, L.H., and Gogas, H.J. (2008). Next generation of immunotherapy for melanoma. J Clin Oncol *26*, 3445-3455.

Klebanoff, C.A., Acquavella, N., Yu, Z., and Restifo, N.P. (2011). Therapeutic cancer vaccines: are we there yet? Immunol Rev *239*, 27-44.

Ko, J.S., Zea, A.H., Rini, B.I., Ireland, J.L., Elson, P., Cohen, P., Golshayan, A., Rayman, P.A., Wood, L., Garcia, J.*, et al.* (2009). Sunitinib mediates reversal of myeloid-derived suppressor cell accumulation in renal cell carcinoma patients. Clin Cancer Res *15*, 2148-2157.

Koo, V., Hamilton, P.W., and Williamson, K. (2006). Non-invasive in vivo imaging in small animal research. Cell Oncol *28*, 127-139.

Krug, A., Uppaluri, R., Facchetti, F., Dorner, B.G., Sheehan, K.C., Schreiber, R.D., Cella, M., and Colonna, M. (2002). IFN-producing cells respond to CXCR3 ligands in the presence of CXCL12 and secrete inflammatory chemokines upon activation. J Immunol *169*, 6079-6083.

Kruit, W.H., Suciu, S., Dreno, B., Chiarion-Sileni, V., Mortier, L., Robert, C., Maio, M., Brichard, V.G., Lehmann, F., and Keilholz, U. (2008). Immunization with recombinant MAGE-A3 protein combined with adjuvant systems AS15 or AS02B in patients with unresectable and progressive metastatic cutaneous melanoma: A randomized open-label phase II study of the EORTC Melanoma Group. J Clin Oncol *26*.

Kunz, M., Toksoy, A., Goebeler, M., Engelhardt, E., Brocker, E., and Gillitzer, R. (1999). Strong expression of the lymphoattractant C-X-C chemokine Mig is associated with heavy infiltration of T cells in human malignant melanoma. J Pathol *189*, 552-558.

Ladoire, S., Mignot, G., Dabakuyo, S., Arnould, L., Apetoh, L., Rebe, C., Coudert, B., Martin, F., Bizollon, M.H., Vanoli, A.*, et al.* (2011). In situ immune response after neoadjuvant chemotherapy for breast cancer predicts survival. J Pathol.

Lanier, L.L. (2005). NK cell recognition. Annu Rev Immunol *23*, 225-274.

Larue, L., and Beermann, F. (2007). Cutaneous melanoma in genetically modified animals. Pigment Cell Res *20*, 485-497.

Le, H.K., Graham, L., Cha, E., Morales, J.K., Manjili, M.H., and Bear, H.D. (2009). Gemcitabine directly inhibits myeloid derived suppressor cells in BALB/c mice bearing 4T1 mammary carcinoma and augments expansion of T cells from tumor-bearing mice. Int Immunopharmacol *9*, 900-909.

Legha, S.S., Ring, S., Eton, O., Bedikian, A., Buzaid, A.C., Plager, C., and Papadopoulos, N. (1998). Development of a biochemotherapy regimen with concurrent administration of cisplatin, vinblastine, dacarbazine, interferon alfa, and interleukin-2 for patients with metastatic melanoma. J Clin Oncol *16*, 1752-1759.

Lengagne, R., Graff-Dubois, S., Garcette, M., Renia, L., Kato, M., Guillet, J.G., Engelhard, V.H., Avril, M.F., Abastado, J.P., and Prevost-Blondel, A. (2008). Distinct role for CD8 T cells toward cutaneous tumors and visceral metastases. J Immunol *180*, 130-137.

Lengagne, R., Le Gal, F.A., Garcette, M., Fiette, L., Ave, P., Kato, M., Briand, J.P., Massot, C., Nakashima, I., Renia, L.*, et al.* (2004). Spontaneous vitiligo in an animal model for human melanoma: role of tumor-specific CD8+ T cells. Cancer Res *64*, 1496-1501.

Lev, D.C., Onn, A., Melinkova, V.O., Miller, C., Stone, V., Ruiz, M., McGary, E.C., Ananthaswamy, H.N., Price, J.E., and Bar-Eli, M. (2004). Exposure of melanoma cells to dacarbazine results in enhanced tumor growth and metastasis in vivo. J Clin Oncol *22*, 2092-2100.

Levina, V., Su, Y., Nolen, B., Liu, X., Gordin, Y., Lee, M., Lokshin, A., and Gorelik, E. (2008). Chemotherapeutic drugs and human tumor cells cytokine network. Int J Cancer *123*, 2031-2040.

Liao, C.P., Zhong, C., Saribekyan, G., Bading, J., Park, R., Conti, P.S., Moats, R., Berns, A., Shi, W., Zhou, Z.*, et al.* (2007). Mouse models of prostate adenocarcinoma with the capacity to monitor spontaneous carcinogenesis by bioluminescence or fluorescence. Cancer Res *67*, 7525-7533.

Lim, D.M., and Wang, M.L. (2011). Toll-like receptor 3 signaling enables human esophageal epithelial cells to sense endogenous danger signals released by necrotic cells. Am J Physiol Gastrointest Liver Physiol.

Lizee, G., Cantu, M.A., and Hwu, P. (2007). Less yin, more yang: confronting the barriers to cancer immunotherapy. Clin Cancer Res *13*, 5250-5255.

Ljunggren, H.G. (2008). Cancer immunosurveillance: NKG2D breaks cover. Immunity *28*, 492-494.

Louahed, J., Gruselle, O., Gaulis, S., Coche, T., Eggermont, A.M., Kruit, W., Dreno, B., Chiarion Sileni, V., Lehmann, F., and Brichard, V.G. (2008). Expression of defined genes identified by pretreatment tumor profiling: Association with clinical responses to the GSK MAGE- A3 immunotherapeutic in metastatic melanoma patients. J Clin Oncol *26(suppl)*.

Lyons, S.K. (2005). Advances in imaging mouse tumour models in vivo. J Pathol *205*, 194-205.

Mack, M., Riethmuller, G., and Kufer, P. (1995). A small bispecific antibody construct expressed as a functional single-chain molecule with high tumor cell cytotoxicity. Proc Natl Acad Sci U S A *92*, 7021-7025.

Mackenzie, M.A., Jordan, S.A., Budd, P.S., and Jackson, I.J. (1997). Activation of the receptor tyrosine kinase Kit is required for the proliferation of melanoblasts in the mouse embryo. Dev Biol *192*, 99-107.

Mankoff, D.A., Dehdashti, F., and Shields, A.F. (2000). Characterizing tumors using metabolic imaging: PET imaging of cellular proliferation and steroid receptors. Neoplasia *2*, 71-88.

Mankoff, D.A., Shields, A.F., and Krohn, K.A. (2005). PET imaging of cellular proliferation. Radiol Clin North Am *43*, 153-167.

Mantovani, A., Allavena, P., Sozzani, S., Vecchi, A., Locati, M., and Sica, A. (2004). Chemokines in the recruitment and shaping of the leukocyte infiltrate of tumors. Semin Cancer Biol *14*, 155-160.

Maric, M., and Liu, Y. (1999). Strong cytotoxic T lymphocyte responses to a macrophage inflammatory protein 1alpha-expressing tumor: linkage between inflammation and specific immunity. Cancer Res *59*, 5549-5553.

Mellado, M., de Ana, A.M., Moreno, M.C., Martinez, C., and Rodriguez-Frade, J.M. (2001a). A potential immune escape mechanism by melanoma cells through the activation of chemokine-induced T cell death. Curr Biol *11*, 691-696.

Mellado, M., Rodriguez-Frade, J.M., Vila-Coro, A.J., Fernandez, S., Martin de Ana, A., Jones, D.R., Toran, J.L., and Martinez, A.C. (2001b). Chemokine receptor homo- or heterodimerization activates distinct signaling pathways. EMBO J *20*, 2497-2507.

Menard, C., Martin, F., Apetoh, L., Bouyer, F., and Ghiringhelli, F. (2008). Cancer chemotherapy: not only a direct cytotoxic effect, but also an adjuvant for antitumor immunity. Cancer Immunol Immunother *57*, 1579-1587.

Meyer, C., Sevko, A., Ramacher, M., Bazhin, A.V., Falk, C.S., Osen, W., Borrello, I., Kato, M., Schadendorf, D., Baniyash, M.*, et al.* (2011). Chronic inflammation promotes myeloid-derived suppressor cell activation blocking antitumor immunity in transgenic mouse melanoma model. Proc Natl Acad Sci U S A *108*, 17111-17116.

Middleton, J., Neil, S., Wintle, J., Clark-Lewis, I., Moore, H., Lam, C., Auer, M., Hub, E., and Rot, A. (1997). Transcytosis and surface presentation of IL-8 by venular endothelial cells. Cell *91*, 385-395.

Middleton, J., Patterson, A.M., Gardner, L., Schmutz, C., and Ashton, B.A. (2002). Leukocyte extravasation: chemokine transport and presentation by the endothelium. Blood *100*, 3853-3860.

Middleton, M.R., Grob, J.J., Aaronson, N., Fierlbeck, G., Tilgen, W., Seiter, S., Gore, M., Aamdal, S., Cebon, J., Coates, A.*, et al.* (2000). Randomized phase III study of temozolomide versus dacarbazine in the treatment of patients with advanced metastatic malignant melanoma. J Clin Oncol *18*, 158-166.

Mlecnik, B., Tosolini, M., Charoentong, P., Kirilovsky, A., Bindea, G., Berger, A., Camus, M., Gillard, M., Bruneval, P., Fridman, W.H.*, et al.* (2010). Biomolecular network reconstruction identifies T-cell homing factors associated with survival in colorectal cancer. Gastroenterology *138*, 1429-1440.

Mohty, A.M., Grob, J.J., Mohty, M., Richard, M.A., Olive, D., and Gaugler, B. (2010). Induction of IP-10/CXCL10 secretion as an immunomodulatory effect of low-dose adjuvant interferon-alpha during treatment of melanoma. Immunobiology *215*, 113-123.

Mondino, A., Dardalhon, V., Hess Michelini, R., Loisel-Meyer, S., and Taylor, N. (2010). Redirecting the immune response: role of adoptive T cell therapy. Hum Gene Ther *21*, 533-541.

Monteagudo, C., Martin, J.M., Jorda, E., and Llombart-Bosch, A. (2007). CXCR3 chemokine receptor immunoreactivity in primary cutaneous malignant melanoma: correlation with clinicopathological prognostic factors. J Clin Pathol *60*, 596-599.

Morgan, R.A., Dudley, M.E., Wunderlich, J.R., Hughes, M.S., Yang, J.C., Sherry, R.M., Royal, R.E., Topalian, S.L., Kammula, U.S., Restifo, N.P.*, et al.* (2006). Cancer regression in patients after transfer of genetically engineered lymphocytes. Science *314*, 126-129.

Morse, M.A., Clay, T.M., and Lyerly, H.K. (2002). Current status of adoptive immunotherapy of malignancies. Expert Opin Biol Ther *2*, 237-247.

Mrass, P., Kinjyo, I., Ng, L.G., Reiner, S.L., Pure, E., and Weninger, W. (2008). CD44 mediates successful interstitial navigation by killer T cells and enables efficient antitumor immunity. Immunity *29*, 971-985.

Mroz, E.A., and Rocco, J.W. (2010). Functional p53 status as a biomarker for chemotherapy response in oral-cavity cancer. J Clin Oncol *28*, 715-717.

Mule, J.J., Custer, M., Averbook, B., Yang, J.C., Weber, J.S., Goeddel, D.V., Rosenberg, S.A., and Schall, T.J. (1996). RANTES secretion by gene-modified tumor cells results in loss of tumorigenicity in vivo: role of immune cell subpopulations. Hum Gene Ther *7*, 1545-1553.

Mullins, I.M., Slingluff, C.L., Lee, J.K., Garbee, C.F., Shu, J., Anderson, S.G., Mayer, M.E., Knaus, W.A., and Mullins, D.W. (2004). CXC chemokine receptor 3 expression by activated CD8+ T cells is associated with survival in melanoma patients with stage III disease. Cancer Res *64*, 7697-7701.

Munoz-Fontela, C., Macip, S., Martinez-Sobrido, L., Brown, L., Ashour, J., Garcia-Sastre, A., Lee, S.W., and Aaronson, S.A. (2008). Transcriptional role of p53 in interferon-mediated antiviral immunity. J Exp Med *205*, 1929-1938.

Naito, Y., Saito, K., Shiiba, K., Ohuchi, A., Saigenji, K., Nagura, H., and Ohtani, H. (1998). CD8+ T cells infiltrated within cancer cell nests as a prognostic factor in human colorectal cancer. Cancer Res *58*, 3491-3494.

Nardin, A., Wong, W.C., Tow, C., Molina, T.J., Tissier, F., Audebourg, A., Garcette, M., Caignard, A., Avril, M.F., Abastado, J.P*., et al.* (2011).

Dacarbazine promotes stromal remodeling and lymphocyte infiltration in cutaneous melanoma lesions. J Invest Dermatol *131*, 1896-1905.

Nathan, F.E., and Mastrangelo, M.J. (1998). Systemic therapy in melanoma. Semin Surg Oncol *14*, 319-327.

Nausch, N., and Cerwenka, A. (2008). NKG2D ligands in tumor immunity. Oncogene *27*, 5944-5958.

NCT00480025 ([updated 02.06.2011]). GSK1572932A antigen-specific cancer immunotherapeutic as adjuvant therapy in patients with non-small cell lung cancer (MAGRIT trial).

Nelson, A.L., Algon, S.A., Munasinghe, J., Graves, O., Goumnerova, L., Burstein, D., Pomeroy, S.L., and Kim, J.Y. (2003). Magnetic resonance imaging of patched heterozygous and xenografted mouse brain tumors. J Neurooncol *62*, 259-267.

Nelson, D., and Ganss, R. (2006). Tumor growth or regression: powered by inflammation. J Leukoc Biol *80*, 685-690.

Niiya, M., Niiya, K., Kiguchi, T., Shibakura, M., Asaumi, N., Shinagawa, K., Ishimaru, F., Kiura, K., Ikeda, K., Ueoka, H.*, et al.* (2003). Induction of TNF-alpha, uPA, IL-8 and MCP-1 by doxorubicin in human lung carcinoma cells. Cancer Chemother Pharmacol *52*, 391-398.

O'Connell, J., O'Sullivan, G.C., Collins, J.K., and Shanahan, F. (1996). The Fas counterattack: Fas-mediated T cell killing by colon cancer cells expressing Fas ligand. J Exp Med *184*, 1075-1082.

Obeid, M., Tesniere, A., Ghiringhelli, F., Fimia, G.M., Apetoh, L., Perfettini, J.L., Castedo, M., Mignot, G., Panaretakis, T., Casares, N.*, et al.* (2007). Calreticulin exposure dictates the immunogenicity of cancer cell death. Nat Med *13*, 54-61.

Offner, S., Hofmeister, R., Romaniuk, A., Kufer, P., and Baeuerle, P.A. (2006). Induction of regular cytolytic T cell synapses by bispecific single-chain antibody constructs on MHC class I-negative tumor cells. Mol Immunol *43*, 763-771.

Ostrand-Rosenberg, S. (2010). Myeloid-derived suppressor cells: more mechanisms for inhibiting antitumor immunity. Cancer Immunol Immunother *59*, 1593-1600.

Pages, F., Galon, J., Dieu-Nosjean, M.C., Tartour, E., Sautes-Fridman, C., and Fridman, W.H. (2010). Immune infiltration in human tumors: a prognostic factor that should not be ignored. Oncogene *29*, 1093-1102.

Palucka, K., Ueno, H., and Banchereau, J. (2011). Recent developments in cancer vaccines. J Immunol *186*, 1325-1331.

Pamment, J., Ramsay, E., Kelleher, M., Dornan, D., and Ball, K.L. (2002). Regulation of the IRF-1 tumour modifier during the response to genotoxic

stress involves an ATM-dependent signalling pathway. Oncogene *21*, 7776-7785.

Paoletti, S., Petkovic, V., Sebastiani, S., Danelon, M.G., Uguccioni, M., and Gerber, B.O. (2005). A rich chemokine environment strongly enhances leukocyte migration and activities. Blood *105*, 3405-3412.

Perrone, F., Bossi, P., Cortelazzi, B., Locati, L., Quattrone, P., Pierotti, M.A., Pilotti, S., and Licitra, L. (2010). TP53 mutations and pathologic complete response to neoadjuvant cisplatin and fluorouracil chemotherapy in resected oral cavity squamous cell carcinoma. J Clin Oncol *28*, 761-766.

Pertl, U., Luster, A.D., Varki, N.M., Homann, D., Gaedicke, G., Reisfeld, R.A., and Lode, H.N. (2001). IFN-gamma-inducible protein-10 is essential for the generation of a protective tumor-specific CD8 T cell response induced by single-chain IL-12 gene therapy. J Immunol *166*, 6944-6951.

Poznansky, M.C., Olszak, I.T., Foxall, R., Evans, R.H., Luster, A.D., and Scadden, D.T. (2000). Active movement of T cells away from a chemokine. Nat Med *6*, 543-548.

Prestwich, R.J., Errington, F., Hatfield, P., Merrick, A.E., Ilett, E.J., Selby, P.J., and Melcher, A.A. (2008). The immune system--is it relevant to cancer development, progression and treatment? Clin Oncol (R Coll Radiol) *20*, 101-112.

Proost, P., Wuyts, A., and Van Damme, J. (1996). Human monocyte chemotactic proteins-2 and -3: structural and functional comparison with MCP-1. J Leukoc Biol *59*, 67-74.

Puaux, A.-L., Ong, L.C., Jin, Y., Teh, I., Hong, M., Chow, P., Golay, X., and Abastado, J.-P. (2011). A comparison of imaging techniques to monitor tumor growth and cancer progression in living animals. Mol Imaging Biol.

Purdy, A.K., and Campbell, K.S. (2009). Natural killer cells and cancer: regulation by the killer cell Ig-like receptors (KIR). Cancer Biol Ther *8*, 2211-2220.

Rabinovich, G.A., Gabrilovich, D., and Sotomayor, E.M. (2007). Immunosuppressive strategies that are mediated by tumor cells. Annu Rev Immunol *25*, 267-296.

Rasku, M.A., Clem, A.L., Telang, S., Taft, B., Gettings, K., Gragg, H., Cramer, D., Lear, S.C., McMasters, K.M., Miller, D.M.*, et al.* (2008). Transient T cell depletion causes regression of melanoma metastases. J Transl Med *6*, 12.

Raulet, D.H. (2004). Interplay of natural killer cells and their receptors with the adaptive immune response. Nat Immunol *5*, 996-1002.

Ray, P., Wu, A.M., and Gambhir, S.S. (2003). Optical bioluminescence and positron emission tomography imaging of a novel fusion reporter gene in tumor xenografts of living mice. Cancer Res *63*, 1160-1165.

Reed, J.C. (2006). Drug insight: cancer therapy strategies based on restoration of endogenous cell death mechanisms. Nat Clin Pract Oncol *3*, 388-398.

Rehemtulla, A., Stegman, L.D., Cardozo, S.J., Gupta, S., Hall, D.E., Contag, C.H., and Ross, B.D. (2000). Rapid and quantitative assessment of cancer treatment response using in vivo bioluminescence imaging. Neoplasia *2*, 491-495.

Richards, J.M., Mehta, N., Ramming, K., and Skosey, P. (1992). Sequential chemoimmunotherapy in the treatment of metastatic melanoma. J Clin Oncol *10*, 1338-1343.

Richmond, A. (2002). Nf-kappa B, chemokine gene transcription and tumour growth. Nat Rev Immunol *2*, 664-674.

Rosano, L., Cianfrocca, R., Spinella, F., Di Castro, V., Nicotra, M.R., Lucidi, A., Ferrandina, G., Natali, P.G., and Bagnato, A. (2011). Acquisition of chemoresistance and EMT phenotype is linked with activation of the endothelin A receptor pathway in ovarian carcinoma cells. Clin Cancer Res.

Rosenberg, L.B., Gibson, K., and Shulman, J.F. (2009). When cultures collide: female genital cutting and U.S. obstetric practice. Obstet Gynecol *113*, 931-934.

Rosenberg, S.A., and Dudley, M.E. (2009). Adoptive cell therapy for the treatment of patients with metastatic melanoma. Curr Opin Immunol *21*, 233-240.

Rosenberg, S.A., Lotze, M.T., Yang, J.C., Aebersold, P.M., Linehan, W.M., Seipp, C.A., and White, D.E. (1989). Experience with the use of high-dose interleukin-2 in the treatment of 652 cancer patients. Ann Surg *210*, 474-484; discussion 484-475.

Rosenberg, S.A., Yang, J.C., and Restifo, N.P. (2004). Cancer immunotherapy: moving beyond current vaccines. Nat Med *10*, 909-915.

Rosenblum, J.M., Shimoda, N., Schenk, A.D., Zhang, H., Kish, D.D., Keslar, K., Farber, J.M., and Fairchild, R.L. (2010). CXC chemokine ligand (CXCL) 9 and CXCL10 are antagonistic costimulation molecules during the priming of alloreactive T cell effectors. J Immunol *184*, 3450-3460.

Ruffini, P.A., Morandi, P., Cabioglu, N., Altundag, K., and Cristofanilli, M. (2007). Manipulating the chemokine-chemokine receptor network to treat cancer. Cancer *109*, 2392-2404.

Ruggeri, L., Mancusi, A., Burchielli, E., Aversa, F., Martelli, M.F., and Velardi, A. (2007). Natural killer cell alloreactivity in allogeneic hematopoietic transplantation. Curr Opin Oncol *19*, 142-147.

Salcedo, M., Bercovici, N., Taylor, R., Vereecken, P., Massicard, S., Duriau, D., Vernel-Pauillac, F., Boyer, A., Baron-Bodo, V., Mallard, E.*, et al.* (2006).

Vaccination of melanoma patients using dendritic cells loaded with an allogeneic tumor cell lysate. Cancer Immunol Immunother *55*, 819-829.

Sangro, B., Mazzolini, G., Ruiz, J., Herraiz, M., Quiroga, J., Herrero, I., Benito, A., Larrache, J., Pueyo, J., Subtil, J.C*., et al.* (2004). Phase I trial of intratumoral injection of an adenovirus encoding interleukin-12 for advanced digestive tumors. J Clin Oncol *22*, 1389-1397.

Sato, E., Olson, S.H., Ahn, J., Bundy, B., Nishikawa, H., Qian, F., Jungbluth, A.A., Frosina, D., Gnjatic, S., Ambrosone, C*., et al.* (2005). Intraepithelial CD8+ tumor-infiltrating lymphocytes and a high CD8+/regulatory T cell ratio are associated with favorable prognosis in ovarian cancer. Proc Natl Acad Sci U S A *102*, 18538-18543.

Schall, T.J., Bacon, K., Camp, R.D., Kaspari, J.W., and Goeddel, D.V. (1993). Human macrophage inflammatory protein alpha (MIP-1 alpha) and MIP-1 beta chemokines attract distinct populations of lymphocytes. J Exp Med *177*, 1821-1826.

Schmitt, T.M., Ragnarsson, G.B., and Greenberg, P.D. (2009). T cell receptor gene therapy for cancer. Hum Gene Ther *20*, 1240-1248.

Schreiber, R.D., Old, L.J., and Smyth, M.J. (2011). Cancer immunoediting: integrating immunity's roles in cancer suppression and promotion. Science *331*, 1565-1570.

Schumann, G., Loth, E., Banaschewski, T., Barbot, A., Barker, G., Buchel, C., Conrod, P.J., Dalley, J.W., Flor, H., Gallinat, J.*, et al.* (2010). The IMAGEN study: reinforcement-related behaviour in normal brain function and psychopathology. Mol Psychiatry *15*, 1128-1139.

Schwartzentruber, D.J., Lawson, D., Richards, J., Conry, R.M., Miller, D., Triesman, J., Gailani, F., Riley, L.B., Vena, D., and Hwu, P. (2009). A phase III multi-institutional randomized study of immunization with the gp100: 209-217(210M) peptide followed by high-dose IL-2 compared with high-dose IL-2 alone in patients with metastatic melanoma J Clin Oncol *27*, abstract CRA9011.

Sebastiani, S., Danelon, G., Gerber, B., and Uguccioni, M. (2005). CCL22-induced responses are powerfully enhanced by synergy inducing chemokines via CCR4: evidence for the involvement of first beta-strand of chemokine. Eur J Immunol *35*, 746-756.

Seliger, B. (2008). Different regulation of MHC class I antigen processing components in human tumors. J Immunotoxicol *5*, 361-367.

Sertoli, M.R., Bernengo, M.G., Ardizzoni, A., Brunetti, I., Falcone, A., Vidili, M.G., Cusimano, M.P., Appino, A., Doveil, G., Fortini, C.*, et al.* (1989). Phase II trial of recombinant alpha-2b interferon in the treatment of metastatic skin melanoma. Oncology *46*, 96-98.

Shankaran, V., Ikeda, H., Bruce, A.T., White, J.M., Swanson, P.E., Old, L.J., and Schreiber, R.D. (2001). IFNgamma and lymphocytes prevent primary

tumour development and shape tumour immunogenicity. Nature *410*, 1107-1111.

Sharma, S., Stolina, M., Luo, J., Strieter, R.M., Burdick, M., Zhu, L.X., Batra, R.K., and Dubinett, S.M. (2000). Secondary lymphoid tissue chemokine mediates T cell-dependent antitumor responses in vivo. J Immunol *164*, 4558-4563.

Shrimali, R.K., Yu, Z., Theoret, M.R., Chinnasamy, D., Restifo, N.P., and Rosenberg, S.A. (2010). Antiangiogenic agents can increase lymphocyte infiltration into tumor and enhance the effectiveness of adoptive immunotherapy of cancer. Cancer Res *70*, 6171-6180.

Sikora, A.G., Gelbard, A., Davies, M.A., Sano, D., Ekmekcioglu, S., Kwon, J., Hailemichael, Y., Jayaraman, P., Myers, J.N., Grimm, E.A.*, et al.* (2010). Targeted inhibition of inducible nitric oxide synthase inhibits growth of human melanoma in vivo and synergizes with chemotherapy. Clin Cancer Res *16*, 1834-1844.

Smithies, O., Gregg, R.G., Boggs, S.S., Koralewski, M.A., and Kucherlapati, R.S. (1985). Insertion of DNA sequences into the human chromosomal beta-globin locus by homologous recombination. Nature *317*, 230-234.

Smyth, M.J., Dunn, G.P., and Schreiber, R.D. (2006). Cancer immunosurveillance and immunoediting: the roles of immunity in suppressing tumor development and shaping tumor immunogenicity. Adv Immunol *90*, 1-50.

Smyth, M.J., Hayakawa, Y., Takeda, K., and Yagita, H. (2002). New aspects of natural-killer-cell surveillance and therapy of cancer. Nat Rev Cancer *2*, 850-861.

Sondak, V.K., Liu, P.Y., Tuthill, R.J., Kempf, R.A., Unger, J.M., Sosman, J.A., Thompson, J.A., Weiss, G.R., Redman, B.G., Jakowatz, J.G.*, et al.* (2002). Adjuvant immunotherapy of resected, intermediate-thickness, node-negative melanoma with an allogeneic tumor vaccine: overall results of a randomized trial of the Southwest Oncology Group. J Clin Oncol *20*, 2058-2066.

Sotomayor, E.M., Borrello, I., Tubb, E., Allison, J.P., and Levitsky, H.I. (1999). In vivo blockade of CTLA-4 enhances the priming of responsive T cells but fails to prevent the induction of tumor antigen-specific tolerance. Proc Natl Acad Sci U S A *96*, 11476-11481.

Speiser, D.E., and Romero, P. (2010). Molecularly defined vaccines for cancer immunotherapy, and protective T cell immunity. Semin Immunol *22*, 144-154.

Stadler, R., Luger, T., Bieber, T., Kohler, U., Linse, R., Technau, K., Schubert, R., Schroth, K., Vakilzadeh, F., Volkenandt, M.*, et al.* (2006). Long-term survival benefit after adjuvant treatment of cutaneous melanoma with dacarbazine and low dose natural interferon alpha: A controlled, randomised multicentre trial. Acta Oncol *45*, 389-399.

Staerz, U.D., Kanagawa, O., and Bevan, M.J. (1985). Hybrid antibodies can target sites for attack by T cells. Nature *314*, 628-631.

Stanford, M.M., and Issekutz, T.B. (2003). The relative activity of CXCR3 and CCR5 ligands in T lymphocyte migration: concordant and disparate activities in vitro and in vivo. J Leukoc Biol *74*, 791-799.

Strand, S., Hofmann, W.J., Hug, H., Muller, M., Otto, G., Strand, D., Mariani, S.M., Stremmel, W., Krammer, P.H., and Galle, P.R. (1996). Lymphocyte apoptosis induced by CD95 (APO-1/Fas) ligand-expressing tumor cells--a mechanism of immune evasion? Nat Med *2*, 1361-1366.

Struyf, S., Gouwy, M., Dillen, C., Proost, P., Opdenakker, G., and Van Damme, J. (2005). Chemokines synergize in the recruitment of circulating neutrophils into inflamed tissue. Eur J Immunol *35*, 1583-1591.

Struyf, S., Stoops, G., Van Coillie, E., Gouwy, M., Schutyser, E., Lenaerts, J.P., Fiten, P., Van Aelst, I., Proost, P., Opdenakker, G.*, et al.* (2001). Gene cloning of a new plasma CC chemokine, activating and attracting myeloid cells in synergy with other chemoattractants. Biochemistry *40*, 11715-11722.

Sumantran, V.N., Ealovega, M.W., Nunez, G., Clarke, M.F., and Wicha, M.S. (1995). Overexpression of Bcl-XS sensitizes MCF-7 cells to chemotherapy-induced apoptosis. Cancer Res *55*, 2507-2510.

Sundaresan, S., Chacko, A., Dutta, A.K., Bhatia, E., Witt, H., Te Morsche, R.H., Jansen, J.B., and Drenth, J.P. (2009). Divergent roles of SPINK1 and PRSS2 variants in tropical calcific pancreatitis. Pancreatology *9*, 145-149.

Suzuki, E., Kapoor, V., Jassar, A.S., Kaiser, L.R., and Albelda, S.M. (2005). Gemcitabine selectively eliminates splenic Gr-1+/CD11b+ myeloid suppressor cells in tumor-bearing animals and enhances antitumor immune activity. Clin Cancer Res *11*, 6713-6721.

Swann, J.B., and Smyth, M.J. (2007). Immune surveillance of tumors. J Clin Invest *117*, 1137-1146.

Sznol, M. (2011). Molecular markers of response to treatment for melanoma. Cancer J *17*, 127-133.

Takaoka, A., and Taniguchi, T. (2008). Cytosolic DNA recognition for triggering innate immune responses. Adv Drug Deliv Rev *60*, 847-857.

Tang, L., Hu, H.D., Hu, P., Lan, Y.H., Peng, M.L., Chen, M., and Ren, H. (2007). Gene therapy with CX3CL1/Fractalkine induces antitumor immunity to regress effectively mouse hepatocellular carcinoma. Gene Ther *14*, 1226-1234.

Tannenbaum, C.S., Tubbs, R., Armstrong, D., Finke, J.H., Bukowski, R.M., and Hamilton, T.A. (1998). The CXC chemokines IP-10 and Mig are necessary for IL-12-mediated regression of the mouse RENCA tumor. J Immunol *161*, 927-932.

Taub, D.D., Conlon, K., Lloyd, A.R., Oppenheim, J.J., and Kelvin, D.J. (1993). Preferential migration of activated CD4+ and CD8+ T cells in response to MIP-1 alpha and MIP-1 beta. Science *260*, 355-358.

Teft, W.A., Kirchhof, M.G., and Madrenas, J. (2006). A molecular perspective of CTLA-4 function. Annu Rev Immunol *24*, 65-97.

Teng, M.W., Swann, J.B., Koebel, C.M., Schreiber, R.D., and Smyth, M.J. (2008). Immune-mediated dormancy: an equilibrium with cancer. J Leukoc Biol *84*, 988-993.

Terando, A.M., Faries, M.B., and Morton, D.L. (2007). Vaccine therapy for melanoma: current status and future directions. Vaccine *25 Suppl 2*, B4-16.

Tham, M., and Abastado, J.-P. (2011). Escape of tumor immune surveillance and metastas. Drug Discovery Today: Disease Models (Manuscript submitted).

Thomas, L. (1959). Discussion of cellular and humoral aspects of the hypersensitivity states. (New York, Hoeber-Harper).

Tiligada, E. (2006). Chemotherapy: induction of stress responses. Endocr Relat Cancer *13 Suppl 1*, S115-124.

Ting, A.Y., Kimler, B.F., Fabian, C.J., and Petroff, B.K. (2007). Characterization of a preclinical model of simultaneous breast and ovarian cancer progression. Carcinogenesis *28*, 130-135.

Toh, B., Wang, X., Keeble, J., Sim, W.J., Khoo, K., Wong, W.C., Kato, M., Prevost-Blondel, A., Thiery, J.P., and Abastado, J.P. (2011). Mesenchymal transition and dissemination of cancer cells is driven by myeloid-derived suppressor cells infiltrating the primary tumor. PLoS Biol *9*, e1001162.

Topp, M. (2011). Blinatumomab Produced Complete Remission in ALL. Paper presented at: 16th Congress of the European Hematology Association (London, United Kingdom).

Topp, M.S., Kufer, P., Gokbuget, N., Goebeler, M., Klinger, M., Neumann, S., Horst, H.A., Raff, T., Viardot, A., Schmid, M.*, et al.* (2011). Targeted therapy with the T-cell-engaging antibody blinatumomab of chemotherapy-refractory minimal residual disease in B-lineage acute lymphoblastic leukemia patients results in high response rate and prolonged leukemia-free survival. J Clin Oncol *29*, 2493-2498.

Tow, C. (2010). TLR3 induces hepatocellular carcinoma cell death and increases natural killer cell activity. In Microbiology (National University of Singapore).

Trinchieri, G. (1989). Biology of natural killer cells. Adv Immunol *47*, 187-376.

Trinchieri, G. (2010). Type I interferon: friend or foe? J Exp Med *207*, 2053-2063.

Ugurel, S., Schrama, D., Keller, G., Schadendorf, D., Brocker, E.B., Houben, R., Zapatka, M., Fink, W., Kaufman, H.L., and Becker, J.C. (2008). Impact of the CCR5 gene polymorphism on the survival of metastatic melanoma patients receiving immunotherapy. Cancer Immunol Immunother *57*, 685-691.

Umansky, V., Abschuetz, O., Osen, W., Ramacher, M., Zhao, F., Kato, M., and Schadendorf, D. (2008). Melanoma-specific memory T cells are

functionally active in Ret transgenic mice without macroscopic tumors. Cancer Res *68*, 9451-9458.

Uyttenhove, C., Pilotte, L., Theate, I., Stroobant, V., Colau, D., Parmentier, N., Boon, T., and Van den Eynde, B.J. (2003). Evidence for a tumoral immune resistance mechanism based on tryptophan degradation by indoleamine 2,3-dioxygenase. Nat Med *9*, 1269-1274.

Vanbervliet, B., Bendriss-Vermare, N., Massacrier, C., Homey, B., de Bouteiller, O., Briere, F., Trinchieri, G., and Caux, C. (2003). The inducible CXCR3 ligands control plasmacytoid dendritic cell responsiveness to the constitutive chemokine stromal cell-derived factor 1 (SDF-1)/CXCL12. J Exp Med *198*, 823-830.

Vetter, C.S., Groh, V., thor Straten, P., Spies, T., Brocker, E.B., and Becker, J.C. (2002). Expression of stress-induced MHC class I related chain molecules on human melanoma. J Invest Dermatol *118*, 600-605.

Vianello, F., Papeta, N., Chen, T., Kraft, P., White, N., Hart, W.K., Kircher, M.F., Swart, E., Rhee, S., Palu, G.*, et al.* (2006). Murine B16 melanomas expressing high levels of the chemokine stromal-derived factor-1/CXCL12 induce tumor-specific T cell chemorepulsion and escape from immune control. J Immunol *176*, 2902-2914.

Vijayanathan, V., Thomas, T., and Thomas, T.J. (2002). DNA nanoparticles and development of DNA delivery vehicles for gene therapy. Biochemistry *41*, 14085-14094.

Vooijs, M., Jonkers, J., Lyons, S., and Berns, A. (2002). Noninvasive imaging of spontaneous retinoblastoma pathway-dependent tumors in mice. Cancer Res *62*, 1862-1867.

Waldhauer, I., and Steinle, A. (2008). NK cells and cancer immunosurveillance. Oncogene *27*, 5932-5943.

Wallace, A., LaRosa, D.F., Kapoor, V., Sun, J., Cheng, G., Jassar, A., Blouin, A., Ching, L.M., and Albelda, S.M. (2007). The vascular disrupting agent, DMXAA, directly activates dendritic cells through a MyD88-independent mechanism and generates antitumor cytotoxic T lymphocytes. Cancer Res *67*, 7011-7019.

Walrath, J.C., Hawes, J.J., Van Dyke, T., and Reilly, K.M. (2010). Genetically engineered mouse models in cancer research. Adv Cancer Res *106*, 113-164.

Walser, T.C., Ma, X., Kundu, N., Dorsey, R., Goloubeva, O., and Fulton, A.M. (2007). Immune-mediated modulation of breast cancer growth and metastasis by the chemokine Mig (CXCL9) in a murine model. J Immunother *30*, 490-498.

Weigelin, B., Krause, M., and Friedl, P. (2011). Cytotoxic T lymphocyte migration and effector function in the tumor microenvironment. Immunol Lett *138*, 19-21.

Wherry, E.J., Ha, S.J., Kaech, S.M., Haining, W.N., Sarkar, S., Kalia, V., Subramaniam, S., Blattman, J.N., Barber, D.L., and Ahmed, R. (2007).

Molecular signature of CD8+ T cell exhaustion during chronic viral infection. Immunity *27*, 670-684.

Williams, S.A., Harata-Lee, Y., Comerford, I., Anderson, R.L., Smyth, M.J., and McColl, S.R. (2010). Multiple functions of CXCL12 in a syngeneic model of breast cancer. Mol Cancer *9*, 250.

Wolf, G.T., Bradford, C.R., Urba, S., Smith, A., Eisbruch, A., Chepeha, D.B., Teknos, T.N., Worden, F., Dawson, L., Terrell, J.E.*, et al.* (2002). Immune reactivity does not predict chemotherapy response, organ preservation, or survival in advanced laryngeal cancer. Laryngoscope *112*, 1351-1356.

Wu, G.S. (2004). The functional interactions between the p53 and MAPK signaling pathways. Cancer Biol Ther *3*, 156-161.

Xin, H., Kikuchi, T., Andarini, S., Ohkouchi, S., Suzuki, T., Nukiwa, T., Huqun, Hagiwara, K., Honjo, T., and Saijo, Y. (2005). Antitumor immune response by CX3CL1 fractalkine gene transfer depends on both NK and T cells. Eur J Immunol *35*, 1371-1380.

Yang, C.C., Shiau, Y.C., Sun, S.S., and Kao, C.H. (2003). Detection of bladder cancer using single-photon emission computed tomography of thallium-201: a preliminary report. Anticancer Res *23*, 2977-2980.

Yang, S.C., Hillinger, S., Riedl, K., Zhang, L., Zhu, L., Huang, M., Atianzar, K., Kuo, B.Y., Gardner, B., Batra, R.K.*, et al.* (2004). Intratumoral administration

of dendritic cells overexpressing CCL21 generates systemic antitumor responses and confers tumor immunity. Clin Cancer Res *10*, 2891-2901.

Yoneyama, H., Narumi, S., Zhang, Y., Murai, M., Baggiolini, M., Lanzavecchia, A., Ichida, T., Asakura, H., and Matsushima, K. (2002). Pivotal role of dendritic cell-derived CXCL10 in the retention of T helper cell 1 lymphocytes in secondary lymph nodes. J Exp Med *195*, 1257-1266.

Zhang, J., and Xu, G. (2007). Suppression of FasL expression in tumor cells and preventing tumor necrosis factor-induced apoptosis by adenovirus 14.7K is an effective escape mechanism for immune cells. Cancer Genet Cytogenet *179*, 112-117.

Zhang, N., Lyons, S., Lim, E., and Lassota, P. (2009). A spontaneous acinar cell carcinoma model for monitoring progression of pancreatic lesions and response to treatment through noninvasive bioluminescence imaging. Clin Cancer Res *15*, 4915-4924.

Zhang, T., and Herlyn, D. (2009). Combination of active specific immunotherapy or adoptive antibody or lymphocyte immunotherapy with chemotherapy in the treatment of cancer. Cancer Immunol Immunother *58*, 475-492.

Zhang, T., Somasundaram, R., Berencsi, K., Caputo, L., Gimotty, P., Rani, P., Guerry, D., Swoboda, R., and Herlyn, D. (2006). Migration of cytotoxic T lymphocytes toward melanoma cells in three-dimensional organotypic culture is dependent on CCL2 and CCR4. Eur J Immunol *36*, 457-467.

Zitvogel, L., Apetoh, L., Ghiringhelli, F., and Kroemer, G. (2008). Immunological aspects of cancer chemotherapy. Nat Rev Immunol *8*, 59-73.

Zitvogel, L., Kepp, O., and Kroemer, G. (2011). Immune parameters affecting the efficacy of chemotherapeutic regimens. Nat Rev Clin Oncol *8*, 151-160.

Zitvogel, L., Tesniere, A., and Kroemer, G. (2006). Cancer despite immunosurveillance: immunoselection and immunosubversion. Nat Rev Immunol *6*, 715-727.

Zwijnenburg, P.J., Polfliet, M.M., Florquin, S., van den Berg, T.K., Dijkstra, C.D., van Deventer, S.J., Roord, J.J., van der Poll, T., and van Furth, A.M. (2003). CXC-chemokines KC and macrophage inflammatory protein-2 (MIP-2) synergistically induce leukocyte recruitment to the central nervous system in rats. Immunol Lett *85*, 1-4.

APPENDICES

APPENDICES

Appendix 1 – Sequence of the transgene used to generate the Dct-Luc mice.

```
   1 CCTAGGCTTT TGCAAAAAGC TCGATTCTTC TGACACTAGC GCCACCATGA
  51 TCGAACAAGA CGGCCTCCAT GCTGGCAGTC CCGCAGCTTG GGTCGAACGC
 101 TTGTTCGGGT ACGACTGGGC CCAGCAGACC ATCGGATGTA GCGATGCGGC
 151 CGTGTTCCGT CTAAGCGCTC AAGGCCGGCC CGTGCTGTTC GTGAAGACCG
 201 ACCTGAGCGG CGCCCTGAAC GAGCTTCAAG ACGAGGCTGC CCGCCTGAGC
 251 TGGCTGGCCA CCACCGGCGT ACCCTGCGCC GCTGTGTTGG ATGTTGTGAC
 301 CGAAGCCGGC CGGGACTGGC TGCTGCTGGG CGAGGTCCCT GGCCAGGATC
 351 TGCTGAGCAG CCACCTTGCC CCCGCTGAGA AGGTTTCTAT CATGGCCGAT
 401 GCAATGCGGC GCCTGCACAC CCTGGACCCC GCTACCTGCC CCTTCGACCA
 451 CCAGGCTAAG CATCGGATCG AGCGTGCTCG GACCCGCATG GAGGCCGGCC
 501 TGGTGGACCA GGACGACCTG GACGAGGAGC ATCAGGGCCT GGCCCCCGCT
 551 GAACTGTTCG CCCGACTGAA AGCCCGCATG CCGGACGGTG AGGACCTGGT
 601 TGTCACACAC GGAGATGCCT GCCTCCCTAA CATCATGGTC GAGAATGGCC
 651 GCTTCTCCGG CTTCATCGAC TGCGGTCGCC TAGGAGTTGC CGACCGCTAC
 701 CAGGACATCG CCCTGGCCAC CCGCGACATC GCTGAGGAGC TTGGCGGCGA
 751 GTGGGCCGAC CGCTTCTTAG TCTTGTACGG CATCGCAGCT CCCGACAGCC
 801 AGCGCATCGC CTTCTACCGC TTGCTCGACG AGTTCTTTTA ATGATCTAGA
 851 ACCGGTCATG GCCGCAATAA AATATCTTTA TTTTCATTAC ATCTGTGTGT
 901 TGGTTTTTTG TGTGTTCGAA CTAGATGCTG TCGACCGATG CCCTTGAGAG
 951 CCTTCAACCC AGTCAGCTCC TTCCGGTGGG CGCGGGGCAT GACTATCGTC
1001 GCCGCACTTA TGACTGTCTT CTTTATCATG CAACTCGTAG GACAGGTGCC
1051 GGCAGCGCTC TTCCGCTTCC TCGCTCACTG ACTCGCTGCG CTCGGTCGTT
1101 CGGCTGCGGC GAGCGGTATC AGCTCACTCA AAGGCGGTAA TACGGTTATC
1151 CACAGAATCA GGGGATAACG CAGGAAAGAA CATGTGAGCA AAAGGCCAGC
1201 AAAAGGCCAG GAACCGTAAA AAGGCCGCGT TGCTGGCGTT TTTCCATAGG
1251 CTCCGCCCCC CTGACGAGCA TCACAAAAAT CGACGCTCAA GTCAGAGGTG
1301 GCGAAACCCG ACAGGACTAT AAAGATACCA GGCGTTTCCC CCTGGAAGCT
1351 CCCTCGTGCG CTCTCCTGTT CCGACCCTGC CGCTTACCGG ATACCTGTCC
1401 GCCTTTCTCC CTTCGGGAAG CGTGGCGCTT TCTCATAGCT CACGCTGTAG
1451 GTATCTCAGT TCGGTGTAGG TCGTTCGCTC CAAGCTGGGC TGTGTGCACG
1501 AACCCCCCGT TCAGCCCGAC CGCTGCGCCT TATCCGGTAA CTATCGTCTT
1551 GAGTCCAACC CGGTAAGACA CGACTTATCG CCACTGGCAG CAGCCACTGG
1601 TAACAGGATT AGCAGAGCGA GGTATGTAGG CGGTGCTACA GAGTTCTTGA
1651 AGTGGTGGCC TAACTACGGC TACACTAGAA GAACAGTATT TGGTATCTGC
1701 GCTCTGCTGA AGCCAGTTAC CTTCGGAAAA AGAGTTGGTA GCTCTTGATC
1751 CGGCAAACAA ACCACCGCTG GTAGCGGTGG TTTTTTTGTT TGCAAGCAGC
```

1801 AGATTACGCG CAGAAAAAAA GGATCTCAAG AAGATCCTTT GATCTTTTCT
1851 ACGGGGTCTG ACGCTCAGTG GAACGAAAAC TCACGTTAAG GGATTTTGGT
1901 CATGAGATTA TCAAAAAGGA TCTTCACCTA GATCCTTTTA AATTAAAAAT
1951 GAAGTTTTAA ATCAATCTAA AGTATATATG AGTAAACTTG GTCTGACAGC
2001 GGCCGCAAAT GCTAAACCAC TGCAGTGGTT ACCAGTGCTT GATCAGTGAG
2051 GCACCGATCT CAGCGATCTG CCTATTTCGT TCGTCCATAG TGGCCTGACT
2101 CCCCGTCGTG TAGATCACTA CGATTCGTGA GGGCTTACCA TCAGGCCCCA
2151 GCGCAGCAAT GATGCCGCGA GAGCCGCGTT CACCGGCCCC CGATTTGTCA
2201 GCAATGAACC AGCCAGCAGG GAGGGCCGAG CGAAGAAGTG GTCCTGCTAC
2251 TTTGTCCGCC TCCATCCAGT CTATGAGCTG CTGTCGTGAT GCTAGAGTAA
2301 GAAGTTCGCC AGTGAGTAGT TTCCGAAGAG TTGTGGCCAT TGCTACTGGC
2351 ATCGTGGTAT CACGCTCGTC GTTCGGTATG GCTTCGTTCA ACTCTGGTTC
2401 CCAGCGGTCA AGCCGGGTCA CATGATCACC CATATTATGA AGAAATGCAG
2451 TCAGCTCCTT AGGGCCTCCG ATCGTTGTCA GAAGTAAGTT GGCCGC

Appendix 2a – Microarray: Non-supervised hierarchical clustering of all the chemokine genes and T cell-related genes in 35 resected cutaneous melanoma lesions from 13 patients before and after chemotherapy. Data are color-coded gene expression compared to the median expression of each gene in all samples. Array labels: pre (blue), pre-chemotherapy; pos (red), post-chemotherapy; S (light blue), stable; R (orange), regression; P (purple), progression.

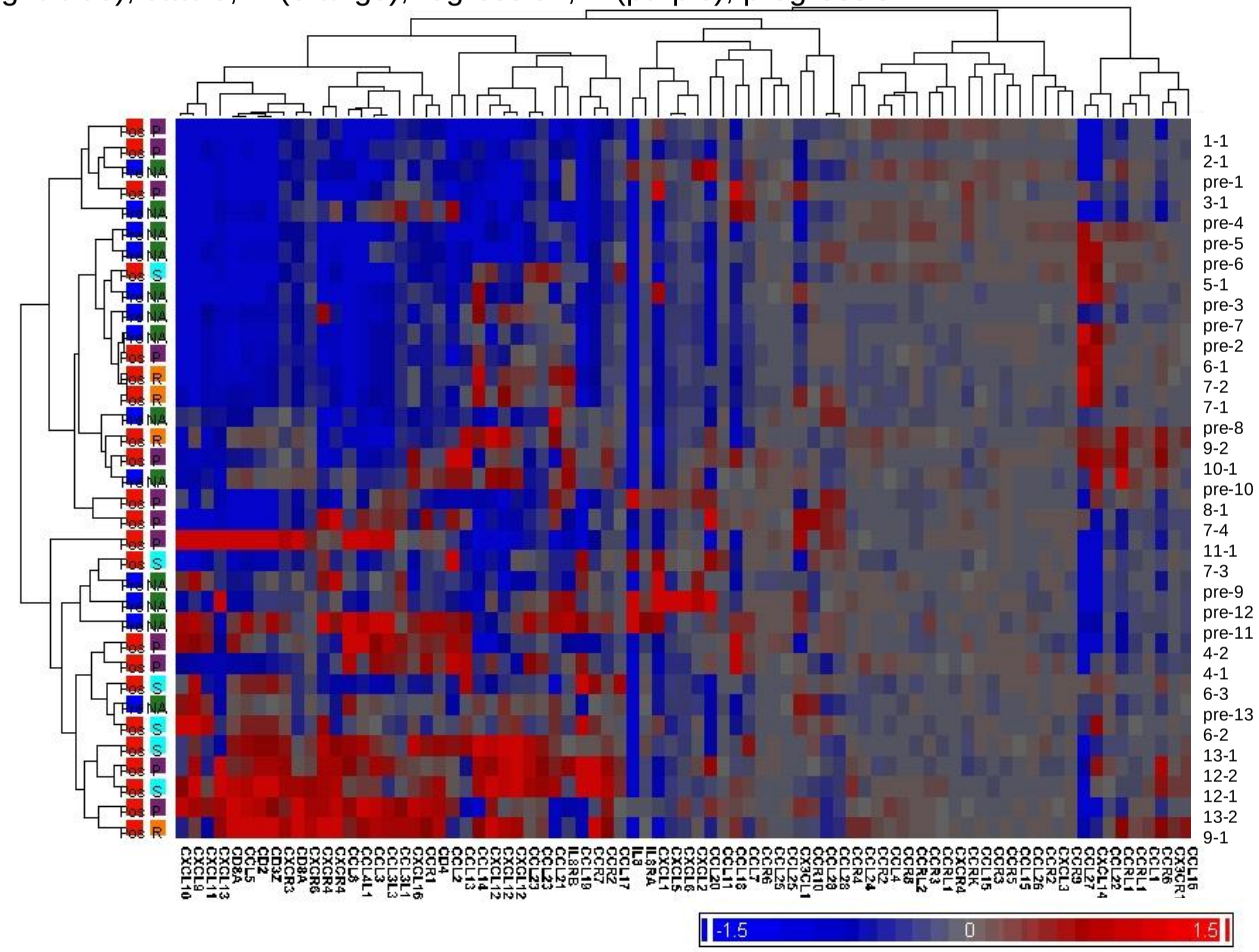

Appendix 2b – Microarray: Correlation between chemokine genes and CD3 (Table A), CD4 (Table B), and CD8A (Table C) expression in resected cutaneous melanoma lesions from patients before and after chemotherapy. P-values for multiple comparisons were adjusted using Bonferroni correction.

Table A

Genes	r-value	bonferroni p-value
CD2	0.9820	1.36E-23
CCL5	**0.9600**	**6.36E-18**
CXCR3	0.9500	2.32E-16
CD8A	0.9448	1.14E-15
CXCL9	**0.9010**	**1.28E-11**
CCR2	0.8217	1.13E-07
CXCL10	**0.8094**	**3.08E-07**
CXCR6	0.8088	3.22E-07
CD8A	0.8025	5.25E-07
CD4	0.7915	1.17E-06
CCR7	0.7842	1.95E-06
CCL8	0.7340	4.09E-05
CCL4L1	0.7298	5.10E-05
CXCL13	0.7083	1.51E-04
CXCL11	0.6972	2.55E-04
CXCL12	0.6525	0.00169
CCL3	0.6354	0.00321
CXCR4	0.6233	0.00495
CXCL12	0.6133	0.00697
CCL19	0.5978	0.01164
CXCL16	0.5829	0.01859
CXCR4	0.5820	0.01909
CXCL12	0.5771	0.02215
CCL3L3	0.5332	0.07585
CCR1	0.5297	0.08320
CX3CR1	0.5252	0.09345
CCL23	0.4981	0.18152
CCL23	0.4755	0.30357
CCL13	0.4245	0.86039
CCR6	0.4208	0.92340
CCR4	0.4156	1.00000
CX3CL1	0.4153	1.00000
CCL2	0.4125	1.00000
CCL15	-0.3758	1.00000
CCL3L1	0.3629	1.00000
CCR3	-0.3610	1.00000
CCL16	0.3551	1.00000
CCL17	0.3518	1.00000
CCL14	0.3202	1.00000
CCRL2	-0.3042	1.00000
CCRK	-0.3006	1.00000
CCL15	-0.2901	1.00000
CXCL3	-0.2450	1.00000
CCL27	-0.2432	1.00000
CCR2	-0.1906	1.00000
CCL28	-0.1857	1.00000
CCL1	0.1754	1.00000
CCR5	-0.1720	1.00000
IL8RB	0.1604	1.00000
CCRL1	-0.1588	1.00000
CCL21	0.1417	1.00000
CCL25	-0.1400	1.00000
CCR8	0.1310	1.00000
CCR9	-0.1249	1.00000
CCL4	-0.1219	1.00000
CCL28	-0.1210	1.00000
CXCL1	-0.1124	1.00000
CCRL1	0.1015	1.00000
IL8RA	0.1009	1.00000
CCR6	0.0901	1.00000
CCR10	-0.0836	1.00000
CCR2	-0.0800	1.00000
CCL24	0.0725	1.00000
CCL18	0.0617	1.00000
CXCL5	-0.0597	1.00000
CCRL1	-0.0594	1.00000
CXCL14	0.0582	1.00000
CCL22	0.0541	1.00000
CCL25	0.0513	1.00000
CCL26	-0.0444	1.00000
CXCL6	0.0390	1.00000
CXCL2	0.0372	1.00000
CXCR4	-0.0355	1.00000
IL8	-0.0354	1.00000
CCL20	-0.0332	1.00000
CCL11	-0.0278	1.00000
CCL7	-0.0223	1.00000
CCR3	-0.0192	1.00000

Table B

Genes	r-value	bonferroni p-value
CCL5	**0.8478**	**1.02E-08**
CD8A	0.8303	5.33E-08
CXCR6	0.8079	3.46E-07
CCR1	0.8072	3.64E-07
CD2	0.8042	4.61E-07
CD3Z	0.7915	1.17E-06
CXCL16	0.7850	1.84E-06
CXCR3	0.7767	3.23E-06
CCL4L1	0.7689	5.35E-06
CCR2	0.7425	2.57E-05
CCL8	0.7323	4.46E-05
CCL3	0.7285	5.45E-05
CXCL12	0.7098	0.00014
CXCR4	0.7080	0.00015
CD8A	0.7030	0.00019
CXCL9	**0.6857**	**0.00043**
CXCR4	0.6623	0.00114
CCL3L3	0.6413	0.00258
CXCL12	0.6379	0.00292
CCL23	0.6347	0.00329
CCR7	0.6241	0.00481
CCL23	0.6197	0.00561
CXCL10	**0.6176**	**0.00602**
CXCL12	0.6084	0.00822
CCL2	0.5411	0.06157
CCL3L1	0.4928	0.20517
CXCL11	0.4809	0.26924
CXCL13	0.4785	0.28435
CCL19	0.4492	0.52926
CX3CR1	0.4305	0.76754
CCL13	0.4222	0.89925
CCL28	-0.3782	1.00000
CCR3	-0.3572	1.00000
CCL18	0.3537	1.00000
CCL28	-0.3484	1.00000
CCL14	0.3340	1.00000
CCR4	0.3239	1.00000
CCL15	-0.2990	1.00000
CXCL3	-0.2874	1.00000
CCR6	0.2750	1.00000
CCL16	0.2718	1.00000
CCL27	-0.2684	1.00000
CCL15	-0.2539	1.00000
CCL7	0.2484	1.00000
CCRL1	-0.2371	1.00000
CCRL2	-0.2238	1.00000
CXCL1	-0.2159	1.00000
CCRK	-0.2018	1.00000
CX3CL1	0.1972	1.00000
CCL24	0.1938	1.00000
IL8RA	0.1898	1.00000
CCL1	0.1817	1.00000
CCL21	0.1665	1.00000
CCR8	0.1639	1.00000
CCL17	0.1555	1.00000
CXCL2	-0.1484	1.00000
CXCL5	-0.1467	1.00000
CCRL1	-0.1395	1.00000
CCR10	0.1181	1.00000
CCL26	0.1115	1.00000
CCR2	-0.1094	1.00000
CCR9	-0.1038	1.00000
IL8RB	0.0984	1.00000
CXCR4	-0.0840	1.00000
CCR6	0.0800	1.00000
IL8	0.0776	1.00000
CCL22	-0.0595	1.00000
CXCL6	-0.0582	1.00000
CCR5	-0.0553	1.00000
CCL25	-0.0460	1.00000
CCR2	-0.0426	1.00000
CCL11	0.0413	1.00000
CCR3	0.0350	1.00000
CCRL1	-0.0350	1.00000
CXCL14	-0.0269	1.00000
CCL25	0.0145	1.00000
CCL4	0.0056	1.00000
CCL20	0.0024	1.00000

Table C

Genes	r-value	bonferroni p-value
CCL5	**0.9819**	**1.49E-23**
CD2	0.9649	7.72E-19
CD3Z	0.9448	1.14E-15
CXCR3	0.9242	1.87E-13
CD8A	0.8861	1.15E-10
CXCL9	**0.8789**	**3.00E-10**
CXCR6	0.8643	1.74E-09
CCL4L1	0.8364	3.08E-08
CXCL10	**0.8340**	**3.83E-08**
CD4	0.8303	5.33E-08
CCL8	0.7568	1.12E-05
CXCL11	0.7486	1.81E-05
CCR2	0.7291	5.30E-05
CCL3	0.6953	0.00028
CXCL13	0.6883	0.00038
CXCL16	0.6569	0.00142
CCR7	0.6426	0.00246
CCL3L3	0.6203	0.00550
CCR1	0.6118	0.00734
CXCR4	0.6075	0.00847
CXCL12	0.5970	0.01196
CXCR4	0.5919	0.01403
CXCL12	0.5646	0.03204
CXCL12	0.5327	0.07688
CCL3L1	0.4573	0.44835
CCL2	0.4502	0.51862
CX3CR1	0.4484	0.53788
CCL19	0.4247	0.85709
CCL23	0.4160	1.00000
CX3CL1	0.3928	1.00000
CCL23	0.3809	1.00000
CCL13	0.3805	1.00000
CCR3	-0.3706	1.00000
CCR4	0.3595	1.00000
CCL15	-0.3291	1.00000
CCR6	0.2873	1.00000
CCRL2	-0.2866	1.00000
CCL16	0.2802	1.00000
CCL27	-0.2779	1.00000
CCL15	-0.2745	1.00000
CXCL3	-0.2585	1.00000
CCL17	0.2538	1.00000
CCL14	0.2021	1.00000
CXCL1	-0.1988	1.00000
CCRK	-0.1767	1.00000
CCL1	0.1742	1.00000
CCL28	-0.1603	1.00000
CCRL1	-0.1596	1.00000
CCL24	0.1458	1.00000
CCR2	-0.1357	1.00000
CCL18	0.1325	1.00000
CCR6	0.1231	1.00000
CCL25	0.1223	1.00000
CCR8	0.1216	1.00000
CCL11	0.1097	1.00000
CCL28	-0.1078	1.00000
CCL26	-0.0872	1.00000
CXCL5	-0.0778	1.00000
CCR5	-0.0740	1.00000
CCR9	-0.0655	1.00000
CCL20	-0.0655	1.00000
IL8	-0.0592	1.00000
CCL4	-0.0568	1.00000
CCR3	-0.0557	1.00000
CCL21	0.0498	1.00000
CXCL14	-0.0495	1.00000
CXCL2	-0.0479	1.00000
CCR2	-0.0456	1.00000
CCL22	-0.0452	1.00000
CCRL1	0.0428	1.00000
CXCL6	0.0393	1.00000
CCR10	0.0355	1.00000
CCRL1	-0.0332	1.00000
IL8RB	-0.0175	1.00000
CCL25	-0.0072	1.00000
IL8RA	0.0070	1.00000
CXCR4	-0.0042	1.00000
CCL7	-0.0035	1.00000